APPLICATION OF GENETIC ALGORITHM TO A FORCED LANDING MANOEUVRE ON TRANSFER OF TRAINING ANALYSIS

by

Peter Tong Cheong Chee

Bachelor of Engineering (Honours) (Queen's University)
Master of Engineering (Queen's University)
Diploma in Education (McGill University)

Submitted to the School of Aerospace, Mechanical and Manufacturing Engineering
in the Faculty of Engineering
in fulfilment of the requirements for the degree of

Doctor of Philosophy

at the

Royal Melbourne Institute of Technology

April 2006

Declaration

I, Peter Tong, certify that except where due acknowledgement has been made, the work is that of the author alone; the work has not been submitted previously, in whole or in part, to qualify for any other academic award; the content of the thesis is the result of work which has been carried out since the official commencement date of the approved research program; and, any editorial work, paid or unpaid, carried out by a third party is acknowledged.

Peter Tong
May 12, 2007

Preface

Intent.

This work has been carried out under a joint scholarship agreement between the Royal Melbourne Institute of Technology (RMIT) and Defence Science and Technology Organisation (DSTO). The work has been conducted within Air Operations Division (DSTO) and School of Aerospace, Mechanical and Manufacturing Engineering (RMIT).

Publications.

During the course of this research program, the author has published or submitted the following publications of relevance to the topic area.

- **Tong, P.** and Bil, C.: "Effects of Errors on Transfer of Aircraft Flight Training," 32nd European Rotorcraft Forum, Maastricht, The Netherlands, 12 – 14 September 2006.

- **Tong, P.** and Bil, C.: "Genetic Algorithm Control Parameters Design for Direct Value and Real Value Encoding," 4th International Conference on Advanced Engineering Design, Glasgow, Scotland, UK, 5 – 8 September 2004.

- **Tong, P.**, Bil, C., and Galanis, G.: "Horizontal Wind Effects on Flight Paths Design for a Forced Landing Manoeuvre," 4th International Conference on Advanced Engineering, Glasgow, Scotland, UK, 5 – 8 September 2004.

- **Tong, P.**, Bil, C., and Galanis, G.: "Genetic Algorithm Technique Applied to a Forced Landing Manoeuvre," 24th International Council of the Aeronautical Sciences, Yokohama, Japan, August 29 – September 3, 2004.

- **Tong, P.**, Bil, C.: "Errors in Helicopter Training," RMIT Report CR 2004, June 2004.

- **Tong, P.**, Bil, C., and Galanis, G.: "The Effect of Vertical Atmospheric Turbulence Velocity on the Sensitivity Analysis to a Forced Landing Manoeuvre," Second MIT Conference on Computational Fluid and Solid Mechanics, Cambridge, Massachusetts, June 17 – 20, 2003.

- **Tong, P.**, Galanis, G. and Bil, C.: "Sensitivity Analysis to a Forced Landing Manoeuvre," Journal of Aircraft, Vol. 40, No. 1, 2003, pp. 208 – 210.

- **Tong, P.**, Bil, C, and Galanis, G.: "Control Parameters for Genetic Algorithms to a Forced Landing Manoeuvre", 2002 Aircraft Performance Symposium, Melbourne, Victoria, Australia, 13th December 2002.

- **Tong, P.** and Galanis, G.: "Simulator Requirements for Optimal Training of Pilots for Forced Landings," SimTect 2001, Canberra, Australia, 28 – 31 May 2001.

Acknowledgements

I would first like to thank my senior supervisor, Associate Professor Cees Bil (RMIT), for his support and supervision over the duration of the research project. His valuable suggestions and comments are greatly appreciated. I would next like to thank my second supervisor, Dr. George Galanis (DSTO), whose experience as a research scientist and a flight instructor has proved extremely valuable during the course of this research. My thanks are also extended to the Air Operations Division (AOD) of DSTO and RMIT for their financial support in the form of a joint scholarship. The computing facilities provided by AOD are also greatly appreciated.

As with every great project, there are always the supporting "crew" whose contribution may or may not be so obvious. I would like to express my appreciation to all the individuals who have assisted me along during this long and winding road to completing this thesis. They include colleagues from AOD and postgraduate students from RMIT Bundoora East campus. They have on many occasions been a sounding board and provided many informal discussions that paved other avenues of thoughts. A special thanks to Satya Prasad Mavuri for his help in Matlab programming.

The continuous support from my family is also greatly appreciated. This work has been made possible with the support of my parents, sisters and brothers-in-law, and my wife – Michelle Wee. They have been extremely patient and supportive to me throughout my "roller coaster ride" and have always been there whenever I hit rough seas. They rode the rough seas with me and helped me through by providing sunshine and rainbows. Michelle, thank you for your encouragement, inspiration, patience and extreme tolerance throughout my many years of studies and in putting up with "Hang on," "Give me 2 minutes," "I'll do it some other time". You are my pillar of support. As I complete this chapter of my life, Michelle and I are awaiting the arrival of our first baby.

Finally, I would like to thank the examiners for their time and patience in assessing this work.

To my teacher and my mentor, Professor Emeritus Patrick Oosthuizen,
who helped me to look from outside the box and gave me the encouragement that "IT" is possible.

To Jane Paul,
who provided a spark in finding the career that I most enjoy.

Table of Contents

Nomenclature

$V_{climb\ out}$	= climb out velocity
$V_{L/D\ max}$	= maximum L/D velocity
$V_{R/C\ max}$	= maximum R/C velocity
g	= acceleration due to gravity
D	= drag
L	= lift
R	= radius of turn
T	= trust
W	= weight
n	= load factor
β	= sideslip angle
ϕ	= bank angle
θ	= angle into the turn
γ	= glide angle
χ	= heading angle
ω	= turn rate
dh/dt	= sink rate with respect to time
dh/dθ	= sink rate with respect to angle turned
$\Phi_{ug,}\ \Phi_{vg,}\ \Phi_{wg,}$	Spectral density. (turbulence component?)
Ω	Spatial frequency (ω/V_T) (radians/ unit length).
$\sigma_u,\ \sigma_v,\ \sigma_w,$	Turbulence intensity.
ω	Temporal frequency (radians/unit time).
$L_{u,}\ L_{v,}\ L_w$	Characteristic Scale Length.
V_T	Aircraft's true speed.

Subscripts

u	Longitudinal
v	Lateral
w	vertical

List of Tables

List of Figures

ABSTRACT

Flight simulators are becoming more sophisticated in replicating actual flying manoeuvres and conditions. Despite the advancement of technology, a flight simulator cannot perfectly represent a particular aircraft in all aspects. For example, the mathematical model of the aircraft is never fully accurate, the motion and visual systems have physical limitations that make the full representation of the sensation of flying less than perfect. Regulatory authorities around the world are beginning to approve—or are considering the approval of—single engine gas turbine (SEGT) aircraft for regular public transport (RPT) operations. This will require the flight simulator industry to consider exploring the use of flight simulators for SEGT aircraft in RPT operations.

The application of flight simulators for initial pilot training for both civil and military pilots is still relatively unexploited. For example, training of ab-initio pilots in emergencies such as forced landings is still carried out in aircraft. Similarly, almost all training of combat manoeuvres for military pilots is also carried out in aircraft. The issues involved in doing such training in simulators are not well developed in the literature. This study raises some issues for training pilots to fly forced landings and examines the impact that these issues may have on the design of simulators for such training. In particular, it focuses on the trajectory that a pilot must fly after an engine failure and how pilots could be trained for this manoeuvre in a simulator.

A sensitivity study of the effects of errors in the aerodynamic parameters was carried out and the requirements for determining these parameters for simulators were examined. This study also investigated the effect that the tolerances prescribed in the Manual of Criteria for the Qualification of Flight Simulators have on the performance of flight simulators used for pilot training. A simplified analytical model for the Beech Bonanza model E33A aircraft with retractable undercarriage was used to determine the effect of the aforementioned to the tolerances on forced landings. It was found that the effect of the tolerances is highly sensitive on the nature of the manoeuvre flown and that in some cases, negative transfer of training may be induced by the tolerances. For an engine failure height at 650 ft AGL, the results show that, following a turn around manoeuvre for landing, the touchdown points vary significantly from the reference model. This issue is of concern to flight simulator manufacturers in determining their tolerance standards.

An investigation on the effect vertical atmospheric turbulence, based on the MIL-F-8785C specifications, has on a forced landing manoeuvre was also carried out. 100 vertical turbulence profiles were randomly generated and were applied to a simplified forced landing analytical model. The results show that the nature of the manoeuvre flown is highly sensitive to the vertical gust and is therefore important to flight simulation. The straight glide to touchdown manoeuvre shows possible touchdown locations that vary from approximately 637 ft to 828 ft from the engine failure location, while for the continuous 360° attempt, it ranges from 0 ft to 396 ft. The vertical gust has the most effect during the initial phase of the forced landing flight manoeuvre since a small deviation in the glide angle due to vertical gust will have a nonlinear effect on the horizontal distance. The effect for a 360° turn to touchdown is least affected since the turn radius is less susceptible to vertical gust. Therefore, it can be concluded that vertical turbulence has the most effect on the straight glide to touchdown manoeuvre and lesser effect on the turning manoeuvre.

This analysis demonstrates the importance of analyses of vertical gust to flight simulation and the consideration of such requirements within the context of particular manoeuvres to be flown, as in some cases, negative transfer of training may be induced by the vertical gust. The vertical gust sensitivity analysis shows that a simulator may incur significant errors in the task of handling an engine failure after take-off for a single engine aircraft. This raises the question of the ability to use simulators to train pilots aptly for engine failure after take-off using the tolerances as specified in current regulations since the resultant errors are manoeuvre dependent.

A forced landing trajectory optimisation was carried out using Genetic Algorithm (GA). The selection of GA control parameters can have a significant impact on the effectiveness of this optimisation algorithm. Therefore, the selection for a suitable set of control parameters in the GA analyses for both direct-value and real-value encoding was carried out to determine the best selection of population size, crossover rate, mutation rate and coefficients for non-uniform. The results show that there is minimal or no improvement in the fitness value when the population size exceeds four times the chromosome length and the computational cost increases linearly with the population size.

The forced landing manoeuvre analyses with pre-selected touchdown locations and pre-selected final headings were carried out for an engine failure at 650 ft AGL for bank angles varying from banking left at 45° to banking right at 45°, and with an aircraft's speed varying from 75.6 mph to 208 mph corresponding to 5% above airplane's stall speed and airplane's maximum speed respectively. Simulations were carried out for a time averaged atmospheric turbulence model and for a simplified thermal model for various crosswinds at three test locations. The results show that certain pre-selected touchdown locations are more susceptible to horizontal wind. The results for the forced landing manoeuvre with a pre-selected location show minimal distance error while the quality of the results for the forced landing manoeuvre with a pre-selected location and a final heading show that the results depended on the pre-selected location and on the final heading. For certain pre-selected touchdown locations and final headings, the airplane may either touchdown very close to the pre-selected touchdown location but with greater final heading error from the pre-selected final heading or touchdown with minimal final heading error from the pre-selected final heading but further away from the pre-selected touchdown location.

Analyses for an obstacle avoidance forced landing manoeuvre were also carried out where an obstacle was intentionally placed in the flight path as found by the GA program developed for without obstacle. The program developed successfully found flight paths that will avoid the obstacle and touchdown near the pre-selected location. In some cases, there exist more than one ensemble grouping of flight paths. The distance error depends on both the pre-selected touchdown location and where the obstacle was placed. The distance error tends to increase with the addition of a specific final heading requirement for an obstacle avoidance forced landing manoeuvre. Again, as with the case without specific final heading requirement, there is a trade off between touching down nearer to the pre-selected location and touching down with a smaller final heading error.

Although GA is capable of locating some of the best values for optimisation, it does not guarantee that it is a minimum value. Therefore, another optimisation technique, Sequential Quadratic Programming (SQP) was used to find more accurate and precise solutions. The results obtained agree well with the results obtained using GA. This research concludes with a practical forced landing manoeuvre strategy in the presence of unknown wind conditions. The main limitations of the research are highlighted and several areas for further research are suggested.

CHAPTER 1

INTRODUCTION

1.1 Introduction

The advancement of computer technology has made it possible for increasing the role of flight simulators for initial pilot training for both civil and military pilots. It has also enabled pilots to be trained in more complicated and dangerous manoeuvres in emergency procedures without endangering the pilots' lives, and in the development of new methods of achieving operational objectives. The costs of modern aircraft and the increasing complexity of the operating environment are placing more demands on flight simulators to provide more types of training as well as a safe and improved learning environment. Flight simulations provide researchers with the ability to identify and define specific human capabilities and limitations in man/machine interaction. They are also used to explore interrelationships between machines and humans under various configurations and circumstances. Flight simulators are used for three primary purposes: (a) in training individual pilots and other crewmembers; (b) to support initial training of pilots, navigators and systems operators in the Air Force, the Navy and the Army as well as civilian pilots from civilian colleges, universities and flying schools and (c) to train pilots in skills and procedures that they could never practise in a real world setting (Stark 1989).

To date, flight simulators have been widely used by commercial airlines for pilot training. They have become so sophisticated that the highest approved category of simulations allows zero flight time training for commercial airline pilots converting to a new aircraft type. Flight simulations for military use are far more intricate and agile than those for commercial airlines. Despite the advancements, flight simulations are still not widely used in military training. This is because the human perceptual and learning processes involved are still not well enough understood to permit accurate prediction of the levels of information or fidelity required to ensure significant levels of positive transfer of training in many important tasks. The objective determination of the ability of simulator training to transfer to the aircraft has always been recognised as a fundamental problem. This has resulted in a great deal of effort being devoted to designing simulators to provide as many of the characteristics assumed to contribute to transfer as possible (Lintern 1999).

Recent advances in aircraft technology are also creating new ways of using aeroplanes. For example, gas turbine engines are now so reliable that a number of countries including Australia are approving the use of single engine gas turbine aircraft for regular public transport. This has created new opportunities and challenges for the flight simulation industry. One approach to flight simulator development has been to attempt to replicate an entire real world scenario. This method is limited by the physical hardware e.g. computer constraints, visual reproductions and input devices. The other approach has been to define the supporting tasks such as delay compensation, visual fidelity and motion in order to replicate the real world scenarios. An issue associated with this approach is the effect the supporting tasks have on the learning transfer from flight simulation training to real life performance and if there exists a relevant performance correlation between training on a flight simulator and real life performance.

The application of flight simulators for initial pilot training for both civil and military pilots is still relatively unexploited. For example, training of ab-initio pilots in emergencies such as forced landings is still carried out in aircraft. Similarly, almost all training of combat manoeuvres for military pilots is also carried out in aircraft. The issues involved in conducting such training in simulators are not well developed in the literature. The basic piloting tasks for the approach and landing are similar for most aircraft and these tasks can be as demanding as any of the complete mission of an aircraft.

This study focuses on the trajectory that a pilot must fly after an engine failure and how pilots could be trained for this manoeuvre in a simulator. It raises some issues for training pilots to fly forced landings and examines the impact that these issues may have on the design of simulators for such training. Although a high fidelity airplane model can be used to model the aircraft performance but intrinsic tolerance and errors which are inherent to the model will not provide perfect solutions. Therefore a sensitivity study of the effects of errors in the aerodynamic parameters was also carried out and the requirements for determining these parameters for simulators were examined.

Simulator manufacturers assume that flight simulators can train pilots appropriately but how accurate are the training when even with the advancement of technology, a flight simulator cannot perfectly represent a particular aircraft in all aspects. For example, the mathematical model of the aircraft is never fully accurate, the motion and visual systems have physical limitations that make the full representation of the sensation of flying always less than

perfect. The time delay in flight simulation which is also known as transport delay, consists of two components: the constant inherent delay due to processing time from the input device to the visual image or transmission over the physical distance and the variable delay due to traffic or congestion over a network. The inherent transport delay problem in flight simulators may cause the pilot to fly a totally different manoeuvre in real life than in a flight simulator or to even react differently. This raises the issue of the appropriate transfer of training from flight simulators. This study analyzes the effects artefact, such as uncertainties in flying judgement which results in a form of a delay in the decision making, may affect in a forced landing manoeuvre. The effects of delay are represented in the form of wind disturbances in a forced landing analysis since the time used in deciding on how to fly under the influence of wind disturbances has similar effects as the delay in decision making under the influence of wind disturbances. For example, a pilot may have picked an aiming point to land but due to some blurred vision which may be due to weather or poor visibility, or uncertainties in distance or elevation, the pilot's reaction or judgement in landing the airplane may be affected. The uncertainties may be present in a form of wind disturbances. These potential errors and uncertainties are related to the study of transfer of training from flight simulators since the pilot may manoeuvre the aircraft differently according to varying perceptions. How much will the manoeuvre differ from some reference manoeuvre? Will the uncertainties affect the pilot so much so as for the pilot to fly a totally different manoeuvre? Negative transfer of training can lead to unsafe manoeuvres, such as controlled flight into terrain, loss of situational awareness and mid-air collisions.

The forced landing manoeuvre after an engine failure at low altitude considered in this study will also serve as a preliminary configuration to a simplified representation of a fighter combat pursuit-evasion scenario. Here, the unpowered airplane and the stationary landing point represent the pursuit and the evader aircraft respectively. By introducing velocity to both the unpowered airplane and the stationary landing point, the analysis can be used as a preliminary understanding and as corner stones to the formulation of a fighter combat pursuit-evasion manoeuvre analysis. Hence, the present study on a forced landing was carried out to serve as a preliminary investigation to a fighter combat pursuit-evasion manoeuvre analysis, which is of interest to the Australian Defence Force. The effects artefacts such as delays may also have an affect on the players' decision in the pursuit evasion game and in networked flight simulations. An open-loop control analysis was applied to find the optimal flight trajectory synthesis given a pre-selected touchdown location and a specific final heading as a function of time through an iterative search procedure. The

results for this study will then form the basis for further research on the requirement for both stand alone and networked flight simulators.

This research project was conducted in collaboration with the Defence Science and Technology Organisation (DSTO) at Fishermens Bend. This study on the effects artefacts have on flight simulations along with DSTO's research on task-relevant cues on simulation design (Galanis, Jennings *et al.* 1997) and modelling of human perception for manned simulation (Galanis, Jennings *et al.* 1998) support the DSTO's research program of enabling work for the creation of synthetic environments. The research program incorporates virtual simulation and constructive simulation technology which contributes to the development of both research and training simulators. Currently, the Australian Department of Defence spends a substantial portion of its budget on pilot training and on maintaining constant flight training operations. The development of sophisticated flight simulations can help reduce airborne training and operating costs, which will be beneficial to Australia in the form of financial savings. It will also reduce the wear and tear on the aircraft and have a less destructive impact on the environment in the form of reduced noise and fuel pollution. Further benefits can be gained by reducing flight-training accidents whilst enabling pilots to explore more dangerous flying situations.

The focus of this study is on the search for better flight trajectories in the presence of wind disturbances so as to provide pilots with rules of thumb, which can be memorized for forced landings after engine failure at low altitude. It is not on the search for optimal trajectories as this implies an outcome of a single best solution. However, it concentrates on the effects delay has on an ensemble of intended flight paths.

The main aim of this research can be summarised as:

> To develop and to gain better understanding on skills transfer from flight simulators, especially on the effects artefacts have on a forced landing manoeuvre after an engine failure and to use genetic algorithm as a search method to generate an ensemble of probable flight paths to a forced landing manoeuvre with and without obstacle for simulator flight training purposes.

1.2 Background

Whilst flight simulators are commonly used to train pilots worldwide, there still exist questions on the effectiveness on the transfer of training from flight simulators to a real flying environment. This work examined the effects the tolerances prescribed in the Manual of Criteria for the Qualification of Flight Simulations (ICAO 1995) have on the flight simulators' performance used for pilot training. It addressed some issues for training pilots to fly such phases of flight and examined the impact that these issues may have on the design of simulators for such training.

This work demonstrated the importance of analyses of simulator requirements and the consideration of such requirements within the context of particular manoeuvres to be flown. The sensitivity analysis shows that a simulator may incur potentially significant errors in the task of handling an engine failure after takeoff for a single engine aircraft. It is not sufficient to assume that the present simulator regulations will be adequate for such operations. New applications of flight simulators will also require new types of data to be collected from flight tests. For example, the data collection methods should ensure that the tolerances achieved in the simulators are relevant for the specific training tasks performed in the simulators.

The forced landing performance and sensitivity analysis show that the universally recommended speed at maximum lift to drag ratio may not be the best speed to fly for a forced landing manoeuvre. The manoeuvre to fly depends on where the engine failure occurs and on the atmospheric conditions.

The forced landing analysis in this study utilised Genetic Algorithm (GA) as a search technique for the optimal landing trajectory since it is a relatively simple procedure. The selection of GA control parameters can have significant impact on the effectiveness of this optimisation algorithm. Since GAs rely on stochastic processes and are optimisation objective dependent, a control parameter design analysis was carried out and the combination of control parameters that are most suitable for use in different problems and for different encoding is recommended. The suggested combination of control parameters provides beneficial information and guidelines to GA users on control parameters selection for a wide range of engineering and industrial applications. One of the drawbacks in using GA for optimisation is that it cannot guarantee that a minimum or a maximum value has been found. However, the results found will be very close to the relative extrema, if not the absolute extrema by fine-tuning the control parameters during the search process.

The results from the GA search optimisation method was used to determine an ensemble of successful forced landing manoeuvres in the presence of unknown atmospheric conditions and horizontal crosswinds. They were also used to determine an ensemble of successful obstacle avoidance forced landing manoeuvres.

1.3 Thesis Outline

This thesis contains 9 main chapters, including Introduction and Conclusion. A brief content description of each chapter will be given here. However, more comprehensive details are contained in the opening sections of each chapter.

Chapter 1 – Introduction introduces the scope of the research and gives a brief description of the nature of the research. This chapter also introduces the motivation behind the research and its benefits. It also discusses the area in which this research lies and gives a brief overview of the structure of the thesis.

Chapter 2 – Background gives the history and current applications of flight simulators. It also provides a review on some of the issues on transfer of training, skills transfer and on how artefacts affect the transfer of training from flight simulators. Reviews on aircraft trajectory optimisation and on different techniques used in a forced landing are presented. Overall this chapter does not provide many technical details on trajectory optimisation but comments are made regarding the relevancy of certain optimisation methods. For more technical details, referrals can be made to the work cited.

Chapter 3 – Aircraft Dynamics Model and Atmospheric Model provides the theoretical development of the aircraft model and the atmospheric disturbance models used for this research. The Beech Bonanza E33A single engine aircraft model and a brief review on the atmospheric turbulence models and thermal models are presented in this chapter.

Chapter 4 – Problem Formulation contains the problem formulation for the forced landing considered in this study. It presents the problem description and setting the objectives and constraints based on the aircraft model and vertical wind models described in Chapter 3. This chapter includes an exhaustive search on a forced landing manoeuvre for different touchdown

locations whose flight trajectories will be used to serve as reference flight trajectories for subsequent chapters.

Chapter 5 – Forced Landing Performance and Sensitivity Analysis presents the effects that different turn speeds have on a forced landing manoeuvre. It also presents the sensitivity analysis results on the effects that ICAO's tolerance standards have on flight simulators used for pilot training with and without vertical disturbances.

Chapter 6 – Genetic Algorithm in a Forced Landing Manoeuvre presents the necessary background to the genetic algorithm theory as used in the analysis on a forced landing manoeuvre. It includes a genetic algorithm control parameter analyses for both direct value and real value representations to allow for efficient use of genetic algorithm in the forced landing problem considered. The forced landing manoeuvre analyses were carried out in the presence of vertical disturbances and constant horizontal wind. Additional genetic algorithm analyses in a forced landing manoeuvre include landing at a pre-selected location with a specified final heading and analyses on obstacle avoidance in a forced landing manoeuvre. The analyses have successfully found flight trajectories that will manoeuvre around the obstacle and touchdown as close as possible to the pre-selected locations and specific final headings, with and without the presence of constant horizontal wind.

Chapter 7 – Sequential Quadratic Programming in a Forced Landing Manoeuvre presents the necessary background to grasp the Sequential Quadratic Programming theory for use in the analysis on a forced landing manoeuvre. The results obtained using this optimisation method for a specified pre-selected touchdown location were used to compare and to support the results found by using the genetic algorithm method. Forced landing manoeuvre analyses at higher engine failure altitude were also carried out for the specific pre-selected landing location.

Chapter 8 – Practical Forced Landing Manoeuvre Strategy with Unknown Atmospheric Wind Conditions discusses how the findings from the present work can be applied to a forced landing manoeuvre with unknown atmospheric wind conditions.

Chapter 9 – Conclusions discusses some of the key results of this study. Those areas requiring further work and, possible areas of future research are identified. Other

applications based on the results of this study are also suggested. Finally a brief conclusion on the outcome of the research is given.

CHAPTER 2

BACKGROUND

2.1 Introduction

This chapter presents an overview of research and technical reports regarding flight simulations, transfer of training, aircraft landing trajectories and flight trajectory optimisation. These topics are reviewed in this chapter while an in depth analysis on the specific methods used can be found in subsequent chapters. Flight simulation encompasses a very broad range of technical areas. Therefore, only publications that are specifically related to the pertaining work contained are provided. A brief review on the historical background, the efficiency and effectiveness of skill transfer from flight simulators, and some of the inherent problems associated with flight simulation such as delay are presented. A general description on different approaches for various situations on an aircraft landing manoeuvre are also reviewed.

2.2 Flight Simulations

Flight simulations enable a user to experiment with various systems configurations and modes of operations without the need of building an actual system. A flight simulator uses mathematical expressions to describe the major characteristics of the system whose output represents the response to the control inputs and environmental effects. A mathematical model may also be used to represent the human-in-the-loop operator. However, the accuracy of the mathematical model may be limited or there are restrictions in the hardware, for example in the visual display system or motion base. Hence, it may require a complex system to estimate the relative value of the system configurations and its characteristics. The most important role of a flight simulator is to train pilots, however they are also used for basic and applied research into establishing human capabilities and limitations, as well as to explore how humans and systems interact under various circumstances and conditions.

A brief history of flight simulation was compiled by (Baarspul 1990) and pilot training has been considered of vital importance since the beginning of manned flight. The first synthetic flight training device, the Antoinette trainer, consisted of two half-sections of a barrel. Its

motion was manually controlled by instructors in order to simulate the pitch and roll motion of an aircraft, and the pilot was required to align the reference bar with the horizon using the device controls. Over time, following some trial and error experiments, improvements were made on the manual motion by replacing both the mechanical or electrical actuators that were linked to the training device controls. The Link Trainer was the most successful and well-known training device of this type. This training device, which was also known as the blue box-link simulator, was patented by Edwin Link in 1930. Advancements in flight simulations were made during World War II with the use of a differential analyser within an analogue computer to solve the airplane's equations of motion. In 1941, the Telecommunications Research Establishment in Britain designed and built an electronic simulator that solved the aircraft equations of motion.

From the 1950's, flight simulators continued to improve with the addition of cockpit motion systems and in 1964 research on flight simulator motion began at the Faculty of Aerospace Engineering of Delft University of Technology (DUT). With the introduction of the three Degrees of Freedom (DOF) motion system (roll, pitch and heave), this faculty developed flight simulators that used hydraulic actuators in hydrostatic bearings. The motion systems continued to improve and the first commercially available six DOF motion system was developed by LMT (Thompson CSF) in 1977. In the late 1960s and early 1970s, Evans & Sutherland (E&S) of Salt Lake City, Utah developed a night landing and carrier landing flight simulator program based on a Digital Equipment PDP 11/45 and the E&S Picture Systems 1. This was considered a major break through at the time. The system was based on a line drawing display, hence, the limitation to night landings. Subsequent flight simulation systems from E&S were raster scan based, e.g., CT-5, which were acquired by most airlines and branches of the military. Visual systems were then added and the first Computer Generated Image (CGI) system for simulation was produced by the General Electric Company (Stark 1989). Since then, flight-training devices have improved tremendously and technology has been driving the development of Full Flight Simulators (FFS).

Using flight simulators for pilot training has many advantages over training in a real aircraft. For example, flight simulators are safer, more convenient, more flexible and more economical than training in a real aircraft. They enable task specific training where additional skills can be acquired upon mastering basic skills, and they allow pilots to learn and practice critical, complex, and dangerous manoeuvres without risking lives. Flight simulators provide a dedicated and effective learning and practice environment. They are

particularly valuable in support of training for emergency procedures such as flying in an adverse weather environment or at the edge of the flight envelope. (Ray 1999) provided a list of nine training accidents where forty-five lives were lost and nine aircraft were destroyed. (Teunissen 1999) compiled a list of flight accidents that resulted from military and civil flight training from 1965 – 1998 and there were more than 250 dead in 30 years. These training accidents could have been avoided had today's flight simulator existed and used.

The role of a flight simulator is to provide a tool with which student pilots learn how to fly and to demonstrate proficiency in flying an aircraft. In flying a real aircraft, the student pilot cannot afford the consequences of his or her incorrect control inputs. On the contrary, the use of a flight simulator allows the student pilot to experience improper pilot actions or even to fail in any given manoeuvre while eliminating potential catastrophic training accidents or risking their lives. It has been well accepted in the field of behavioural psychology that failure is a powerful feedback to human learning ability.

The growing role of flight simulation for training, both civil and military, generates a potential market for more effective simulation systems. Another benefit in using flight simulators for flight training is in cost savings. In 1976, the use of flight simulators for training had an estimated saving of about $25 million per year in training cost for a particular airline by using an average of 26,000 flight simulator hours and for about 1100 hrs on an aircraft (Orlansky and String 1980). In 1972, the use of the UH-1 helicopter military flight simulators for training reduced actual flight hours from 116 hours to 26.5 hours, which translated to a saving of over $4,000 per student (Stark 1989). Some of the indirect saving in using flight simulators is the cost involved in the support of flying the actual aircraft such as ground personnel and facilities needed to support flight operations, and in aircraft wear and tear. Student pilots also save time by using the flight simulator for training. For example, if students were training for a specific task such as a landing manoeuvre, the students would have to take-off and fly the circuit for the landing manoeuvre. In a flight simulator, the student pilots can virtually spend the entire practice session on the particular landing manoeuvre task. Currently, in the whole of Europe, only a handful of airports allow unrestricted training flights and the number is decreasing (Teunissen 1999). Hence, the demand for using flight simulators to train pilots is increasing.

Flight simulators are also being used for training military and civilian transport pilots. In training civilian pilots, FFS has been recognized as an integral part of flight training from ab

initio pilot training to advanced training including type conversion. The military use flight simulators for training specific tasks but they are mainly used for dedicated ongoing proficiency training. (Farrow 1982) discussed how the use of flight simulators has reduced the risks for military aircrew. Some of the applications of military flight simulators include training or practicing for evading air-to-air missiles, evading surface-to-air missiles, air-to-air combat, airborne surveillance and as a mission simulator. This advanced follow-on training has driven the requirement for sophisticated simulation technology. The Air Education and Training Command of the U.S. Air Force conducted an analysis and evaluation of its flying program. It identified some current and future training problems and challenges that could be met by infusion of advanced modelling and simulation technologies (Andrews, Edwards *et al.* 1996).

Flight simulators have been used to study the greater operational potential on approach and Microwave Landing System (MLS) by (Erkelens 1988). His investigation was on the evaluation of the feasibility of MLS guided interception procedures by considering the appropriate turn techniques and the required avionics equipment. His research also included an investigation on the approach path parameters for curved paths. However, the MLS was only marginally implemented in the United States and curved approach paths are now being considered for the Global Positioning System (GPS) Wide Area Augmentation System (WAAS). A study on the effects of different levels of wake turbulence on final approach using a research simulator for a B737-100 airplane was conducted by (Stewart 1998). His data shows a large amount of variation between pilots and the results obtained appear to be more conservative than the results from his previous studies.

2.2.1 Transfer of Training

The use of flight simulators to effectively train pilots has always been recognised as a fundamental problem. As a result, significant effort has been dedicated into designing flight simulators that will provide as many of the characteristics assumed to contribute to the transfer of training. It is very difficult to accurately predict the levels of information required to ensure significant levels of positive transfer of training since the human learning and perceptual processes are not well understood (Stark 1989). The development of Full flight simulators has been driven by either the training establishment or the technological advances. It is important that the training community is aware of some of the inherent shortfalls that are associated with using flight simulators to train pilots. They should focus on the significant

potential benefits while at the same time be aware of the current limitations of the commercially available flight simulators.

Some common questions in using flight simulators to train pilot are “How well do flight simulators train pilots?” “What constitutes learning?” “What are the positive skill transfers and how do we recognize the potentially negative skills transfer?”, “What is expected from student pilots after a successful completion of the training?”. Despite the advancement of technology, a flight simulator cannot perfectly represent a particular aircraft in all aspects. For example, the mathematical model of an aircraft is never fully accurate, the motion and visual systems have physical limitations that make the full representation of the sensation of flying always less than perfect. The motion systems cannot fully replicate vertical motion, sustained linear and rotational accelerations as present in roll, pitch, and yaw accelerations, and as well as in the normal load factor “g’s” but a certain level of fidelity may be achieved albeit at high cost. Pilots have to be aware of the limitations of sensory feedbacks that are provided and not to rely on them completely.

Flight simulators are not designed to simulate the whole spectrum of flight operation and therefore caution should be observed when using flight simulators out of the “normal operating envelope”, e.g. the simulation to accurately teach a pilot to recover from post stall or unusual attitudes/upset manoeuvres or engine failures after take-off. A potential improper application of flight simulators is in accident investigation. The National Transportation Safety Board (NTSB) has cautioned that the use of flight simulators in accident investigations should be approached judicially (Ray 1999).

The training qualities and effectiveness from flight simulators are dependent on a number of factors, which include the quality of the simulator, the instructor's skill and the teaching curriculum. Flight simulators provide invaluable training in preparing pilots to cope with extreme conditions but awareness should be applied in recognizing the basic limitations of flight simulators such as the effect of restricted motion cues and how such limitations might impact individual exercises. The time constraint in completing the curriculum also hampers the opportunity to explore situations that are outside the syllabus. Instead of asking, "What is the envelope of the flight simulator?” the question should be rephrased to "What is my specific training objective and can the flight simulator support it?” Often a simple approach in flight simulators yields good results if not better.

(Pouliot, Gosselin *et al.* 1988) conducted an experiment and their results show that in most cases, a 3-DOF simulator is capable of producing motion simulation quality comparable to that produced by a 6-DOF simulator. Implementing a complex model may seem beneficial but shortcomings such as the lack of repeatability may prevail over the benefits of a sophisticated model since the degree of the effect is dependent upon the profile flown by the pilot. However, simple models may not allow more sophisticated simulation training or exploration of other more dangerous manoeuvres. It may also not expose some fundamental flaws of aircraft manufacturing or current procedures.

Modelling must be the best achievable if the aircraft systems and procedures were to be questioned with any confidence. In addition, low quality flight simulators may produce negative transfer of training. Most flight simulator users are unaware of the implementation and modelling techniques, and are therefore uninformed of the limitations and short falls. These issues require flight simulator users to be educated by the industry (Stephens and Seymour 1999).

Pilots have reported that flight simulators are typically harder to fly than the real aircraft that they represent. Some of the difficulties in simulated flying are the limited field of view, scene distortion, absence of depth perception, attenuation or absence of motion cues, and response delays that are inconsistent with visual, motion and instruments (Katz 1991). For example, a curve vision is better for flight simulation as in a screen that wraps around the simulator cockpit since it will provide the pilot the same type of view available during flight (Mattoon 1996). Modelling requirements also affect flight simulation and have been dictated by computing equipment limitations. Some of these issues and concerns are discussed by (Barnes 1994).

Technology has always been driving the development of FFS. Despite having discussed some of the flight simulators' shortfalls and limitations, FFS have become very sophisticated and significant achievements have resulted in the highest approved category of simulators that allows zero flight time for training pilots converting to a new aircraft type – the level D FFS. With the high level of maturity in FFS, training requirements should be driving further development of training and simulation. From a training point of view, raises the following question "What is effective and efficient training?" An attempt to answering this question would entail establishing the training needs, what should be trained and how should training be carried out? According to (Teunissen 1999) "effective training" is to ensure that all

training objectives are met and " efficient training" is training in the shortest possible time at the lowest cost while meeting all training objectives with the least chance of failure.

2.2.2 Skills Transfer

The use of a virtual environment has potential for training of complex and real-world tasks. However, there will be considerable danger if ineffective research methodologies are being used in flight simulation research and this will result in failure to resolve crucial issues for the same reasons. Designing virtual training is more than just an engineering problem; it is also on effective transfer of training of virtual environments or any other form of real-time simulations. Contrary to intuition, students who performed well in a flight simulator do not necessary perform well in real life situation. Studies on skills transfer have been conducted where poor transfer performance is associated with good training performance. There is no evidence to support that the much desired properties of high fidelity and sense of psychological immersion do anything to enhance training effectiveness of simulations or virtual environments (Reardon, Oliver *et al.* 1987; Lintern, Roscoe *et al.* 1990; Lintern 1991; Lintern).

Skill transfer occurs when an individual is able to perform a task easier as a result of having previously practised a different task. Identification of the elements that support transfer and development of instructional strategies that selectively enhance a trainee's skill with those elements could contribute substantially to the design principles of training devices. (Gopher, Weil *et al.* 1992) conducted a study on the transfer of skill from a computer trainer to actual flight and found that those trained with a computer game as part of their training performed better and have higher final percentage of graduation than those who did not. Hence, computer based training has proven to be valid but there remain questions as to what skills are exactly being transferred and how. The success in using a flight simulator for training purposes for example has led the Israeli air force personnel to incorporate the computer game into their regular training program.

(Lintern, Roscoe *et al.* 1990) conducted a quasi transfer experiment using augmented visual feedback that used 8 pairs of "F-poles" to define the boundary of the desired path to the runway landing point and an automatic adaptive flight path predictor symbol as guidance to indicate the azimuth and elevation directions. A quasi transfer experiment is one that is trained with different simulator configurations then followed by testing on a criterion

simulator configuration. Their experiments show that the quasi transfer landing experiment yielded good results if a moderately detailed pictorial airport scene was used in early training and the overall quasi transfer experiments demonstrated a relationship between training in a research simulator and the performance in an aircraft. Their results show that students who received landing practice in a simulator performed better than those without. This represented a potential savings of 1.5 pre solo flight hours per student, which translates to an effectiveness ratio of 0.75.

Contrary to intuition, in an experimental study carried out by (Lintern 1992), a transfer of training to crosswind conditions was found to be better following training without crosswind than following training with crosswind. This type of result shows that there is a need for theoretical conception of skill transfer that does not rely on the notion of fidelity. (Oldaker 1996) pointed out the importance of how pilot training should be carried out and how accident prevention is being approached from the wrong direction - that is by regulating what pilots should or should not do rather than training them to deal with the situation effectively.

A common response from commercial airline pilots to the question, "How would you land an aircraft should you suffer an engine failure during flight?" is to land straight ahead from the aircraft's current heading position. This well ingrained procedure is a very common technique taught by flight instructors, which the FAA has recommended for such situations. However, not all geographical scenarios allow a straight ahead landing such as a well-developed urban area that lies ahead of the engine failure point. How different would the training have been if there were suitable landing fields on the right or left or even behind the engine failure point? It is important that student pilots are trained effectively because certain piloting habits are hard to change once they are developed in the early stages of the student pilot training program.

(Mason and Eichner 1996) carried out a series of tests on training methods and their results show that subjects preferred flight simulator training over a lecture styled format. Although flight simulators are capable of replicating scenarios, there are no guidelines or curricula that can increase the awareness of aeromedical issues. Their experimental results show that their simulator-based curriculum was assessed to be 250% - 350% higher than the existing conventional training. Some of the improvements identified in their experiment include improvement in cognitive domain from comprehension to evaluation, improvement in

psychomotor domain from set to origination and improvement in affective domain from responding to characterization.

(Adams 1979) discussed some issues on the evaluation of training devices such as flight simulators for aircrew training. This is an important issue since millions are spent on flight simulators and evaluations are not tested against criteria that prevail in systems engineering. He presented arguments that both the transfer of training experiment, where competence in the aircraft is required as evidence of a simulator's training value, and the rating methods (Cooper and Harper 1969; Gerlach, Bray *et al.* 1975) of evaluating the merits of a simulator are flawed.

2.2.3 Artefacts – Delay in Modelling

Despite the advancement of technology, a flight simulator cannot perfectly replicate a flying environment. The simulation fidelity of flight simulators is dependent on the accuracy of the aircraft model and the update rate of the model dynamics. At present, the flight simulation industry is still trying to understand and overcome the effect that delay has on the transfer of training. Transport delay is the time between the input to and output from a flight simulator that is not due to the aircraft dynamics. This inherent problem, which destabilizes the system in flight simulation, is inevitable since a finite amount of time is required by the hardware and software to recreate the virtual environment. Typically, hardware transport delay is the largest contributor to the overall transport delay.

The effects of delay on flight simulators can be generalized to either control degradation or simulator sickness. Experiments on simulating demanding tasks have shown that time delays can significantly degrade the flying qualities. Time delays, which are often associated with the control systems time delay, has profound effects on the longitudinal and the lateral flying qualities for precision fighter manoeuvring tasks since the allowable time delay and the rate of flying qualities degradation with time delay are function of the level of task precision, the pilot's technique and the subsequent pilot's response (Smith and Sarrafian 1986). "High stress" tasks will expose some of the flying qualities problems related to time delay, therefore, flying qualities evaluation criteria should include time delay (Smith and Bailey 1982). As mentioned by (Levison and Papazian 1987) delays have a greater effect on simulating high-performance fighter aircraft than for simulating heavy transport aircraft that are used for less demanding tasks.

(Hess 1984) carried out an experiment and an analytical pilot modelling study to investigate the effect time delay has in manual control systems. He studied the effects time delay has on the human-operator controlled-element transfer function and its performance scores. His results show that for a variety of controlled elements, time delay can cause significant regression in pilot-vehicle crossover frequencies and significant pilot lead generation. He concluded that there is a definite link between system time delay and pilot workload since pilot lead generation has been shown to contribute directly to pilot workload. (Gum and Martin 1987) conducted a research on how time delay manifests itself into the flight simulator in both the time domain and frequency domain. They also investigated the effect integration methods have on delay and suggested various compensation techniques that can help to reduce time delays. (Riccio, Cress *et al.* 1987) conducted an experiment on the effect delays have on performance, control behaviour and transfer of training in simulated aircraft with different dynamic responses using persons with no experience with flight control tasks. Their results show that delay has a greater effect on the transfer of training for aircraft with sluggish dynamics and it also contributed to pilot-induced oscillations.

(Horowitz 1987) carried out an experiment on transport delay and the effects they have on the training effectiveness of simulation. He found that transport delay has essentially stayed constant even with the increase in sophistication in simulators, which correspond to an increase in computational complexity since they are being compensated by an increase in computing speed. However, the effects delays have on training effectiveness are not constant due to the complexity of how computers are networked together. The average delay in his experiment was 148 ms and comments from pilots were that it did not fly like the real thing although all tasks could be accomplished without much difficulty.

(Ricard and Harris 1980)'s experiment show that the flying performance is tolerable up to a maximum delay of 141 ms while (Middendorf and Fiorita 1991)'s simulation experiment reported that their subjects cannot clearly distinguish delays between 90 ms and 200 ms but the effects of a high delay of 300 ms can always be experienced along with an associated increase in workload. (Bailey, Knotts *et al.* 1987) conducted a study on the effects time delay has on manual flight control and on flying qualities. Their findings show that as the time delay increases, the aircraft has the tendency to overshoot and oscillations became evident leading to pilot induced oscillations. A time delay of up to 150 ms was found to be tolerable in their simulation experiment. Transport delay is also known to affect landing manoeuvres

and formation flying (Berry, Powers *et al.* 1982). In a sidestep landing manoeuvre experiment carried out by (Whiteley and Lusk 1990), a delay of up to 200 ms was found to be acceptable but a delay of 300 ms caused difficulty for pilots to align their aircraft to the runway.

Visual and motion system delays are deleterious and detrimental to both an individual's control performance and well-being but visual delay is far more disruptive to a simulator operator's performance and physical comfort than is motion delay (Conklin 1957; Bakker 1982; Frank, Casali *et al.* 1988; Merriken, Johnson *et al.* 1988; Dumas and Klee 1996). An extensive list of references on the effects of delay was reviewed by (Ricard 1994) and delays ranging from 100 ms to 200 ms from CGIs have been known to have an effect on the control behaviour of pilots in flight simulators.

Data transmission over long distances introduces data latency that can introduce artefacts in the simulation. In a networked pursuer-evader simulation, delay in an aircraft's simulated flight path can cause the attacking pilot to change tactics in order to improve positioning, hence, affecting flying strategy in a real life situation. Analysis of delays from networked flight simulators carried out by (Menhaj and Hagan 1994) revealed that intra-simulator delay is a significant problem for flight task simulations such as air-to-air-combat, formation flight, air-to-air-refuelling, and target hand-off. A delay of 250 ms was found to be acceptable with little degradation in a networked simulation of two-aircraft air-to-air combat simulation, (Malone, Horowitz *et al.* 1987). A delay of up to 300 ms was found to be tolerable by the defender, in an investigation on the effect delay has on dome-to-dome simulation link for different air combat manoeuvring with emphasis on scoring, guns and missiles (Johns 1988).

Time delay affects the transfer of training in a simulator and some compensation methods for reducing time delay in flight simulations have been suggested by (Gum and Albery 1977; Merriken, Johnson *et al.* 1988; Howe 1990; Smith 1992; Lampton, Kolasinski *et al.* 1994; Dumas and Klee 1996; Gillespie and Handley 1996). In summary, many experiments have shown that a time delay of up to 200 ms is tolerable but the FAA's recommendation is to keep it below 150 ms (Ricard and Harris 1978; Bailey, Knotts *et al.* 1987; Katz 1991; Smith 1991; Smith 1992; Ricard 1995). The military specifications for vehicle flying qualities (MIL-F-8785C) are 100 ms, 200 ms and 250 ms for Level 1, 2 and 3 respectively (Bailey, Knotts *et al.* 1987).

2.3 Aircraft Trajectories

This section reviews some of the research conducted on aircraft trajectory optimisation during the landing phase, including the optimisation methods used in trajectory optimisation and the forced landing manoeuvres for an aircraft after engine failure that are relevant to the current study.

2.3.1 Aircraft Trajectory Optimisation

Aircraft trajectory optimisation has been the subject of many investigations. There exist many numerical optimisation methods which are suitable for solving aircraft trajectory optimisation problems. The primary goal in selecting optimisation methods is to find methods that, given a good starting point, require the least number of iterations to find the solution. However, most of the research work reviewed has been for segments of a trajectory. In general, a trajectory optimisation problem can be formulated as a collection of N phases where the independent variable, time, is used to indicate the phase k, in the region within the time interval. A set of dynamic variables is used to describe the dynamics of the system within phase k and the dynamics of the system are described by a system of equations. Solving optimisation problems involves solving the system of equations for a given initial set of conditions and terminal conditions subject to a given path constraint. The process of deriving the equations of motion, analytical solutions and the properties of optimal trajectories are available in many texts (Houghton and Brock 1960; Vinh 1981; Shevell 1989; Asselin 1997).

(Betts 1998) conducted an extensive survey on methods for trajectory optimisation and regarded his survey a daunting task, hence, decided to only focus on the direct and the indirect methods. He reviewed non-linear programming methods such as Newton's method, unconstrained optimisation and with equality constraints and inequality constraints. His review also included direct shooting, indirect shooting, multiple shooting, indirect transcription and direct transcription. Most of the research on aircraft trajectory optimisation has been on segments of a trajectory such as minimum fuel path (Ringertz 2000), minimum time path (Hedrick and Arthur E. Bryson 1971; Hedrick and Arthur E. Bryson 1972; Ringertz 2000; Jardin and Arthur E. Bryson 2001), and minimum time to climb as reviewed by (Schultz and Zagalsky 1972). Research on optimum horizontal guidance techniques and on aircraft trajectory optimisation in the horizontal plane was also carried out by (Erzberger and Lee 1971; Kishi and Pfeffer 1971; Heymann and Ben-Asher 1997). Other research on

trajectory optimisation, such as for noise abatement due to aircraft departures and landings, were conducted by (Ohta 1982; Pierson 1985; Visser and Wijnen 2001; Visser and Wijnen 2001).

(Virtanen, Ehtamo *et al.* 1997; Raivio, Virtanen *et al.* 1998; Virtanen, Ehtamo *et al.* 1999) developed, Visual Interactive Aircraft Trajectory Optimisation (VIATO), which is an aircraft trajectory optimisation software that consists of a graphical user interface, an optimisation server, and a model server. This software was developed for the Finish Air Force. It is capable of solving minimum time to climb, minimum time trajectory to a fixed or moving target on the vertical plane, 3-D interception problems and tracking problems where an aircraft is required to be as close as possible to a given reference flight path. The software represents different types of aircraft by a set of parameters, which is stored in the software library. The equations of motion and state equations as well as control constraints are fixed in advance. The dynamics of an aircraft are described by a system of differential equations that represent the state equations for the optimisation problem. The objective function is also specified. Convergence is improved by converting the original optimal control problem into a finite dimensional optimisation problem. The optimisation server discritises the trajectory optimisation problem using direct collocation or a scheme based on differential inclusions. A non-linear programming package NPSOL, an implementation of Sequential Quadratic Programming (SQP), is used to solve the finite dimensional approximation of the original optimal control problem. The model server created and used continuous smooth approximation instead of interpolation to fill the gap to aircraft parameters that were only available at discrete points in the model library.

The basic piloting tasks for an approach and landing are similar for most aircraft and these tasks can be as demanding as any other task in the complete mission of an aeroplane. They are also considered to be the most demanding task in transport aircraft operations. Numerous research activities have been performed on the landing segment of aircraft trajectory optimisation. Some of the research on aircraft landing reviewed were numerical studies on real-time generation of near-optimal trajectories for an air vehicle descent/landing on aircraft carriers (Yakimenko and Kaminer 1999), experimental investigation on how the overhead landing approach pattern should be flown for different lift to drag ratio during the approach and landing segment (Matranga and Armstrong 1959), simulation studies of low visibility approaches and landings at night (Brown 1971), and fundamental study on safe landing using the Two Phase Optimisation method (Obata 1972). A bidimensional optimal landing

problem was carried out by (Lefebvre 1998) and he presented a model for the height and the vertical velocity of an airplane to use for obtaining the value of the control that leads to an optimal landing of an airplane.

Research on effects of wind during the final approach such as optimal aircraft landing trajectories in the presence of windshear have also been carried out by (Frost and Reddy 1978; Miele, Wang *et al.* 1987; Bulirsch, Montrone *et al.* 1991; Bulirsch, Montrone *et al.* 1991; Semonov 1993; Berkmann and Pesch 1995) and optimal lateral-escape manoeuvres in a microburst wind field during final approach was carried out by (Visser 1994).

Research from soaring flights were also reviewed since forced landing after an engine failure is similar to landing a glider. The MacCready theory is a popular technique, which is used to suggest the speed to fly for soaring pilots and is used by most soaring pilots for travelling maximum distance. (Metzger and Hedrick 1975) used quadratic approximations to the polars to obtain numerical optimisation of a maximising cross-country speed with zero net altitude loss for gliders in various atmospheric vertical velocity distributions. (Arho 1972) used calculus of variations to numerically solve for the optimal speed for a particular case of a straight dolphin soaring with a sinusoidal atmospheric vertical velocity distribution. (Gedeon 1972) carried out a computer study on a dolphin style sustained thermal cross-country flight using a finite-element method. His results show that a course can be completed faster using the proper MacCready speed along with some pull up manoeuvres at optimal positions. (Sheu, Chen *et al.* 1998) used the Second-Order Gradient Method (SOGM) and the Singular Perturbation Method (SPM) to solve for maximum range glide problem. Their results show that the SPM computed the results very much faster that the SOGM with a slight trade off in optimal results. (Fukada 2000) utilised risk management to access the risk in landing out using mathematics, and stochastic models of the spatial and strength distributions of thermals to obtain definite values of flight techniques. (Edwards 1983) used a stochastic process to discuss the trade offs in increase in average speed versus the reduction in probability of arrival for soaring pilots.

Various techniques have been used to solve trajectory optimisation problems. Table 2.1 shows a brief summary of the work reviewed on the different optimisation methods used to solve aircraft trajectories optimisation.

Table 2.1 Optimisation Methods

Method	Reference	Notes
Novel hybrid approach	(Karatas and Bullo 2001)	A novel hybrid approach to trajectory design using the best features of randomised incremental searches and collocation methods.
Parameter optimisation method	(Rader and Hull 1975)	Used the applicability of parameter optimisation method to compute the optimal aircraft trajectory for a minimum time to climb.
Direct Method	(Yakimenko 2000)	Used direct method of calculus of variations to generate near-optimal aircraft trajectories of short-term manoeuvres onboard a flying vehicle.
Direct multiple shooting method and direct collocation method	(Gath and Well 2001) (Fan, Lutze *et al.* 1995)	Used the Graphical Environment for Simulation and OPtimisation (GESOP), which includes two optimisation methods: the direct multiple shooting method PROMIS (PaRameterised Optimal Control using Multiple Shooting) and the direct collocation method TROPIC (Trajectory Optimisation by direct Collocation) to solve trajectory optimisation for spacecraft. Used GESOP, PROMIS and to solve the optimal lateral manoeuvres for an aircraft during power-on-approach-to-landing.
Sequential Quadratic Programming	(Hargaves and Paris 1987)	Used an embedded collocation scheme in conjunction with mathematical programming in a trajectory optimisation method to solve a minimum time to climb problem.
Direct Transcription Method	(Betts and Huffman 1993)	Used the direct transcription method that combines a non-linear programming algorithm with discretisation of trajectory dynamics to solve path-constrained trajectory optimisation.
Non-linear Programming	(Betts and Huffman 1992)	Presented a method for solving trajectory optimisation problem using a sparse non-linear programming algorithm
Inverse Dynamic Approach	(Lu 1993)	Used inverse dynamic approach to solve a trajectory optimisation problem for minimum fuel consumption and minimum peak dynamic pressure for an aerospace plane.
Pontryagin's minimum principle	(Seywald, Cliff *et al.* 1994)	Used Pontryagin's minimum principle to solve range optimal trajectories for an aircraft flying in the vertical plane.
Total Energy Control (TECS)	(Wu and Guo 1994)	Used Total Energy Control System (TECS) to solve the guidance technique for optimal vertical flight trajectory.
Continuous Simulated Annealing	(Lu and Khan 1994)	Developed a new global trajectory optimisation tool for nonsmooth dynamic system using a continuous simulated annealing.

In addition to the optimisation methods mentioned in Table 2.1, there exist several specific software packages for solving aerospace optimisation problems such as Non-linear Programming for Direct Optimisation Of Trajectories (NPDOT), Variational Trajectory Optimisation Tool Set (VTOTS), Program to Optimise Simulated Trajectories (POST), Recursive Integration Optimal Trajectory Solver (RIOTS), Trajectory Optimisation by Mathematical Programming (TOMP), Optimal Trajectories by Implicit Simulation (OTIS), Direct Collocation Program (DIRCOL) and OptiA as reviewed by (Virtanen, Ehtamo *et al.* 1999). The Aero-Astronautics Group of Rice University has also performed some work on the algorithms for the numerical solutions of optimal control problems and their application to the computation of optimal flight trajectories or aircraft and spacecraft (Miele 1990).

2.3.2 Forced Landing

On August 24, 2001, Air Transat flight TSC236, an Airbus A330 twin engine aircraft was on route from Toronto, Ontario, Canada to Lisbon, Portugal when a fuel starvation problem occurred at approximately 300 nm northeast of Terciera Island, Azores, Portugal while it is still 886 nm from its destination. Since the final destination distance was still too far away, the pilot had to carry out a forced landing manoeuvre and a much closer landing location had to be selected – Lajes Airport, Terceira Island. The pilot successfully flew the airplane without power, which in effect glided for approximately 17 to 18 minutes and landed with all the passengers alive while the aircraft sustained minor damage during landing.[*]

An infamous incident occur in aviation history on July 23, 1983 when Air Canada flight AC 143, a Boeing 767, twin engine aircraft was on route from Montreal to Ottawa and on to Edmonton when fuel starvation occurred and the pilot was forced to carry out a forced landing manouevre. The final destination was still far away when the pilots were forced to select another landing location that was within reach. Owing to the co-pilot's familiarity to the geographical location, he selected his former RCAF base at Gimli as the landing location, which was 12 miles from the engine failure position. Neither the pilot nor the co-pilot was trained to glide a Boeing 767 and Boeing never anticipated anyone to try and glide any of its larger passenger jets. Using his glider pilot knowledge and applying his skills in an emergency situation, the pilot successfully landed the aircraft with relatively minor damage to the airplane and none of the 61 passengers were hurt during the landing.[†]

Emergency landings such as forced landing that involves partial or complete engine failure can occur despite the reliability of present-day aeroplanes and pilots should be properly trained and prepared for such moments. A competent pilot should constantly search for suitable forced-landing locations, which is not an easy task given that many terrains are possible, and the wind direction and speed conditions may not be in favour in assisting the pilot for an emergency landing. Other factors affecting a judgment in forced landing may be due to insufficient altitude, ground obstacles and distance to a suitable airfield. The forced landing manoeuvre is mostly dependent by the wind speed and the wind direction along its chosen trajectory and failure altitude is usually the governing factor for a successful forced landing.

[*] http://www.gpiaa.gov.pt/upldocs/RF-2001%2022.ACCID.01%20AIRTRANSAT%20C-GITS.pdf
[†] http://www.wadenelson.com/gimli.html

Forced landing manoeuvres require the pilot to consider many more factors than for a normal power-assisted landing. Pilots undergo frequent checks to keep their license current and more importantly it is to refresh their emergency procedures. Air combat pilots are constantly undergoing training and exercises to prepare for emergency situations, which does not occur everyday but the skills in being able to perform emergency landings has to be present at all times. A significant amount of training is being emphasised in training for emergency situations. Hence, training on forced landing cannot be overly stated and flight simulators are very useful tools to be trained and practiced on.

The glide approach during the final approach segment to landing happens when an aeroplane is forced to land without power. (Bramson 1982) suggested that the landing techniques for glide approach differ from landing with power in that a higher approach speed of about 5 to 10 knots than that recommended be used for with power and a steeper glide path which entails a larger change in pitch angle during the round-out. The excess energy in height can be dispersed but not the reverse and more importantly it requires a higher judgment on height, direction, distance, heading and positioning. Also, there is only one speed for best glide performance – speed for best lift to drag ratio, which is usually stated in the pilot's operating handbook for the aircraft's gross weight. Any attempt to fly at a different speed will only decrease the gliding distance.

(Thom 1997) suggested some forced landing scenarios and techniques in his book entitled "The Air Pilot's Manual". He suggested that good airmanship includes being aware of the surface wind, which could be indicated by windsock, smoke, cloud shadows, the drift angle of the aeroplane or wind lanes on water. His conservative estimated gliding range in still air upon engine failure is approximately 10° below the horizon as shown in Figure 2.1. For example, at 1000 ft AGL, the range will be approximately 5671 ft or 1.07 nm.

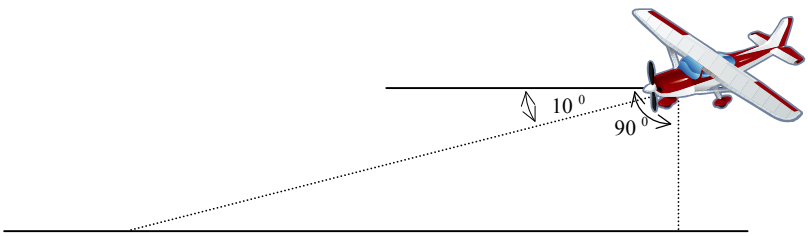

Figure 2.1 Estimated Gliding Range for a Forced Landing in no Wind condition

However, the range will be affected by the presence of different wind conditions. The effect of horizontal wind such as a headwind will reduce the gliding range while a tail wind will increase it as shown in Figure 2.2.

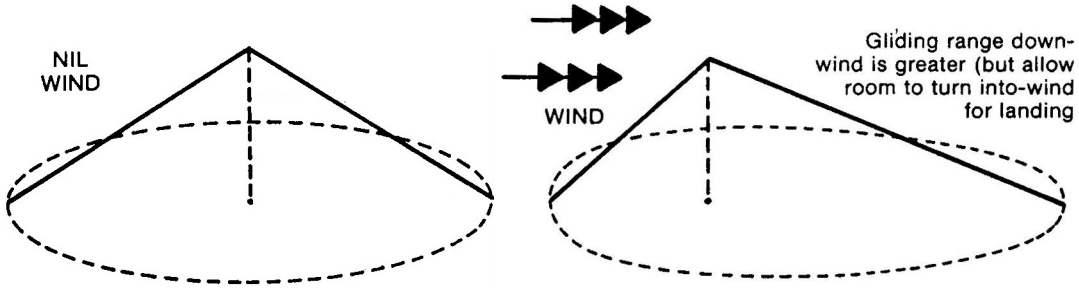

Figure 2.2 Horizontal Wind Effects on Gliding Range (after Thom 1997)

There is no one correct method but several suggested manoeuvres for planning the approach for a forced landing since different flying schools and different instructors have their preferred method. Thom described two landing manoeuvre methods for a forced landing above 3000 ft AGL. Method A is the "1000 ft AGL close base leg" technique where the pilot is to be at 1000 ft AGL close to the base leg. The engine failure's position will help decide if a left or right 1000 ft AGL base point should be selected for a long base leg and a short final leg landing. A suitable downwind leg distance is approximately 1/3 nm from the selected landing path as shown in Figure 2.3.

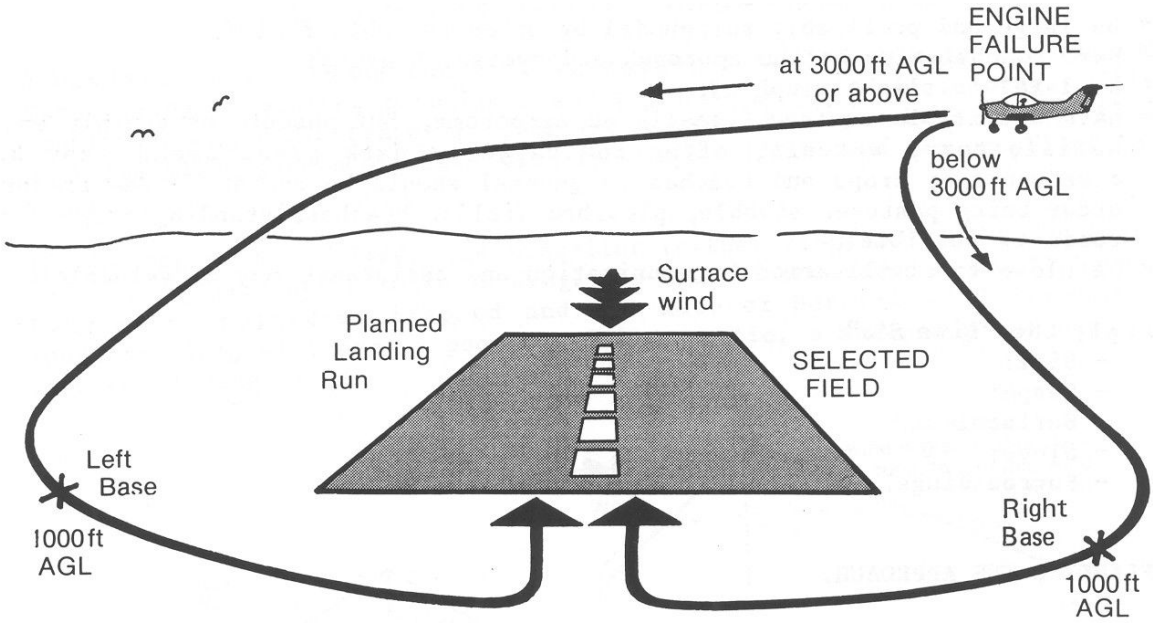

Figure 2.3 A Very Basic Circuit Plan for Forced Landing (after Thom 1997)

Method B is the “high key” and “low key” technique where the pilot descends to a “high key” of 2500 ft AGL. This position ranges from approximately 0.75 nm to 1 nm upwind from the selected landing spot and the pilot maintains the selected landing site in sight as shown in Figure 2.4(a). This procedure is then followed by the “low key” technique, which is similar to the method described in the previous method for an altitude at 1500 ft AGL. The descend to the key points should also be monitored for a long base leg and a short final leg; if the aeroplane is too high at this point, a wider path should be flown and if the aeroplane is too low, a narrower path should be flown as shown in Figure 2.4(b).

During the commencement to final approach, the advantage of flying a long base leg and a short final leg allows for correction to a successful touchdown as shown in Figure 2.5. If the aeroplane is too low, the pilot will turn earlier into the final leg and if the aeroplane is too high it can delay its turn or fly a slightly longer path during the final leg. This will also allow for the headwind or the tailwind variations during the base leg and the final leg, which will affect the touchdown point. Headwinds on the base or final leg will effectively decrease the air speed during the final leg. This will lead to undershooting the touchdown point while tailwinds will effectively increase the air speed that will lead to overshooting the touchdown point.

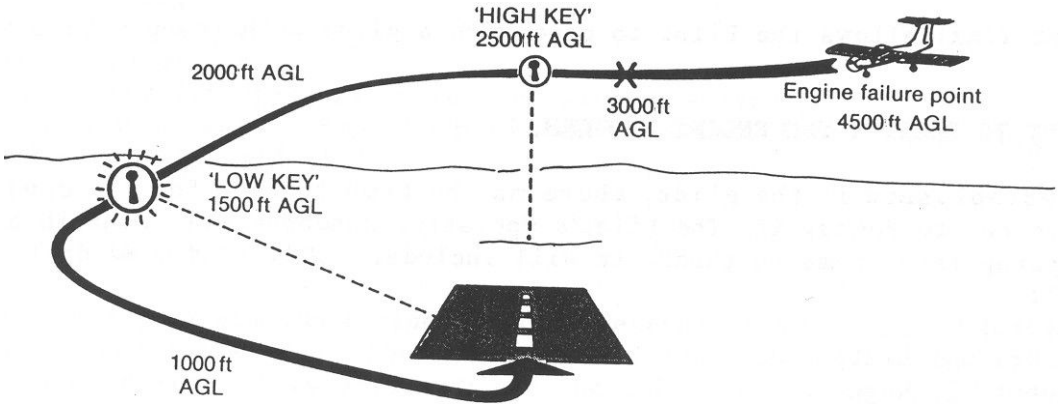

(a)

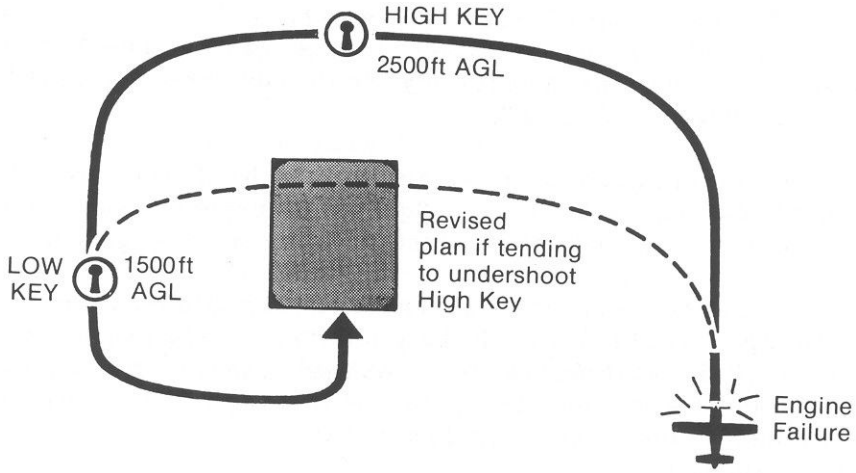

(b)

Figure 2.4 The High Key and the Low Key (after Thom 1997)

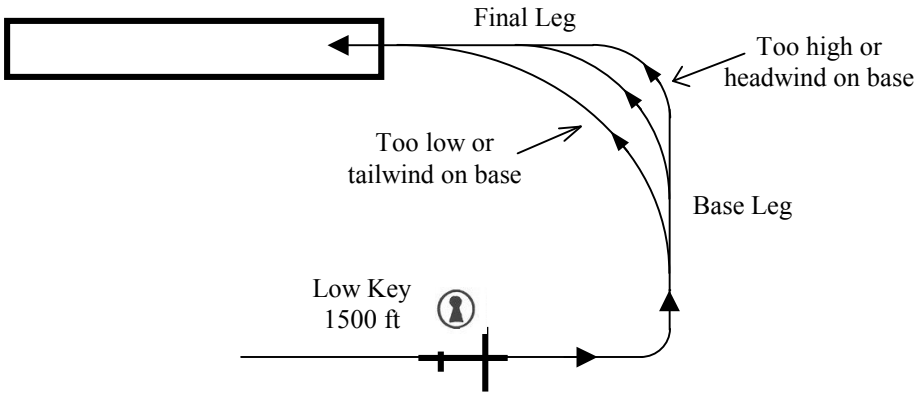

Figure 2.5 Base Leg Manoeuvre for Variational Wind on Base and Final Leg (after Thom 1997)

Another forced landing technique has been suggested by (Stewart-Smith 1999) which recommends choosing the landing spot well inside the wing tips and that the ideal forced

landing site is the site directly underneath the failure point. His method, "The Constant Aspect Approach", stresses two key points: the Initial Aiming Point (IAP) and the Sight Line Angle (SLA), are shown in Figures 2.6 and 2.7.

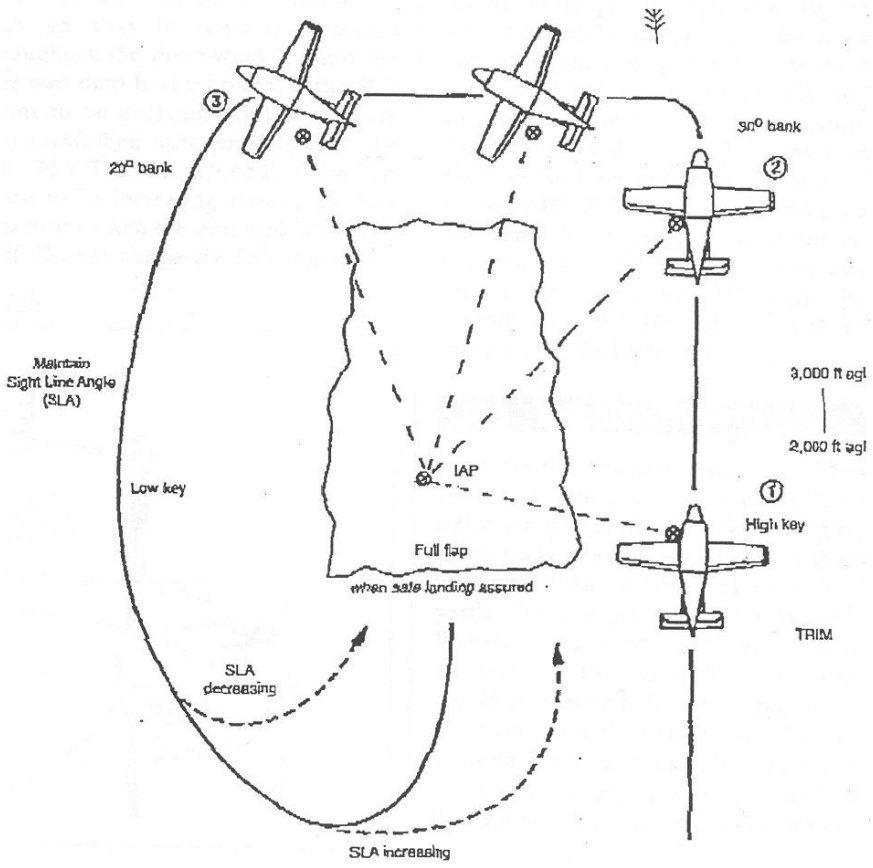

Figure 2.6 The Constant Aspect Approach (after Stewart-Smith 1999)

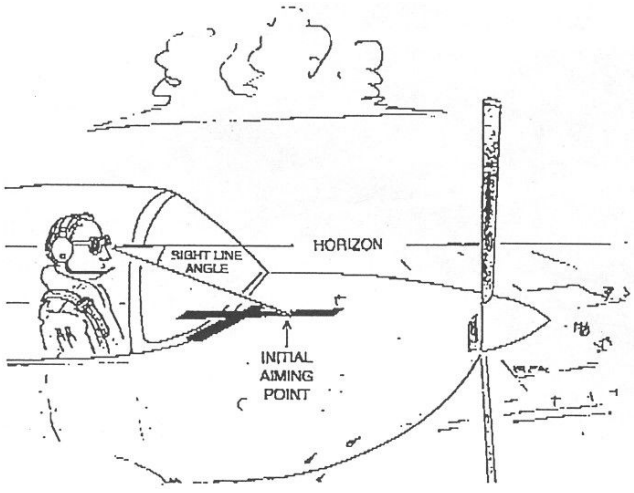

Figure 2.7 Sight Line Angle (after Stewart-smith 1999)

The IAP is the pivoting point on the downwind position, at which the aeroplane is flown for the entire forced landing pattern. It is the runway threshold plus 1/3 the runway length and

the ideal touchdown point plus 200 yards for a field landing. The SLA is the angle between the horizon and the IAP. This forced landing manoeuvre is flown around the surface of an irregular cone whose apex is at the IAP and its angle is the aircraft's gliding angle. The SLA is to be maintained constant throughout the downwind leg and the base leg before turning to the final leg. An increase in SLA indicates an overshooting of the IAP while a decrease in SLA indicates an undershooting of the IAP. The path projected on the ground will vary automatically due to wind and the rate of descent, which may be a continuous gentle curve instead of a rectangular track as recommended by traditional forced landing method.

Landing an aircraft that has suffered an engine failure just after take-off is one type of a forced landing. (Thom 1997)'s recommendation for forced landings after take-off is to first maintain the flying speed. The height at which an engine failure occurs determines the flying manoeuvre. For example, it is not recommended to return to the take-off runway when an engine failure occurs at an altitude of less 500 ft AGL, but instead, if possible select the best landing area from the area available ahead that are within ±30°, otherwise within 60° making gentle turns with maximum bank angle of 15° as shown in Figure 2.8. For an engine failure at higher altitude, different landing manoeuvres and landing trajectories may be used.

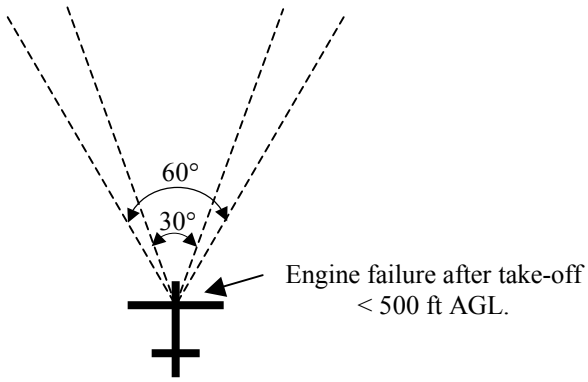

Figure 2.8 Landing Area for an Engine Failure after take-off

In the specific case of an engine failure after take-off before a suitable altitude is reached, the general recommendation in aviation literature for such a situation is to land directly ahead (Bramson 1982; Thom 1987; Stewart-Smith 1999) or slightly to either side of the take-off path as recommended by the Federal Aviation Authority (FAA) and (Thom 1997). For example, the FAA regulations recommend that pilots land straight ahead and should never attempt track reversals in an effort to land on the departure runway. This ingrained training procedure was confirmed by an experiment carried out by (Jett 1982). He found that when pilots were given this exercise, 85% of the pilots landed straight ahead after an engine failure

at 500 ft AGL. This straight-ahead landing procedure is certainly the recommended case for failures up to about 200 ft AGL. However, (Rogers 1995) suggests that, for forced landings from a higher altitude, a different manoeuvre may be flown since the higher altitude allows for more time in the air giving the pilot more options. The forced landing manoeuvre not only depends on the failure altitude but also on the ambient wind conditions such as headwinds and crosswinds, the aircraft parameters such as bank angle (ϕ), maximum lift coefficient (C_{Lmax}), wing loading (W/S), lift to drag ratio (L/D), and the surrounding terrain such as hills or valleys, open fields, buildings, bridges or other obstructions.

(Rogers 1995) conducted an analysis on track reversals for the Beech Bonanza E33A on optimum flight path following an engine failure after take-off. He compared the parameters he used in his simplified analytical model in a forced landing due to an engine failure after take-off manoeuvre analysis with (Schiff 1985)'s and (Eckalbar 1992)'s for the various climb out velocities, turn velocities, and bank angles combinations for the Beech Bonanza single engine aircraft. A table of comparison for the different forced landing parameters used by the different researchers is shown in Table 2.2. Schiff's experimental results identified an optimum bank angle of 45° and a teardrop-shaped for optimum flight path. However, he used a non-optimum velocity for maximum straight-ahead glide ratio ($V_{L/Dmax}$) in the turn and velocity for maximum rate of climb ($V_{R/Cmax}$) during climb out. Eckalbar's analytical results showed that incorrect parameters were recommended and will result in failure to land successfully on a typical departure runway of 3000 ft for this category of aeroplanes.

Table 2.2 Comparison of Parameters for Forced Landing (Rogers 1995)

Investigator	$V_{climb\ out}$	V_{turn}	ϕ	V_{glide}
Schiff	$V_{R/C\ max}$ [a]	$V_{L/D\ max}$ [b]	45°	$V_{L/D\ max}$
Eckalbar	$V_{R/C\ max}$	$\frac{1.3V_{stall(clean)}}{\sqrt{\cos\phi}}$ [d]	35°	$V_{L/D\ max}$
Rogers	$V_{\gamma\ max}$ [c, d] $V_{R/C\ max}$ [d]	$\frac{1.05V_{stall(clean)}}{\sqrt{\cos\phi}}$	45°	$V_{L/D\ max}$

[a] R/C_{max} = maximum rate of climb.
[b] L/D_{max} = maximum life to drag ratio.
[c] γ_{max} = maximum climb angle.
[d] Gear and flaps retracted.

Rogers' landing profile following an engine at failure height of 650 ft AGL after take-off is shown in Figure. 2.9. His analysis began at the brake release point, which was used as the reference distance for all distances calculated for his analysis. The pilot flew along the runway centreline at both the velocity for maximum climb angle and the velocity for maximum rate of climb to a failure height of 650 ft AGL. At this point in the forced landing manoeuvre the pilot could either land straight-ahead (gliding at maximum lift to drag velocity) or turn (at 5% above the stall velocity with a 45^0 bank angle) and glide to touchdown at the maximum lift to drag velocity. The second alternative produced a trajectory that resembled a teardrop shape. Rogers' analytical results, for the case of a teardrop landing profile, are shown in Figure. 2.10. His results show successful landing within the typical 3000 ft runway for such aeroplane type. He also carried out analyses on the effects climb velocity, bank angle, failure altitude, and wind have on the landing profile following an engine failure after take-off.

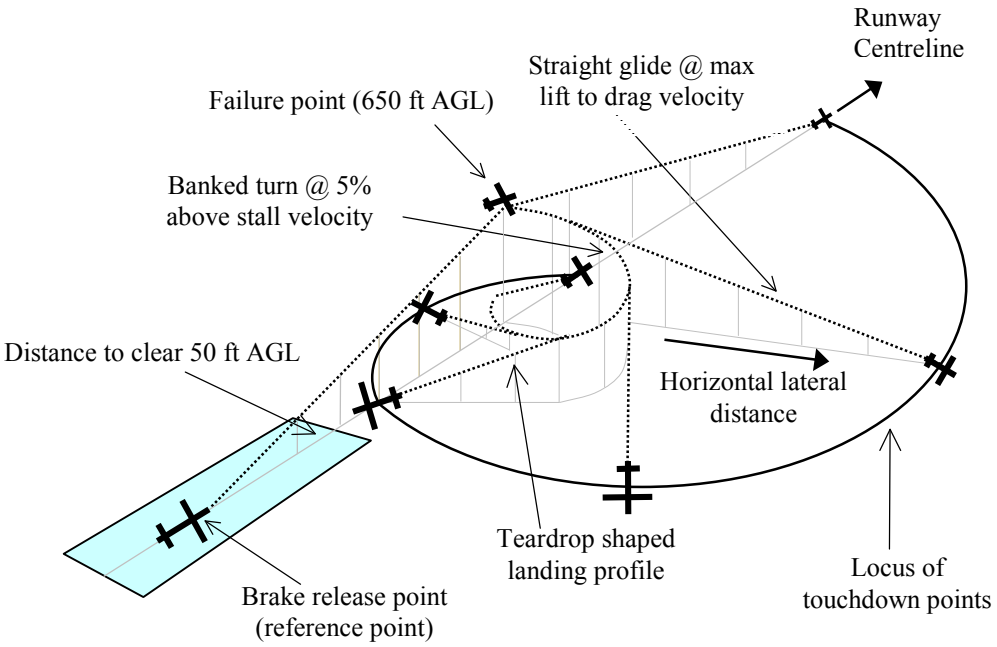

Figure 2.9 Locus of Touchdown Points

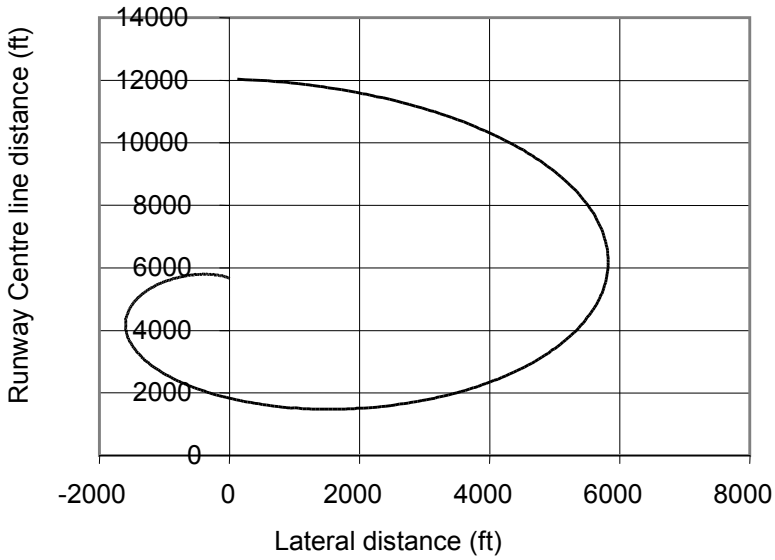

Figure 2.10 Rogers' Locus of Touchdown Points

Research on forced landings has its application in energy-preserving manoeuvres after an engine failure. One such application is on optimal trajectory control after an engine failure. Flying an optimal trajectory will allow the aircraft to land safely or if an energy-preserving manoeuvre is flown, valuable time could be gained which may allow the pilot more time to restart the aircraft even if there are no suitable landing locations. The landing manoeuvres should be simple and general for pilots to carry out the manoeuvres and should not be overly sensitive to the flying manoeuvres.

(Hoffren and Raivio 2000) carried out a numerical study on the controls and trajectories for a BAe Hawk Mk. 51 after an engine failure due to a fuel system failure, using optimisation and simulation for maximising the gliding distance into a given direction. The aircraft was assumed to be at an altitude of 3900 ft ISA with an equivalent airspeed of 460 kts, a flight path angle of –10°, and banking left at an angle of 60°. In order to turn to the nearest runway, the aircraft has to turn right 113° from the engine failure position with final conditions of an equivalent airspeed of 175 kts and a corresponding flight path of – 4.7°.

Their calculations were based on numerical time integration, standard aircraft equations of motion for a pure point-mass model and for an inertial flat earth base. Only three force equations instead of the full 6 equations were used since the primary focus is on the aircraft trajectory performance. Their objective was to find the lift coefficients and bank angles that will allow maximum gliding range along a given direction. However, due to the problems encountered in the computational factors, the problem was transformed into a multi-objective optimization problem where the first objective is to maximize the glide range and the second

objective is to minimize the final time. Since the objective functions are conflicting, Pareto-optimal solutions were used where sets of solutions were found without necessarily worsening the other one. The flight path consisted of three segments: (1) initial transient where velocity was traded for altitude until a velocity and flight path corresponding to the best glide ratio was attained, (2) steady-state glide at optimal speed and (3) final transient to guide the aircraft to landing. The last segment was disregarded since it was assumed that the gliding distance was lengthy. In all of their calculations the engine failure point was used as the reference point and the glide range was the sum of the transient distance and the steady-state glide distance. Their results show that many of the solutions (paths) gave the same performance index, i.e. the solutions are insensitive to the solution trajectory in the neighbourhood of the optimal solution space. Their numerical solution was solved with the direct transcription approach (Hargaves and Paris 1987) and the Sequential Quadratic Programming (SQP) algorithm in the NPSOL software package (Raivio, Ehtamo *et al.* 1996).

Hoffren and Raivio's initial calculated results for the optimal flight path showed some inaccuracies during the initial attitude transients in the optimal solution. This was because a simple flight-mechanical point mass model was used. In addition, the manoeuvre for the initial calculated flight path was very difficult for a pilot to fly in an emergency situation. Hence, an easier flying manoeuvre was required. Further calculations revealed that the trajectories were not very sensitive to the details of the control or to the modelling of the attitude transients for such a manoeuvre. Their calculations for a simplified, approximate optimal flight path were computed. The outcome was a climbing turn at a constant angle of attack of 4.3° with a constant bank angle of 53° until the desired heading was reached at a climb angle of 41°, followed by a constant load factor of 0.2 until the glide phase. Thus, only two manoeuvres were required to head toward the desired landing location and this reduced the pilot's workload significantly. Sensitivity on the performance and control strategy on suboptimal controls were also carried out to demonstrate the importance of efficient manoeuvring after a high-speed engine failure. Their results verified that the optimal solution was not overly sensitive to the modelling of a simple flight-mechanical point mass model or to the details of the control application.

They also conducted tests on the effects initial heading, airspeed, altitude and weight have on the optimal manoeuvre and found the following results. The effect of initial heading is the strong dependence of the required bank angle on the initial heading and the initial speed. An

increasing initial heading error will cause an increase in load factor and in maximum glide path angles. The effects of initial equivalent airspeed are large for the optimal controls and the related trajectories. The effects of initial altitude is on the elongation of time scales but is benign compared to the effect initial speed or initial heading has on the flight path and the overall shapes do not change significantly. The effects of initial weight are on the flight path, the bank angles, the time to complete the manoeuvre and most significantly on the horizontal distance.

They concluded that a simple point mass model is adequately realistic for such study on forced landing after an engine failure and the optimal trajectories were not overly sensitive to the control details or weight. The optimal controls were case dependent with initial heading and airspeed being the strongest factors and speed has the greatest effect on the achievable trajectories. It appears not possible to devise an optimal control strategy for pilots to fly following an engine failure since the flight path parameters are strongly affected by the initial conditions and variations in time.

2.4 Concluding Remarks

This chapter presents a review on the importance of flight simulation development along with some of its inherent problem such as transport delay and visual delay, and how it affects the transfer of training. Despite some of the issues associated in using flight simulators to train pilots, the present day flight simulators have become very sophisticated and have achieved the highest approved category of simulation that allows zero flight time for aeroplane type conversion.

A general review on trajectory optimisation was also presented along with a more specific review on forced landings after an engine failure for both after take-off and at mid-flight. The different forced landing manoeuvres reviewed were situation dependent and the effects of atmospheric turbulence were not considered.

The research reviewed is used in the present study to assist in flight simulator development and in the better use of the flight simulators for forced landing training. One of the objectives in this study is to investigate if there exist a general optimal forced landing manoeuvre after an engine failure or if there exist a simple forced landing manoeuvre for pilots to fly.

CHAPTER 3

AIRCRAFT DYNAMICS MODEL & ATMOSPHERIC TURBULENCE MODELS

3.1 Introduction

This chapter presents a simplified mathematical model for a general-aviation aircraft model and for two atmospheric turbulence models used in this research. Although there are many atmospheric models available to study the effect of low frequency vertical turbulence on the aircraft trajectory, they are either inconvenient or not easily adaptable for used in the present study because of their complexities in integrating the atmospheric model into a simple aircraft model. Research on forced landings using point mass model have been used by (Hoffren and Raivio 2000; Brinkman and Visser 2007) to obtain acceptable results. Therefore, two approximated vertical atmospheric turbulence models were applied to a simple point mass aircraft model to study the effects on forced landing trajectories. The atmospheric disturbances were vectorially added to the aircraft's point mass model. Thus, simplifying mathematical modelling calculations.

3.2 Aircraft Model

The mathematical model for a general-aviation aircraft comprises of two principal components: the force model and the kinematic model. For this research, it is assumed that the moments about the center-of-mass (CM) are zero (trimmed condition) and that the flight is quasi-steady. Since the objective of this research is on the forced landing trajectory such simplifications and assumptions will not have a major effect on the accuracy of the overall results. Furthermore, a point-mass model is assumed and as a result, Newton's second law governs the equations of motion of the aircraft. A mass and the relation between the lift and drag are sufficient to describe the aircraft motions since a simple model is used in this analysis and the flight path is the direction of motion. Therefore, only the force model is used as shown in Figure 3.1.

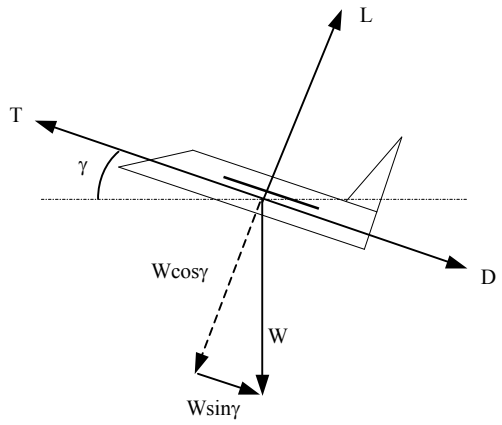

Figure 3.1 Forces on Aircraft in Level Flight

The equations of motion are obtained by applying Newton's second Law along the flight path:

$$T - D - W\sin\gamma = m\frac{dV}{dt} \qquad \text{Eqn. 1}$$

and perpendicular to the flight path:

$$L - W\cos\gamma = -mV\frac{d\gamma}{dt} \qquad \text{Eqn. 2}$$

These forces are expressed with respect to an axis system that is fixed to the aircraft with its origin at the aircraft's CM. This axis system is referred to as the aircraft body coordinate (ABC) frame and the aircraft body coordinates are aligned with x forward, y to the right and z down as shown in Figure 3.2.

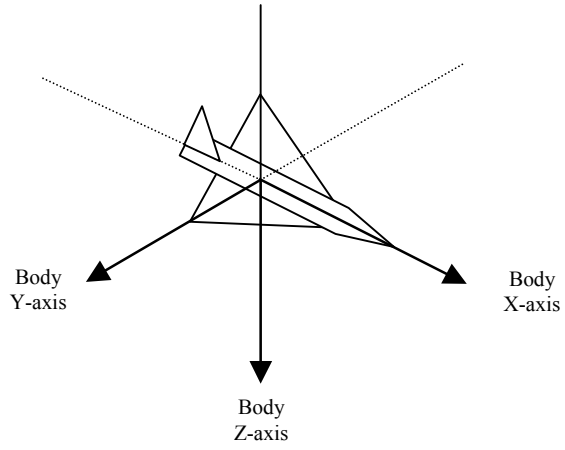

Figure 3.2 Aircraft Body Axes

It is assumed that the Earth's surface is flat and serves as an inertial reference point and navigation is only required over a small distance. Consequently, the inertia coordinate system is fixed to the Earth with the origin at or near sea level. The x-axis points in the longitudinal direction on the plane of symmetry while the y-axis points in the lateral direction forming the horizontal plane, and the z axis is directed or points down. This orthogonal axis system is assigned to the three directions North, East, and Down (NED) and the gravitational force is assumed to be acting down.

The force model is used to develop the general equations of motion for an aircraft in a steady, coordinated turn with bank (ϕ) and sideslip (β) in a turning flight as shown in Figure 3.3.

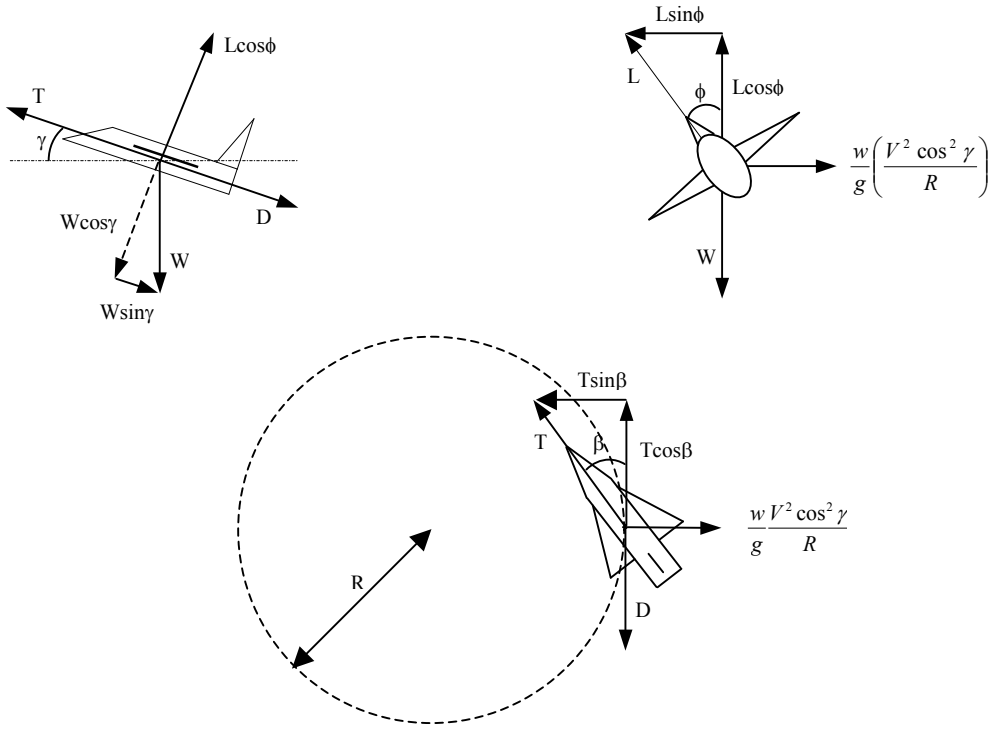

Figure 3.3 Forces on Aircraft During Turn

The governing equations along the flight path are:

$$T\cos\beta - D - W\sin\gamma = 0 \qquad \text{Eqn. 3}$$

along the normal is:

$$L\cos\phi - W\cos\gamma = 0 \qquad \text{Eqn. 4}$$

and along the binormal is:

$$T\sin\beta + L\sin\phi - \left(\frac{WV^2\cos^2\gamma}{gR}\right) = 0 \qquad \text{Eqn. 5}$$

while the kinematics equations are:

$$\frac{dx}{dt} = V\cos\gamma\cos\chi \qquad \text{Eqn. 6}$$

$$\frac{dy}{dt} = V\cos\gamma\sin\chi \qquad \text{Eqn. 7}$$

$$\frac{dh}{dt} = V\sin\gamma \qquad \text{Eqn. 8}$$

The area of interest in this research is on forced landing after an engine failure (T=0) with a coordinated turn, i.e. no sideslip (β=0), a heading angle (χ=0) which coincides with the airplane's fuselage and the effects of windmilling, are assumed to be zero. However, if a more accurate model is required for further research, the windmilling drag can be incorporated in the overall aircraft drag coefficient. Also, the dynamic response of the airplane is not being examined and in other words the airplane will always simply be carried by the wind. Therefore, the above set of governing equations can be reduced to the following.

Along the flight path:

$$D = W\sin\gamma \qquad \text{Eqn. 9}$$

along the normal:

$$L\cos\phi = W\cos\gamma \qquad \text{Eqn. 10}$$

along the binormal:

$$L\sin\phi = \left(\frac{WV^2\cos^2\gamma}{gR}\right) \qquad \text{Eqn. 11}$$

Other useful flight parameters that are used in the analytical model can be obtained by simultaneously solving Equations 6 – 10:

Load factor (n)

$$n = \frac{\cos\gamma}{\cos\phi} \qquad \text{Eqn. 12}$$

Velocity (V)

$$V = \sqrt{\frac{2nW}{\rho S C_L}} \qquad \text{Eqn. 13}$$

Radius (R)

$$R = \frac{V^2\cos\gamma}{g\tan\phi} \qquad \text{Eqn. 14}$$

Bank angle (ϕ)

$$\tan\phi = \frac{V^2\cos\gamma}{Rg} \qquad \text{Eqn. 15}$$

Glide angle (γ) $$\tan\gamma = \frac{D}{L\cos\phi}$$ Eqn. 16

Rate of turn (ω) $$\omega = \frac{V\cos\gamma}{R} = g\frac{\tan\phi}{V}$$ Eqn. 17

Height lost during turn: $$\Delta h = V\sin\gamma\Delta t = V\sin\gamma\frac{\theta}{\omega}$$ Eqn. 18

Since this is a low subsonic aircraft, the drag polar can be approximated by:

$$C_D = C_{Do} + kC_L^{\ 2}$$ Eqn. 19

and the lift coefficient is: $$\boldsymbol{C_L = \frac{L}{\frac{1}{2}\rho V^2 S}}$$ Eqn. 20

where lift is equal to weight.

The glide angle during a turn can be determined by solving equations 12, 16, 19 and 20 simultaneously which results in the quadratic equation:

$$\sin^2\gamma\left[\frac{2kW}{\rho SV^2\cos^2\phi W}\right] + \sin\gamma[1] - \left[\frac{C_{Do}\rho^2 S^2 V^4\cos^2\phi + 4kW^2}{2\rho SV^2\cos^2\phi W}\right] = 0$$ Eqn. 21

As can be seen from the above equation, the glide angle during banking is also a function of the turn velocity. Hence, a change in the turn velocity will have a major effect on the parameters used in determining the forced landing trajectory.

The calculations performed in this study were based on the Beech Bonanza Model E33A as shown in Table 3.1 and it is the same aircraft used in Rogers' forced landing analysis as reviewed in Chapter 2.3.2. The data for initial takeoff ground roll and distance to clear a 50 ft obstacle are obtained from Rising Up Aviation Resources‡

‡ Data available online at http://www.risingup.com/planespecs/info/airplane117.shtml

Table 3.1 Beech Bonanza Model E33A characteristics (Rogers 1995)

Parameter	Value
Gross Weight, lb	3300
Wing Area, ft^2	181
L/D_{max}	10.56
Power, brake horsepower	285
Propeller	Constant speed-3 blade
V_{max}, mph	208
V_{cruise} at 65%, mph	190
$V_{stall(clean)}$ [a] power off, mph	72
$V_{stall(dirty)}$ power off, mph	61
$V_{L/Dmax}$ [b], mph	122
$V_{\gamma max}$ [c] at sea level, mph	91
$V_{R/Cmax}$ [d] at sea level, mph	112.5
R/C at sea level and 3300 lb, ft/min	1200
Parabolic drag polar	$C_D = 0.019 + 0.0917C_L^2$
Takeoff: Ground roll, ft	880
Takeoff: Over 50 ft obstacle, ft	1225
Landing: Ground roll, ft	625
Landing: Over 50 ft obstacle, ft	1150

[a] Gear and flaps retracted.
[b] L/D_{max} = maximum lift to drag ratio based on the aircraft's gross weight.
[c] γ_{max} = maximum climb angle.
[d] R/C_{max} = maximum rate of climb.

3.3 Aircraft Model with Wind Disturbances

The mathematical model for a general aircraft with wind disturbances is based on the mathematical model presented in the previous section. The addition of the wind velocities is simply being vectorially added to the aircraft's airspeed. This is made possible since a point-mass model is assumed and is acceptable for a small, light aircraft. The mathematical vector addition of the random vertical wind disturbance is as shown in Figure 3.4, where the aircraft's airspeed (V) is separated into its horizontal (V_h) and vertical (V_v) components and the resultant airspeed (V_r) is assumed through vectorial addition of wind velocity (V_w). The vertical wind component is vectorially added to the aircraft's vertical airspeed component, resulting in an updated aircraft's airspeed (V_r) and glide angle (γ).

Updraft *Downdraft*

Figure 3.4 Aircraft Velocity and Vertical Wind Speed Vectors

Similarly, the constant horizontal crosswind vectors will be also be vectorially added in the form of longitudinal and lateral components relative to the aircraft's initial horizontal airspeed as shown in Figure 3.5. The vertical disturbance velocities and the horizontal crosswinds will have an overall three dimensional effect on the aircraft's ground speed.

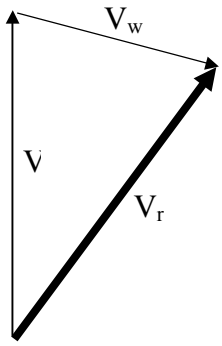

Figure 3.5 Aircraft Velocity and Crosswind Vectors

3.4 Atmospheric Turbulence Models

The use of the correct atmospheric turbulence model is of considerable importance in any aircraft simulation and in trajectory optimisation. In general, atmospheric disturbances can be catagorised into short period and long period. An example of a short period atmospheric disturbance is the turbulence that an aircraft experiences as it flies through an air pocket and thermal disturbance is an example of a long period atmospheric disturbance. Atmospheric turbulence is random by nature and so are its magnitudes and the frequencies of occurrence. They are affected, for example, by the geographical location, the weather and the time of the year. A convenient approach in choosing a suitable atmospheric model is to select the disturbance model in the order of time constant matching the aircraft's model. Since atmospheric turbulence vary widely, two models were used in this research to represent the atmospheric turbulence spectrum, the simulated thermal model and time averaging the von Karman turbulence model respectively.

The thermal turbulence model was used in this study because of its long period characteristics and landing an aircraft without power as in the case of an engine failure of a single engine gas turbine aircraft is very similar to flying a glider. Soaring pilots in particular have an interest in thermal structures since thermals provide energy to their flying and frequently use thermal distribution models to assist them in determining the best gliding speed and flying manoeuvres. In short, thermals are columns of rising air, not necessarily perfect columns of air but twisted and meander horizontally, bifurcated and merge as they rise, which are

consequences of heated air due to incoming solar energy. Thermals also depend on the irregularities of the Earth's surface such as the amount of vegetation, the ground moisture content, the ground heat flux, the terrain topology, the barometric pressure, urban development and the wind speed. Thermals typically range from 500 m to 1000 m in diameter with broad areas of sink spacing of 1 km to 2 km between thermals. They are not uniform and do not have sharp edges, and usually have warm, fairly smooth core thermals that are surrounded by turbulent edges.

Since thermal models are random in nature and are dependent on many different parameters such as the different seasons of the year and the latitude, different thermal distribution models have been developed. They are either based on experiments or on mathematical idealizations with no physical justification other than the smooth gradation of velocity with distance from the axis criteria. (Konovalov 1970) conducted an experiment on thermal distributions and identified two basic types of thermals: type "*a*" which contains several maxima with depressions in between and type "*b*" which contains one pronounced maximum. The type "*b*" resembles a triangle wave whilst type "*a*" exhibits characteristics with a much wider region of strong lift. (Johnson 1978) investigated thermal strengths between thermals in Texas and found that the inter-thermal varies from zero to more than three-tenths of the gross thermal strength. He concludes that the average apparent inter-thermal downdraft strength is roughly one-tenth of the gross thermal strength and that the average thermal height is roughly one-tenth of the thermal spacing. (Milford 1972) investigated the cross section of thermals using an instrumented glider and concluded that a more systematic study of thermals will be useful using powered gliders. (Irving 1999) presented mathematical thermal models which included the power-law velocity distribution, $V_T/V_{TO} = 1-(r/R)^n$, where V_{TO} is the vertical velocity on the axis where $r = 1$, and R is the "thermal radius" and the n index is assumed to be an integer. (Quast 1965) proposed a mathematical parabolic thermal, $V_T = ar^2 + br + c$, where a suitable set of parameters could be used to for a, b, c to describe a strong or a weak thermal, while (Gedeon 1972) proposed a modified parabolic distribution, $V_T/V_{TO} = \left[1-(r/R)^2\right]\exp\left[-(r/R)^2\right]$.

(Fukada 2000) used mathematical and stochastic models to approximate the spatial and the thermal strength of a simple thermal distribution to investigate the problem of the speed management on the risk of landing short or long. He assumed an arbitrary numerical density to a random spatial thermal distribution and the thermal strength was assumed to have a

normal distribution. The high ends of the strength were truncated based on the estimated maximum strength of the thermals for a particular day and the thermal density, which was the reciprocal of the thermal spacing, decreases uniformly with an increase in thermal strength. (Arho 1972) assumed a sinusoidal atmospheric vertical velocity distribution in his research on optimal speeds to fly on a straight dolphin soaring manoeuvre using calculus of variations. (Metzger and Hedrick 1975) modelled the vertical component of the atmospheric velocity distribution as a series of step-like velocities that consisted of constant rising speed and constant sinking speed and applied this to the problem of optimal flight paths for soaring flight with zero net altitude loss. Their vertical velocity distributions were composed of several combinations of lifting portion lengths ratios to the total length. Their horizontal atmospheric distribution velocity components were assumed constant with respect to both altitude and downrange distance and the effects of wind distributions with respect to altitude and downrange distance were not considered. (Mathar 1996) modelled the random lift intensity of a stochastic model of a thermal convection by using a discrete probability model or a continuous exponential distribution model with probability density. For a full stochastic model, the Markov jump process was used as one of the many empirical rules to model the thermal distribution, which depends on only a few parameters. (Edwards 1983) used an exponentially distributed probability density to model adjacent thermals while (Cochrane 1999) used empirical thermal models that were calibrated based on his own experience for different geographical locations in the United States to determine the MacCready flight speed.

Predicting the thermal distribution is a complex exercise. Researchers have used Synergie as a powerful integrated tool for the forecaster to interact with weather data in obtaining atmospheric conditions for gliding meteorology (Benichou and Santurette 1998) and synoptical data could be obtained from national weather services to support glider competitions (Heise 1999). There are also web links to obtain forecasting of thermal soarings and techniques to estimate thermal modelling (Wang 1997). Geographical signatures for thermal convection climatology and new approaches to climatology of thermal soaring conditions have been used by (Kindemann and Asseng 1998; Liechti and lorenzen 1998) to estimate thermal activities. Climatology of thermal soaring conditions can also be modelled based on a numerical convection model using ALPTHERM – a PC based model for atmospheric convection over a complex topography (Liechti and Neininger 1994).

As can be seen from the atmospheric model literature reviewed, various types of thermal models exist whilst there is no one type that is better than the other. For this research, thermal models consisting of thermal velocities varying from –9.84 ft/sec to +9.84 ft/sec in discrete step size of 3.28 ft/sec were used and no allowance for boundary layer or velocity gradient close to the ground were made. The "jump times" will be discussed in Section 3.5. An example of the general thermal distribution used is shown in Figure 3.6.

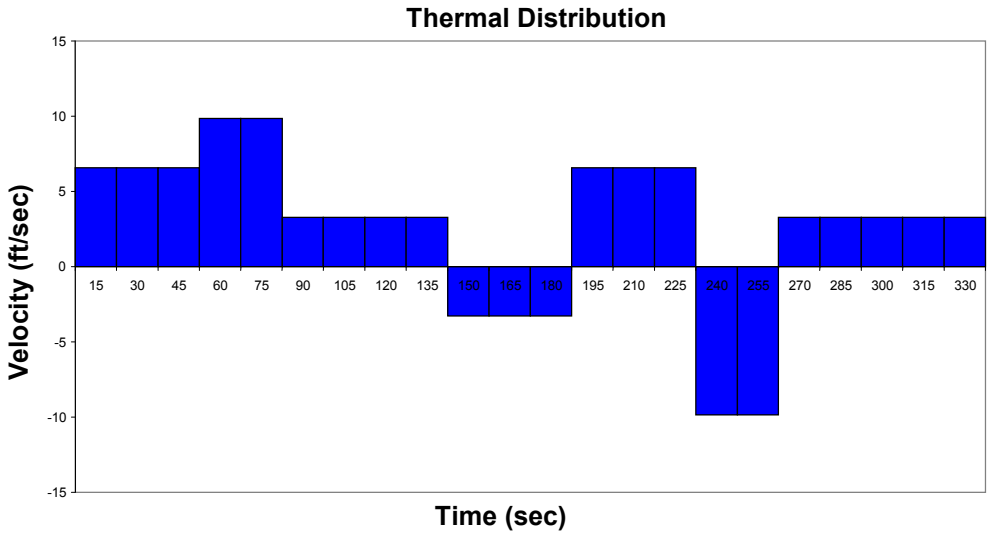

Figure 3.6 Thermal Distribution

The fluctuations in turbulence velocity on an airplane flying through atmospheric turbulence are functions of time and are therefore a stochastic or random process. Since atmospheric disturbances are short period and random in nature, one method of representing the atmospheric disturbance is to time average the atmospheric turbulence.

Studies on the turbulence atmosphere have long been carried out to better understand and to predict its behaviour. A review on atmospheric turbulence and its relevance to the design and flight of aircraft was conducted by (Houbolt 1973). His work provided insight to various phases of turbulence encounter such as atmospheric turbulence, turbulence types, mathematical modelling, turbulence measurements, aircraft design, and response analysis methods. Statistical properties were used to describe the random turbulence chaotic motion of the air. The main statistical features are the probability distributions, the correlations and spectra, homogeneity, isotropy, time, and distance scales. Turbulence is a vector process in which the velocity vector is a random function of position and time. Understanding the atmospheric turbulence behaviour is important to aircraft designers and operators. It affects the pilot's workload significantly and therefore, plays and important role in the training of

emergency procedures. It also allows them to evaluate aircraft structural loads and aircraft handling qualities. Realistic turbulence models have been shown to affect the Instrument Flight Rule (IFR) handling-quality in the presence of simulated turbulence. (Jacobson and Joshi 1978) conducted a pilot task performance test based on four basic turbulence models and their results show that the realism of a turbulence model is closely linked to the physical properties of the real atmosphere. However, the degree of physical realism needed remained a controversial issue but pilot ratings on the Cooper-Harper scale show the expected trends with increasing turbulence intensity (Etkin 1981) .

Atmospheric turbulence modelling is also of importance to flight simulation development and to trajectory optimisation. There exists a few atmospheric turbulence models; the Dryden model, the von Karman model (Anon 1980), the low-altitude turbulence model (Lappe 1966) which was later modified at Lockheed-Georgia and others (Firebaugh 1967). Of these, the Dryden model and the von Karman model are most frequently used. Improvement to the fine structure of atmospheric turbulence to the von Karman model was also suggested by (Gedeon 1996). A comparison between the Dryden and the Kolmogorov turbulence forms was performed by (McMinn 1997) where he described enhancements that added functionality to the Kolmogorov turbulence model. An algorithm for digital implementation of the von Karman model, where a potential reduction of approximately 60% in computational time was identified at the expense of a reduction of accuracy using digital filtering algorithms to the Dryden model was proposed by (Beal 1993).

The von Karman low altitude model and the medium altitude model for atmospheric turbulence model based on the MIL-F-8785C specifications were used to simulate the atmospheric turbulence model (Anon 1980). Since this study investigated the landing segment of a forced landing flight manoeuvre, the aircraft was considered as being in a terminal (Category C) flight. The low altitude model, for height between ground level and 2000 ft AGL, assumed homogenous turbulence characteristics in the longitudinal and the lateral directions but changed rapidly in vertical direction. Thus, the disturbances are function of height for the low altitude model. A reference mean wind speed, U_{20}, is assumed to exist at 20 ft AGL for different atmospheric turbulence intensities. A typical wind speed for “light” turbulence is 15 kts, for “moderate” turbulence is 30 kts and for “severe” turbulence is 45 kts. The medium altitude model, for height above 2000 ft AGL assumed isotropic and homogeneous turbulence and can be considered frozen pattern in space.

In this research, only the vertical component was considered since one of the aims is to study the effect vertical atmospheric turbulence has on a forced landing manoeuvre. The von Karman form for the spectra for vertical atmospheric turbulence velocity is:

$$\Phi_{w_g}(\Omega) = \sigma^2{}_w \frac{L_w}{\pi} \frac{1+\frac{8}{3}(1.339L_w\Omega)^2}{[1+(1.339L_w\Omega)^2]^{11/6}} \qquad \text{Eqn. 21}$$

For the low altitude model, the turbulence intensities in the wind axes, σ_w, is $0.1U_{20}$ and the turbulence scale length in wind axes are:

$$\begin{aligned} L_w &= 10\,ft && for \quad h \le 10\,ft \\ &= h\ ft && for \quad 10\,ft < h < 1000\,ft \\ &= 1000\,ft && for \quad 1000\,ft \le h \end{aligned}$$

The medium altitude model, for height above 2000 ft AGL, is assumed to be isotropic where the turbulence scale length, L_w, is 2500 ft and σ_w was obtained from (Anon 1980, pg. 49). The atmospheric turbulence velocity for this research was calculated using (Newman and Wong 1993)'s approximated transfer function from the von Karman spectrum through a rational polynomial approximation using the frequency domain relation between the power spectral densities and the transfer function:

$$|T_g(i\omega)|^2 = \Phi_g(\omega) \qquad \text{Eqn. 22}$$

and related the spatial and the temporal frequencies through the aircraft's true airspeed as:

$$\Omega = \frac{\omega}{V_T} \qquad \text{Eqn. 23}$$

The approximated vertical transfer function is:

$$T_{wg}(s) = \sigma_w \sqrt{\frac{L_w}{\pi}} \frac{2.619\left(\frac{L_w}{V_T}\right)^2 s^2 + 37.63\left(\frac{L_w}{V_T}\right)s + 12.64}{\left(\frac{L_w}{V_T}\right)^3 + 24.22\left(\frac{L_w}{V_T}\right)^2 s^2 + 40.88\left(\frac{L_w}{V_T}\right)s + 12.64} \qquad \text{Eqn. 24}$$

The rational transfer function was converted to time domain gust velocity where a Gaussian random number with zero mean, unit variance input was used to generate a time-varying gust velocity. The time domain the vertical gust is:

$$\begin{bmatrix} \dot{X}_{w_1} \\ \dot{X}_{w_2} \\ \dot{X}_{w_3} \end{bmatrix} = \begin{bmatrix} -24.22\left(\frac{V_T}{L_w}\right) & -40.88\left(\frac{V_T}{L_w}\right)^2 & -12.64\left(\frac{V_T}{L_w}\right)^3 \\ 1 & 0 & 0 \\ 0 & 1 & 0 \end{bmatrix} \begin{bmatrix} X_{w_1} \\ X_{w_2} \\ X_{w_3} \end{bmatrix} + \begin{bmatrix} \sigma_v \sqrt{\frac{L_v}{\pi}} \\ 0 \\ 0 \end{bmatrix} \begin{bmatrix} W_{ran_{vw}} \end{bmatrix} \quad \text{Eqn. 25}$$

$$\begin{bmatrix} W_g \end{bmatrix} = \begin{bmatrix} 2.619\left(\frac{V_T}{L_w}\right) & 37.63\left(\frac{V_T}{L_w}\right)^2 & 12.64\left(\frac{V_T}{L_w}\right)^3 \end{bmatrix} \begin{bmatrix} x_{w_1} \\ x_{w_2} \\ x_{w_3} \end{bmatrix} \quad \text{Eqn. 26}$$

Figure 3.7 shows a sample of the vertical atmospheric turbulence profile. These profiles were incorporated into the aircraft force model where Genetic Algorithm and Sequential Quadratic Programming were used to search for the optimal landing trajectories. The vertical turbulence velocity terms were vectorially added to the aircraft's velocity and were assumed to have an instantaneous change to the aircraft's vertical velocity. The aircraft was also assumed to be flying through a one-dimensional gust field where only the vertical velocity changed and it was assumed that the turbulence encountered was independent of time. In other words, the turbulence profile was frozen or fixed in space and time.

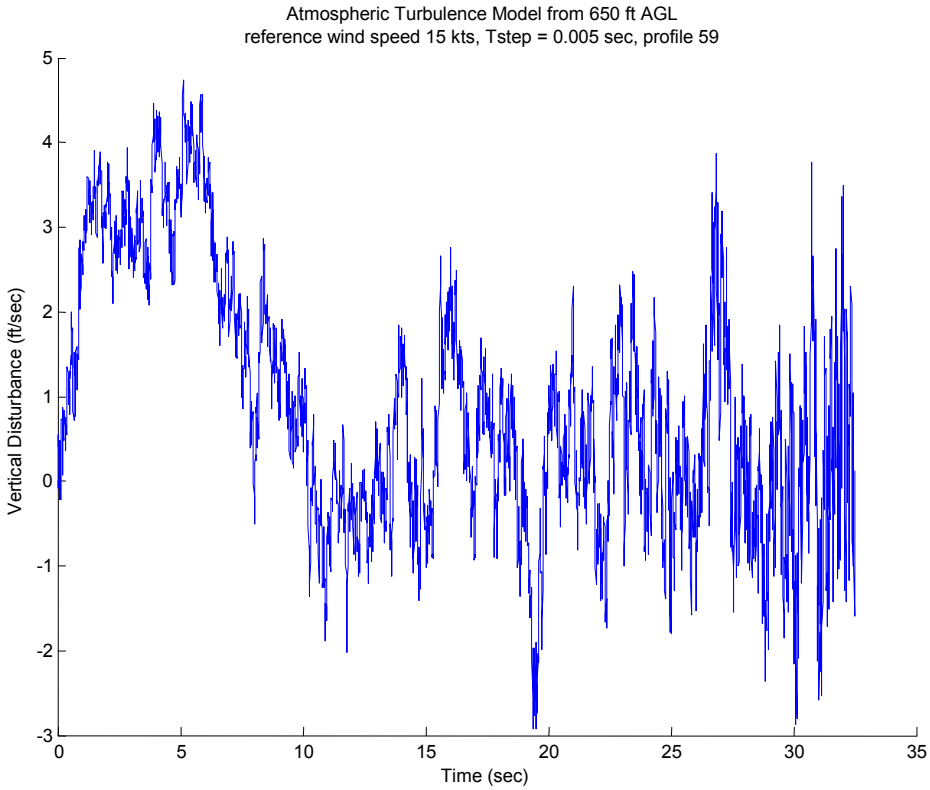

Figure 3.7 Vertical Atmospheric Turbulence

3.5 Atmospheric Models for Forced Landing Manoeuvres

One of the objectives for this research is to study the effects delay has on a forced landing manoeuvre and delay has been indirectly represented by atmospheric disturbances. The influence of wind velocities have on an aircraft could be roughly separated into 2 parts. The flight performance description of an aircraft depends on the low frequency part of the wind vector, the wind shear component. It is only the low frequency part of the wind that influences the energy relation of the aircraft and wind shear is not being considered in this study. The high frequency wind components in the atmospheric turbulence and gust are considered high frequency and have no effect on the aircraft trajectory. Their effects are on the aircraft's loading, the structural fatigue, the pilot's workload, passenger comfort, and on the flying qualities of the aircraft. The eigenmotions of the aircraft, the phugoid and the short period motion are important frequencies for the separation effects. If the frequency of the wind perturbation is less than the phugoid frequency, the change of aircraft trajectory is directly proportional to the wind angle of attack, meaning the low frequency directly changes the aircraft trajectory. If the range of frequency is above the short period motion, the inertia of the aircraft avoids large change of trajectory. In other words the flight path is only affected in phugoid mode where the pitch angle follows the flight path angle (Schanzer 1989; Hahn, Heintsch *et al.* 1990; Hahn, Heintsch *et al.* 1990). Using the airplane's stall speed (V_s = 72 mph) and the well-known phugoid period equation, the phugoid period was found to be

$$T_{Phugoid} = \frac{\sqrt{2}\pi V}{g} \approx 15\,\text{sec}.$$

Although there exist several atmospheric models as discussed in Chapter 3.3, there is no one atmospheric model that is perfectly suitable for the nature of this research on a forced landing of a single engine aircraft after an engine failure. This is because there are no suitable low frequency atmospheric models available that are applicable for researching the effects atmospheric disturbances have on the final landing segment of a forced landing manoeuvre. Therefore, the two proposed atmospheric models are implemented for this study. They are the simulated discrete steps thermal distribution and the time averaged of the von Karman atmospheric turbulence model.

For this study, the thermal distribution models with velocities varying from –9.84 ft/sec to +9.84 ft/sec in discrete step size of 3.28 ft/sec are assumed to "jump" from one state to another. For convenience, the thermal jumps are assumed to occur at every 350 ft drop in altitude, regardless of the horizontal distance traveled since calculations were carried out for

every 50 ft drop in altitude. The approximation step size of 350 ft drop in altitude was used because while using an estimated average sink rate of 20 ft/sec, the thermals change state every 16.25 secs, which is very close to the estimated phugoid period of 15 sec. Therefore, 49 different thermal distributions, with one "jump", were used to simulate the forced landing manoeuvre with thermal distribution for an engine failure altitude at 650 ft AGL as shown in Figure 3.8. Note that discritising the thermal distributions in terms of altitude drop resulted in thermals with various horizontal sizes. This is because the up and down drafts affect the aircraft's net sink rate during the descend manoeuvre, which in turn affects the horizontal distance travelled.

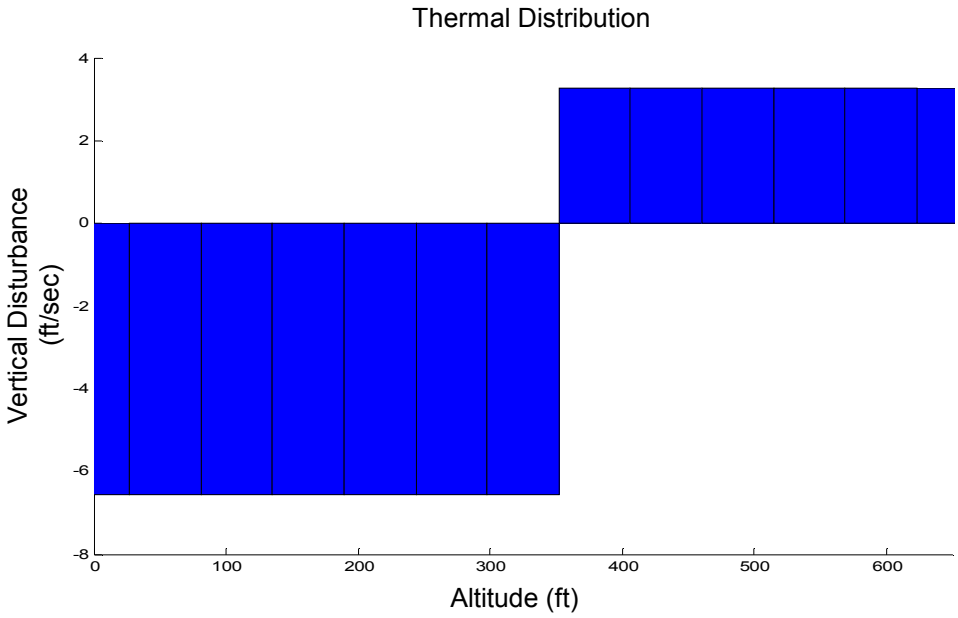

Figure 3.8 Vertical Thermal Distribution

100 atmospheric turbulence profiles were generated for a reference speed of 15 kts at 650 ft AGL using the von Karman atmospheric turbulence model as described in Chapter 3.3. An improvisation to the atmospheric turbulence model was made by time averaging the von Karman atmospheric turbulence model to coincide with the airplane's approximated phugoid mode of 15 secs. An example of such atmospheric turbulence profile is shown in Figure 3.9. Time averaging the velocity was carried out in order to obtain an improvised low frequency atmospheric distribution pattern, which is one method of obtaining the low frequency velocity representations from high frequency velocity representations. The effect of short period is the "diffusion of paths" where the noise in the atmosphere is filtered by the airplane. The maximum time averaged atmospheric turbulence updraft is 1.48 ft/sec and the maximum downdraft is 1.67 ft/sec.

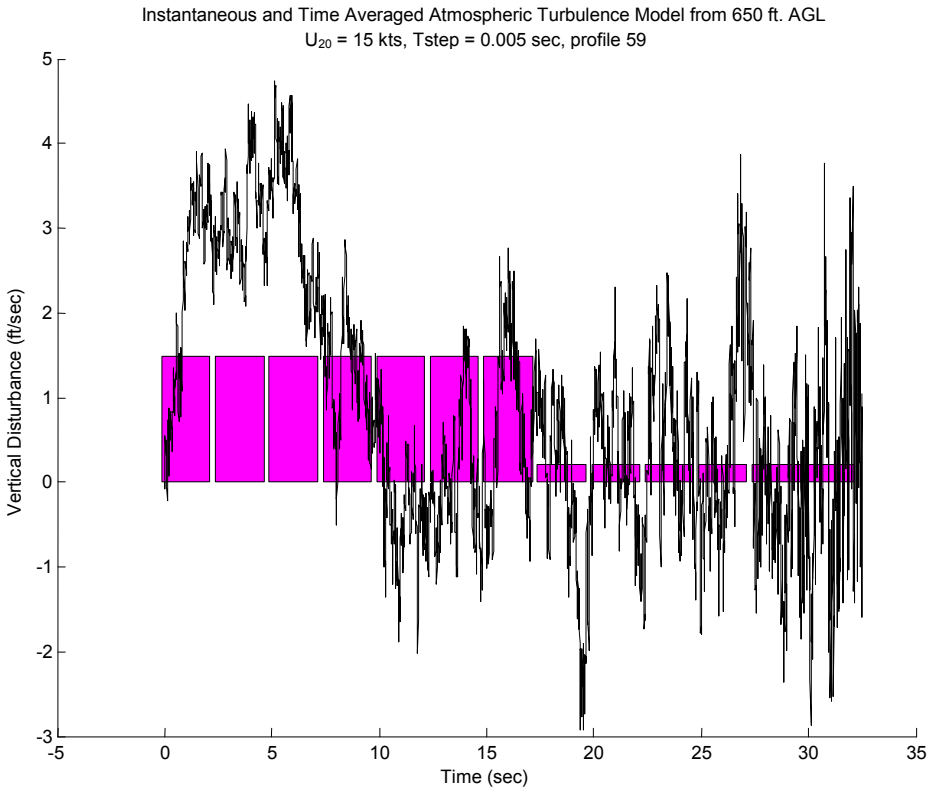

Figure 3.9 Time Averaged Vertical Atmospheric Turbulence

The turbulence wind models used in this simulation affected the aircraft trajectory through the aircraft force equations, which were calculated with reference to the aircraft wind axes. In addition to the vertical atmospheric disturbances described, horizontal wind variations with fixed constant wind magnitude and direction components were also incorporated into the forced landing analysis. In reality, the magnitude and direction of the wind will depend on the surrounding terrain. The constant horizontal wind components considered all the different head wind combinations of 10 mph, 20 mph, and 30 mph at –45°, 0° and +45° relative to aircraft's direction of motion at engine failure after take-off. The tail wind conditions relative to the initial engine failure position were not considered since it was assumed that aircrafts normally take-off into the wind.

3.6 Concluding Remarks

A point mass model was used to represent the aircraft model since this study is on trajectory manoeuvres and no transients were assumed. Other researchers have used the point mass model assumption and found acceptable results on flight trajectory studies (Hoffren and Raivio 2000) and (Brinkman and Visser 2007). The models used for this study have been

made as accurate as possible. However, it is accepted that large discrepancies in the atmospheric model could be possible. It is believed that simulating it repeatedly by randomly generating the atmospheric turbulence model and the thermal model described could compensate for this draw back. If higher accuracy is needed, better atmospheric data can be obtained using Global Positioning System (GPS). The atmospheric turbulence profiles generated were applied to the forced landing Genetic Algorithm program in Chapter 6 and to Sequential Quadratic Programming in Chapter 7 to test their effects on forced landing trajectories.

The atmospheric disturbance models presented do not contain any significant advances in the field of simulation. However, their representation in simulating aircraft trajectories for the problem considered in this study is an important step in flight simulator development.

CHAPTER 4

PROBLEM FORMULATION

4.1 Introduction

This chapter discusses the problem formulation and the analyses involved for this study. The objective of this study is to understand the effects artefacts such as delay have on the transfer of training. An indirect method of representing delay is to represent it with atmospheric disturbances. Wind disturbances were used to a means to represent the delay in decision-making in flying an airplane since wind disturbances may contribute to the minute variations in any flight path and the pilot has to manoeuvre the aircraft accordingly to maintain its original flight path. Therefore, a particular flight manoeuvre, the forced landing manoeuvre after an engine failure under the influence of atmospheric disturbances was carried out. A description on the forced landing problem and the atmospheric models used are provided. Since this research focuses on finding successful landing trajectories for an aircraft after an engine failure, a brief discussion on optimisation and search techniques will also be provided. It concludes with an exhaustive search for a forced landing manoeuvre after an engine failure at 650 ft AGL. The results obtained from the exhaustive search analysis will serve as a building block and a benchmark for comparison with the results obtained from a search and an optimisation technique.

4.2 Problem Description: Forced Landing

The study of safe landing of aeroplanes is a very important issue in the aviation field and is considered by pilots as the most demanding task in every flight. Many accidents have occurred during the landing phase of flights, some of which were beyond the pilot's control, some were due to human error, while some could have been successful if only a more optimal landing manoeuvre was carried out. Unfortunately, it is the disastrous failed landings that became a statistics with the National Transportation Safety Board (NTSB) and those who landed safely or with minor damage generally are not reported to Federal Aviation Authority (FAA) or NTSB. Hence, the statistics gathered are skewed or biased towards failed attempts.

The research problem in this study has its interest in the search for the best landing trajectories, landing closest to a pre-selected location and within a small deviation from a pre-defined final heading, for a forced landing manoeuvre after an engine failure with and without the influence of vertical disturbances and horizontal crosswinds as mentioned in Chapter 3. Such situation could occur after take-off (Rogers 1995) or during a level flight at any altitude above ground level (Hoffren and Raivio 2000) as reviewed in Chapter 2.3.2. When an engine failure occurs on an aircraft and no additional power is available, the pilot must select a suitable location to land safely with the limited amount of energy available from the engine failure position. The general recommendation for this situation is to land straight ahead and (Jett 1982) confirmed this ingrained technique in his study whereby 85% of his subjects followed this procedure. However, (Rogers 1995) suggests that, for forced landings from a higher altitude, a turnback manoeuvre may be flown because higher altitude allows for more time in the air. This research is also an extension of Rogers' forced landing manoeuvre where the search for optimal landing paths began after the pilot has selected a practical landing location on the ground that was within range after an engine failure. A graphical interpretation of the forced landing after an engine failure at an arbitrary altitude is shown in Figure 4.1. This research takes the approach of an ensemble of probability of landing within a specified tolerance from a pre-selected location and not as an optimal control problem of the deviation from the flight trajectory during a forced landing manoeuvre. In other words, what are the chances of the pilot performing the landing task with a maximum probability of landing at a pre-selected landing site?

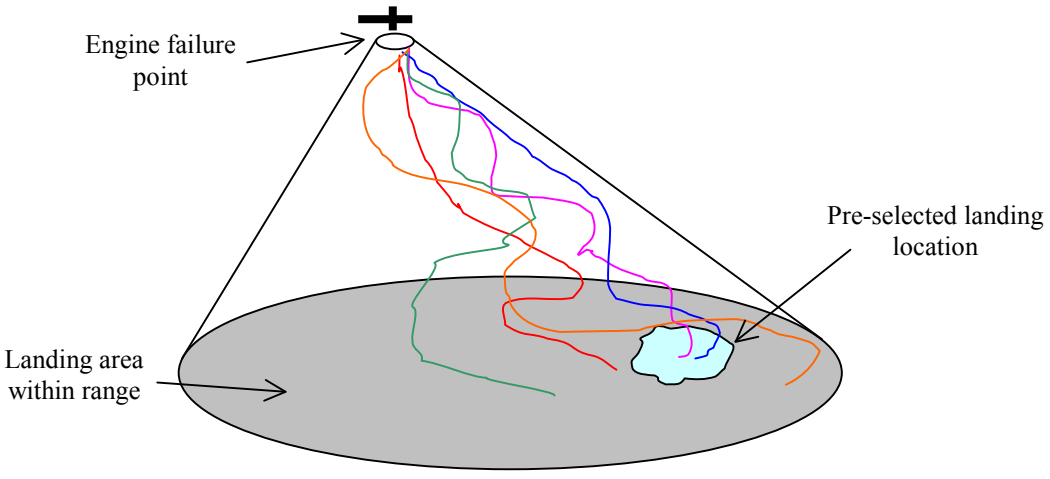

Figure 4.1 Forced Landing Area

Since the aircraft's flying manoeuvres are governed by the aircraft's parameters such as bank angle, glide angle, minimum turn radius and minimum speed, there will be some regions in

space as shown in Figure 4.2 that the aircraft will never fly through for a successful landing at a pre-selected location. On the contrary, the aircraft have to be in a certain region in space if it is to land successfully at a pre-selected location.

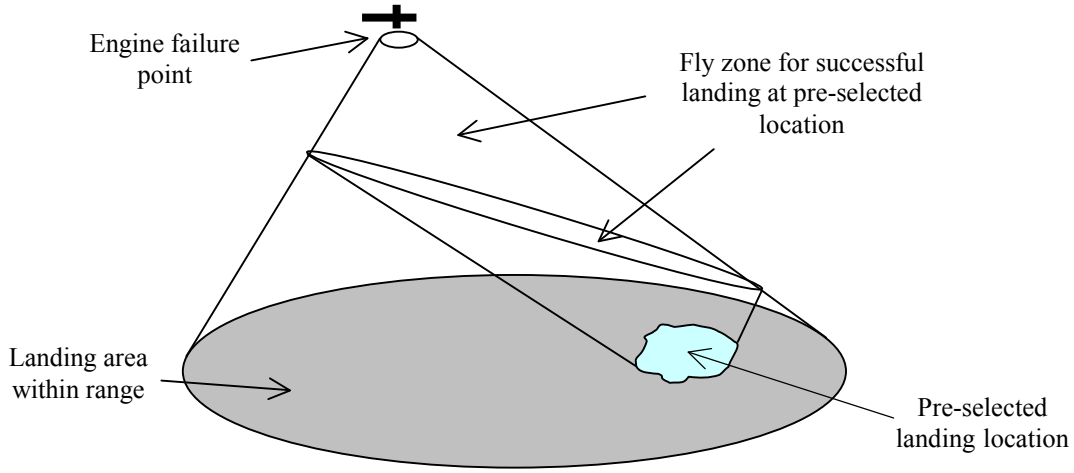

Figure 4.2 Flight Path Zones

This research also searches for some of the best obstacle avoidance flight paths in a forced landing manoeuvre. Such situations occur in real life situation where there are buildings in close proximity to the flight paths during take-offs and landings. An illustration of an aircraft's flight path avoiding an obstacle is shown in Figure 4.3.

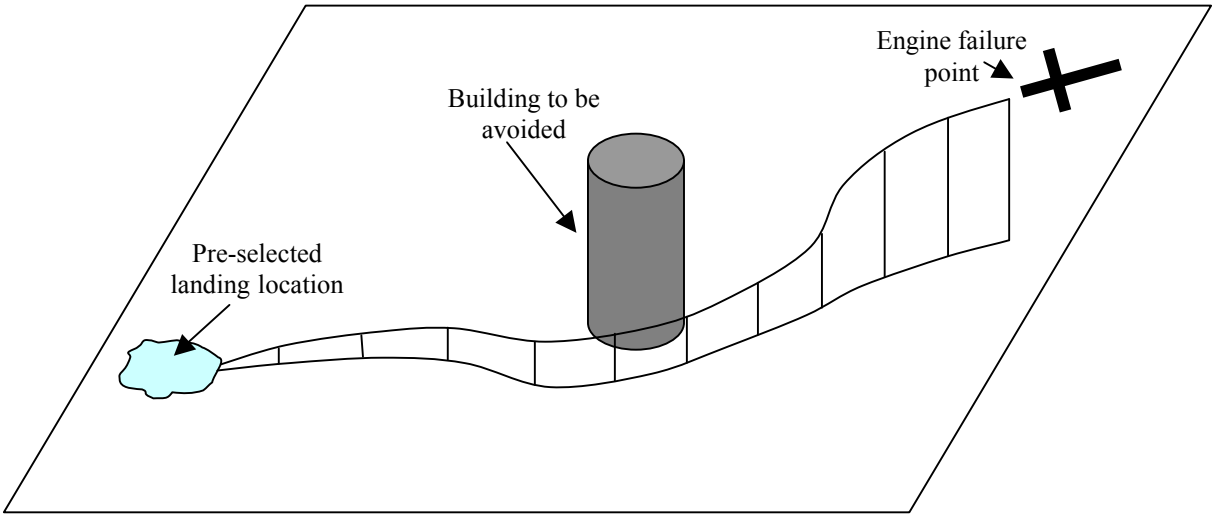

Figure 4.3 Obstacle Avoidance Flight Path

The performance index for this forced landing problem is the search for flight paths, ignoring time to flare, landing closest to a pre-selected landing location (x, y) with and without pre-

selected final headings (ψ) as shown in Equations 22 and 23. The weighting factors for equation 23 will be further discussed in Chapter 6.7.

$$Performance\ Index = \sum\left[(x - x_{pre-selected})^2 + (y - y_{pre-selected})^2\right] \qquad \text{Eqn. 22}$$

$$Performance\ Index = \sum\left[(x - x_{pre-selected})^2 + (y - y_{pre-selected})^2\right]/100 + \sum\left[(\psi - \psi_{pre-selected})\right]/\ 10 \qquad \text{Eqn. 23}$$

Solving the forced landing after an engine failure problem using search technique involves satisfying several aerodynamic constraints and keeping the pilot's workload to a minimum so that the execution of an emergency procedure could be carried out rapidly. The following boundary conditions and variables were used for the point mass model and the Beech Bonanza Model E33A aeroplane whose characteristics are as shown in Table 3.1.

$$-45° \leq Bank\ angle \leq +45°$$
$$-7.5° \leq Glide\ angle \leq -5.4°$$
$$110.88\ ft/sec \leq Velocity \leq 305.49\ ft/sec$$

Simulations for this study were performed at every 50 ft drop in altitude from the engine failure altitude and the option for trading speed for an increase in altitude or to maintain altitude were not being considered in this research since the analysis for engine failure after take-off usually occurs at relatively low altitudes. The calculations were carried out at discrete altitude to conveniently suit the search method used and to ensure that the airplane touches down at the final sector of the calculations. The range of bank angle used is the same as the range used by (Rogers 1995) in his analytical forced landing analysis. The maximum glide angle (*-7.5*°) is governed by 5% above the stall speed (75.6 mph) allowed while the minimal glide angle (*-5.4*°) is governed by the speed for maximum lift to drag (122 mph). The minimum speed is the velocity at 5% above stall speed (72 mph) while the upper speed limit is the aircraft's maximum speed (208 mph).

In reality, the presence of atmospheric disturbances will complicate a forced landing manoeuvre and this research is limited to investigating the effects vertical disturbances and crosswind have on a forced landing manoeuvre. At low altitudes an updraft may cause the

aircraft to overshoot the pre-selected landing location while a downdraft may cause the aircraft to undershoot the pre-selected landing location. Although a sideslip landing will generate greater drag, thereby, allowing a steeper approach and thus avoiding overshooting, it is not being considered in this study because sideslip also increases the risk of errors. At high altitudes the vertical disturbances, which affect the specific energy, may completely change the forced landing flying manoeuvre since the airplane's sink rate is being affected by the specific energy drain and therefore complicating the landing procedure.

4.3 Optimisation/Search Methods

According to the American Heritage dictionary, optimisation means the procedure or procedures used to make a system or design as effective or functional as possible that involves mathematical techniques. In other words, it is the process of making something better by trying variations on the initial concept and using informed knowledge for improvement. Optimisation involves the search for the "best" solution, which implies that there may be more than one possible solution, some of which may be better than the others. It involves the minimisation or maximisation of functions or functionals. The output from the optimisation process is usually the cost function that is either the minimal value in which case it is known as a minimization process or the maximum value in which case it is known as a maximization process. A minimum cost function can easily be turned into a maximum cost function by simply multiplying it by a minus sign. In general, there are six categories of optimisation algorithms as shown in Figure 4.4 and they are not necessarily mutually exclusive. A brief description for each category is presented as follows (Haupt and Haupt 1998):

Trial & error vs. function. This category simply involves experimenting the process without much knowledge on how the process affects the outcome. Function, on the other hand assumes that the process can be mathematically described.

Single parameters vs. multi parameters. The optimisation problem may involve only one parameter or it may involve multiple parameters, which involves multidimensional optimisation and increased level of difficulties.

Static vs. dynamic. The static optimisation results are independent of time while the dynamic optimisation results are time dependent.

Discrete vs. continuous. The optimisation parameters may be discrete where there are finite number of possible values, or continuous where there are infinite number of possible values. Discrete parameter optimisation is also known as combinatorial optimisation.

Constrained vs. unconstrained. Constraint optimisations require the parameter equalities and inequalities to be part of the cost function while unconstraint optimisation allows the parameter of any values. A linear program consists of a constraint optimisation, which only involves linear equations and linear constraints while a non-linear programming problem involves non-linear cost functions and/or non-linear constraints.

Random vs. minimum seeking. Random methods use probabilistic algorithms to seek for solutions and are generally slower but have greater success in find the global minimum. Minimum seeking algorithms are usually calculus-based methods, which may be easily trapped, in local minima but they tend to be find a solution relatively fast.

With the current advancements in computers, simulations can be carried out effectively to perform optimisation. A more detailed description of the optimisation methods used in this study will be provided in the respective chapters.

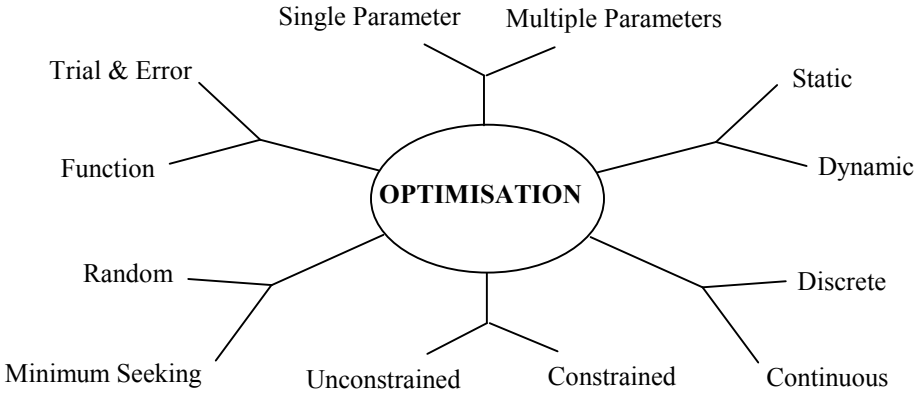

Figure 4.4 Optimisation Categories

The heart of all optimisation routines is the search for the minimum cost value. In general, there exist three main types of search techniques for optimisation; calculus based, enumerative and random as shown in Figure 4.5 (Goldberg 1989). The calculus based

techniques use a set of governing equations along with some specific conditions to solve an optimisation problem. They can be subdivided into two main classes: indirect and direct methods. Indirect methods search for local extrema by solving the usually non-linear set of equations resulting from setting the gradient of the objective function equal to zero. These methods are restricted to smooth continuous functions where the search for possible solutions – the function peaks, starts by restricting the search to points with zero slopes in all directions. The direct methods, such as Newton and Fibonacci, search for the local optima by "hopping" on the function and moving in a direction related to the local gradient. This is simply the notion of "hill climbing" where it searches for the extrema by climbing the steepest permissible gradient. The drawback in these two methods is that the results may converge to a local extrema should there be a multiple-peak function. The enumerative technique, such as dynamic programming which suffers "the curse of dimensionality", searches every point in the objective function's domain space. It requires tremendous amount of computational time making it impractical and very inefficient for large domain space. This technique also includes constraint optimisation whose efficiency may be improved significantly when constraint propagation is used. The guided random search techniques have its roots from the enumerative technique but use additional information to guide the search. This technique can be subdivided into two classes: simulated annealing and evolutionary algorithms. The former uses thermodynamic evolution process to locate the minimum energy states while the later are based on natural selection principles. The evolutionary algorithms subdivides into evolutionary strategy and genetic algorithms (Filho and Treleavan 1994).

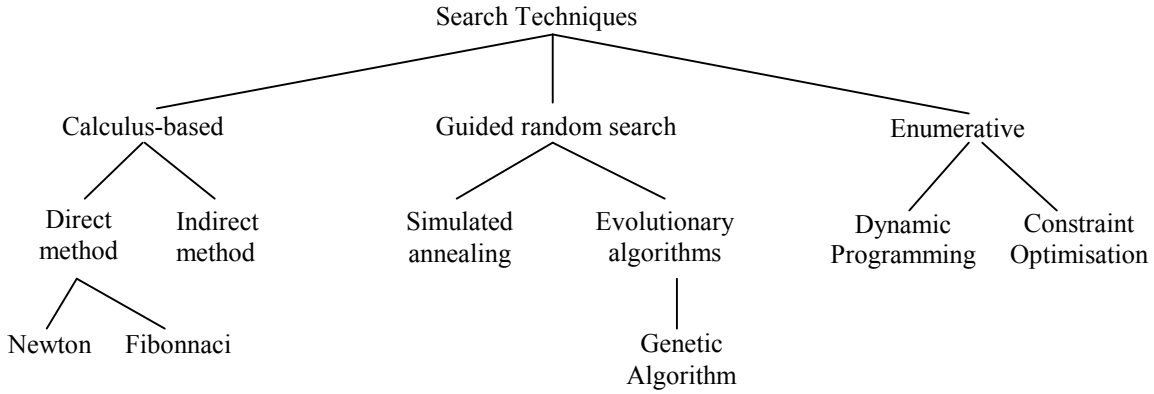

Figure 4.5 Search Techniques

A primary goal for the selection of an optimisation method is to find a method that, given high-quality starting points or poor initial guesses, will require only a small number of iterations for the arrival to some optimal point or points. Optimisation consists of two parts:

the optimisation process and the arrival to the optimum solution(s). When selecting an optimisation technique, it is common to focus on the end results, i.e. its convergence to the best solution. However, its interim performance is usually overlooked. This is because optimisation has its origin in calculus, which is driven by the end results obtained. However, this is not a natural emphasis. Improvement is the most important goal for optimisation. For a complex system, the improvement is more important than the attainment of the optimal solution. This issue can be illustrated if the exhaustive search method were used on a complex problem where the best solution could be obtained if the entire solution space were searched. However, this may not be possible or practical. In this case, a local optimal solution may be found from the limited search space within the allocated finite amount of time.

Therefore, optimisation can be further broken down into global optimisation and local optimisation. Global optimisation finds the best solution from the set of all solutions and will always find the same solution regardless of the optimisation's starting point but it will require more computation power and time. Local optimisation finds the best solution, local optimum, from a set of limited solutions that are close to one another and is dependent on the optimisation's starting point. In many practical problems it may not be possible to search for the global optimal solution and at times finding the local optimal quickly is more desirable than finding the absolute best solution.

There exist many different approaches to optimisation and the most suitable approach is best found by considering the nature of the problem and the resources available. Some of the optimisation methods used in aerospace problems are mentioned in Chapter 2.3.1. For this study, three optimisation techniques were considered for the forced landing manoeuvre. An exhaustive search method was carried out to a coarsely sampled solution space with discrete flying manoeuvres. It would be impossible to apply the exhaustive search method to the forced landing problem where variable real value and atmospheric disturbances were being considered. Therefore, genetic algorithm was chosen for its simplistic and easy to formulate algorithm. However, since this method does not guarantee if a maximum point can be found, another optimisation method, sequential quadratic programming was also being selected as comparison and support to the results obtained using the former method.

4.4 Exhaustive Search Applied to a Forced Landing Manoeuvre

An initial approach to the forced landing problem considered for this study was to use an exhaustive search technique even though this method proved to be very inefficient, if not impossible as there are infinite number of combinations of variables and aircraft parameters for the aircraft to land closest to a pre-selected location. A coarsely sampled exhaustive search method was carried out as a building block to locate flight trajectories landing closest to three pre-selected locations. These results were used a reference for comparison with other search methods on the forced landing manoeuvre of a single engine aircraft after engine failure. The performance index for this exhaustive search is to land as close as possible to the target touchdown point as shown in Equation 22.

A forced landing manoeuvre upon engine failure at 650 ft AGL during take off was undertaken for a Beech Bonanza E33A aircraft. An exhaustive search method for a discrete altitude drop of every 50 ft for a forced landing manoeuvre for three possible turn manoeuvres; glide straight at the maximum lift to drag velocity (122 mph), turn right or left by banking ±45° while flying at $1.05V_{stall(clean)} / \sqrt{\cos\phi}$ § was carried out using aircraft data as shown in Table 3.1. If a pre-selected location on the ground was specified, paths landing closest to the pre-selected location could be found from the database of touchdown locations generated. However, the accuracy of the solution is dependent on the sampled points resolution.

A database that contains all possible flight paths for every 50 ft drop in altitude from the initial engine failure altitude of 650 ft AGL to touchdown was generated. By specifying a pre-selected location on the ground, a search through the database was conducted to locate all possible flight paths from the engine failure location that will land closest to the pre-selected touchdown. This search method requires colossal amount of memory space whereby the amount of memory required grows exponentially with increase resolutions or variables. For example, at an engine failure altitude of 650 ft AGL, the pilot has three turn options; straight ahead, left turn or right turn. At 600 ft AGL, there exist another three turn options to each of the previous turn decisions, thus, resulting in nine possible paths. The number of possible flight paths will grow according to 3^n, where n is the number of steps or constant altitude decrement it takes to reach the ground as shown in Figure 4.6.

§ Where ϕ = bank angle during turn.

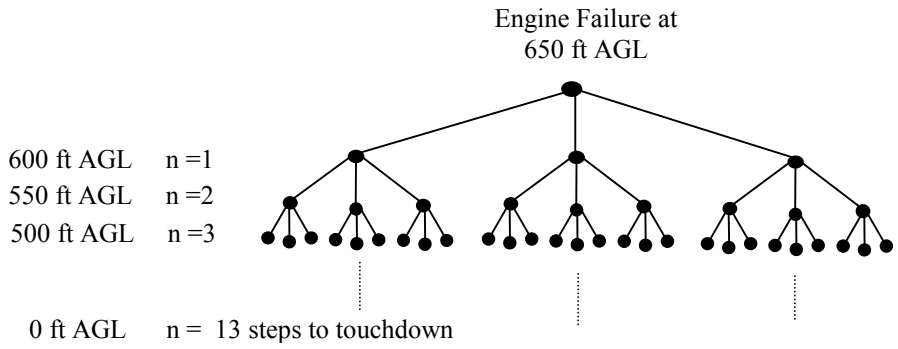

Figure 4.6 Tree Structure for Exhaustive Search Method to a Forced Landing

This exhaustive search method is not efficient for the case of an engine failure at higher altitude since it involves more steps to touchdown or for higher resolution in bank angles or velocities, which involves more manoeuvre options at each node. In fact this search method will not be feasible or practical if variable bank angles and variable velocities, and smaller altitude decrement were used since it will require an extremely large amount of memory to store the database of all the possible flight paths locations in space. Nevertheless, it was carried out for the three turn decisions described for 13 steps to touchdown to serve as a benchmark for the Genetic Algorithm search method and the Sequential Quadratic Programming method, which is described in Chapter 6 and 7 respectively.

Three touchdown points were chosen to illustrate the exhaustive search technique using the engine failure point as the reference for these calculations. The three touchdown points were located at a lateral distance of 0 ft and longitudinal distance of -3100 ft, at lateral distance of 3000 ft and longitudinal distance of 3000 ft, and at lateral distance of 500 ft and longitudinal distance of 200 ft. The accuracy of the best trajectory paths selected is dependent on the database's resolution generated since discrete turn options, bank angles, velocity and altitude were used in generating the database. Figures 4.7 to 4.9 shows the best paths for the three pre-selected locations using the database of points generated.

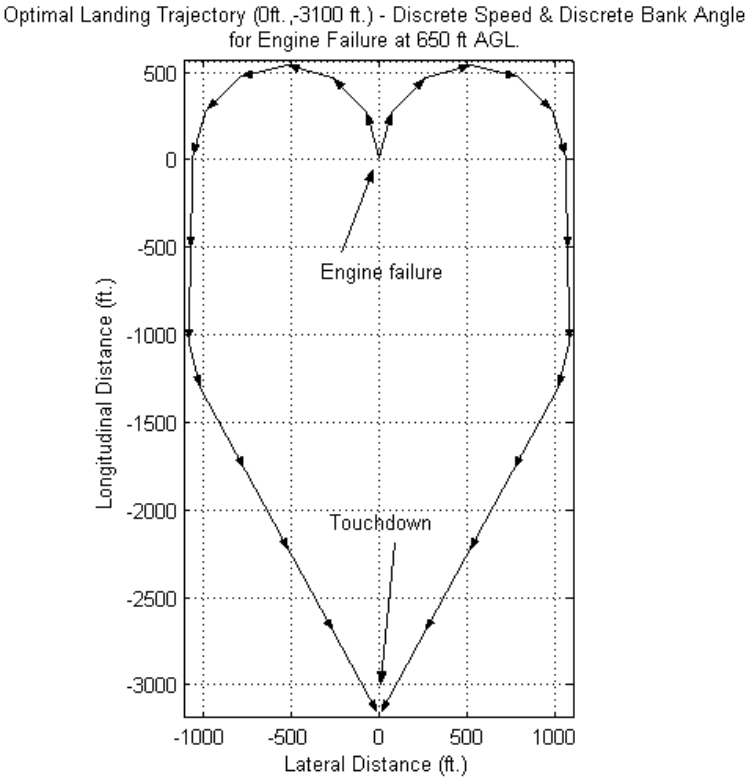

Figure 4.7 Optimal Landing Trajectory (0 ft, -3100 ft) for Engine Failure at 650 ft AGL.

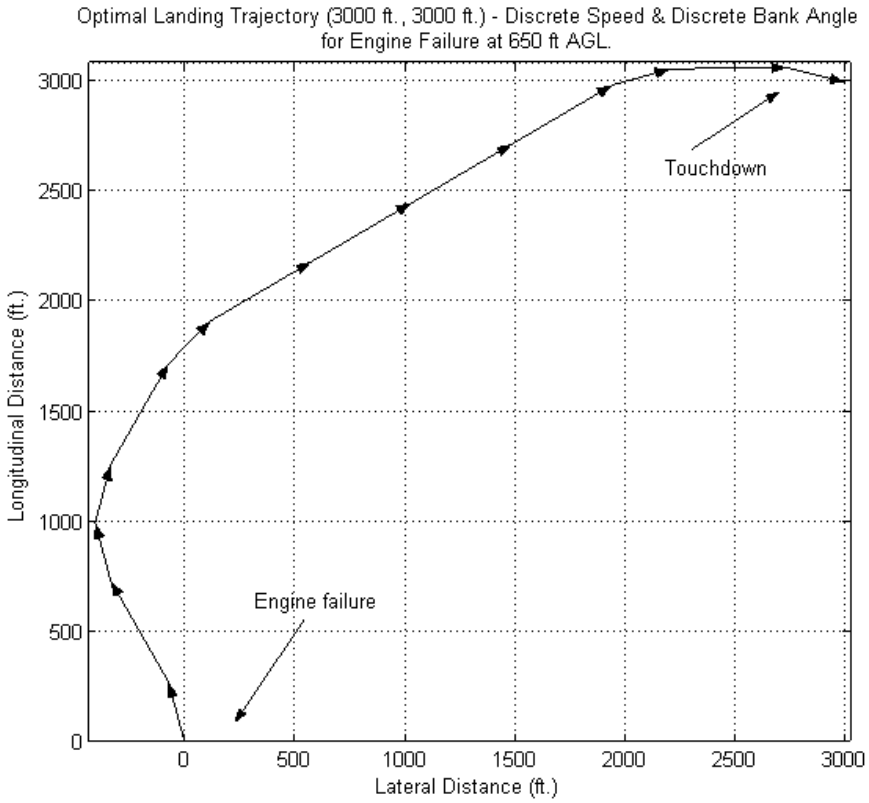

Figure 4.8 Optimal Landing Trajectory (3000 ft, 3000 ft) for Engine Failure at 650 ft AGL.

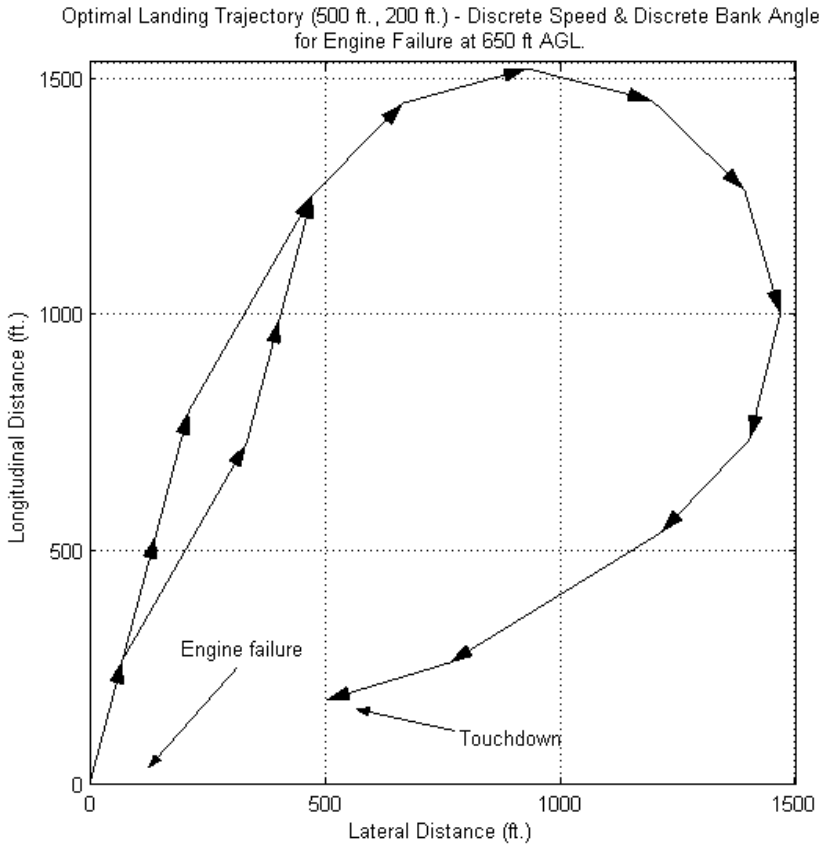

Figure 4.9 Optimal Landing Trajectory (500 ft, 200 ft) for Engine Failure at 650 ft AGL.

4.5 Concluding Remarks

This chapter describes the problem formulation for the forced landing manoeuvre after an engine failure based on the Beech Bonanza Model E33A and the atmospheric models used to simulate the disturbances considered in this study. A brief description on different optimisation methods is also presented. An exhaustive search was carried out for three pre-selected landing locations for an engine failure at 650 ft AGL. These results will be used as benchmark for the other optimisation methods and for forced landing manoeuvres in the presence of winds in the next two subsequent chapters.

CHAPTER 5

FORCED LANDING PERFORMANCE AND SENSITIVITY ANALYSIS

5.1 Introduction

This chapter examines the effect different turn velocities have on forced landing performance for a particular touchdown location. The forced landing manoeuvre for this sensitivity study uses (Rogers 1995)'s teardrop turn around manoeuvre for the Beech E33A Bonanza as described in Chapter 2.3.2 is shown in Figure 5.1. The analysis uses different combinations of turn velocities to calculate the touchdown. It also investigates the effect that the tolerances prescribed in the Manual of Criteria for the Qualification of Flight Simulators (ICAO 1995) have on the performance of flight simulators used for pilot training.

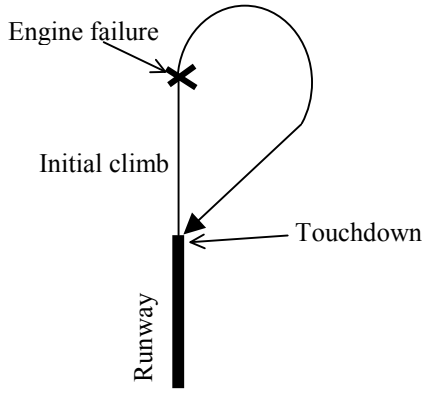

Figure 5.1 Rogers' Teardrop Flight Path

5.2 Forced Landings Performance Analysis

As mentioned in Chapter 2, landing an aircraft that has suffered an engine failure after take-off is one of the classifications of a forced landing. A forced landing performance analysis was carried out to study the effects turn velocity has on the parameters used in determining the landing footprint. This analysis replicated (Rogers 1995)'s results using the general governing equations of motions as described by (Pamadi 1998). A comparison between different turn velocities with different glide velocities and modifications to account for the instantaneous change in velocity during the turn from the engine failure height and gliding to touchdown was carried out. The effects of different turn velocities, glide velocities, and

modifications of instantaneous change in velocity at the end of a turn and at 90° into the turn will affect the landing footprint since glide angle and sink rate changes with respect to angle turned during the glide manoeuvre.

5.2.1 Turn and Glide Velocity Combinations

An analysis of the effects of different turn and glide velocity combinations have on the locus of touchdown points was carried out based on the data shown in Table 3.1. The engine failure point is used as the reference for all calculations. As described in Chapter 2.3.2, Rogers' combination of a turning velocity of 5% above the stall velocity and a gliding velocity of maximum lift to drag ratio (case 1) yielded the optimal path back to the runway as shown in Figure 5.2. His optimal results are fully supported by an analytical result that minimizes the energy (altitude) loss for a turn to a given heading (Rogers 1995). A number of combinations of turning velocities and stall velocities were also tested. For example, it is possible to fly the turn at the velocity for the best lift to drag ratio and continue the straight segment at the same velocity (case 2). However, it was found that if this was done the turn radius will increase and the aircraft must then travel further. Thus, reducing the range available for returning to the runway. Flying the turn at 5% above stall velocity and continuing the straight glide segment at the same velocity (case 3) will result in a smaller turn radius and a landing footprint that is closer to the runway centreline and engine failure point. Therefore, the approach for this research is validated by Rogers' analytical results.

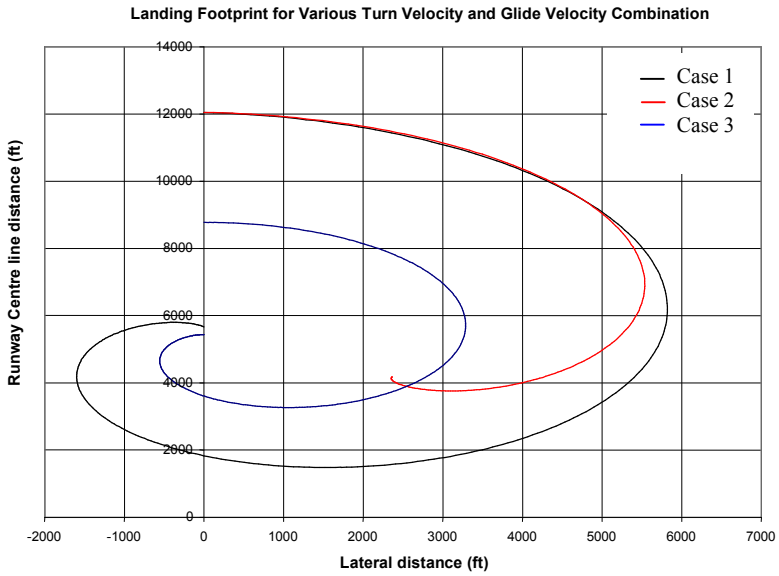

Figure 5.2 Landing Footprints for Different Turn Velocity and Glide Velocity

5.2.2 Velocity Variations Between Turn Velocity and Glide Velocity During Turn

An analysis was performed on the turning velocities and glide velocities combinations to verify some of Rogers' underlying assumptions. For example, Rogers assumes that changes in velocity occur instantaneously and that the increase in velocity from the turn velocity to the best glide velocity at the end of the turn incurs at no height loss. In reality, this increase in velocity requires the pilot to use gravity to accelerate the aircraft thus losing altitude. Modifications were made to Rogers' analytical model to account for this change. Rogers' results (case A) were compared to two other cases. One being the instantaneous change in velocity at the end of the turn (case B) where the change in velocity occurred at the end of the turn manoeuvre over a 1° turn in change of heading. This generated a higher turn velocity, larger turn radius, shallower glide angle during the turn, a smaller turn rate and a higher sink rate with respect to angle turned ($dh/d\theta$) just before entering the glide to landing manoeuvre (Tong and Galanis 2001).

Case C consists of an intermediate velocity of 5% above stall velocity for the first 90° of the turn after an engine failure. Then, the rest of the turn onwards is assumed to be at the average velocity between the initial turn velocity at the beginning of the turn and the best straight glide velocity. This analysis was carried out to study the effect of an intermediate increase in turn velocity during the turn. As shown in Figure 5.3, no modification in turn velocity was made for the turning angle between 0° and 90° since the aircraft is still heading away from the runway. From 90° onwards, the aircraft begins to change its direction towards the runway and therefore the optimal speed is not the previous minimal sink rate velocity (dh/dt) but rather some velocity between minimum sink rate and best straight glide velocity 90° into the turn. The 90° point also serves as an appropriate point for the turn velocity to increase since it is best to fly as slowly as possible while heading away from the runway in order to minimise the distance flown from the runway. The velocity transition between the end of the turn and the glide sector was assumed to increase instantaneously and its effect is assumed to be negligible.

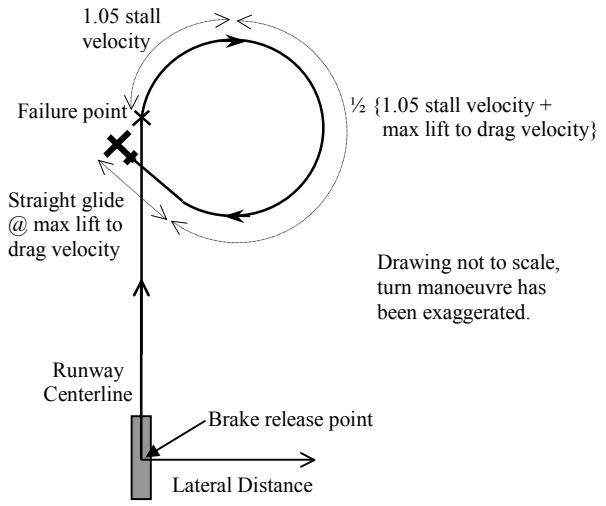

Figure 5.3 Various turn velocities during turn manoeuvre for case C

As shown in Figure 5.4, the footprint for an instantaneous transition from the climb velocity at engine failure to the turning velocity and an instantaneous change in velocity at the end of the turn (case B) is almost identical to Rogers' analysis. It is concluded that the loss in height for acceleration is minimal. Thereafter, whilst gliding at maximum lift to drag velocity, the height and the glide angle are the only factors affecting the glide path. The footprints for case C and case A differ due to the larger changes in heading. The footprints for heading changes between 0° and 90° are similar to Rogers', since no modifications were made. However, between 90° and the gliding point, an average velocity between the turn velocity and the glide velocity is used. This change in intermediate velocity from 90° onwards will not allow the aircraft to complete a 360° turn to touchdown on the runway, but will intersect the runway at an earlier turn angle. This is because from 90° into the turn onwards, a higher turn velocity will cause a larger turning radius and a higher sink rate with respect to angle turned. The reason is that both the radius and the height are proportional to the square of the velocity. Hence, the footprint is further sideways from the runway due to the bigger turning radius from 90° onwards and lacks the height needed to glide to touchdown. Case C is a more detailed model than case A and B. Even though case C is not a high fidelity model for this manoeuvre, it nevertheless indicates that a more detailed model should be investigated to ensure that case C does capture the critical aspects of forced landings.

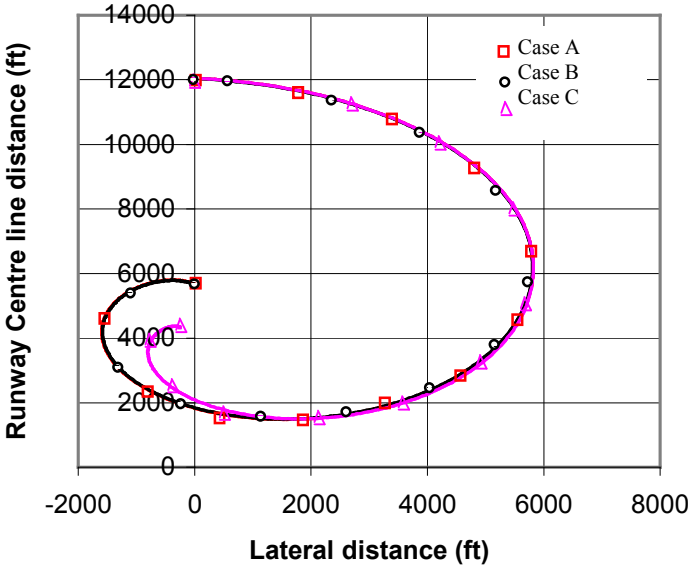

Figure 5.4 Landing Footprint Comparison for Change in Velocity During Turn

5.3 Sensitivity Analysis on Flight Simulator Requirements

The advancement of computer technology has made it possible for increasing the role of flight simulators for initial pilot training for both civil and military pilots. It has also enabled pilots to be trained in more complicated and dangerous manoeuvres in emergency procedures without endangering the pilots' lives or damaging expensive equipment, and in developing new methods for achieving operational objectives. The costs of modern aircraft and the increasing complexity of the operating environment are placing more demands on flight simulators to provide more types of training as well as a safe and improved learning environment. Flight simulators have become so sophisticated in replicating actual flying manoeuvres and conditions that the highest approved category of simulators allows zero flight time for training pilots converting to a new aircraft type.

Despite the advancement in technology, a flight simulator cannot perfectly represent a particular aircraft in all aspects. For example, the mathematical model of the aircraft is never fully accurate, the motion and visual systems have physical limitations that make the full representation of the sensation of flying always less than perfect. Recent advances in aircraft technology are also creating new ways of using aeroplanes. For example, gas turbine engines are now so reliable that a number of countries including Australia are approving the use of Single Engine Gas Turbine aircraft (SEGT) for Regular Public Transport (RPT) operations. This will require the flight simulation industry to consider exploring the use of flight

simulators for SEGT aircraft in RPT operations. It also creates new opportunities and challenges for the simulation industry. Pilots of these aeroplanes will require training in glide approaches (forced landings). This is a new area not covered in the flight simulation regulations at present (ICAO 1995).

This analysis investigated the effect that the tolerances prescribed in the Manual of Criteria for the Qualification of Flight Simulators (ICAO 1995) have on the performance of flight simulators used for pilot training. It also raised some issues for training pilots to fly such phases of flight and examines the impact that these issues may have on the design of simulators for such training. In particular, this analysis focused on the pattern that a pilot must fly following an engine failure and how this could be trained for in a simulator especially during the final manoeuvre prior to touchdown. A simplified analytical model for the Beech Bonanza E33A aircraft with retractable undercarriage was used to determine the effect of the aforementioned to tolerances on forced landings. A sensitivity analysis for the analytical model used to describe the track reversal-landing manoeuvre was also carried out.

5.3.1 Sensitivity Analysis on Forced Landing Manoeuvre

Flight test data obtained from actual flight will contain unavoidable errors, and an important consideration is to investigate the effect of these errors on the ability for pilots to perform particular flight manoeuvres. There is also the problem of not being able to fly manoeuvres that will be required for training in flight simulators. The theoretical forced landing manoeuvre for an engine failure at very low altitude (650 ft AGL) considered in this analysis will not be found in any of the qualification documents that are used for evaluating flight simulator performance because it is a manoeuvre for which flight test data would be difficult if not impossible to safely obtain. Hence, this sensitivity analysis was carried out (Tong, Galanis *et al.* 2003) to illustrate the potential deficiency that may arise from the existing flight simulators requirements.

A sensitivity analysis was carried out from brake release to touchdown using general flight dynamics equations (Pamadi 1998) and data based on the Beech Bonanza E33A with retractable undercarriage as shown in Table 3.1. The data for the initial takeoff ground roll and distance to clear a 50 ft obstacle were obtained from *Rising Up Aviation Resources*[§]. The aircraft is assumed to climb at 1200 ft/min, at a constant velocity of 91 mph, and at constant

§ http://www.risingup.com/planespecs/info/airplane117.shtml

runway heading until the engine fails at an altitude of 650 ft AGL. After an engine failure, the flight manoeuvres used and assumptions made are identical to (Rogers 1995) where the calculations for the flying manoeuvre were carried out for every 1° step increment for the turn followed by a straight glide to touchdown at maximum lift to drag velocity. The turning speed is $1.05V_{stall(clean)} / \sqrt{\cos\phi}$ banking at 45°, where ϕ is the bank turn angle, and the gliding to touchdown speed is $V_{L/Dmax}$ (122 mph). It is assumed that the transition from turning speed to gliding speed occurs instantaneously. The sensitivity analysis consisted of varying the parameters defined in the flight simulator regulations by the tolerances specified in the ICAO regulations (ICAO 1995).

Table 5.1 shows the acceptable tolerances for the parameters involved in the track reversal manoeuvre. These are the tolerance parameters during the takeoff distance** phase to at least 200 ft AGL, the climbing to clear 50 ft obstacle phase, the landing phase from a minimum of 200 ft AGL to nosewheel touchdown and the flight and manoeuvre envelope protection functions.

Table 5.1 Flight Simulator Tolerances from the International Standards (ICAO 1995)

Manoeuvre	Tolerance
Takeoff	±200 ft ground roll, ±3 kts airspeed at which the last main landing gear leaves the ground, ±20 ft in height from brake release to at least 200 ft AGL.
Climb	±3 kts airspeed at nominal climb speed and at mid initial climb altitude, Rate of climb ±100ft/min.
Landing	±3 kts airspeed from 200 ft AGL to nosewheel touchdown, ±10ft or 10% in height from a minimum of 200 ft AGL to nosewheel touchdown.
Flight envelope protection functions	±10% bank angle during approach.

For the manoeuvre considered in this analysis, the engine failure analysis was based on an engine failure at a specific altitude. The engine failure altitude occurred at an altitude of 650 ft AGL with a deviation of ±10% in height and ±200 ft in longitudinal distance along the runway that were accumulated from brake release to engine failure. An airspeed variation of ±3 kts and a bank angle variation of ±10° during turn were also used for all the segments of the manoeuvre. This accumulation in error was attributed from the normal flight segments tolerances specified by flight simulator tolerances as shown in Table 5.1. Hence, to determine the magnitude of the sensitivity of the forced landing manoeuvre to the tolerances in this analysis, flight dynamics equations were applied to three engine failure cases: the

** Takeoff distance is the distance from brake release until the aircraft has reached a specified altitude.

reference case, where no tolerance specifications were applied to the flight dynamics equations; the upper limit; and the lower limit that resulted from the different normal flight segments parameters tolerances combinations as specified by the ICAO.

5.3.2 Results

All possible combinations of ground roll, airspeed, height and bank angle tolerances of errors from normal flight segments were considered, and it was found that the upper limit in touchdown location was given by +200 ft in ground roll, +10% in height, -3 kts in velocity, and +10% in bank angle, as specified by the ICAO standards. The combination giving the lower limit in touchdown location is -200 ft in ground roll, -10% in height, +3 kts in velocity, and -10% in bank angle, as specified by the ICAO standards. The tolerances in ground roll and in failure altitude simply transform to a translation in the longitudinal distance along the runway. In addition, it was found that the engine failure altitude has the most effect on the touchdown locations.

Figure 5.5 shows the results from the sensitivity analysis. The non-linear error characteristics due to the ICAO tolerances are indicated by the area bounded by the upper limit (pink line) and the lower limit (blue line). The three curves at A represent the effect of the tolerance on the specific case for a teardrop turnback to the runway. The touchdown point varies from -210 ft to +570 ft. At B, the three curves represent the sensitivity if the pilot attempts a continuous 360° turn and touchdown on the runway. In this case, the touchdown point varies from -1639 ft to +1935 ft, a significantly larger range of error. At C, the three curves represent the case where the pilot glides straight ahead, the procedure recommended by the FAA. The touchdown point varies from -1650 ft to +1800 ft.

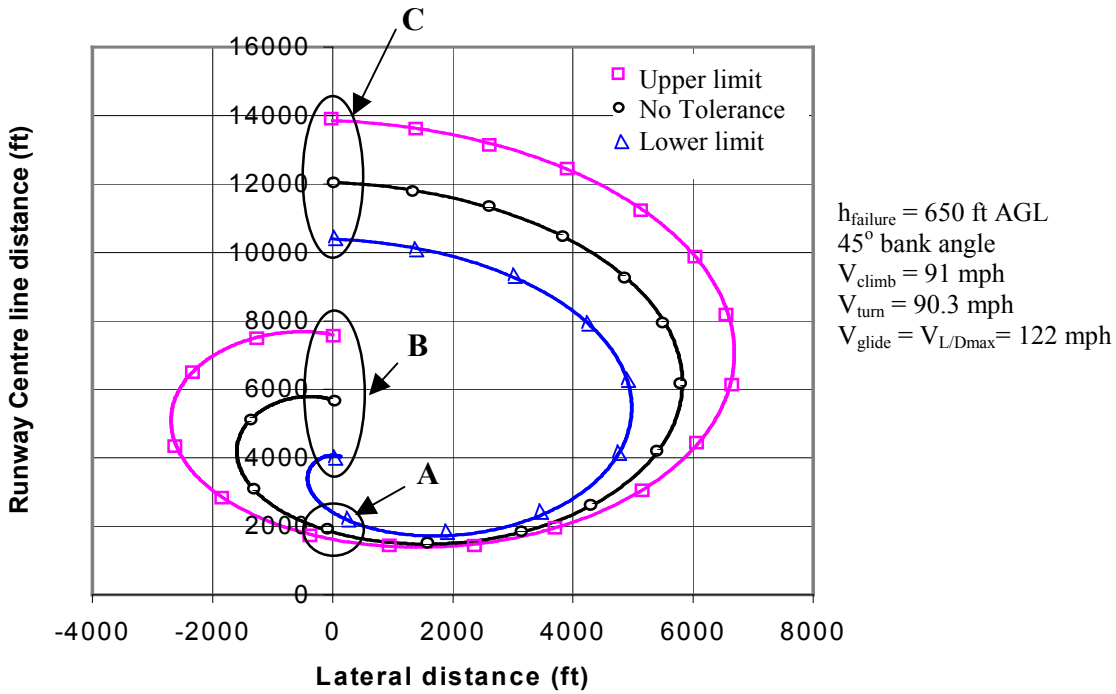

Figure 5.5 Landing Footprint Subject to International Standard Tolerance

There are potentially significant transfer of training issues that arise from this analysis. For example, the turnback procedure A gives a relatively small error. An error of 780 ft in a simulated flight from a typical runway of a length of about 4000 ft would probably not be significant. However, a pilot turning a full 360°, whose heading is now in the same direction as the takeoff direction and touchdown on the same runway (procedure B) as depicted in Figure 5.6 will encounter a possible variation of 3574 ft; clearly a significant error. In addition, if a pilot elected to land straight-ahead (procedure C), there would be an error of 3450 ft. An error of this magnitude could make the difference between whether a suitable field is reached or missed.

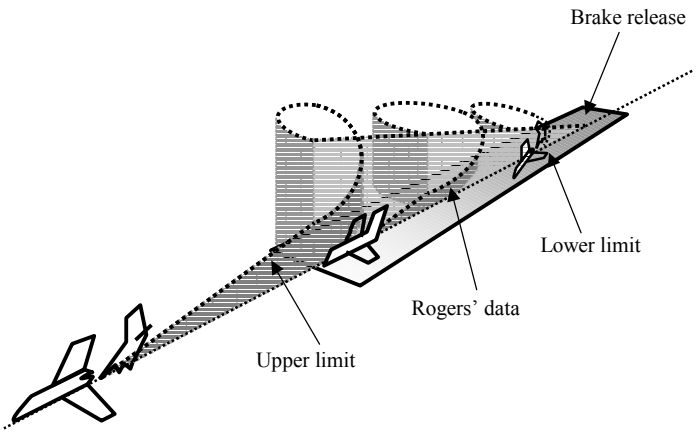

Figure 5.6 Sensitivity Analysis on Landing Footprints Following a 360° Turn Manoeuvre

The critical point here is that the magnitude of performance errors in a flight simulator cannot be assumed to be simply proportional to the tolerances for various individual parameters, but they may be highly dependent on the task being performed. For example, in the turnback case A, the errors appear small. The errors are small because the errors tend to cancel each other out, even in the worst case. In the simple glide straight ahead and in the 360° turn manoeuvre, the errors tend to accumulate due to the task being performed or the flying manoeuvre.

The implications of the sensitivity analysis are shown in Figure 5.7. The shaded area depicts the non-linear error characteristics for the case where no tolerance in error was considered in the analysis for the locus of touchdown points. As the engine failure altitude increases, the error for the 360° turn (case B) will move towards the straight glide to touchdown landing manoeuvre (case C). This result suggests that the simulated performance characteristics of every manoeuvre that is to be flown in a simulator should be validated against data from flight tests in the actual aircraft. It cannot be assumed that just measuring the input parameters alone is sufficient to ensure the simulator will provide adequate accuracy for all training exercises. Although validating the flight simulator data against actual flight tests in an actual aircraft may not be practical but nevertheless it demonstrates how a pilot would have flown the manoeuvre, for example, in one hundred trials, rather than just relying on the tolerances specified by the ICAO standards. Therefore, is it practical not to validate the data?

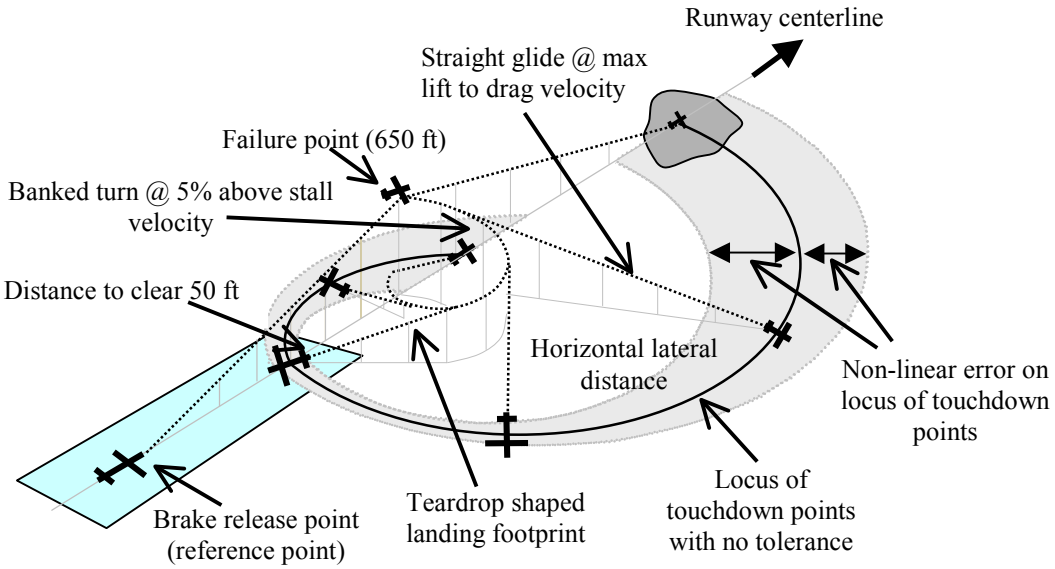

Figure 5.7 Sensitivity of Tolerance on Locus of Touchdown Points

5.3.3 Sensitivity Analysis on Forced Landing Manoeuvre with Vertical Atmospheric Turbulence Velocity

An essential component of any flight simulation is to incorporate an atmospheric model. The effects vertical atmospheric turbulence has on the theoretical forced landing manoeuvre considered here is not found in any of the qualification documents that are used for evaluating flight simulator performance because it is a manoeuvre for which flight test data would be difficult if not impossible to safely obtain. Hence, this analysis was carried out to investigate the effect vertical atmospheric turbulence has on the sensitivity analysis to the forced landing manoeuvre as carried out by (Tong, Bil *et al.* 2003). It investigates the effect vertical atmospheric turbulence, as described in Chapter 3.4, has on the tolerances prescribed in the Manual of Criteria for the Qualification of Flight Simulators (ICAO 1995) and on the performance of flight simulators used for pilot training. The simplified analytical model for the Beech Bonanza E33A with retractable undercarriage used in Chapter 5.2.1 was also used here to determine the effect of the aforementioned to tolerances on forced landings. The analysis was carried out for the following manoeuvre: after engine failure, the aircraft turned at 1° increment and continued with a straight glide to touchdown at maximum lift to drag velocity.

In this analysis, 100 vertical turbulence profiles were randomly generated assuming a reference speed (U_{20}) of 15 kts at 20 ft above mean sea level, an aircraft speed (V_T) of 122 mph, a turbulence scale length (L_w) of 650 ft and a turbulence intensity (σ_w) of $0.1U_{20}$ (15

kts) using the turbulence model described in Chapter 3.4 – Atmospheric Turbulence Models. The vertical turbulence velocities were time averaged from the engine failure point to where the aircraft changes its manoeuvre to straight glide to touchdown and from the beginning of the straight glide manoeuvre to touchdown. Therefore, two turbulent velocity components were added to the trajectory calculations for every turbulence profile simulation. All 100 vertical turbulence profiles were applied to each of the three cases considered in Chapter 5.3.1 – Sensitivity Analysis on Forced Landing Manoeuvre: the upper limit case, the lower limit case and the reference case where no flight simulator tolerance specifications were applied to the flight dynamics equations.

5.3.4 Results

Figure 5.8 shows the results for the vertical gust analysis on the different cases. Regions A, B and C are the touchdown points for the straight glide to touchdown corresponding to the upper limit (ranging from 13475 ft to 14303 ft), the reference case (ranging from 11711 ft to 12442 ft) and the lower limit case (ranging from 10100 ft to 10737 ft) respectively. Regions D, E, and F are the touchdown points if the pilot attempts a continuous 360° turn and touchdown along the runway centreline corresponding to the upper limit (ranging from 7424 ft to 7820 ft), the reference case (ranging from 5620 ft to 5752 ft) and the lower limit case (lack of height to complete a full 360° turn) respectively. The results show that the nature of the manoeuvre flown is highly sensitive to the vertical gust and is therefore important to flight simulation. The straight glide to touchdown manoeuvre shows possible touchdown locations that vary from approximately 637 ft to 828 ft distance, while for the continuous 360° attempt, it ranges from incomplete 360° turn to 396 ft distance. The vertical gust has the most effect during the initial phase of the forced landing flight manoeuvre since a small deviation in glide angle due to vertical gust will have a non-linear effect to the straight glide to touchdown sector, which will be magnified, on the horizontal distance. The effect for a 360° turn to touchdown is least affected since the turn radius is less susceptible to vertical gust. Therefore, it can be concluded that vertical turbulence has the most effect on the straight glide to touchdown manoeuvre and lesser effect on the turning manoeuvre.

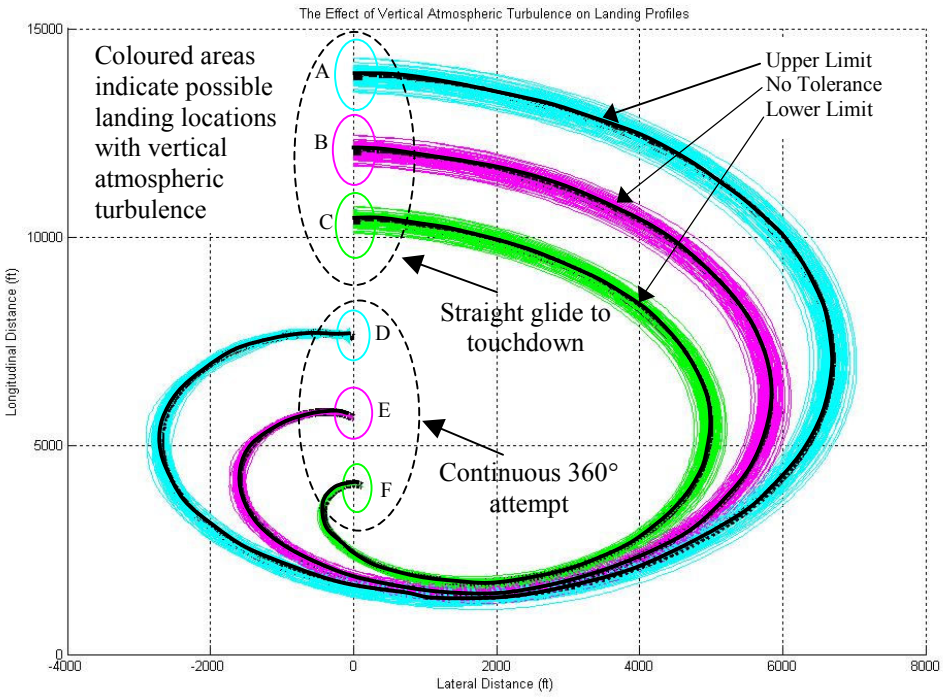

Figure 5.8 Landing Footprints with Vertical Atmospheric Turbulence

5.4 Concluding Remarks

These sensitivity analyses demonstrate the importance of simulator requirements and the consideration of such requirements within the context of particular manoeuvres to be flown, as in some cases, negative transfer of training may be induced since certain errors are manoeuvre dependent. The sensitivity analyses show that a simulator may incur potentially significant errors in the task of handling an engine failure after takeoff for a single engine aircraft. This raises the question of the ability to use simulators to train pilots aptly for engine failure after take-off using the tolerances as specified in current regulations since the resultant errors are manoeuvre dependent. With increasing prevalence of Single Engine Gas Turbine (SEGT) aircraft for Regular Public Transportation (RPT) operations and the increasing usage of flight simulators for smaller aircraft, the problems discussed become more relevant. It is not sufficient to assume that the present simulator regulations will be adequate for such operations. New applications of flight simulators will also require new types of data to be collected from flight tests. For example, the data collection methods should ensure that the tolerances achieved in the simulators are relevant for the specific training tasks performed in the simulators.

CHAPTER 6

GENETIC ALGORITHM IN A FORCED LANDING MANOEUVRE

6.1 Introduction

This chapter presents the analysis on the forced landing manoeuvre trajectory optimisation using Genetic Algorithm (GA), which is a branch of the guided random search technique. This search technique was chosen because of its simplicity in representing the problem mathematically.

6.2 Genetic Algorithm

GA has its roots in Darwin's Theory of Evolution where only the fittest individuals will survive and reproduce. It is also known as the "survival of the fittest". Drawing parallels from natural selection, (Holland 1975) proposed the GAs theory in the early 1970's which imitates the evolutionary processes in nature and it can be used as a search tool in optimisation problems. It performs a parallel, non-comprehensive search in the hope of finding the global maximum, if not a very near optimal solution, to optimisation problems. GA uses crossovers – a probabilistic mechanism, and mutations – a perturbation mechanism, as search mechanisms to generate a sequence of populations. The most rudimentary unit, the gene, which is made up of alleles, is combined to form chromosomes that control the "keys" to survival of the individual in a competitive environment. Evolution occurs when the chromosomes from two parents are combined during reproduction and a new gene pool is formed from combinations generated either through crossover or mutation.

GAs differ from other optimisation methods in its advantages in (a) its ability to solve complex problems by searching a large number of complicated solutions efficiently (implicit parallelism) and to locate a near optimal solution in a relatively short time, (b) the ability to solve non-linear problems such as those that may not be solved directly, analytically, algorithmically or those that do not have a precisely defined solving method or discontinuous functions, (c) problems that may involve contradictory constraints that must be satisfied simultaneously, (d) being less prone to getting stuck at a local optimum than the direct

methods or the indirect methods, (e) the use of probabilistic choice rather than deterministic rules and (f) the generations of results without the expense or effort of an enumerative search technique. One of the advantages in using GA is that it is not necessary to know how to solve the problem but rather to intelligently select and to encourage better offspring through a carefully developed fitness function and genetic operators. It also avoids the use of gradient, derivatives or other auxiliary knowledge, which may lead to pitfalls in hill climbing techniques. Although GAs are quick in locating near optimal solution and very effective in exploring very large solution domain space, they are not proficient for fine-tuning or improvement of the solution but this can be overcome with higher computational expense. However, no proof is available in GA for solution convergence since no gradient information is known but this shortcoming can be compensated with a wider search of the solution landscape or a complex solution domain.

GA can be expressed as a four part procedure of the evolutionary process: evaluation, selection, crossover, and mutation (Goldberg 1989). It begins with an initial population string of "random" characteristics of chromosomes representing the solutions to a problem. The initial population string to the chromosomes can be encoded or represented in ways that are best suited to the nature of the problem considered. It can be encoded (a) as binary where every chromosome is a string of bits of "1" or "0", (b) as permutation encoding where every chromosome is a string of numbers that represents a number in the sequence, (c) as value encoding where every chromosome is a string of some values that can be real numbers, (d) as characters or even some complicated objects or (e) as tree encoding where every chromosome is a tree of some objects such as functions or commands.

In the evaluation phase, the solutions to the combinations of chromosomes are calculated in the fitness function, which is usually the objective function, and those with high values will have a higher probability of ensuring their survival in the selection phase.

In the selection phase, the chromosomes from the evaluation phase are evaluated against the fitness value that is determined by a fitness function that is designed to evaluate potential solutions. The probability selection is based on the chromosomes' value relative to the rest of the population. This phase has an element of randomness, just like the survival of organisms in nature. The probability of being chosen is based on the random number generated which is equal to its relative fitness value and the number of chromosomes selected is equal to the population size specified, keeping the population size constant for subsequent generations.

The best chromosomes will be used for succeeding regenerations and the rest will be rejected. This approach is very effective since it is built on "good" strings from previous generations, making it unnecessary to search the entire field of possible solutions. As it turns out, each trial becomes less and less random. Once the "bad" string is eliminated, its entire subsequent offspring will be eliminated and this helps the process to rapidly converge to a solution. It is possible that some of the chromosomes are being selected more than once due to their high fitness value and multiple copies of the same chromosomes will be used in the crossover phase.

There exist different types of selection methods as described by (Brigger 1995; Obitko 1998). The roulette wheel selection – where parent chromosomes are selected based on their fitness and occupies a sector of the circle accordingly. Chromosomes with more frequent fitness values will be selected more frequently. One drawback with this method is that a fitter chromosome may not be selected and will be lost if it did not occur frequent enough to occupy a bigger sector of the circle for the selection. The rank selection – similar to the roulette method but first ranks the population where every chromosome receives a fitness value from this ranking and occupies a sector of the circle according to their ranking. The tournament selection – two chromosomes are randomly selected from the population and directly compared, and the fitter chromosome is chosen. A variation of the tournament selection is the two-branch tournament selection (Crossley, Cook *et al.* 1999). The steady-state selection – saves a certain number of the better chromosomes to be passed onto the next generation while the chromosomes with low fitness values are removed. A more specific case of this selection method is the elitism method, where a certain number of the best chromosomes are kept for the next generation. This method will always preserve some of the best chromosome structures ensuring that they are never lost in the optimisation process.

In the crossover and mutation phases, the crossovers and mutation genetic operators are applied to the chromosomes to create, promote and juxtapose building blocks in search for better offsprings (Srinivas 1994) . Crossover occurs when a group of genes from one chromosome (parent) is switched with another group of genes from another chromosome (the other parent) at one or more randomly chosen points on the chromosomes. The crossover probability is determined by the crossover rate. Mutation occurs when a minor perturbation randomly changes a single gene or genes on the new chromosome (offspring). The mutation probability is determined by the mutation rate. Mutation is used sparingly to prevent the solutions from converging to a local optimal solution or to prevent premature convergence

and plays a minor role compare to using crossover, which is the driving force of GAs. There has to be a balance in selecting the crossover rate and the mutation rate since crossover has greater influence at the beginning of the algorithm where it combines the best features from the different chromosomes. As the algorithm converges, mutation becomes more important because the chromosomes are now much more alike and mutation will introduce some diversity to the chromosomes.

There exist different types of crossovers as described by (Brigger 1995; Obitko 1998). The single point crossover which produces two different chromosomes that have the 1st part of the chromosome from one parent and the 2nd part of the chromosome from the other parent and vice versa with the other resulting chromosome, is illustrated as follows:

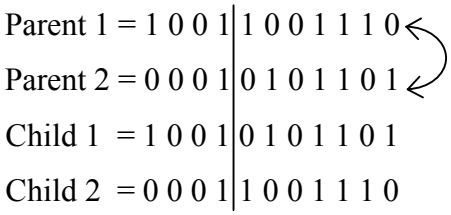

The two-point crossover which is similar to the single point crossover but produces two different chromosomes that have the 1st and the 3rd part of the chromosome from one parent and the 2nd part from the other parent and vice versa with the other resulting chromosome. The uniform crossover which randomly selects genes from the 1st and the 2nd parent is known have better performances (Syswerda 1989; Eshelman and Schaffer 1991; Eshelman and Schaffer 1993).

The GA cycle to solve a complex problem as shown in Figure 6.1 is to define the search space and to custom design a coding scheme for the solutions in the search space that are tailored to the problem. This is known as genetic representation. A fitness function is then designed to evaluate the potential solutions where the better solutions are kept for subsequent regenerations and the "inferior" solutions are discarded. The solutions are selected based on their fitness value to build the next generation. Elitism will ensure that a certain number of the current best chromosomes are kept for the next generation and they cannot be destroyed through crossover or mutation but can only be replaced by a fitter chromosome when a better offspring is found in the subsequent generations. The next generation of solutions are created by applying genetic operators such as crossover and mutation to evolve solutions for further fitness evaluations. The optimisation process will terminate when either an acceptable

tolerance in the results is obtained or when it has processed a specific number of generations or when no improvement in fitness value is encountered after a number of consecutive generations. The three most important features in GAs are the objective functions, the genetic representations and the genetic operators.

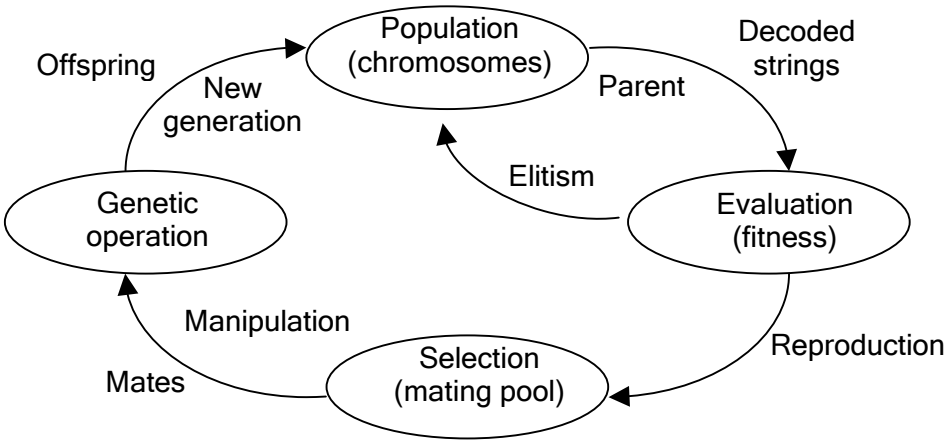

Figure 6.1 Genetic Algorithm Cycle

This relatively new optimisation method has been successfully used in aerofoil design such as topological design of nonplanar wings (Gage and Kroo 1993), subsonic wing design (Anderson 1995), subsonic wing design with pareto (Anderson 1996), transonic wing design (Obayashi and Yamaguchi 1997), Navier-Stokes optimisation of supersonic wings (Sasaki, Obayashi *et al.* 2002) and redesign of compressor cascade model (Obayashi 1998). GA has also been used in parametric and conceptual design of aircraft (Bramlette and Cusic 1989; Blasi, Iuspa *et al.* 2000; Ali and Behdinan 2002), conceptual helicopter design (Crossley and Laananen 1996) and in preliminary design of turbine engines (Tong and Gregory 1990). It has also been applied to missile and hybrid rockets optimisation (Anderson, Burkhalter *et al.* 2000; Schoonover, Crossley *et al.* 2000), multi-scenario force structuring and THUNDER Campaign model optimisation and repair time analysis (Hill, McIntyre *et al.* 2002), and to structural design problems (Hajela 1990; Crossley, Cook *et al.* 1999).

In this study, GA was used to search for optimal trajectories in a forced landing manoeuvre problem using method and assumptions made by Rogers as described in Chapter 2.3.2. The flight dynamics described in Chapter 3.2 were applied to a forced landing with discrete speed and discrete bank angle, and for a forced landing with variable speed and variable bank angle. The analyses were carried out in still air condition and with vertical disturbances such as vertical atmospheric turbulence and thermals flow field, and with horizontal wind.

6.3 Genetic Algorithm in a Forced Landing with Discrete Speed and Discrete Bank Angle

A complete evaluation of all possible trajectories for a forced landing manoeuvre is extremely computationally intense and is not practical if it is used to obtain optimal forced landing trajectories of acceptable resolutions. In this study, GA was used as a search technique to locate some of the optimal trajectories to a forced landing of a single engine aircraft after an engine failure. A fitness function was developed using the general flight dynamics equations (Pamadi 1998) based on the Beech Bonanza E33A single engine aircraft data as shown in Table 3.1. The problem considered for this analysis assumes an engine failure at 650 ft AGL after take-off. The engine failure point was used as the reference point for all distances calculated and calculations were carried out at a constant altitude decrement of 50 ft. Upon engine failure, the pilot can either turn right or left by banking ±45° flying at $1.05V_{stall(clean)}/\sqrt{\cos\phi}$, or glide straight at the maximum lift to drag velocity (122 mph). At every 50 ft drop in altitude, the pilot continuously has three options until he touches down. It assumes instantaneous transition from turning speed to gliding speed and the effects of landing gear retraction/extension are not considered. The aircraft is also assumed to be continuously dropping in attitude while manoeuvring its glide to touchdown.

The GA computer codes were developed in Matlab 5.3 for this implementation and were run on a Pentium 3, 600Mhz with 512Mb RAM. The GA optimisation procedure is shown in Figure 6.2.

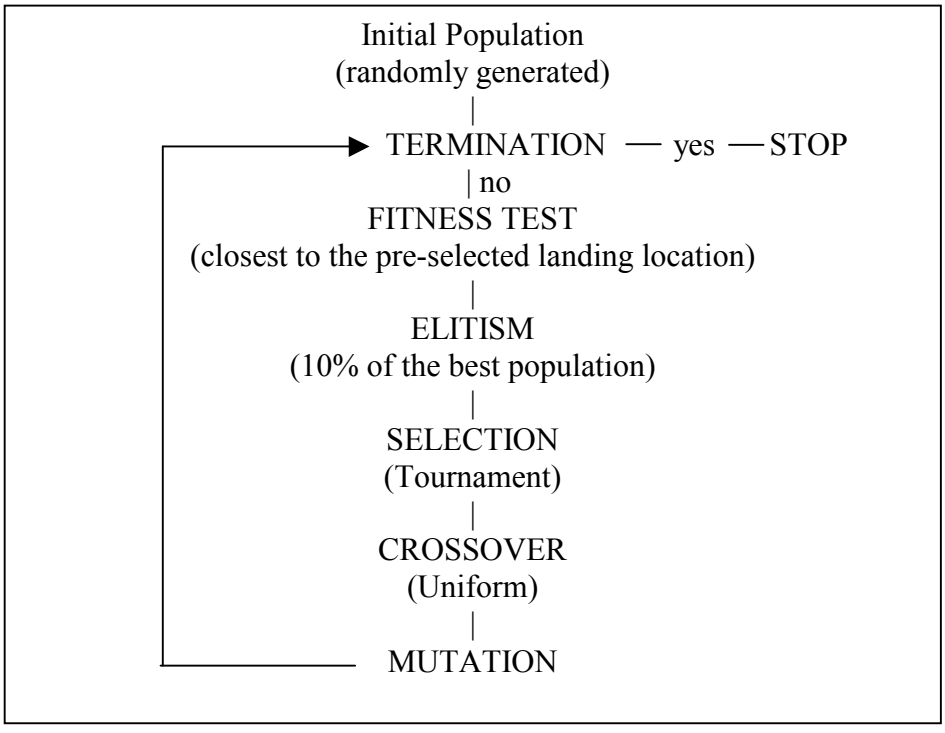

Figure 6.2 Genetic Algorithm Programming Cycle

6.3.1 Direct-Value Control Parameters Selection

A common issue that arises in using GA as an optimisation method is the proper selection of parameter settings (Goldberg 1985; Grefenstette 1986; Srinivas 1994). Using a large population of chromosomes will increase computational time but it will prevent premature convergence to a local optimum while using a small population of chromosomes will reduce computational time but it may converge prematurely to a sub optimal solution. In general, a high crossover rate increases the recombination of building structures but an excessive crossover rate may lead to high-performance structures being discarded faster than the selection process is able produce improvement while a low crossover rate may stagnate the optimisation process. The selection of the crossover rate also depends on the population sizes where higher crossover rate for smaller populations can prevent premature convergence while lower crossover rate be used for larger populations since they have larger search space. A high mutation rate, which is more important in later generations, resembles a random search but it may help to reintroduce lost structure while a low mutation rate may lead to a convergence to a local optimum.

(Williams and Crossley 1998) conducted an empirical study on the effects of how population sizes and mutation rates affect the GAs performances when binary coding and uniform crossover were used. They carried out a GA parameter test for three test problems for N varying from l to $8l$ at $2l$ increments, where N and l are the population size and the number of bits used in the chromosome representation respectively. Their mutation rate tests were conducted for $\frac{(3l-1)}{2Nl}, \frac{1}{N}, \frac{(l+1)}{2Nl}, \frac{1}{Nl}$ *and* $\frac{1}{2Nl}$. They suggested using uniform crossover with a crossover rate of 50% which is equivalent to 50% crossover points on strings with length l. Their results shows that a population size of $4l$ and a mutation rate of $(l + 1)/2Nl$ will make a good guideline for direct-value control parameters selection.

Since GA method relies on stochastic processes and is optimisation objective dependent, a control parameter test using direct-value representation was carried out to determine the proper selection of the population size, the number of generations, the crossover rate and the mutation rate for the forced landing problem with discrete speed and discrete bank angle. Numerical computations were carried out for three sets of test touchdown locations that are located at 0 ft laterally and –3100 ft longitudinally and at 3000 ft laterally and 3000 ft longitudinally from the engine failure point. Calculations were carried out at a constant discrete height decrement of 50 ft. A preliminary parameter test was carried out for

population sizes ranging from 500 to 2000 at an increment of 500, with number of generations varying from 50 to 200 at an increment of 50, with uniform crossover rates varying from 50% to 90% at an increment of 20% and with mutation rates varying from 10% to 90% at an increment of 20%. These preliminary results show that a mutation rate of 10% and a population size of 500 will achieve the desired fitness value.

Although GAs are robust optimisation techniques and only require customisation of fitness function to the specific problem considered, an enhanced fine-tuning of the GA can improve its performances. The GA fine-tuning procedure may include different combinations of genetic operators and better selection of parameters or techniques to boost its adaptation to the design space size and topology. Further fine tuning of genetic operators was conducted using guidelines from (Williams and Crossley 1998) and a uniform crossover rate of 50% was used as suggested by (Eshelman and Schaffer 1991; Eshelman and Schaffer 1993). A test was carried out for a 13 bits string length for population size ranging from 26 ($2l$) to 156 ($12l$) at an increment of 26 ($2l$), for a mutation rate of 1% to 9% at an increment of 2% and for an elitism of 10% of the population size for subsequent generations. The GA in this test used tournament selection whereby two chromosomes were compared at any one time rather than comparing an individual chromosome to the entire population. This selection method prevented fitness scaling where a few highly fit chromosomes may dominate the parent population. A stopping criterion of 100 generations and repetitions of 100 GA runs were carried out on each of the 30 combinations of parameters to reduce the effect of probabilistic "noise".

For each run, the best fitness value and the frequency of the best fitness value were recorded as measures for the GA's performance. These values were averaged over the 100 runs for each combination of population size and mutation rates to provide a representative performance of a general GA run. The average performance values for each combination were normalised with respect to those values from runs with a population size of 13 (l) and a mutation rate of 1%. The computation cost is defined as a product of the population size and the minimum number of generations it takes to obtain the minimum value for each trial limited to the stopping criterion of 100 generations used. Larger population sizes usually provide a more accurate solution, however, there is very little improvement in fitness value for population sizes above $4l$ (N = 52) as shown in Figures 6.3 and 6.4. This minimal improvement in fitness value is at the expense of greater computational cost, which in general is a linear increase of computational effort for an increase in population size.

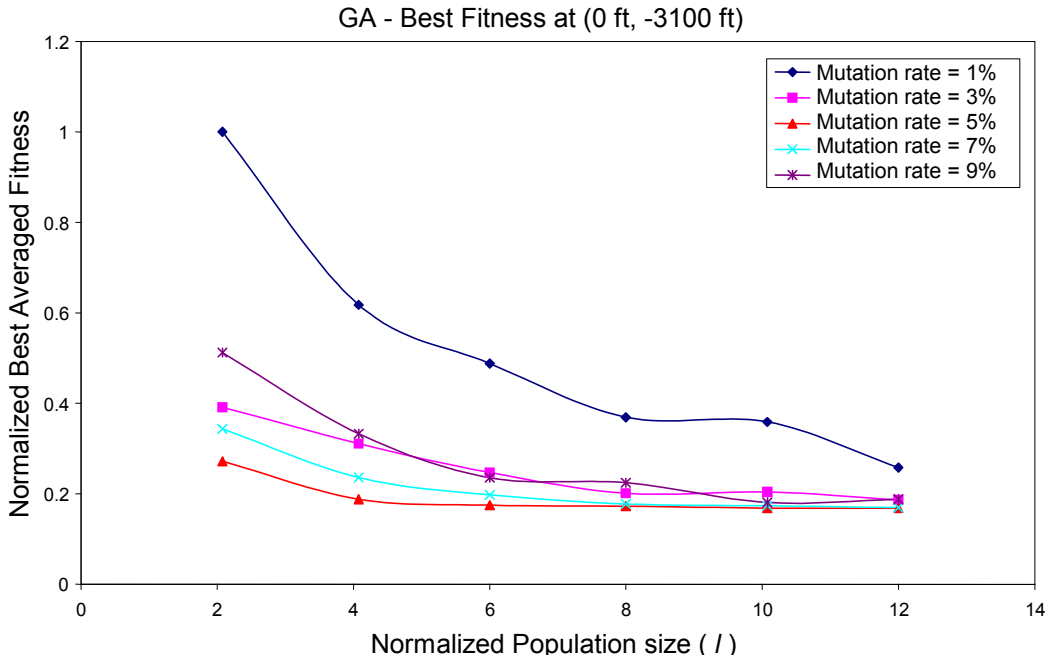

Figure 6.3 Direct-Value GA Control Parameter - Best Fitness at (0 ft, -3100 ft)

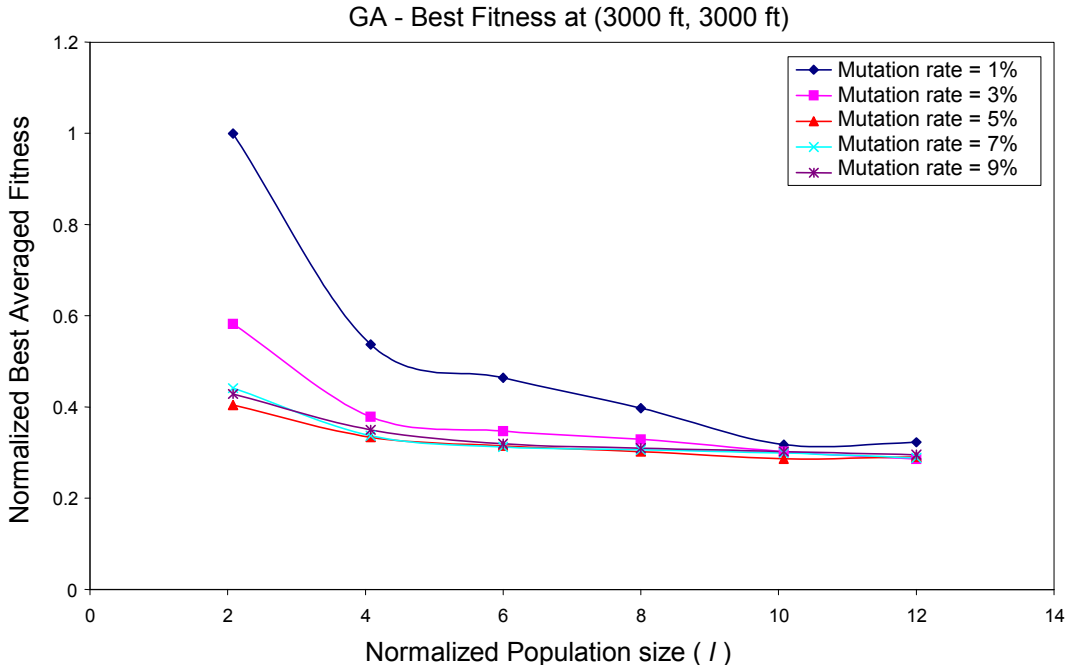

Figure 6.4 Direct-Value GA Control Parameter - Best Fitness at (3000 ft, 3000 ft)

While there is a minimal improvement in the best fitness for populations greater than 6*l* for mutation rate greater than 1%, the computational effort continues to increase as shown in Figures 6.5 and 6.6. The results suggest that a population size of $N = 4l$ ($N = 52$) is an appropriate compromise for the best fitness value and a reasonable computational effort.

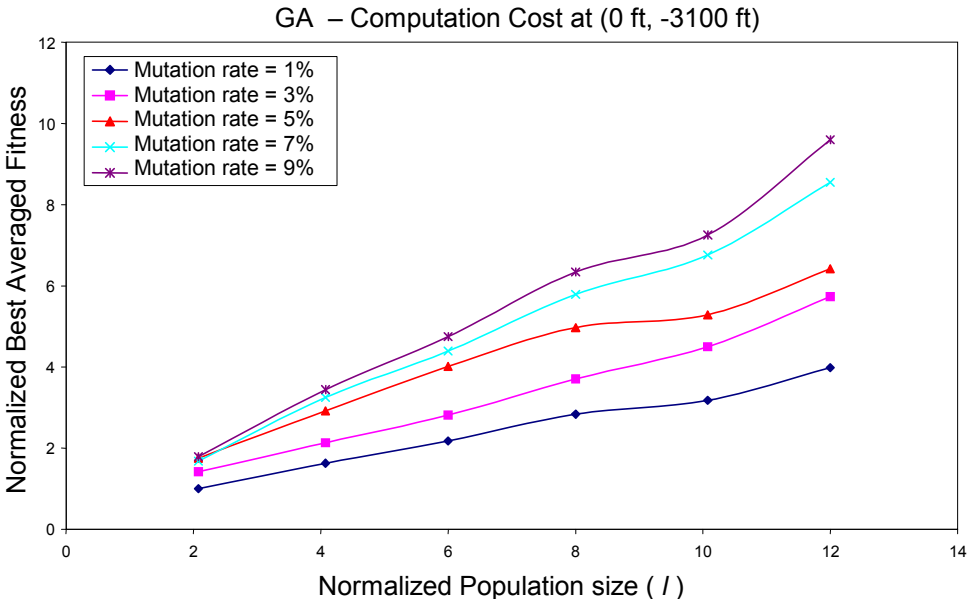

Figure 6.5 Direct-Value GA Control Parameter - Computational Cost at (0 ft, -3100 ft)

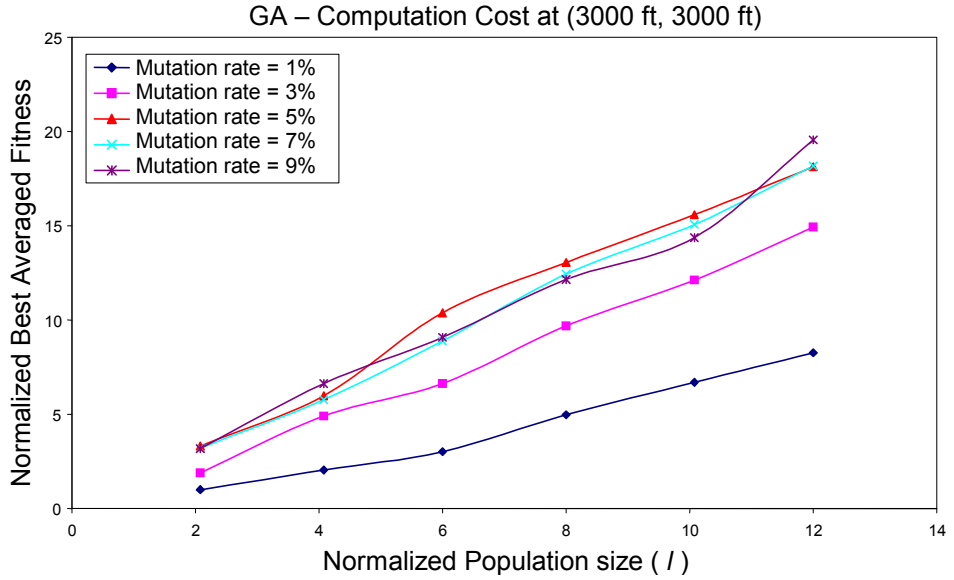

Figure 6.6 Direct-Value GA Control Parameter - Computational Cost at (3000 ft. 3000 ft)

Although a mutation rate of 5% provides the best minimum averaged fitness value for the touchdown location at 0 ft laterally and –3100 ft longitudinally, a mutation rate of 7% gives the best result in locating the global optimum value for all the three touchdown locations tested. A slightly higher mutation rate increases the probability of locating the global minimum value when there exist several neighbourhood values of very small differences from the global minimum value in the solution space. Based on the GA direct-value control parameter analysis carried out, a population size of 52, a uniform crossover rate of 50%, a mutation rate of 7% and tournament selection will be used for GA with discrete speed and discrete bank angle for trajectory optimisation for a forced landing manoeuvre after an engine failure. The best fitness values found by the GA search method were compared to the best fitness values found by the exhaustive search method. The GA search method successfully located the best fitness values as found by the exhaustive search method for all the three-touchdown locations considered.

For the two touchdown locations considered, similar trends of best fitness and computational cost performance versus population size are observed. The fitness performance improves with increasing population size and with mutation rate greater than 3%. This continues until the population size begins to exceed 52 ($4l$) where little or no improvement in fitness performance is observed beyond a population size of 52 ($4l$). In general, the computational cost increases linearly with population size and with mutation rate. Hence, increasing the population size beyond $4l$ does not appear to be worth the related computational cost. For small population sizes, the mutation rates appear to have a significant effect on the fitness performance but as the population sizes increases beyond $4l$, the effect becomes minimal. For larger population sizes, the improvement in fitness value in increased mutation rate is smaller than the improvement in fitness value in an increase in population size. A mutation rate of 7% is deemed to be the best rate for locating the best fitness value to the forced landing of an aircraft after an engine failure for discrete speed and discrete bank angle considered in this analysis. GA convergence history is important to the understanding of its behaviour as sometimes the number of generations ran may not be sufficient for it to find the exact optimum. Figure 6.7 illustrates the typical convergence histories for 100 generations for each of the 100 trials for a particular direct-value control parameter combination obtained from the direct-value control parameter selection analysis. No premature convergence is observed and running it for 100 generations has allowed a satisfactory development of the population.

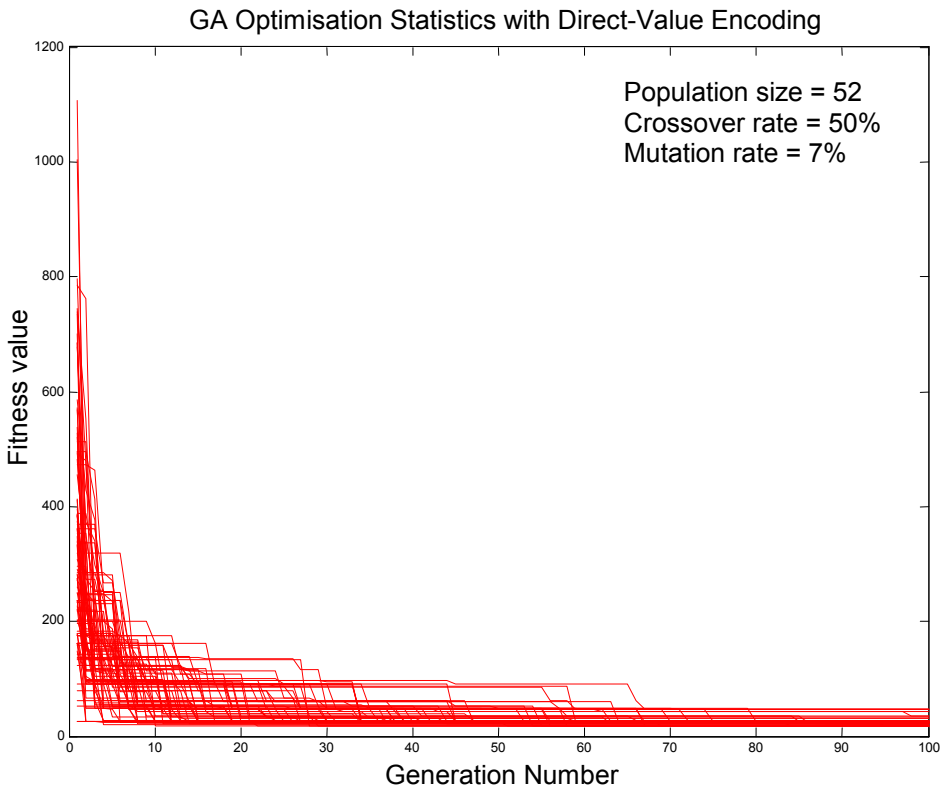

Figure 6.7 Direct-Value GA Evolution History for 100 Trials

6.3.2 GA Results for a Forced Landing with Discrete Speed and Discrete Bank Angle

A forced landing with discrete speed and discrete bank angle using direct-value representation GA was carried out for three test locations; (0 ft, -3100 ft), (3000 ft, 3000 ft) and at (500 ft, 200 ft), where the 1st component represents the lateral distance and the 2nd component represents the longitudinal distance from the engine failure point. A discretisation error analysis for different number of discrete steps in altitude drop to touchdown was also carried out for the three pre-selected locations to gain in-sight the numerical error that the different step sizes might have on the results. The GA forced landing trajectory simulations, for an engine failure at 650 ft AGL, were discritised at every 50 ft, 25 ft and 10 ft drop in altitude which corresponded to calculations for 13 discrete steps, 26 discrete steps and 65 discrete steps to touchdown respectively. For this analysis, the GA population size used the product of four times the chromosome length as suggested in the section on Direct-Value Control Parameters Selection and the chromosome length in this analysis is the number of steps used in the simulation. Therefore, the population sizes used were 52, 104 and 260, which corresponded to discretisation at an altitude drop of 50 ft, 25 ft and 10 ft respectively. It also used a mutation rate of 7%, a crossover rate of 50% and

tournament selection as determined in the previous section for GA with Direct-Value Control Parameter Analysis. A repetition of 100 trials was carried out for each test location to reduce the effect of probabilistic "noise" since GA is a probabilistic guided-search method. This GA search method used the fitness criteria of touching down closest to the pre-selected location. The computational time for the different number of discritisation steps to touchdown were normalised with respect to the case for 13 discrete steps to touchdown (Computing time 1X). The results for the GA with discrete speed and discrete bank angle for touchdown distance from the respective pre-selected landing locations are shown in Table 6.1 – 6.3.

Table 6.1 Results for Forced Landing with Discrete Speed and Discrete Bank Angle for Discritisations at Every 50 ft Drop in Altitude

Statistics	Pre-Selected Location		
	(0 ft, -3100 ft)	(3000 ft, 3000 ft)	(500 ft, 200 ft)
Minimum Distance (ft)	65.2443	17.2520	21.6141
Average Distance (ft)	77.8297	25.8025	28.1311
Maximum Distance (ft)	208.6568	49.4178	62.8629
Standard Deviation	38.9020	6.6946	12.4130
Probability of Landing < 10ft	0 %	0 %	0 %
Probability of Landing < 50ft	0 %	100 %	89 %
Probability of Landing < 100ft	92 %	100 %	100 %
Probability of Landing at Minimum Distance	81%	1%	77%

Computing time 1x

Table 6.2 Results for Forced Landing with Discrete Speed and Discrete Bank Angle for Discritisations at Every 25 ft Drop in Altitude

Statistics	Pre-Selected Location		
	(0 ft, -3100 ft)	(3000 ft, 3000 ft)	(500 ft, 200 ft)
Minimum Distance (ft)	15.2838	0.9126	1.3937
Average Distance (ft)	301.6279	11.8877	15.8839
Maximum Distance (ft)	493.5270	26.8114	35.1971
Standard Deviation	102.7215	5.8957	7.6426
Probability of Landing < 10ft	0 %	41 %	27 %
Probability of Landing < 50ft	3 %	100 %	100 %
Probability of Landing < 100ft	4 %	100 %	100 %

Computing time 4x

Table 6.3 Results for Forced Landing with Discrete Speed and Discrete Bank Angle for Discritisations at Every 10 ft Drop in Altitude

Statistics	Pre-Selected Location		
	(0 ft, -3100 ft)	(3000 ft, 3000 ft)	(500 ft, 200 ft)
Minimum Distance (ft)	709.1898	0.3230	21.4545
Average Distance (ft)	1038.1	4.7183	251.9339
Maximum Distance (ft)	1322	13.8913	448.9114
Standard Deviation	120.6026	2.4636	95.2381
Probability of Landing < 10ft	0 %	99 %	0 %
Probability of Landing < 50ft	0 %	100 %	2 %
Probability of Landing < 100ft	0 %	100 %	6 %

Computing time 24x

For the pre-selected location at (0 ft, -3100 ft), the results for minimum distance closest to the pre-selected location were found when discretisation occurred at every 25 ft drop in altitude. However, the minimum average distance and the shortest maximum distance closest to the pre-selected location were found when discritisation occurred at every 50 ft drop in altitude. It also has the lowest standard deviation and the highest probability of landing less than 100 ft from the pre-selected location. For the pre-selected location at (3000 ft, 3000 ft), the best results in all categories were obtained when discretisation occurred at every 10 ft drop in altitude. However, the quality in such high precision is at the expense of a very long computing time of 24 times when compared to discritisation at every 50 ft drop in altitude. For the pre-selected location at (500 ft, 200 ft), the best results in all categories were obtained when discretisation occurred at every 25 ft drop in altitude. However, the quality in results requires a computing time of 4 times the computing time for discretisation at every 50 ft drop in altitude.

The results seem to show that the touchdown distance from the pre-selected location are location dependent and smaller discrete step size in altitude drop may not necessarily provide better results as shown in the case for discritisation at every 10 ft drop in altitude. This may also be due to the insufficient number of generations used (100) in the GA program for discritisation at 10 ft drop in altitude, although the same number of generations may be adequate for discritisation at 50 ft and 25 ft drop in altitude. Running the GA program for more generations will increase the computing time exponentially of more than 24X and therefore proof very inefficient. The higher quality in results may not necessarily worth the extra computing time. Based on all the factors considered, calculations at every 50 ft drop in altitude will be used for the forced landing analysis in this study.

In order the to test the validity and the reliability of the GA search procedure developed, an exhaustive search was carried out for discritisation at every 50 ft drop in altitude and the minimum distances found using GA for all three test locations are the same as those obtained using the exhaustive search method. The global minimum distances found using the GA search technique are indeed the nearest distances from each of the pre-selected location when constant discrete speed, bank angle and height decrement intervals for discrete calculation steps were used. Note that the used of constant values in the calculations have also contributed to the difference in the distance between the touchdown locations and the pre-selected locations found. The very low probability of 1%, as shown in Table 6.1, in landing at the global minimum distance for the location (3000 ft, 3000 ft) is due to the nature of the

solution landscape. For fitness values with neighbourhood values of very small differences, GA will have a very low probability in locating the global minimum value if not nil since GA concentrates in that solution space and the nearby adjacent values maybe found instead as shown by the high probability of 100% in landing within 50 ft from the pre-selected location. A slightly higher mutation rate may assist in locating the global minimum value in such a solution landscape. Both the direct-value representation GA search method and the exhaustive search method found the same global minimum distances from the pre-selected locations and the same unique trajectory paths for each of the three pre-selected locations. The quality of the results obtained for all three locations can be observed from the high probability in landing less than 50 ft from the pre-selected locations, except for the case of (0 ft, -3100 ft). This is because the minimum possible distance for the calculation resolution used is 65.24 ft and it has a 92% probability of landing less than 100 ft from the pre-selected location. The quality in the results obtained using GA is due to numerical error in the resolution used in the calculations and not in the technique used.

Figure 6.8 shows the optimal and the unique forced landing flight paths found from the 100 GA runs for the pre-selected location at (0 ft, -3100 ft). The flight manoeuvre for this forced landing can generally be described as follow. Upon engine failure at 650 ft AGL, the pilot can either turn right or turn left banking at 45° while flying at $1.05V_{stall(clean)}/\sqrt{\cos\phi}$ (89.9 mph) and at an approximate heading of 180° descending until 300 ft AGL. The pilot then continues gliding straight ahead at maximum lift to drag velocity (122 mph) until 250 ft AGL where the pilot continues turning towards the pre-selected location flying at 89.9 mph and banking at 45° for the next 50 ft descend in altitude. From here onwards, the pilot continues gliding at the maximum lift to drag velocity (122 mph) while heading towards the pre-selected location of (0 ft, -3100 ft) until he touches down. The landing manoeuvre found is very similar to (Rogers 1995)'s teardrop turn around manoeuvre to runway.

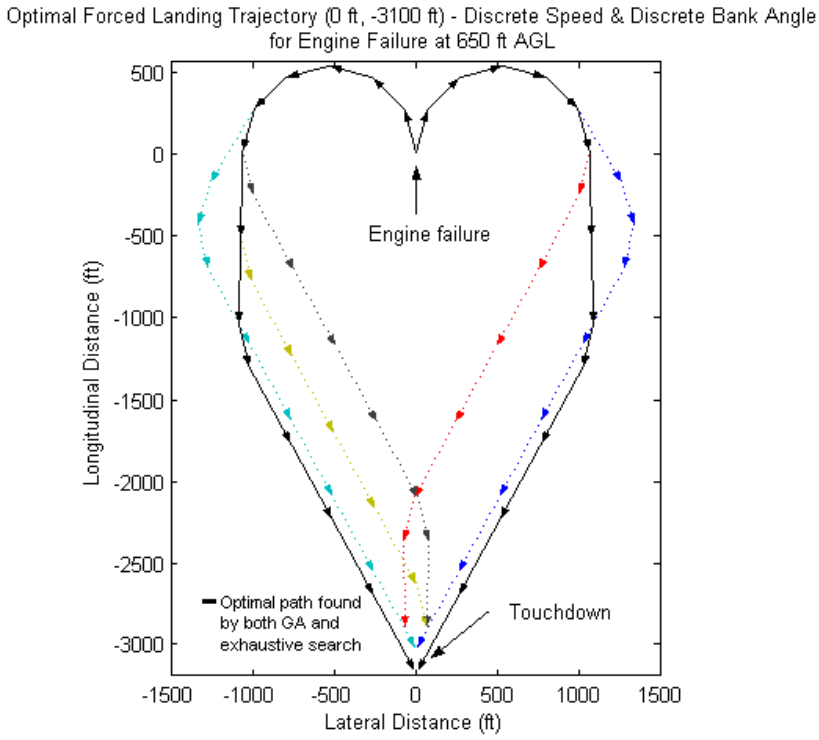

Figure 6.8 Optimal Forced Landing Trajectory Discrete Speed and Discrete Bank Angle (0 ft, -3100 ft) for Engine Failure at 650 ft AGL

Figure 6.9 shows the optimal and the unique forced landing paths found from the 100 GA runs for the pre-selected location at (3000 ft, 3000 ft). The flight manoeuvre for this forced landing can generally be described as follow. Upon engine failure at 650 ft AGL, the pilot banks left at 45° while flying at $1.05V_{stall(clean)}/\sqrt{\cos\phi}$ (89.9 mph) and at a heading of approximately left 30° for a 50 ft descend in altitude. This is followed by gliding straight ahead at the maximum lift to drag velocity (122 mph) for the next 50 ft descend in altitude. The pilot then continues banking right at 45° while flying at 89.9 mph for the next 150 ft descend in altitude. From here onwards, the pilot continues flying at maximum lift to drag velocity (122 mph) towards the pre-selected touchdown location of (3000 ft, 3000 ft). The optimal flight path follows a route that requires the pilot to initially bank away from the pre-selected location. This is because the GA program developed for an engine failure at 650 ft AGL did not consider flying directly to the vicinity of the touchdown point and then circle to touchdown due to the low engine failure altitude which may not allow the airplane to complete its orbit.

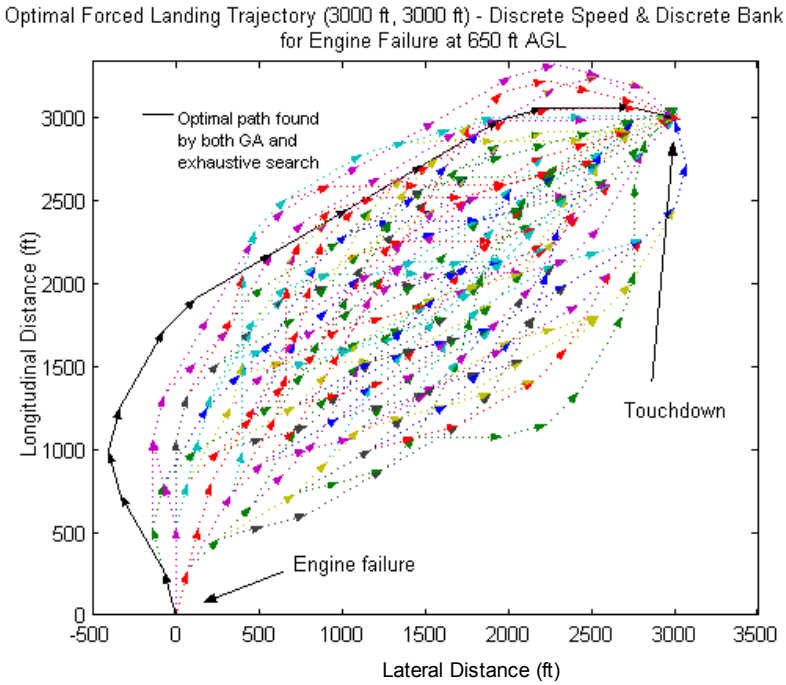

Figure 6.9 Optimal Forced Landing Trajectory Discrete Speed and Discrete Bank Angle (3000 ft, 3000 ft) for Engine Failure at 650 ft AGL

Figure 6.10 shows the optimal and the unique forced landing paths found from the 100 GA runs for the pre-selected location at (500 ft, 200 ft). The results show 2 general flight paths since the pre-selected location is located very near the airplane's line of symmetry at engine failure point. However, the optimal flight path for this pre-selected location is to turn towards the destination. The flight manoeuvre for this forced landing can generally be described as follow. Upon engine failure at 650 ft AGL, the pilot turns right by banking 45° while flying at $1.05V_{stall(clean)}/\sqrt{\cos\phi}$ (89.9 mph) for a 50 ft descend in altitude. This is followed by gliding straight ahead at the maximum lift to drag velocity (122 mph) and a heading of 30° right for the next 100 ft to 150 ft descend. The pilot then continues banking right at 45° while flying at approximately 89.9 mph for the next 250 ft to 350 ft descend and heads toward the pre-selected touchdown location flying at the maximum lift to drag velocity (122 mph). The optimal flight path follows a route that seems to fly further away from the pre-selected location. This is to allow for a higher success rate in landing closer to the pre-selected touchdown point since the engine failure height is at a low altitude, which may not allow the airplane to complete its orbit.

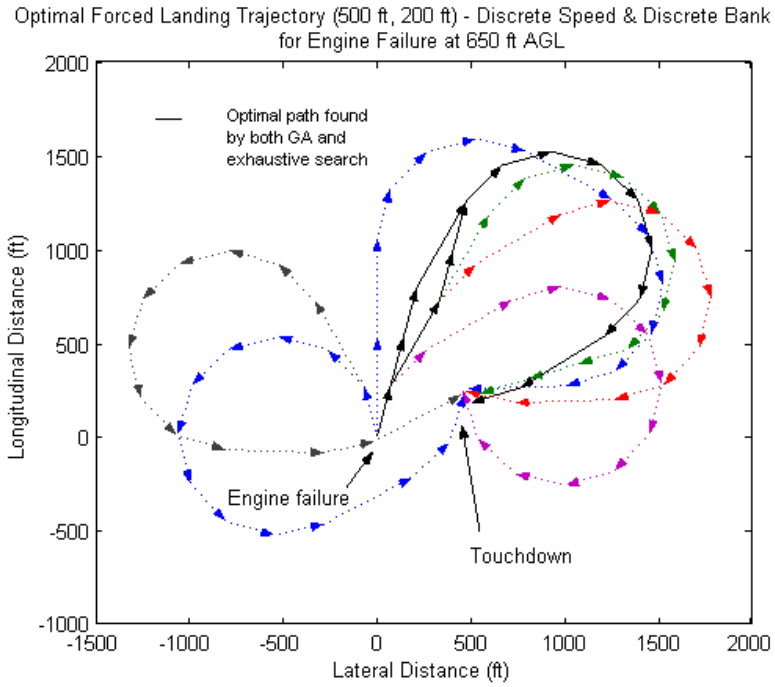

Figure 6.10 Optimal Forced Landing Trajectory Discrete Speed and Discrete Bank Angle (3000 ft, 3000 ft) for Engine Failure at 650 ft AGL

6.4 Genetic Algorithm in a Forced Landing with Variable Speed and Variable Bank Angle

The direct-value representation used in the GA with discrete speed and discrete bank angle lacked the exploitation of mathematical characteristics of the solution space. It also suffered a precision in locating more accurate touchdown locations since constant discrete values were used to represent the two flying speed (5% above stall speed and maximum lift to drag speed) and the three direction headings (straight, right – banking at +45°, left – banking at -45°). Although the precision in the direct-value representation can be increased with longer direct-value length, it suffers an exponential increase in computational time and disruptions in the building blocks known as Hamming cliff (Goldberg 1989), which affects the fitness landscape in the solution space. Hence, for the forced landing GA search analysis with variable speed and variable bank angle, a real-value representation in the chromosomes was also carried out to allow for a wider domain representation without sacrificing precision for larger domain size given a fixed chromosome length. It also allowed for a continuous search for the aircraft's speed and bank angle parameters instead of the discrete values used in the previous version of the GA search for a forced landing manoeuvre. A real-value representation also helped to exploit the numerical properties of a candidate solution by exploiting the solution gradients and information from the function's landscape.

Using the procedures and the results obtained from the GA forced landing search with discrete bank angle and discrete speed, the GA Matlab codes developed were modified to allow for variable bank angle and variable speed for a real-value representation of the chromosomes. The forced landing manoeuvre analysis was carried out at an engine failure height of 650 ft AGL for bank angle varying from banking left at 45° to banking right at 45° and with the aircraft's speed varying from 75.6 mph to 208 mph corresponding to 5% above aircraft's stall speed and maximum speed respectively. The calculations were performed at a fixed number of altitude decrement since GA requires a predetermined number of chromosomes in the genetic representations. It is assumed that the airplane is constantly loosing altitude and the updraft turbulence is less than the airplane's sink rate. Calculations were carried out at constant discrete height decrement of 50 ft for convenience instead of at constant time interval since constant discrete time interval may not allow the GA to terminate at exactly 0 ft AGL due to the different descent speed used for straight glides and for glide turns. A chromosome length of 26 is used since there are 13 discrete steps of 50 ft drop in altitude to ground level for an engine failure height at 650 ft AGL and two variables (speed and bank angle) for each step.

6.4.1 Genetic Operators

The GA real-value chromosome is represented by a vector $\vec{x} = (x_{1, \ldots} x_n)$, where n is the chromosome length. The chromosome length for a real-value representation is equivalent to the number of variables used to represent the domain while the chromosome length used for a direct-value representation depends on the precision used to represent the domain. Each gene, (x_k), in the chromosome is bounded by an upper limit (x_{max}) and a lower limit (x_{min}) specific to the gene. A brief description from (Michalewicz 1996) is presented here for the different operators used for a real-value representation. The genetic operators used in this analysis consist of three types of mutation operators and three types of crossover operators:

Uniform mutation randomly mutates a gene in the chromosome with uniform probability distribution to any value within the real-value domain range. This operator is important in the early phases of the evolution process, as the solutions are free to move within the search space.

Boundary mutation mutates a gene to either the lower boundary value or the upper boundary value for the real-value range. This operator is very useful for GAs with constraints.

Non-uniform mutation mutates a gene by a factor that is a function of the difference in value between that particular gene and either of its boundary value, and the generation number. This mutation probability will decrease to 0 as the generation number increases. This type of mutation is used for local fine-tuning of genes where the operator will initially search the space uniformly and very locally at later generations. The particular element (x_k) that is to be mutated within a population will be mutated as follow,

$$x'_k = \begin{cases} x_k + \Delta(t, \text{right}(k) - x_k) & \text{if a random binary digit is 0} \\ x_k - \Delta(t, x_k - \text{left}(k)) & \text{if a random binary digit is 1} \end{cases}$$

where right(k) = upper boundary domain value

left(k) = lower boundary domain value

and the function $\Delta(t,y) = y \bullet r(1-t/T)^b$

where b = coefficient for non-uniform mutation

r = random number from [0..1]

t = generation number

T = total number of generations

Arithmetic crossover linearly combines the genes from two parents to produce two children; $Child_1 = a*Parent_1 + (1-a)*Parent_2$; $Child_2 = (1-a)*Parent_1 + a*Parent_2$, where a is a random value $a \in [0..1]$.

Simple crossover is very similar to the traditional one-point crossover where a random point in the chromosome is selected as the crossover point. The offspring are formed when the genes from the 1st part of one parent is combined with genes from the 2nd part of the other parent. If $Parent_1 = (x_1, \ldots x_n)$ and $Parent_2 = (y_1, \ldots y_n)$, $Child_1 = (x_1, \ldots x_k, y_{k+1}, \ldots y_n)$ and $Child_2 = (y_1, \ldots y_k, x_{k+1}, \ldots x_n)$.

Heuristic crossover uses the values of the objective function in determining the direction of the search and it may or may not produce an offspring. It is responsible for local fine-tuning and search in the promising direction. It creates a single offspring, $Child_1$, from two parents, $Parent_1$ and $Parent_2$. $Child_1 = r * (Parent_2 - Parent_1) + Parent_2$, where r is a random number $r \in [0..1]$ and $Parent_2$'s fitness value is better than $Parent_1$'s fitness value. If

the random number *r* did not produce a feasible offspring, another *r* will be generated to produce another offspring. If no feasible offspring is generated after a specific number of attempts, no offspring will be produced.

All of the six genetic operators described were required to explore the search space adequately and were used equally to prevent premature convergent without regard to fitness. For example, arithmetical crossover will tend to drive the population to the numerical center of the search space very quickly, regardless if it yields good fitness values and boundary mutation will set the gene to either of its boundary value. However, the use of other operators prevented such problem. It is through the combination of these powerful crossover and mutation operators developed by (Michalewicz 1996) that the search space can be explored and good genetic material exploited.

In order to randomise the use of the three types of crossovers and mutations uniformly, the populations were randomly chosen for the different types of crossovers and mutations. The three types of crossovers and mutations were applied equally to all the randomised populations in every generation to allow for equal distribution.

6.4.2 Real-Value Control Parameters Selection

An analysis on the control parameters selection for real-value encoding as shown in Appendix A was carried out to test its suitability for simple two-dimensional, uni-modal problems with increasing number of state variables and complexity levels to multi-modal functions. The results show that real-value representation is suitable for the problem considered in this study. As mentioned in Chapter 6.2, although GAs are robust optimisation techniques and only require customisation of fitness function to the specific problem considered, fine-tuning will conduct the search more efficiently and improve its performances. A genetic operator control parameter selection process using real-value representation as shown in Table 6.4 was carried out at three test locations: at (3000 ft, 3000 ft), at (0 ft, -3100 ft) and at (500 ft, 200 ft) to obtain a set of suitable control parameters for use in the forced landing manoeuvre with variable speed and variable bank angle. The GA in this analysis used tournament selection, an elitism of 10% of the population size for subsequent generations and a stopping criterion of 100 generations. The actual population size used may be adjusted, if necessary, to coincide with multiples of chromosome lengths to ensure that an even number of chromosomes are available for the crossover process since

some of the best chromosomes are kept for elitism. A repetition of 100 GA runs was carried out on each of the 200 combinations of parameters for each test location to reduce the effect of probabilistic "noise".

Table 6.4 Real-Value Control Parameters Selection

GA Control Parameters	Range	Step Size
Generations	100	1
Coef. for non-uniform mutation	2 – 8	2
Crossover ratio	30% – 40%	10%
Population size (N)	52 – 260	52
Mutation rate	1% – 9%	2%
Repetition for each test	100	1

For each run, the best fitness value and the frequency of the best fitness value were recorded as measures for the GA's performance. These values were averaged over 100 runs for each set of population sizes, crossover ratios, coefficient for non-uniform mutation and mutation rates to provide representative performance of a general GA run. The average performance values for each set were normalised with respect to those values from runs with population size of 52 ($2l$[**]) and a mutation rate of 1% for the two different crossover ratios and the four different coefficients for non-uniform mutation used. The computation cost is defined as a product of the population size and the minimum number of generations it takes to obtain the minimum fitness value for each trial limited to the stopping criterion of 100 generations used.

For the three touchdown locations considered, similar trends of best fitness and computational cost performance vs. population size were observed. The fitness performance improves with increasing population size for all the mutation rates considered in the control parameters selection analysis and larger population sizes provide more accurate solution. Figure 6.11(a) shows that for mutation rates of less than 5%, there is relatively little improvement in the fitness value for the population size above $4l$ (N = 104) and fitter values are obtained using a crossover rate of 30% as shown in Figure 6.11(b). This minimal improvement in fitness value is at the expense of greater computational cost, which in general is a linear increase in computational effort for an increase in population size. While there is minimal improvement in the best fitness for populations greater than $4l$, the computational effort continues to increase as shown in Figures 6.12. Hence, increasing the population size beyond $4l$ does not appear to be worth the related computational cost. The results suggests that a population size of $N = 4l$ (N = 104) is an appropriate compromise for the best fitness value and a reasonable computational effort which agrees well with (Williams and Crossley

[**] l = a 26 real-valued string length chromosome.

1998). A coefficient for non-uniform mutation of 2 provides a fitter and a more consistent best fitness value for the different control parameters combinations tested. Very similar results for computational cost are observed for mutation rates ranging from 3% to 9%. Figure 6.12 also shows that as the population size increases, the number of generations require for the fitness function to obtain the minimum value decreases for mutation rates ranging from 3% to 9%. Nevertheless, the fitness value for these mutation rates are not as fit as the fitness values found for a mutation rate of 1%. As the mutation rate increases, the fitness values seem to deteriorate and this may be due to the excessive increase of mutation in the chromosomes. For smaller population sizes, the mutation rates appear to have a significant effect on the fitness performance but as the population sizes increase beyond 4*l*, the effect is reduced. For larger population sizes, the improvement in fitness value in increase mutation rate is less than the improvement in fitness value in an increase in population size.

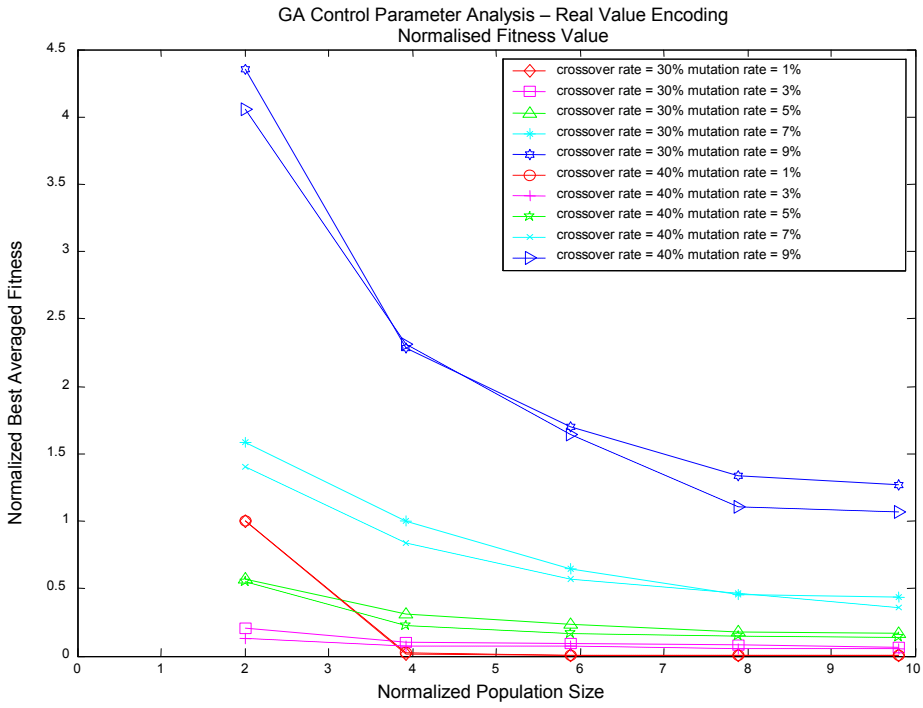

(a)

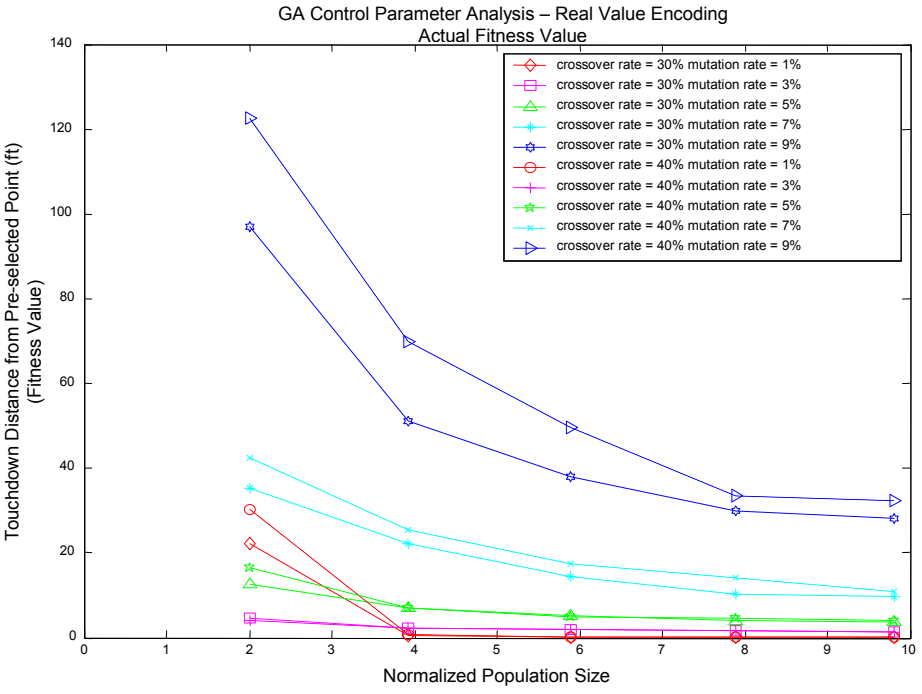

(b)

Figure 6.11 Real Value GA Control Parameter Analysis – Best Fitness

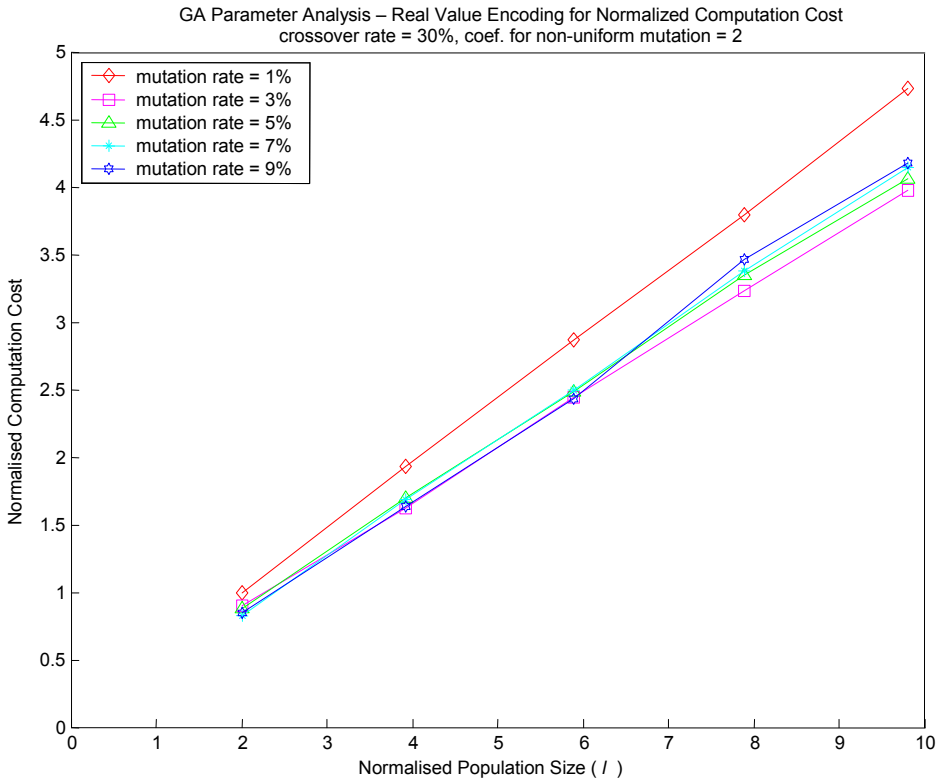

Figure 6.12 Real Value GA Control Parameter Analysis – Computation Cost

Results with similar characteristics in best fitness value and computational cost were observed for the different combinations of mutation rates, crossover rates, coefficients for non-uniform mutation and population sizes.

Based on the GA for variable speed and variable bank angle parameter analysis carried out, a population size of 104, a coefficient for non-uniform mutation of 2, a crossover ratio of 30%, a mutation rate of 1%, tournament selection with an elitism of 10% of the population size for subsequent generations and a stopping criterion of 100 generations were found suitable for use in GA on trajectory optimisation for a forced landing manoeuvre after engine failure with variable speed and variable bank angle. Figure 6.13 shows the typical convergence histories for 100 generations for each of the 100 trials for a particular control parameter combination obtained from the control parameter selection analysis. No premature convergence was observed and running it for 100 generations has allowed for a satisfactory development of the population.

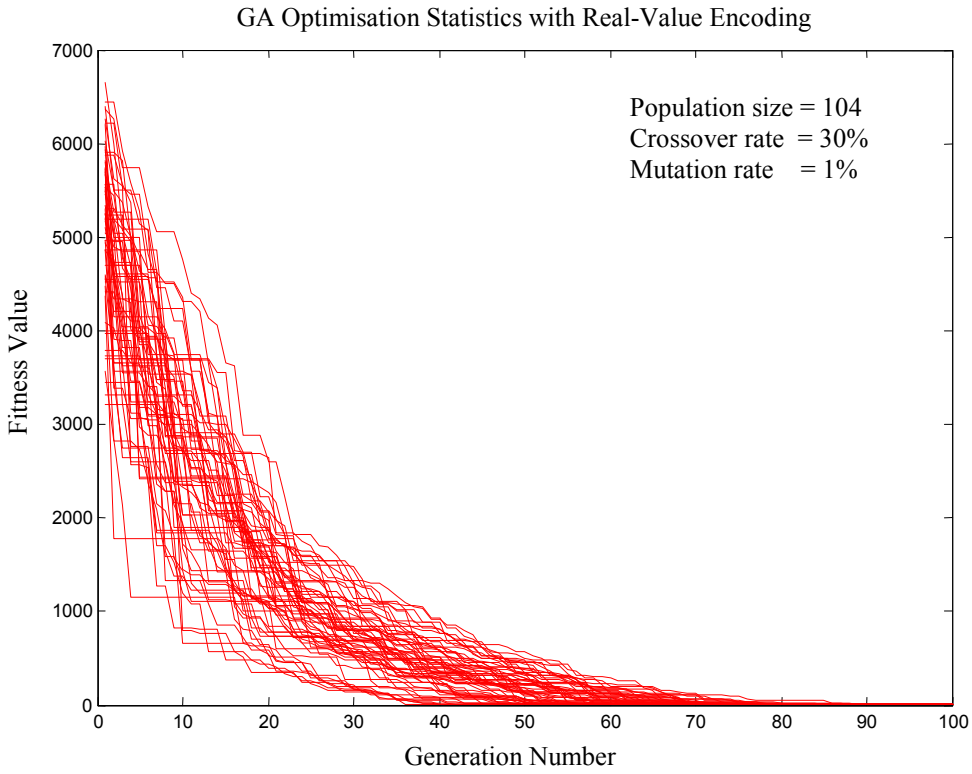

Figure 6.13 Real-Value GA Evolution History for 100 Trials

6.4.3 GA Results for a Forced Landing with Variable Speed and Variable Bank Angle

A GA for forced landing with variable speed and variable bank angle was carried out for three test locations: (0 ft, -3100 ft), (3000 ft, 3000 ft) and at (500 ft, 200 ft), where the 1st component represents the lateral distance and the 2nd component represents the longitudinal distance from the engine failure point. It used real-value representation and the control parameters as suggested in the previous section. An analysis for different number of discrete steps in altitude drop to touchdown was also carried out for the three pre-selected locations. The GA forced landing trajectory simulations, for an engine failure at 650 ft AGL, were discritised at every 50 ft, 25 ft and 10 ft drop in altitude which corresponded to calculations for 13 discrete steps, 26 discrete steps and 65 discrete steps to touchdown respectively. For this analysis, the GA population size used the product of four times the chromosome length as suggested in the section on Real-Value Control Parameters Selection. The chromosome length in this analysis is the product of the number of variables (two – velocity and bank angle) and number of steps used in the simulation. Therefore, the population sizes used were 104, 208 and 520, which corresponded to discretisation at an altitude drop of 50 ft, 25 ft and 10 ft respectively. A repetition of 100 trials was carried out for each test location to reduce the effect of probabilistic "noise" since GA is a probabilistic guided-search method. This GA

search method used the fitness criteria of touching down closest to the pre-selected location. The computational time for the different number of discritisation steps to touchdown are normalized with respect to the case for 13 discrete steps to touchdown (Computing time 1X). The results for the GA with variable speed and variable bank angle for touchdown distance from the respective pre-selected landing locations are shown in Table 6.5 – 6.7.

Table 6.5 Results for GA with Variable Speed and Variable Bank Angle for Discritisations at Every 50 ft Drop in Altitude

Statistics	Pre-Selected Location		
	(0 ft, -3100 ft)	(3000 ft, 3000 ft)	(500 ft, 200 ft)
Minimum Distance (ft)	0.0069	0.0029	0.0082
Average Distance (ft)	0.2486	0.0610	0.0605
Maximum Distance (ft)	5.0038	0.1754	0.1698
Standard Deviation	0.6784	0.0398	0.0336
Probability of Landing < 1ft	97 %	100 %	100 %
Probability of Landing < 10ft	100 %	100 %	100 %
Probability of Landing < 50ft	100 %	100 %	100 %
Probability of Landing < 100ft	100 %	100 %	100 %

Computing time 1x

Table 6.6 Results for GA with Variable Speed and Variable Bank Angle for Discritisations at Every 25 ft Drop in Altitude

Statistics	Pre-Selected Location		
	(0 ft, -3100 ft)	(3000 ft, 3000 ft)	(500 ft, 200 ft)
Minimum Distance (ft)	0.0974	0.0541	0.0552
Average Distance (ft)	16.8201	0.3865	0.5247
Maximum Distance (ft)	109.4551	0.9570	1.9499
Standard Deviation	20.8261	0.2218	0.3321
Probability of Landing < 1ft	9 %	100 %	92 %
Probability of Landing < 10ft	53 %	100 %	100 %
Probability of Landing < 50ft	94 %	100 %	100 %
Probability of Landing < 100ft	99 %	100 %	100 %

Computing time ~3.3x

Table 6.7 Results for GA with Variable Speed and Variable Bank Angle for Discritisations at Every 10 ft Drop in Altitude

Statistics	Pre-Selected Location		
	(0 ft, -3100 ft)	(3000 ft, 3000 ft)	(500 ft, 200 ft)
Minimum Distance (ft)	747.1561	0.0561	541.9353
Average Distance (ft)	1134	0.6293	764.7394
Maximum Distance (ft)	1504.6	1.7559	961.4899
Standard Deviation	123.6180	0.3557	92.6561
Probability of Landing < 1ft	0 %	86 %	0 %
Probability of Landing < 10ft	0 %	100 %	0 %
Probability of Landing < 50ft	0 %	100 %	0 %
Probability of Landing < 100ft	0 %	100 %	0 %

Computing time ~29x

Counter to intuition, the results show that discretisation at every 50 ft drop in altitude provides the smallest minimum distance error and smallest minimum average distance error from the pre-selected location and the smallest maximum distance error closest to the pre-

selected location. It also has the lowest standard deviation and the highest probability of landing less than 1 ft from the pre-selected location. This is due to the nature of the solution landscape where GA concentrates in that solution space and nearby adjacent values maybe found instead.

Based on the results obtained, the GA with variable speed and variable bank angle search method has successfully found suitable combinations of aircraft speed and bank angle to land extremely close to the pre-selected locations with very high probability of landing less than 1 ft from the pre-selected location as shown in Table 6.5. In order to test the validity and the reliability of the real-value representation GA search procedure developed, the GA fitness results for a forced landing with variable speed and variable bank angle were compared to the GA fitness results for a forced landing with discrete speed and discrete bank angle using the fitness criteria of touching down closest to the pre-selected location. The flight paths obtained are similar to the GA search with discrete speed and discrete bank angle. However, the minimum touchdown distances from the pre-selected locations are much less than the case of discrete speed and discrete bank angle since the speed and bank angle are allowed to take on any continuous value instead of at discrete values. The touchdown distance from the different pre-selected locations for GA with variable speed and variable bank angle improves significantly over GA with discrete speed and discrete bank angle because variable real-value parameters were used to represent the airplane's speed and bank angle.

Two general flight paths for the pre-selected location (0 ft, -3100 ft) exist since this location is located along the airplane's line of symmetry at engine failure point. The best flight paths found from each of the 100 runs and their average motion variables for turning right are shown in Figure 6.14. The results show that in order to land at the pre-selected location with high probability, the pilot flies the following manoeuvre. Upon engine failure point at 650 ft AGL, the pilot begins a tight turn either by banking steeply right or left at approximately 40° while flying at 76 mph. This is followed by an increasing airplane's speed towards 107 mph and widening of the turn radius by gradually reducing the bank angle to 23° as it descends to approximately 200 ft AGL. The pilot then continues flying at approximately 106 mph while further reducing the bank angle towards 0° until touchdown.

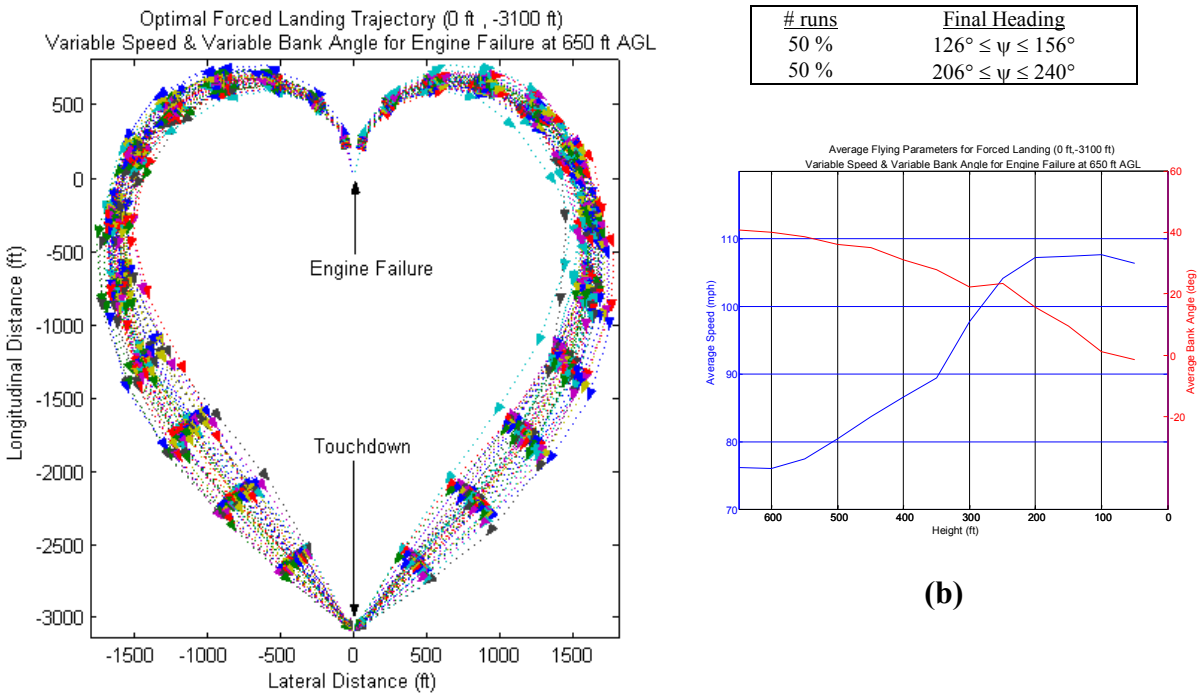

Figure 6. 14 Optimal Forced Landing (0 ft, -3100 ft) Variable Speed and Variable Bank Angle at 650 ft AGL

The best flight paths found from each of the 100 runs and their average motion variables for the pre-selected location (3000 ft, 3000 ft) are shown in Figure 6.15. The general flying manoeuvre to land at the pre-selected location of (3000 ft, 3000 ft) is, upon engine failure at 650 ft AGL, to begin with a left bank of approximately 9° at 96 mph. This is followed by a right bank until approximately 15° at 500 ft AGL and a further right bank towards 22° while gradually decreasing the airplane's speed until approximately 87 mph at 250 ft AGL. The pilot then increases the airplane's speed to approximately 91 mph along with a gradual decrease in right bank angle towards 7° until touchdown. The landing manoeuvre for this pre-selected location resembles the 90° landing approach in general aviation for flying from the base leg to the final leg where the pilot begins to turn towards the pre-selected location when it is at 45° from the current position. The results also show the double base leg flight paths where at engine failure point the aeroplane turns right and then followed by a left turn to touchdown. Although these are feasible flight paths, they are generally not recommended since they are harder to fly and will cause an increase in the pilot's workload.

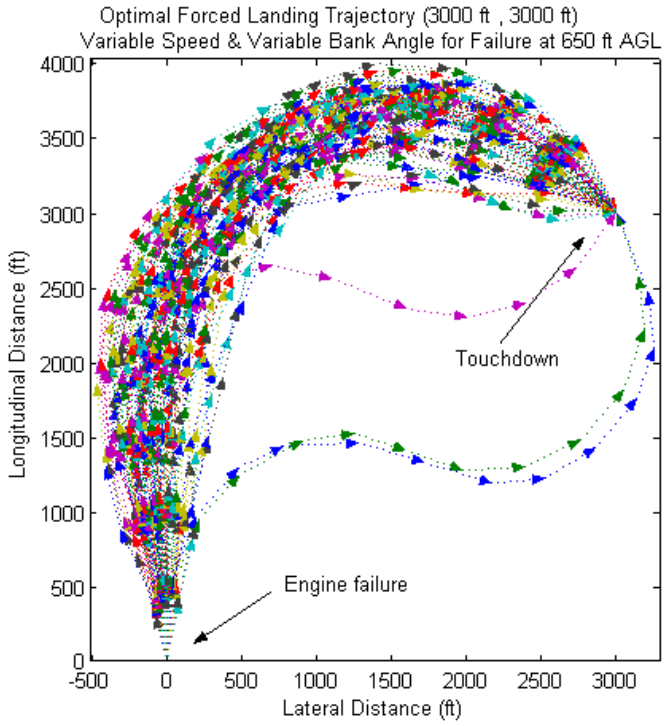

(a)

# runs	Final Heading
1 %	000° ≤ ψ < 045°
2 %	045° ≤ ψ < 090°
53 %	090° ≤ ψ < 135°
42 %	135° ≤ ψ < 180°
2 %	336° ≤ ψ < 340°

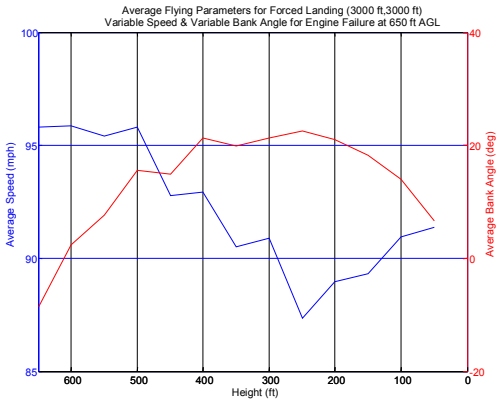

(b)

Figure 6. 15 Optimal Forced Landing (3000 ft, 3000 ft) Variable Speed and Variable Bank Angle at 650 ft AGL

The majority of the initial flight paths for the pre-selected location (500 ft, 200 ft) show that 95% of the flight paths turn toward the pre-selected location while 5% of the counter intuitive flight paths turn away from the pre-selected location. The counter intuitive manoeuvre was also found since the pre-selected location is located near the airplane's line of symmetry at engine failure point. The best flight paths found from each of the 100 runs and their average motion variables for both right and left turns for the pre-selected location (500 ft, 200 ft) are shown in Figure 6.16. The general flying manoeuvre to land at the pre-selected location of (500 ft, 200 ft) for the turn towards the pre-selected location (see Figure 6.16 b) is, upon engine failure, to fly at 100 mph, banking left at approximately 7°, then gradually decreasing the airplane's speed to approximately 79 mph while increasing the right bank angle towards 37° until 350 ft AGL. The pilot then maintains the flying speed at 79 mph while maintaining the bank angle at 37° until 250 ft AGL. This is followed by a gradually increasing airplane's speed towards 96 mph and decreasing the bank angle towards 12° until touchdown. The general flying manoeuvre for the counter intuitive manoeuvre (see Figure 6.16 c) is to fly at 96 mph, banking left at approximately 5.5°, gradually decreasing the airplane's speed to approximately 77 mph while increasing the left bank angle towards 37° until 550 ft AGL. The pilot then maintains the flying speed at 75 mph while maintaining the left bank angle at 40° until 250 ft AGL. This is followed by a gradually increasing airplane's speed towards

100 mph and decreasing the left bank angle towards 21° until touchdown. This is a result of interest because pilots are taught to fly the final part of the approach at maximum lift to drag velocity and this example shows that this approach velocity for maximum range may not be necessary or applicable for all situations. The landing manoeuvres for both cases for this pre-selected location resemble the 180° and 270° landing approach in general aviation in flying from the base leg to the final leg where the pilot begins to turn towards the pre-selected location when the pilot is abreast with the pre-selected landing location.

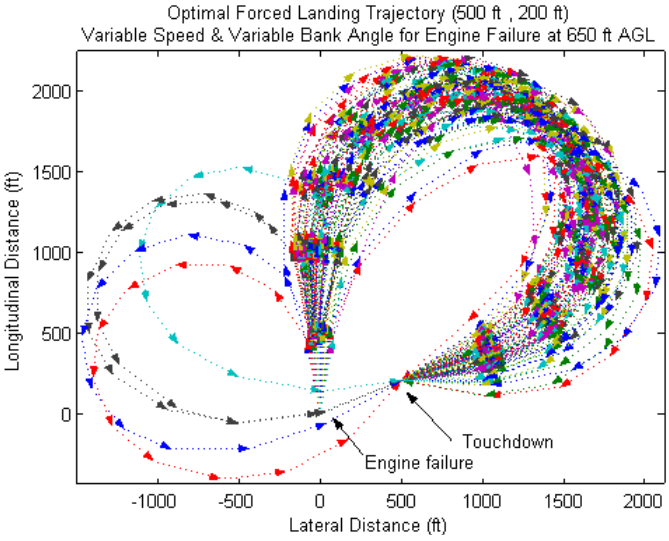

# runs	Final Heading
5 %	$032° \leq \psi \leq 073°$
95%	$222° \leq \psi \leq 288°$

(a)

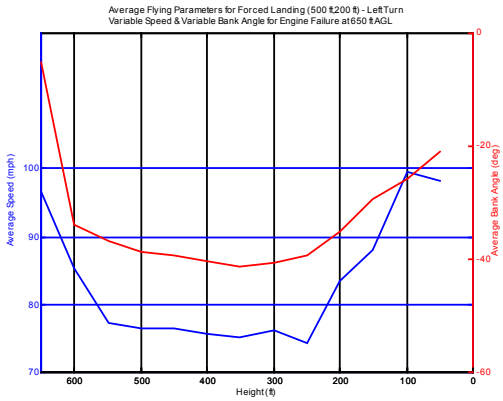

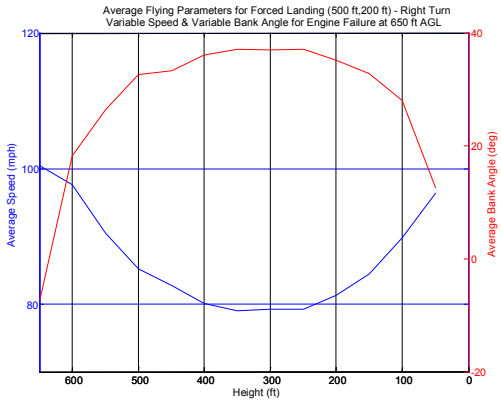

(c) **(b)**

Figure 6. 16 Optimal Forced Landing (500 ft, 200 ft) Variable Speed and Variable Bank Angle at 650 ft AGL

6.5 Genetic Algorithm in a Forced Landing Manoeuvre with Vertical Disturbances

The GA with variable speed and variable bank angle used in the previous section have successfully located optimal trajectories to a forced landing trajectory optimisation for all the three pre-selected locations considered. Further improvement in realism can be achieved with the addition of vertical disturbances into the flight dynamics model for the GA with variable speed and variable bank angle. The two atmospheric models described in Chapter 3.4 were used to generate one hundred vertical atmospheric turbulence profiles and the forty-nine thermal profiles as described in Chapter 3.5. They were used to study the effect vertical atmospheric disturbances have on a forced landing of an aircraft after engine failure. In order to reduce the effect of probabilistic "noise", 100 GA runs were carried out on every vertical atmospheric turbulence profile and thermal profile for each test location. The three similar pre-selected landing locations at ground level were chosen as test locations: (0 ft, -3100 ft), (3000 ft, 3000 ft) and (500 ft, 200 ft), where the 1st component represents the lateral distance and the 2nd component represents the longitudinal distance from the engine failure point.

6.5.1 Results with Time Averaged Vertical Atmospheric Turbulence

The results for the GA with variable speed and variable bank angle, and with atmospheric turbulence for touchdown distance from the respective pre-selected landing locations are shown in Table 6.8. The best landing paths from each of the 100 turbulence profiles and their average flying parameters as shown in Figures 6.17 – 6.19 resemble the flight paths found for both the GA with discrete speed and discrete bank angle, and the GA with variable speed and variable bank angle. For all the three pre-selected landing locations, the flight paths with vertical atmospheric turbulence trace a slightly wider landing flight path envelope than in still air condition (See Chapter 6.4.3).

Table 6.8 Results for GA with Variable Speed, Variable Bank Angle and Vertical Atmospheric Turbulence

Pre-selected Location	Global Minimum Distance	Average of the Minimum Distance from each Turbulence Profile	Average Minimum Distance from 10,000 trials	Probability of Landing ≤ Average Minimum Distance from 10,000 trials
(0 ft, -3100 ft)	1.4847×10^{-4} ft	0.0123 ft	0.7244 ft	93 %
(3000 ft, 3000 ft)	9.2037×10^{-4} ft	0.0045 ft	0.0625 ft	61 %
(500 ft, 200 ft)	1.4374×10^{-4} ft	0.0044 ft	0.0718 ft	70 %

The results show that the GA with variable speed, variable bank angle and vertical atmospheric turbulence have successfully found suitable combinations of the aeroplane's speed and bank angle to land very close to the pre-selected locations. The GA with vertical atmospheric turbulence found very minute global minimum distance from each of the three pre-selected locations. Comparatively, the average touchdown distances from all the pre-selected locations with vertical atmospheric turbulence are farther than in still air condition. This is as expected since vertical atmospheric turbulence is a form of disturbances and uncertainties to the flying manoeuvre. A very high probability (93%) of landing within the average minimum distance from the 10,000 trials was obtained for the pre-selected location (0 ft, -3100 ft) but a relatively low probability (61%) was obtained for the pre-selected location (3000 ft, 3000 ft). This observation is consistent with the results obtained in still air condition. The lower probability (61%) in locating paths that are within the average minimum distance is because GA concentrates in that solution space nearby where adjacent values were found instead. This is because GA will locate values that are very close to the minimum value but the lack of gradient information cannot guarantee a minimum value.

Figure 6.17-a shows the best forced landing flight paths with vertical atmospheric turbulence from each of the 100 turbulence profiles runs for the pre-selected location (0 ft, -3100 ft). Two general forced landing paths exist since the pre-selected location is located along the airplane's line of symmetry at engine failure point. The aeroplane's average flying speed and bank angle at each 50 ft decrement in altitude, and the airplane's final heading statistics to land at the pre-selected location are shown in Figure 6.17-b. The average flying parameters with vertical atmospheric turbulence is very similar to the still air condition because of the mild disturbance. The flight path envelope traced by this case is wider than the flight path envelope found for still air condition. The results show that strong continuous downdrafts during both the turn glide manoeuvre and the straight glide manoeuvre will have the most effect in an attempt to land close to this pre-selected location. Downdrafts affect the straight glide manoeuvre more than the turn glide manoeuvre in an attempt to land close to the pre-selected location while updrafts will increase the probability of landing closer to the pre-selected location.

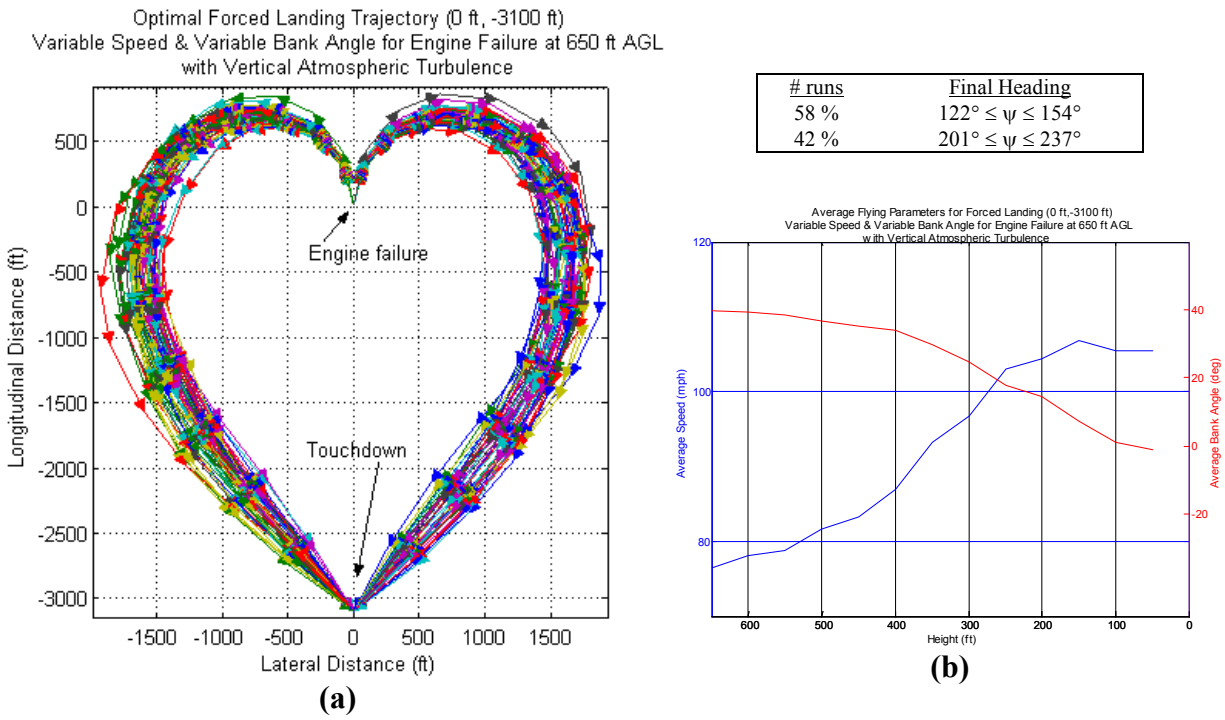

Figure 6. 17 Optimal Forced Landing (0 ft, -3100 ft) Variable Speed and Variable Bank Angle at 650 ft AGL with Vertical Atmospheric Turbulence

Figure 6.18-a shows the best forced landing flight paths with vertical atmospheric turbulence from each of the 100 turbulence profiles for the pre-selected location (3000 ft, 3000 ft). The aeroplane's average flying speed and bank angle at each 50 ft decrement in altitude, and the airplane's final heading statistics to land at the pre-selected location are shown in Figure 6.18-b. The average flying parameters with vertical atmospheric turbulence is very similar to the still air condition since the disturbance is mild. The flight path envelope traced by this case is wider than the flight path envelope for still air condition. The effects updrafts have on this landing manoeuvre is a slightly wider flight path or longer flight path since updrafts decrease the descent rate and longer paths are required to bleed off the excess energy (altitude). Flying longer flight paths also have the effect of touching down at the pre-selected location with final headings near the 180º heading relative to the initial engine failure heading.

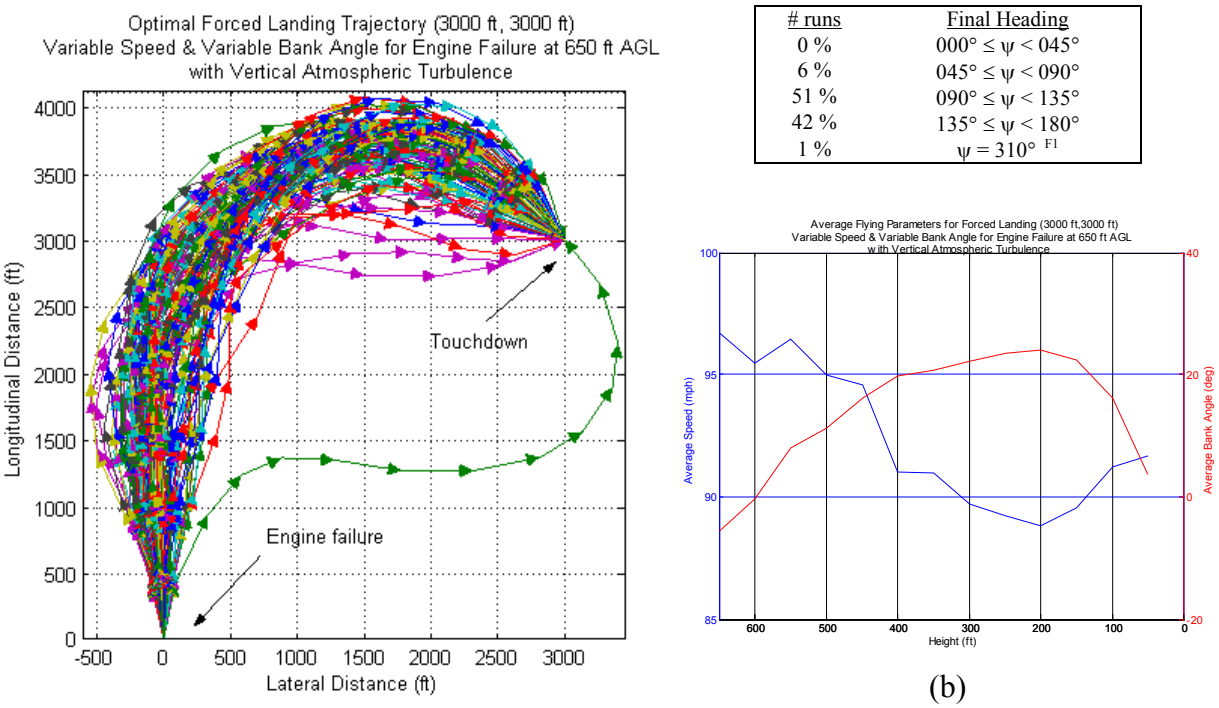

(a) (b)

Figure 6. 18 Optimal Forced Landing (3000 ft, 3000 ft) Variable Speed and Variable Bank Angle at 650 ft AGL with Vertical Atmospheric Turbulence

Figure 6.19-a shows the best forced landing flight paths with vertical atmospheric turbulence from each of the 100 turbulence profiles runs and the airplane's final heading statistics for the pre-selected location (500 ft, 200 ft). The aeroplane's average flying speed and bank angle manoeuvres at each 50 ft decrement in altitude to land at the pre-selected location are shown in Figures 6.19-b,c. The average flying parameters with vertical atmospheric turbulence is very similar to the still air condition since the disturbance is mild. The flight path envelope traced by this case is wider than the flight paths found for still air condition. The random vertical disturbances do not seem to affect its performance in landing close to this pre-selected location since vertical disturbances do not affect the turn manoeuvres as much as the straight glide manoeuvres.

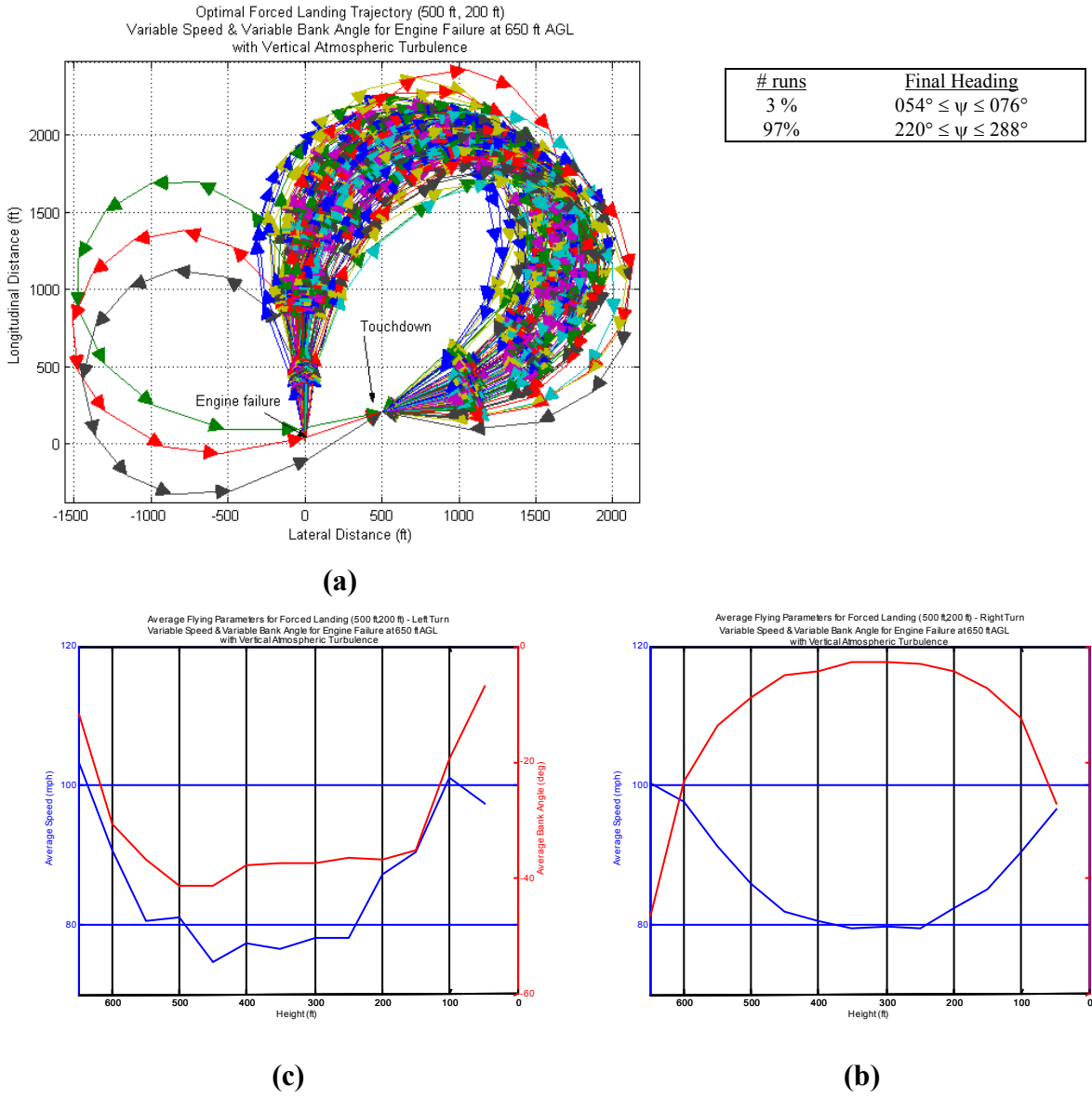

Figure 6. 19 Optimal Forced Landing (500 ft, 200 ft) Variable Speed and Variable Bank Angle at 650 ft AGL with Vertical Atmospheric Turbulence

6.5.2 Results with Thermal Disturbances

The results for the GA with variable speed and variable bank angle, and with thermal disturbances for touchdown distance from the three pre-selected landing locations are shown in Table 6.9. The best landing flight path from each of the 49 thermal profiles and their average flying parameters as shown in Figures 6.20 – 6.22 show general flight paths that resemble the flight paths found for the GA in still air condition. For all the three pre-selected landing locations, the flight paths with thermal disturbances trace flight path envelope that are much broader than in still air condition.

Table 6.9 Results for GA with Variable Speed, Variable Bank Angle and Thermal Disturbances

Pre-selected Location	Global Minimum Distance	Average of the Minimum Distance from each Turbulence Profile	Average Minimum Distance from 4900 trials	Probability of Landing ≤ 1 ft from pre-selected location
(0 ft, -3100 ft)	0.0018 ft	261.4436 ft	294.9192 ft	32 %
(3000 ft, 3000 ft)	0.0004 ft	0.0062 ft	0.1025 ft	49 %
(500 ft, 200 ft)	0.0011 ft	27.3698 ft	42. 4508 ft	40 %

The results show that the GA with variable speed and variable bank angle, and with thermal disturbances has successfully found suitable combinations of the aeroplane's speed and bank angle to land near the pre-selected locations. However, the average distance from the pre-selected location for the location (0, ft, -3100 ft) is far compare to the results for the other two locations but the probability of landing within 1 ft from the pre-selected for all the three locations remain consistent. The overall distance from the pre-selected location with thermal disturbances is farther than for still air condition. This indicates that vertical disturbances have significant effect on the forced landing manoeuvre.

Figure 6.20-a shows the best forced landing flight paths with thermal disturbances for each of the 49 thermal profiles for the pre-selected location (0 ft, -3100 ft). Two general forced landing paths exist since the pre-selected location is located along the airplane's line of symmetry at engine failure point. The aeroplane's average flying speed and bank angle at each 50 ft decrement in altitude, and the airplane's final heading statistics to land at the pre-selected location are shown in Figure 6.20-b. The flight path envelope for this case is a very wide flight path envelope and a wider range in the airplane's final heading compare to the still air condition. The major difference in the average flying parameters with thermal disturbances for this location is a higher airplane's turn speed of approximately 84 mph and a lower bank angle of approximately 30° compare to the still air condition of approximately 76 mph and a bank angle of 40° respectively. These results show that a wider range in vertical disturbance has a significant effect on the forced landing flight paths.

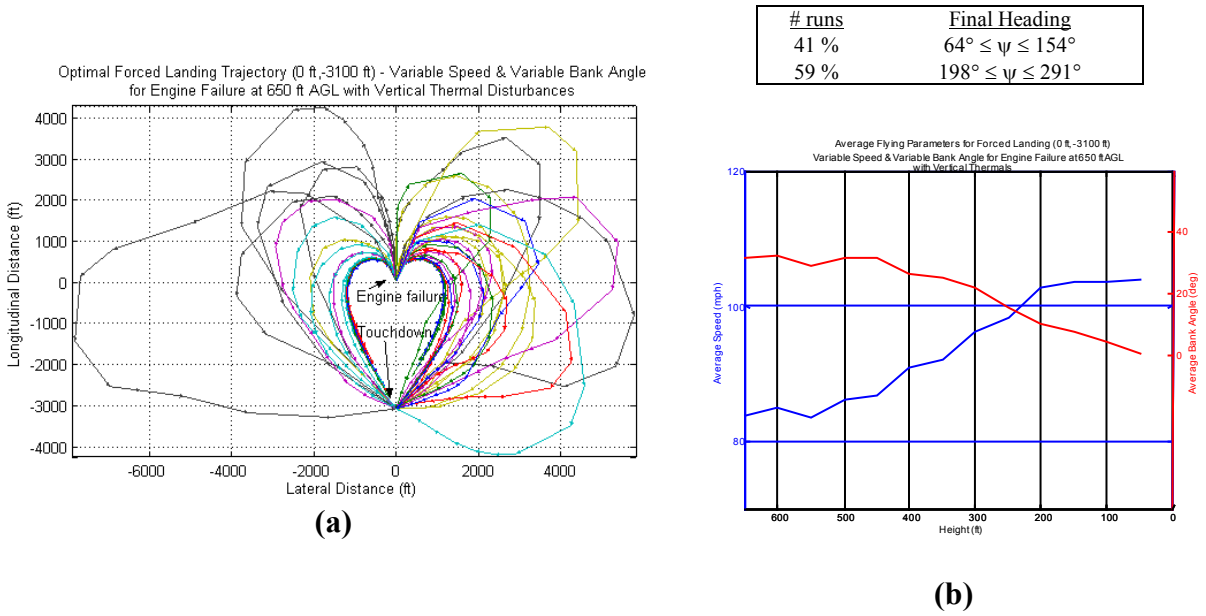

Figure 6. 20 Optimal Forced Landing (0 ft, -3100 ft) Variable Speed and Variable Bank Angle at 650 ft AGL with Vertical Thermals

Figure 6.21-a shows the best forced landing flight paths for each of the 49 thermal disturbances for the pre-selected location (3000 ft, 3000 ft). The aeroplane's average flying speed and bank angle at each 50 ft decrement in altitude, and the airplane's final heading statistics to land at the pre-selected location are shown in Figure 6.21-b. The flight path envelope for this case is very much wider than the flight path envelope in still air condition. The major difference in the average flying parameters with thermal disturbances for this location is a higher initial airplane's turn speed of approximately 99 mph and an approximate zero bank angle for the 1st 50 ft drop in altitude. This is followed by a slight left bank at a reduced airplane's speed for the next 50 ft drop in altitude and a continual decrease in the airplane's speed to approximately 93 mph an a bank angle of approximately 10°. Most of the airplane's final heading is within 090° and 135° but there is a decrease in final heading between 135° and 180° while an increase in final heading between 180° and 270°. This is due to stronger updrafts in the thermal disturbances where the sink rate is reduced and the airplane is required to fly a longer path, hence, arriving at greater than the 180° approach. The stronger downdrafts in the thermals with result in a higher sink rate, hence, a more direct or shorter flight path is necessary.

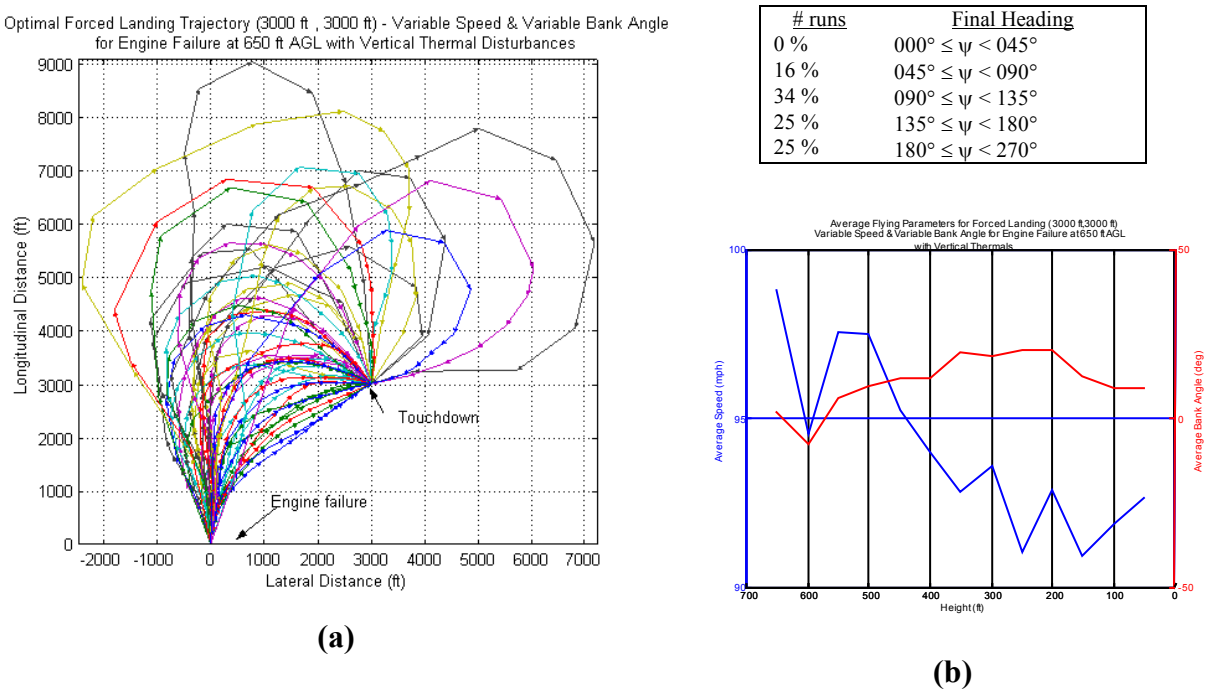

(a) **(b)**

Figure 6. 21 Optimal Forced Landing (3000 ft, 3000 ft) Variable Speed and Variable Bank Angle at 650 ft AGL with Vertical Thermals

Figure 6.22-a shows the best forced landing flight paths for each of the 49 thermal disturbances and the airplane's final heading statistics for the pre-selected location (500 ft, 200 ft). The aeroplane's average flying speed and bank angle at each 50 ft decrement in altitude to land at the pre-selected location are shown in Figures 6.22-b,c. The average flying parameters for this location begins with a higher initial airplane's speed, a higher turn speed, and a lower bank angle during turn compare to still air condition. There is also a reduced number of flight paths that turn toward the pre-selected location and an increased number of flight paths that turn away from the pre-selected location compare to still air conditions. The wider flight paths envelope traced by this case is due to stronger up and down drafts in the thermals, causing the airplane to fly a longer path while the downdrafts in the thermals cause the airplane to fly a smaller radius.

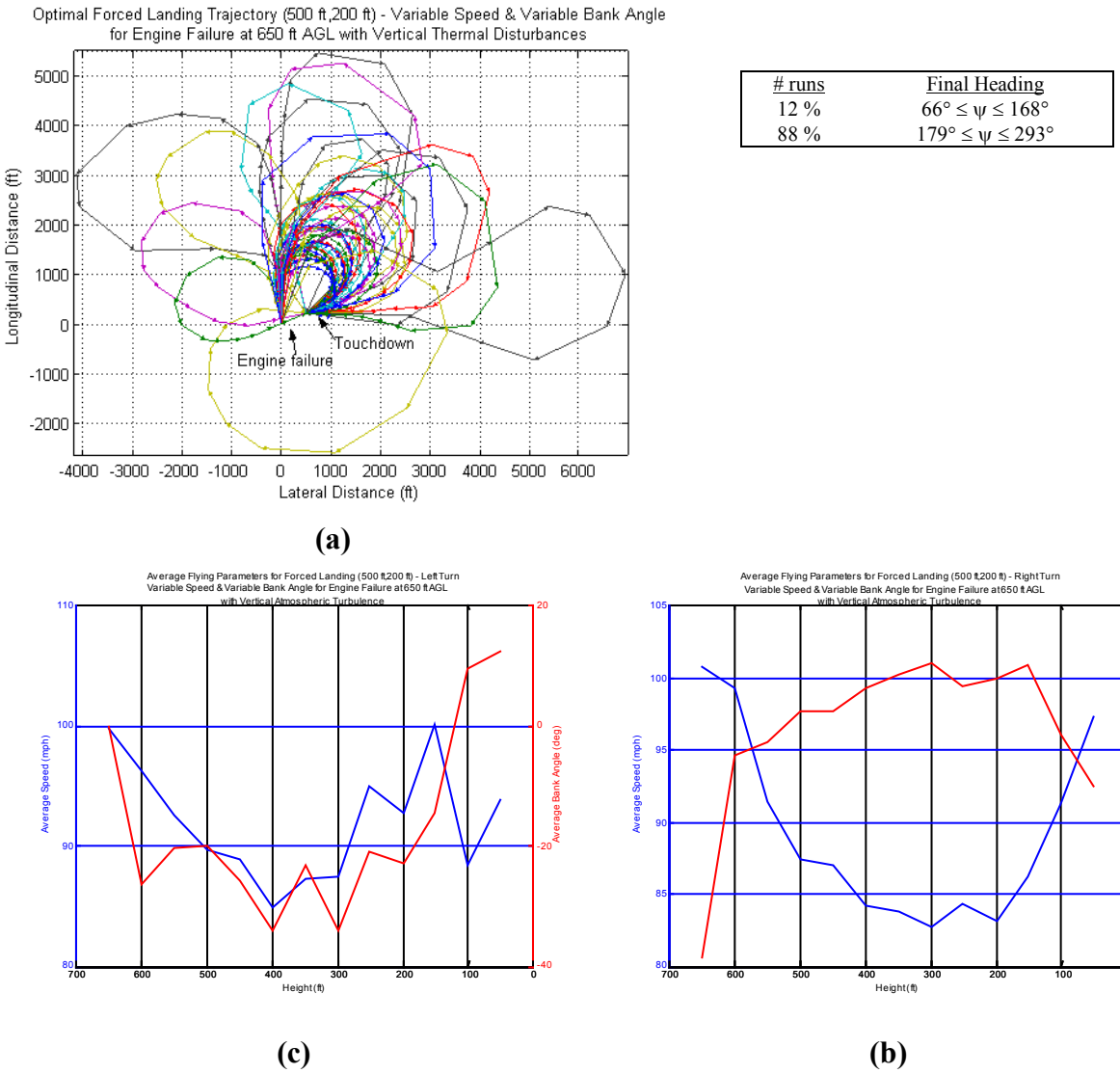

Figure 6. 22 Optimal Forced Landing (500 ft, 200 ft) Variable Speed and Variable Bank Angle at 650 ft AGL with Vertical Thermals

6.6 Genetic Algorithm in a Forced Landing Manoeuvre with Horizontal Wind and Vertical Disturbances

This section examines the effects horizontal winds have on a forced landing manoeuvre using similar GA search method as described in Chapters 6.4 and 6.5. An analysis for horizontal wind at three different combinations of wind speed: 10 mph, 20 mph and 30 mph, and at three wind headings: 45° left of head on wind, 0° (head on wind) and 45° right of head on wind was carried out for three pre-selected touchdown locations. The analysis was also carried out for still air conditions, with vertical atmospheric disturbances and with thermal disturbances as described in Chapter 3.4 and Chapter 3.5. In order to reduce the effects of probabilistic "noise", 100 GA runs were carried out on every vertical atmospheric turbulence

profile and thermal profile for each test location. The pre-selected landing locations at ground level chosen were located at (0 ft, -3100 ft), (3000 ft, 3000 ft) and (500 ft, 200 ft), where the 1st component represents the lateral distance and the 2nd component represents the longitudinal distance from the engine failure point. The pre-selected locations were chosen for consistency and to allow comparison with analysis in previous sections.

6.6.1 Results with Horizontal Wind

This section describes the flight paths and flying parameters for a forced landing manoeuvre for an engine failure at 650 ft AGL with horizontal crosswinds using GA. 100 runs were simulated for each location to reduce the effect of probabilistic "noise". The flight paths for the pre-selected location (0 ft, -3100 ft) as shown in Figure 6.23, show a higher percentage of the airplane landing at the pre-selected location for an initial turn into the crosswind after an engine failure as indicated by the number of flight paths into the wind for both crosswinds at –45° and +45°. The number of flight paths that turn toward the crosswind also increases with increasing crosswind speed. The effects of turning into the crosswind have on the flight path is a smaller turn radius and a slightly longer straight glide to touchdown. As the crosswind speed increases, the flight path envelope widens with a small increase in turn radius during the initial turn towards the crosswind and a wider flight path width for the straight glide to touchdown manoeuvre. The effects of turning away from the crosswind are a small increase in turn radius during the initial turn away from the crosswind and a slightly shorter straight glide to touchdown. Since the pre-selected location is located along the line of symmetry of the airplane's initial flight direction, the effect of increasing headwind has on the flight path is an increase in turn radius which results in a wider flight path width.

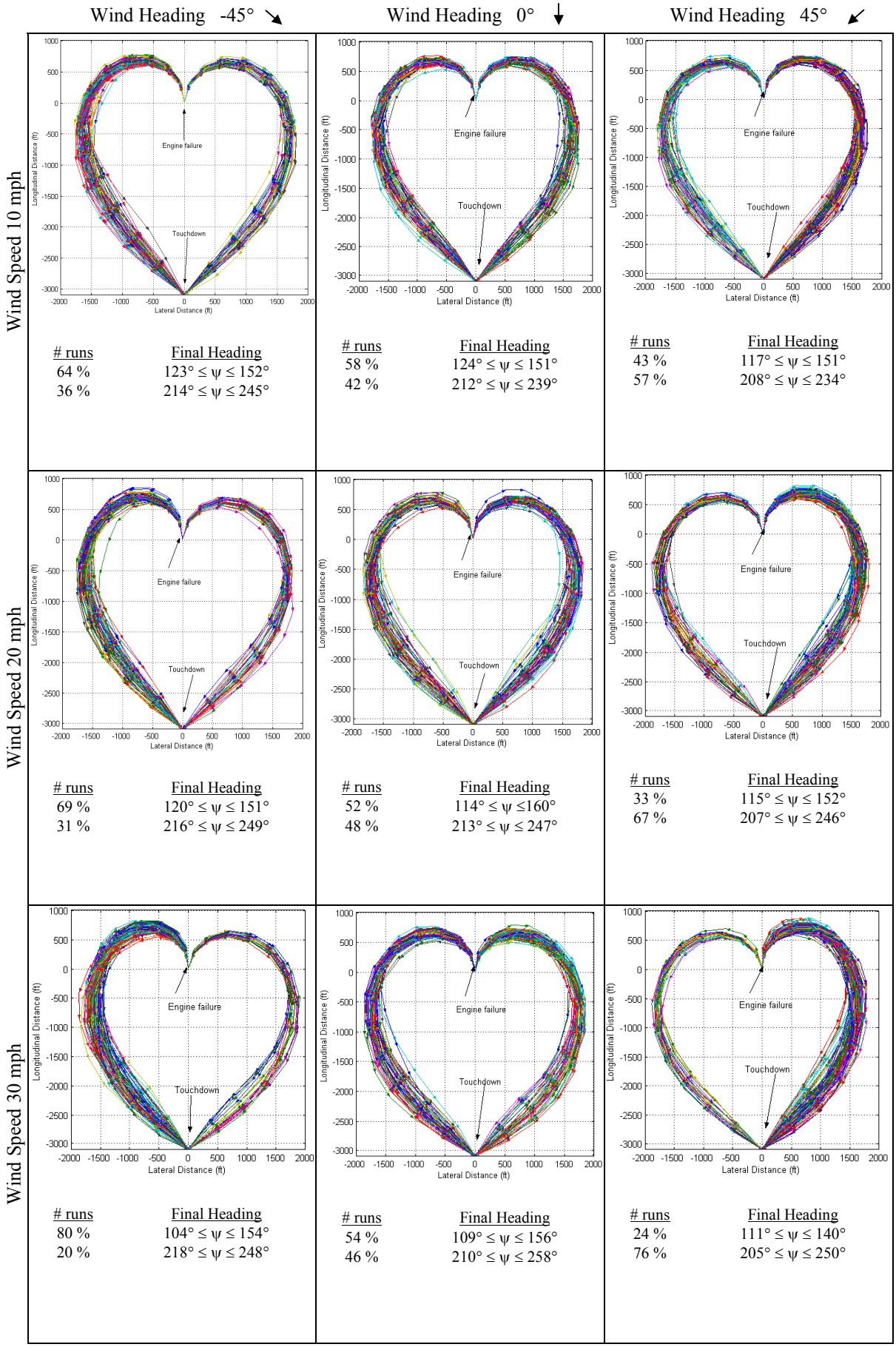

Figure 6.23 Optimal Forced Landing Trajectory – (0 ft, -3100 ft) Variable Speed and Variable Bank Angle for Engine Failure at 650 ft AGL with Horizontal Wind

As can be seen in Figure 6.24, the average initial speed for turning away from crosswind is the lowest among the three different headwinds while higher average initial speed is found for turning into crosswind. However, the reverse holds true during the straight glide to touchdown sector. This is as expected since for the initial turn away from the crosswind, the crosswind has the effect of a tail wind on the airplane and during the straight glide to touchdown sector, the crosswind has an effect of a headwind and this requires the airplane to fly faster. The average initial bank angle for turning away from the crosswind is also the highest among the three different headwind since a smaller turn radius is required to keep the flight path close to the pre-selected location.

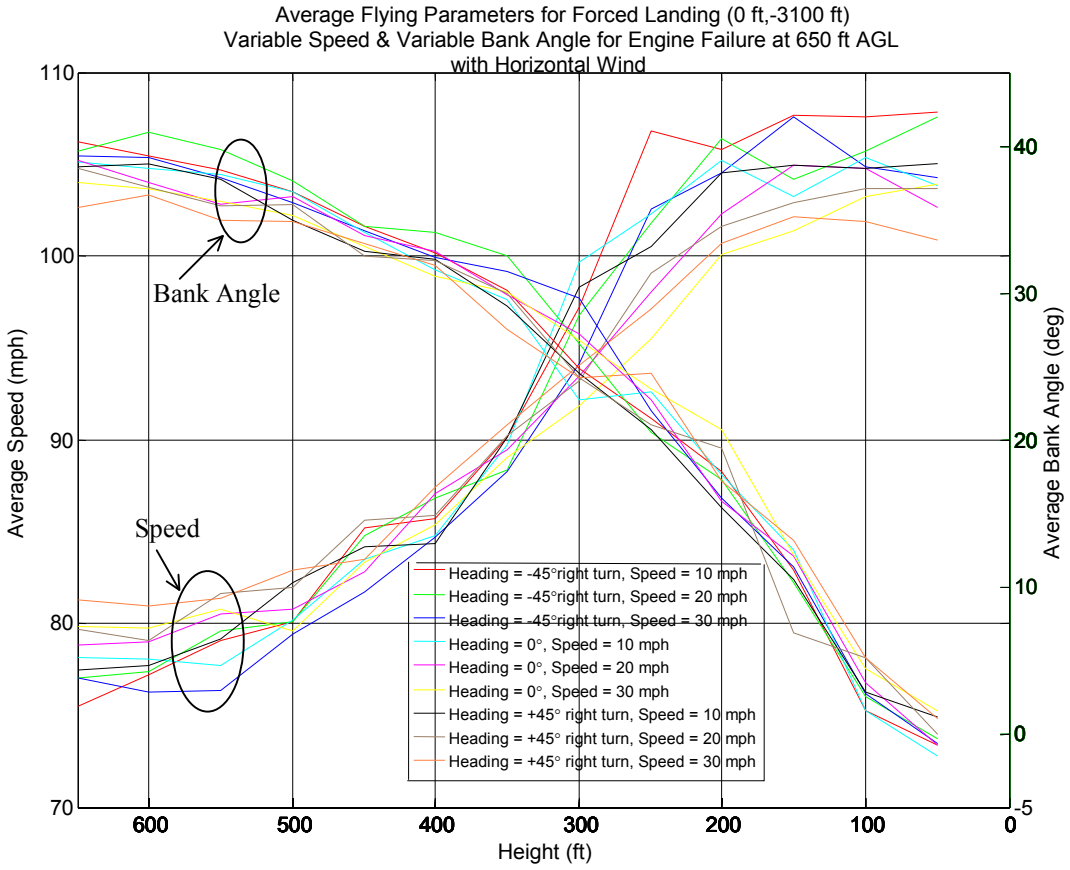

Figure 6.24 Average Flying Parameters for Forced Landing – (0 ft, -3100 ft) Variable Speed and Variable Bank Angle for Engine Failure at 650 ft AGL with Horizontal Wind

The flight paths for the pre-selected location (3000 ft, 3000 ft) as shown in Figure 6.25, show that crosswinds at –45° promotes double base leg turns, which turns that require two opposites turn manoeuvres to land at the pre-selected location and are not encouraged since they increase the pilots' workload and are harder to fly. For direct headwind, an increase in wind speed also promotes double base leg turns which results in an increase in the number flight paths with final heading between 315° and 360°. Overall, the general flight paths for

the different directions and magnitudes in crosswinds resemble the 90° approach to landing. The flying parameters for this pre-selected location are shown in Figure 6.26.

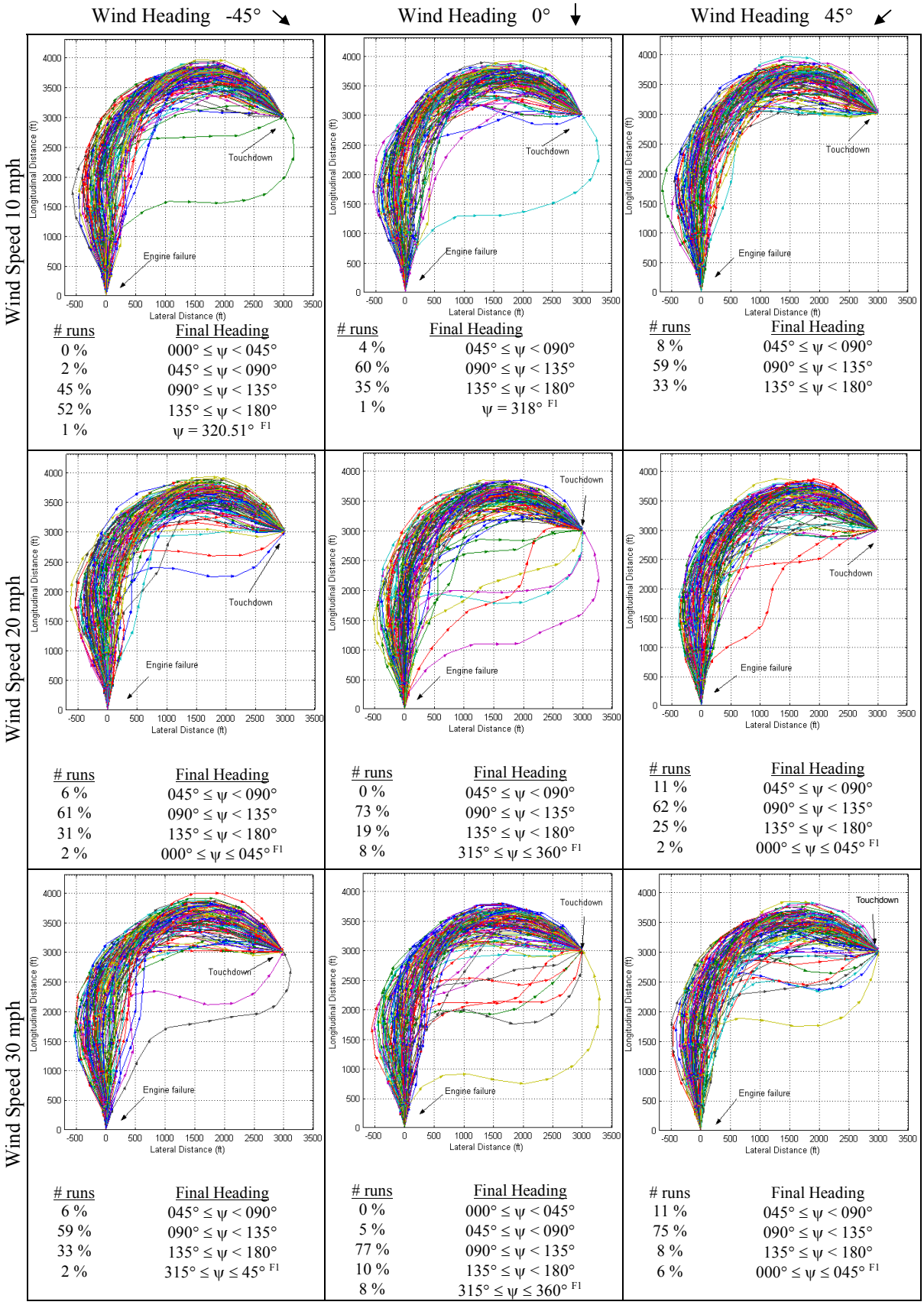

Wind Heading -45°	# runs	Final Heading
Wind Speed 10 mph	0 %	000° ≤ ψ < 045°
	2 %	045° ≤ ψ < 090°
	45 %	090° ≤ ψ < 135°
	52 %	135° ≤ ψ < 180°
	1 %	ψ = 320.51° [F1]
Wind Speed 20 mph	6 %	045° ≤ ψ < 090°
	61 %	090° ≤ ψ < 135°
	31 %	135° ≤ ψ < 180°
	2 %	000° ≤ ψ ≤ 045° [F1]
Wind Speed 30 mph	6 %	045° ≤ ψ < 090°
	59 %	090° ≤ ψ < 135°
	33 %	135° ≤ ψ < 180°
	2 %	315° ≤ ψ ≤ 45° [F1]

Wind Heading 0°	# runs	Final Heading
Wind Speed 10 mph	4 %	045° ≤ ψ < 090°
	60 %	090° ≤ ψ < 135°
	35 %	135° ≤ ψ < 180°
	1 %	ψ = 318° [F1]
Wind Speed 20 mph	0 %	045° ≤ ψ < 090°
	73 %	090° ≤ ψ < 135°
	19 %	135° ≤ ψ < 180°
	8 %	315° ≤ ψ ≤ 360° [F1]
Wind Speed 30 mph	0 %	000° ≤ ψ < 045°
	5 %	045° ≤ ψ < 090°
	77 %	090° ≤ ψ < 135°
	10 %	135° ≤ ψ < 180°
	8 %	315° ≤ ψ ≤ 360° [F1]

Wind Heading 45°	# runs	Final Heading
Wind Speed 10 mph	8 %	045° ≤ ψ < 090°
	59 %	090° ≤ ψ < 135°
	33 %	135° ≤ ψ < 180°
Wind Speed 20 mph	11 %	045° ≤ ψ < 090°
	62 %	090° ≤ ψ < 135°
	25 %	135° ≤ ψ < 180°
	2 %	000° ≤ ψ ≤ 045° [F1]
Wind Speed 30 mph	11 %	045° ≤ ψ < 090°
	75 %	090° ≤ ψ < 135°
	8 %	135° ≤ ψ < 180°
	6 %	000° ≤ ψ ≤ 045° [F1]

Figure 6.25 Optimal Forced Landing Trajectory – (3000 ft, 3000 ft) Variable Speed and Variable Bank Angle for Engine Failure at 650 ft AGL with Horizontal Wind

[F1] Double Base Leg Manoeuvre

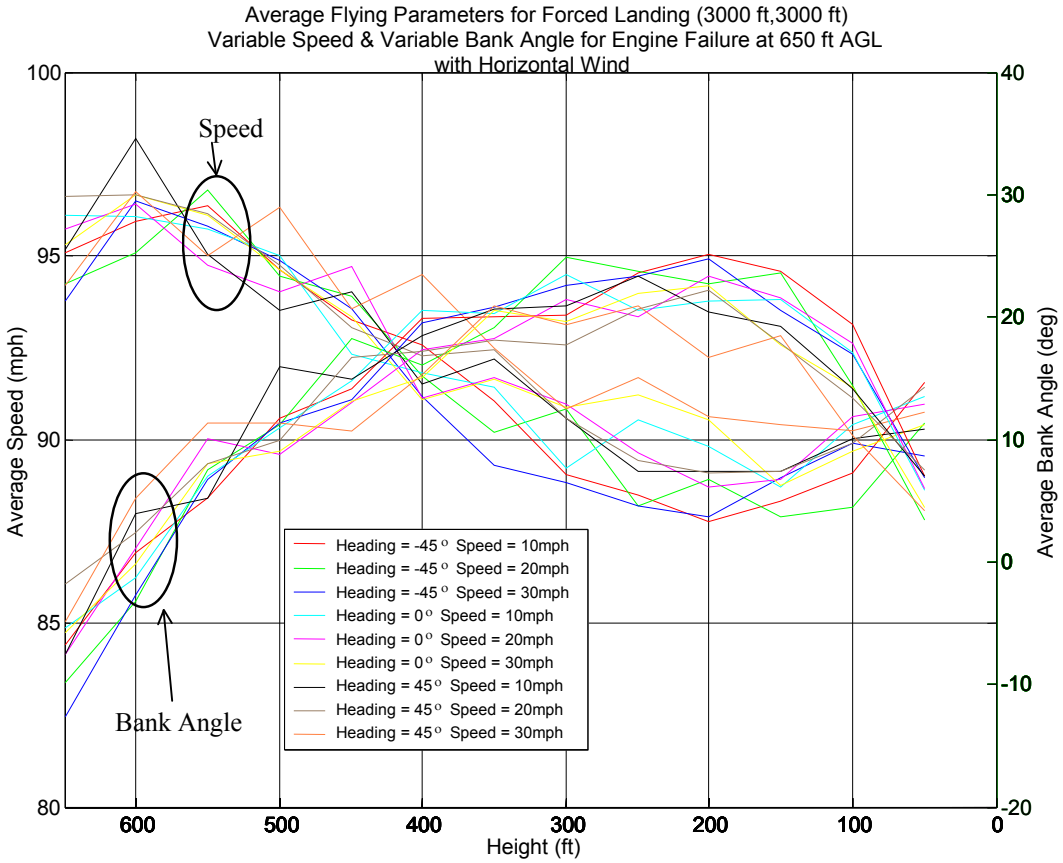

Figure 6.26 Average Flying Parameters for Forced Landing – (3000 ft, 3000 ft) Variable Speed and Variable Bank Angle for Engine Failure at 650 ft AGL with Horizontal Wind

The flight paths for the pre-selected location (500 ft, 200 ft) that are near the aircraft's initial line of symmetry are shown in Figure 6.27. The effect of crosswind at -45° has on the results is an increase in the number of flight paths that turn into the -45° crosswind direction, which also increases with increasing crosswind speed. This is as expected since the pre-selected touchdown location is very near the airplane's initial line of symmetry. The crosswind at this direction causes the airplane to experience a headwind during the initial turn manoeuvre and a tail wind for the later part of the turn manoeuvre. Thus, enhances the probability of touching down closer to the pre-selected landing location. The number of flight paths with initial left turns are reduced for direct headwind since they represent unfavourable crosswind in the later part of the turn manoeuvre. Comparatively, the number of flight paths for crosswind at 45° with initial left turn are reduced to zero with increasing crosswind speed since this crosswind represents strong headwind for the later part of the manoeuvre making it impossible to land at the pre-selected location due to the lack of altitude. Therefore, for the pre-selected locations near the airplane's line of symmetry, turning towards the pre-selected location will have a higher probability of touching down successfully at the pre-selected

location regardless of the crosswind's direction. The flying parameters for this pre-selected location are shown in Figure 6.28.

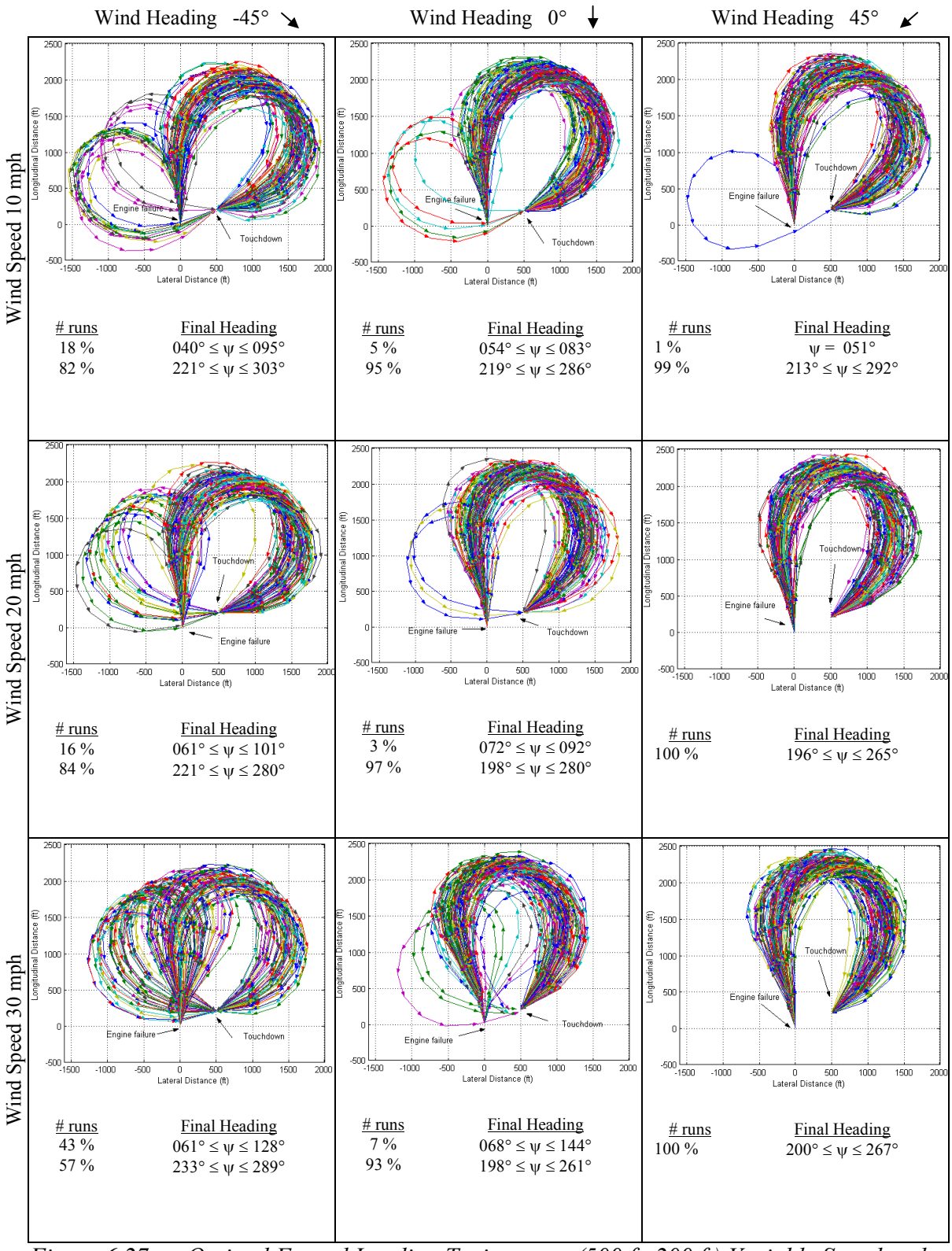

Figure 6.27 Optimal Forced Landing Trajectory – (500 ft, 200 ft) Variable Speed and Variable Bank Angle for Engine Failure at 650 ft AGL with Horizontal Wind

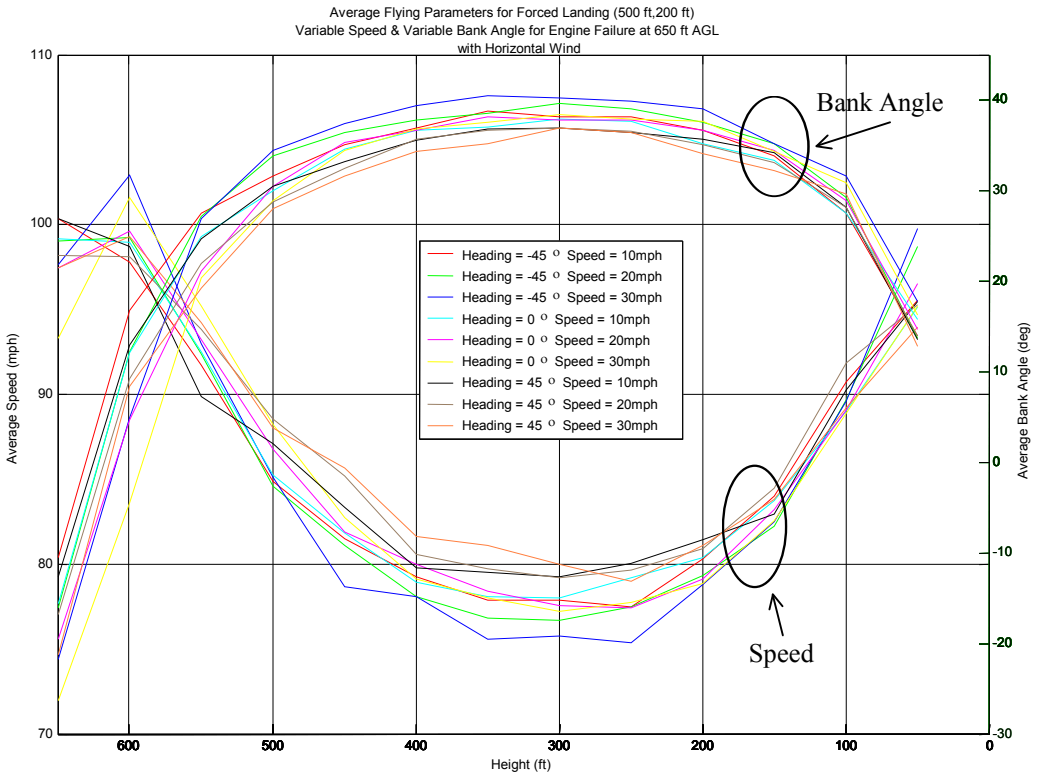

Figure 6.28 Average Flying Parameters for Forced Landing – (500 ft, 200 ft) Variable Speed and Variable Bank Angle for Engine Failure at 650 ft AGL with Horizontal Wind

6.6.2 Results with Horizontal Wind and Time Averaged Vertical Atmospheric Turbulence

This section shows the effects time averaged vertical atmospheric turbulence have on a forced landing manoeuvre with horizontal crosswinds. The results for the pre-selected location (0 ft, -3100 ft) with time averaged vertical atmospheric turbulence are shown in Figures 6.29 – 6.30. These results show very similar trend compare to the results obtained without vertical atmospheric disturbances as shown in Figures 6.23 – 6.24. However, vertical atmospheric turbulence accentuates the flight path characteristics as described in Chapter 6.6.1 and forces the aeroplane to fly a moderately wider flight path.

The results for the pre-selected location (3000 ft, 3000 ft) with time averaged vertical atmospheric turbulence are shown in Figures 6.31 – 6.32. The results show very similar trend compare to the results without vertical atmospheric disturbances as shown in Figures 6.25 – 6.26. However, vertical atmospheric turbulence accentuates the flight path characteristics as described in Chapter 6.6.1 and forces the aeroplane to fly a slightly wider flight path.

The results for the pre-selected location (500 ft, 200 ft) with time averaged vertical atmospheric turbulence are shown in Figures 6.33 – 6.34. The results show very similar trend compare to the results without vertical atmospheric disturbances as shown in Figures 6.27 – 6.28. However, vertical atmospheric turbulence accentuates the flight path characteristics as described in Chapter 6.6.1 and forces the aeroplane to fly a wider flight path.

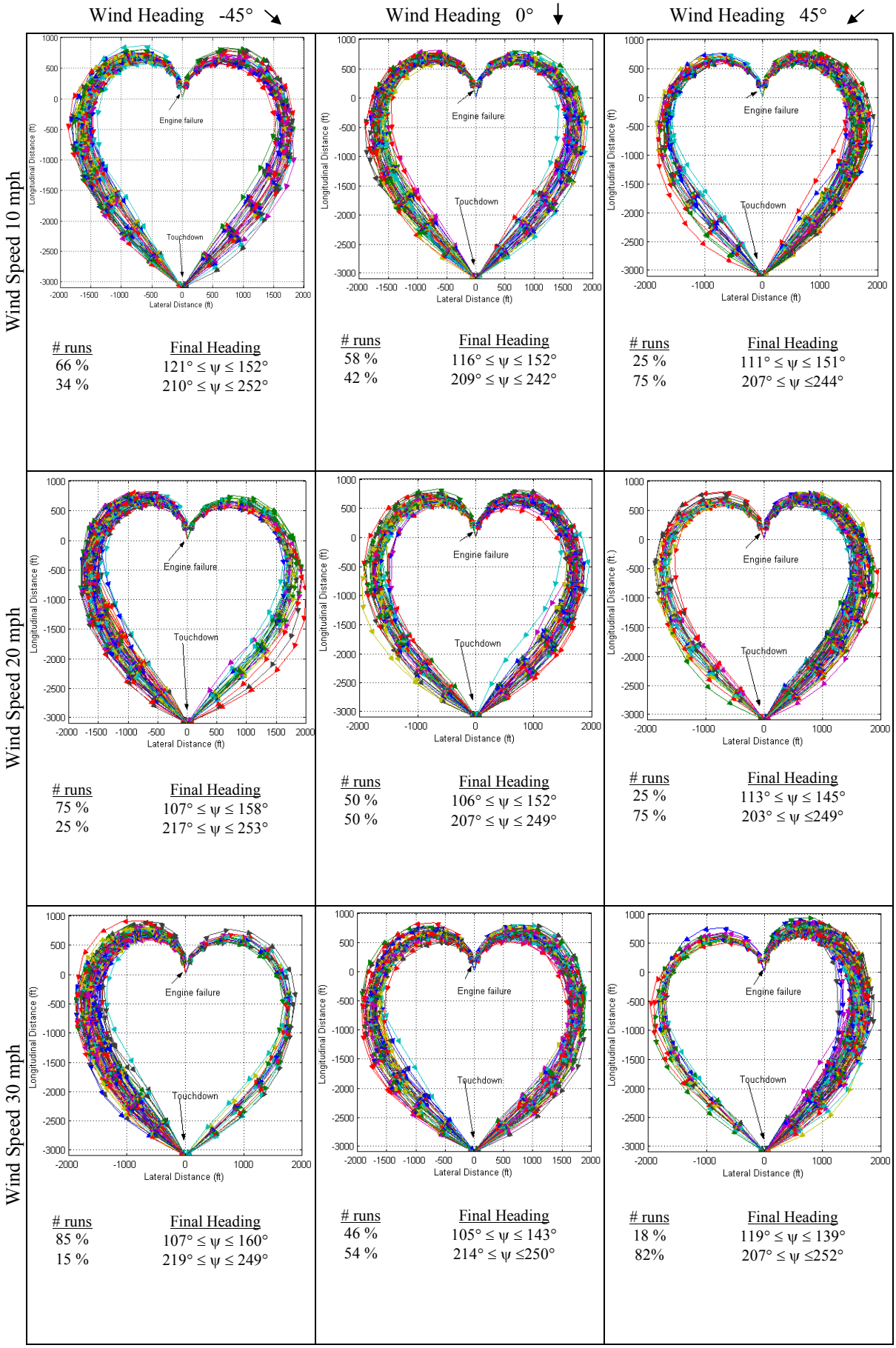

Figure 6.29 Optimal Forced Landing Trajectory – (0 ft, -3100 ft) Variable Speed and Variable Bank Angle for Engine Failure at 650 ft AGL with Horizontal Wind and Vertical Atmospheric Turbulence

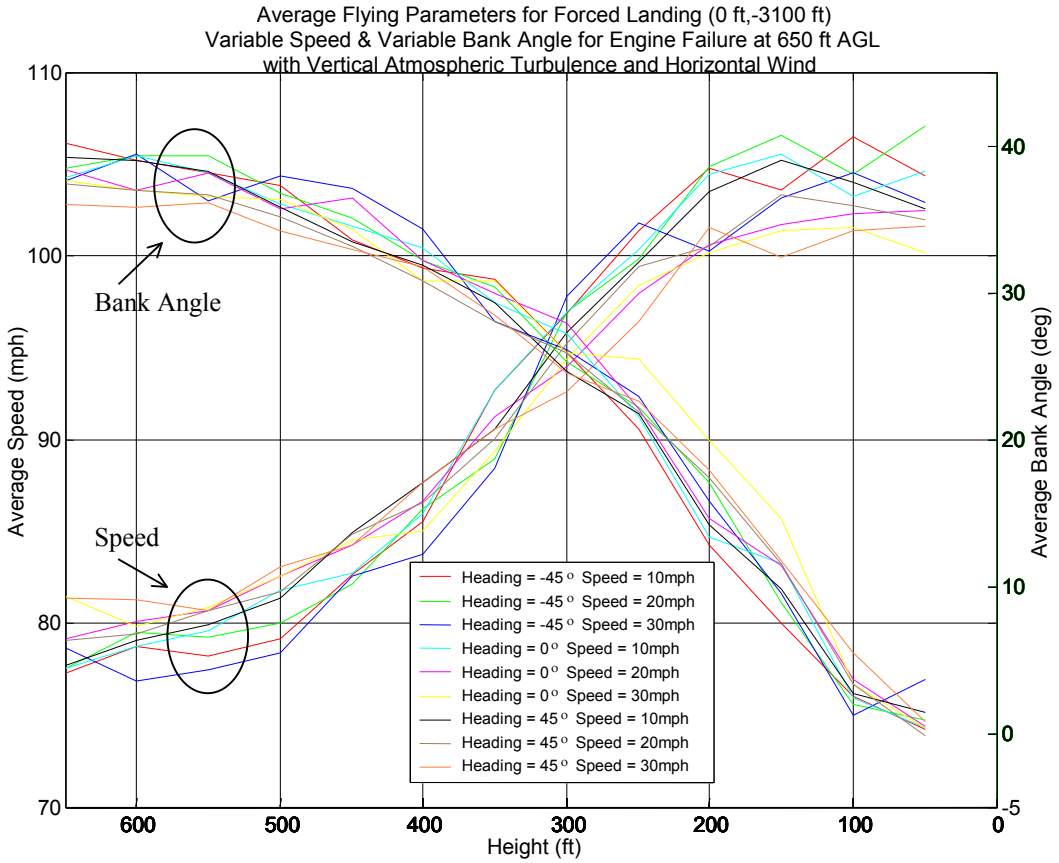

Figure 6.30 Average Flying Parameters for Forced Landing – (0 ft, -3100 ft) Variable Speed and Variable Bank Angle for Engine Failure at 650 ft AGL with Horizontal Wind and Vertical Atmospheric Turbulence – Right Turn

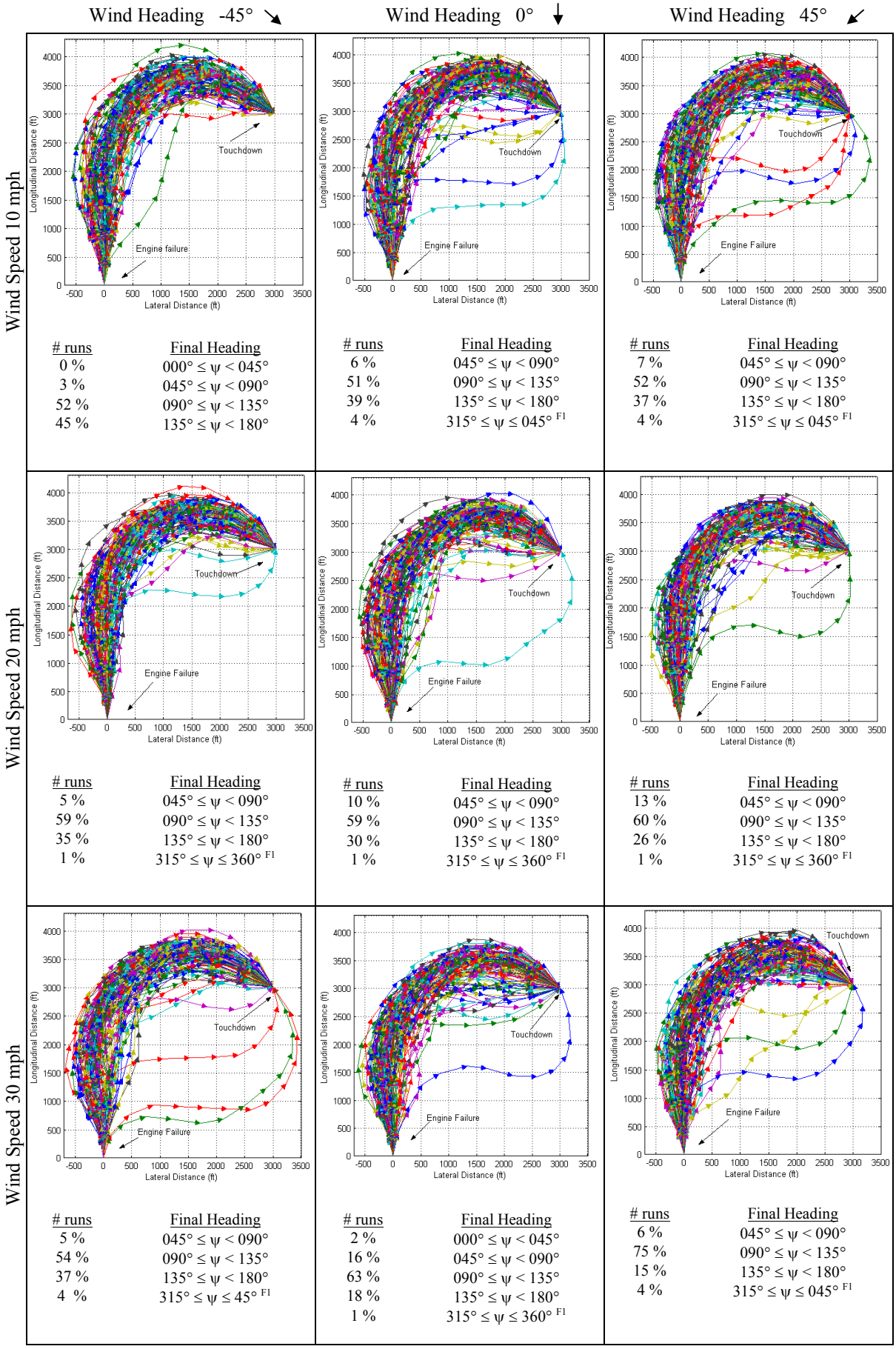

Wind Speed 10 mph	# runs	Final Heading
Wind Heading -45°	0 %	000° ≤ ψ < 045°
	3 %	045° ≤ ψ < 090°
	52 %	090° ≤ ψ < 135°
	45 %	135° ≤ ψ < 180°
Wind Heading 0°	6 %	045° ≤ ψ < 090°
	51 %	090° ≤ ψ < 135°
	39 %	135° ≤ ψ < 180°
	4 %	315° ≤ ψ ≤ 045° [F1]
Wind Heading 45°	7 %	045° ≤ ψ < 090°
	52 %	090° ≤ ψ < 135°
	37 %	135° ≤ ψ < 180°
	4 %	315° ≤ ψ ≤ 045° [F1]

Wind Speed 20 mph	# runs	Final Heading
Wind Heading -45°	5 %	045° ≤ ψ < 090°
	59 %	090° ≤ ψ < 135°
	35 %	135° ≤ ψ < 180°
	1 %	315° ≤ ψ ≤ 360° [F1]
Wind Heading 0°	10 %	045° ≤ ψ < 090°
	59 %	090° ≤ ψ < 135°
	30 %	135° ≤ ψ < 180°
	1 %	315° ≤ ψ ≤ 360° [F1]
Wind Heading 45°	13 %	045° ≤ ψ < 090°
	60 %	090° ≤ ψ < 135°
	26 %	135° ≤ ψ < 180°
	1 %	315° ≤ ψ ≤ 360° [F1]

Wind Speed 30 mph	# runs	Final Heading
Wind Heading -45°	5 %	045° ≤ ψ < 090°
	54 %	090° ≤ ψ < 135°
	37 %	135° ≤ ψ < 180°
	4 %	315° ≤ ψ ≤ 45° [F1]
Wind Heading 0°	2 %	000° ≤ ψ < 045°
	16 %	045° ≤ ψ < 090°
	63 %	090° ≤ ψ < 135°
	18 %	135° ≤ ψ < 180°
	1 %	315° ≤ ψ ≤ 360° [F1]
Wind Heading 45°	6 %	045° ≤ ψ < 090°
	75 %	090° ≤ ψ < 135°
	15 %	135° ≤ ψ < 180°
	4 %	315° ≤ ψ ≤ 045° [F1]

Figure 6.31 Optimal Forced Landing Trajectory – (3000 ft, 3000 ft) Variable Speed and Variable Bank Angle for Engine Failure at 650 ft AGL with Horizontal Wind and Vertical Atmospheric Turbulence

[F1] Double Base Leg Manoeuvre

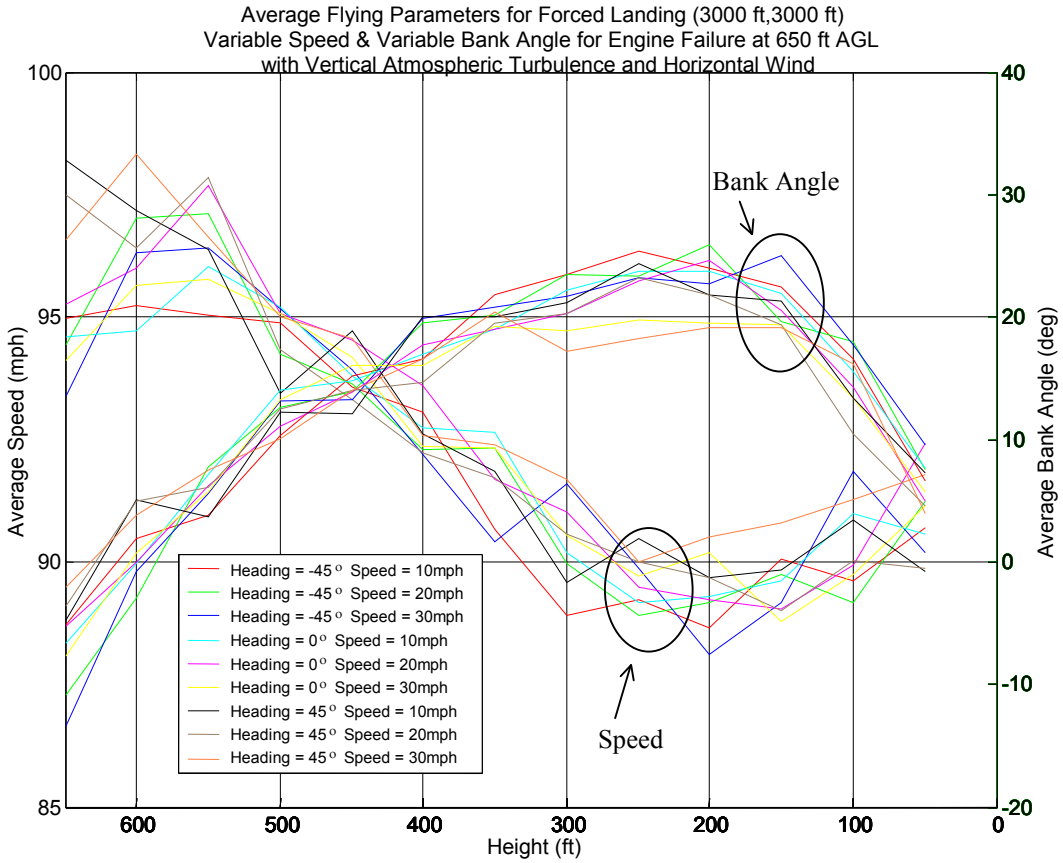

Figure 6.32 Average Flying Parameters for Forced Landing – (3000 ft, 3000 ft) Variable Speed and Variable Bank Angle for Engine Failure at 650 ft AGL with Horizontal Wind and Vertical Atmospheric Turbulence

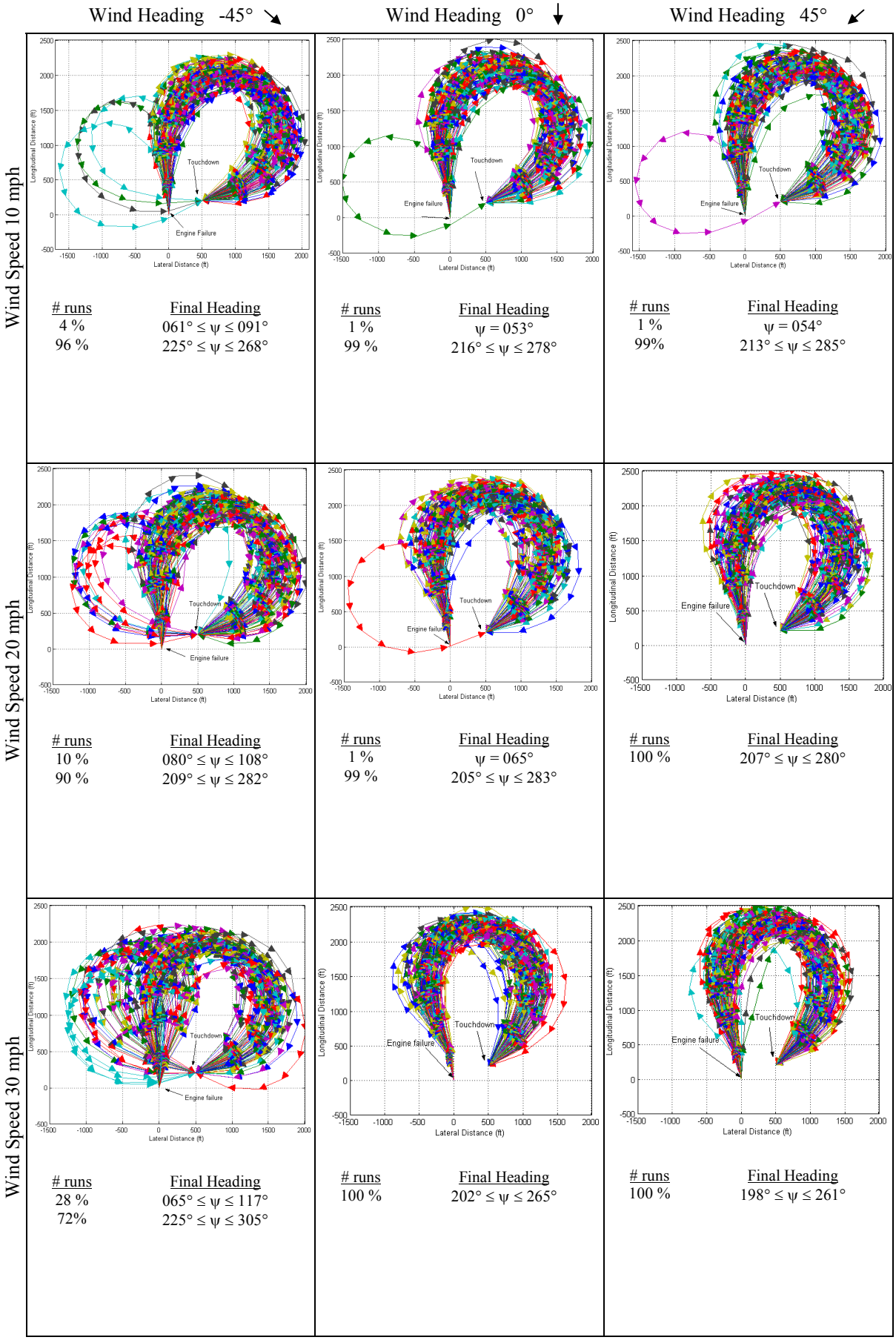

Figure 6.33 Optimal Forced Landing Trajectory – (500 ft, 200 ft) Variable Speed and Variable Bank Angle for Engine Failure at 650 ft AGL with Horizontal Wind and Vertical Atmospheric Turbulence

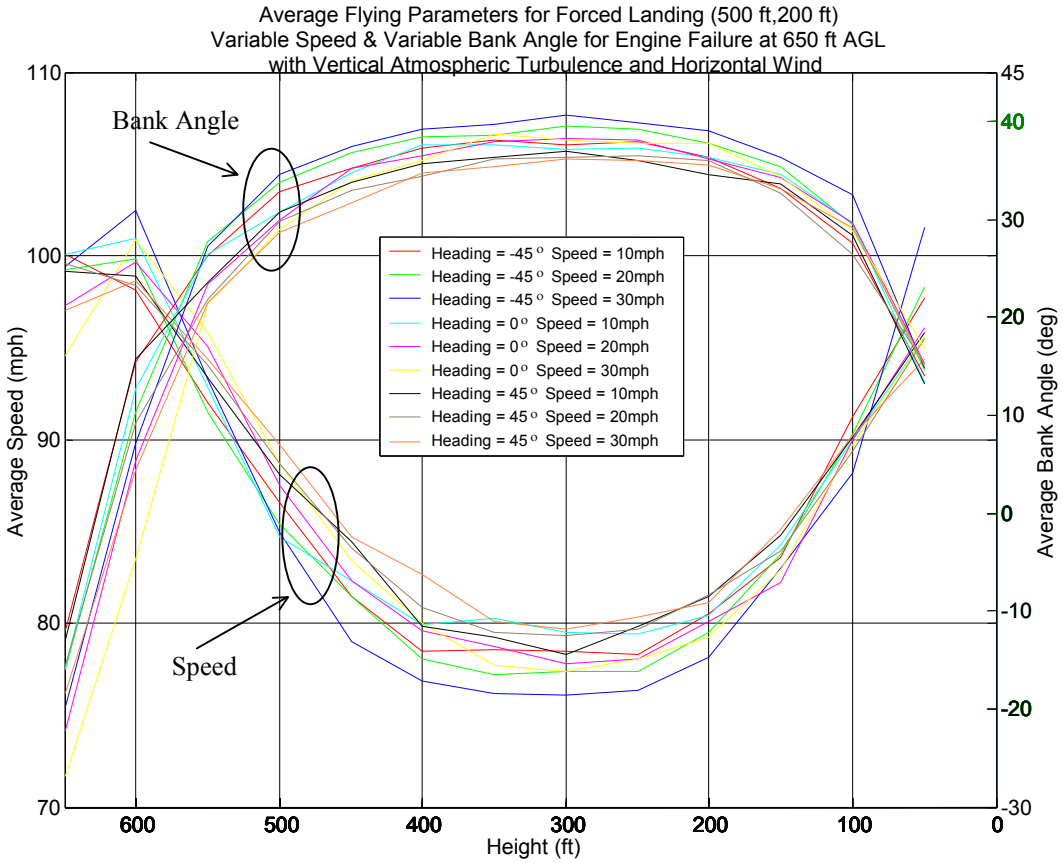

Figure 6.34 Average Flying Parameters for Forced Landing – (500 ft, 200 ft) Variable Speed and Variable Bank Angle for Engine Failure at 650 ft AGL with Horizontal Wind and Vertical Atmospheric Turbulence

Overall, the effects vertical atmospheric disturbances with maximum updrafts and downdrafts of 1.48 ft/sec and 1.67 ft/sec respectively, have on a forced landing resemble the results obtained without vertical disturbances but the flight path characterises are accentuated moderately for all the three pre-selected locations tested.

6.6.3 Results with Horizontal Wind and Thermal Disturbances

This section shows the effects vertical thermals, ranging from –9.84 ft/sec to +9.84 m/s, have on a forced landing manoeuvre with horizontal crosswinds. The results for the pre-selected location (0 ft, -3100 ft) with vertical thermal are shown in Figures 6.35 – 6.36. These results show similar general trend compare to the results obtained without vertical atmospheric disturbances as shown in Figures 6.23 – 6.24. However, the strong vertical thermals accentuate the flight path and flying parameters characteristics significantly, tracing a much longer and wider flight path, and resulting in a wider range of flying parameters compare to without vertical disturbances as described in Chapter 6.6.1.

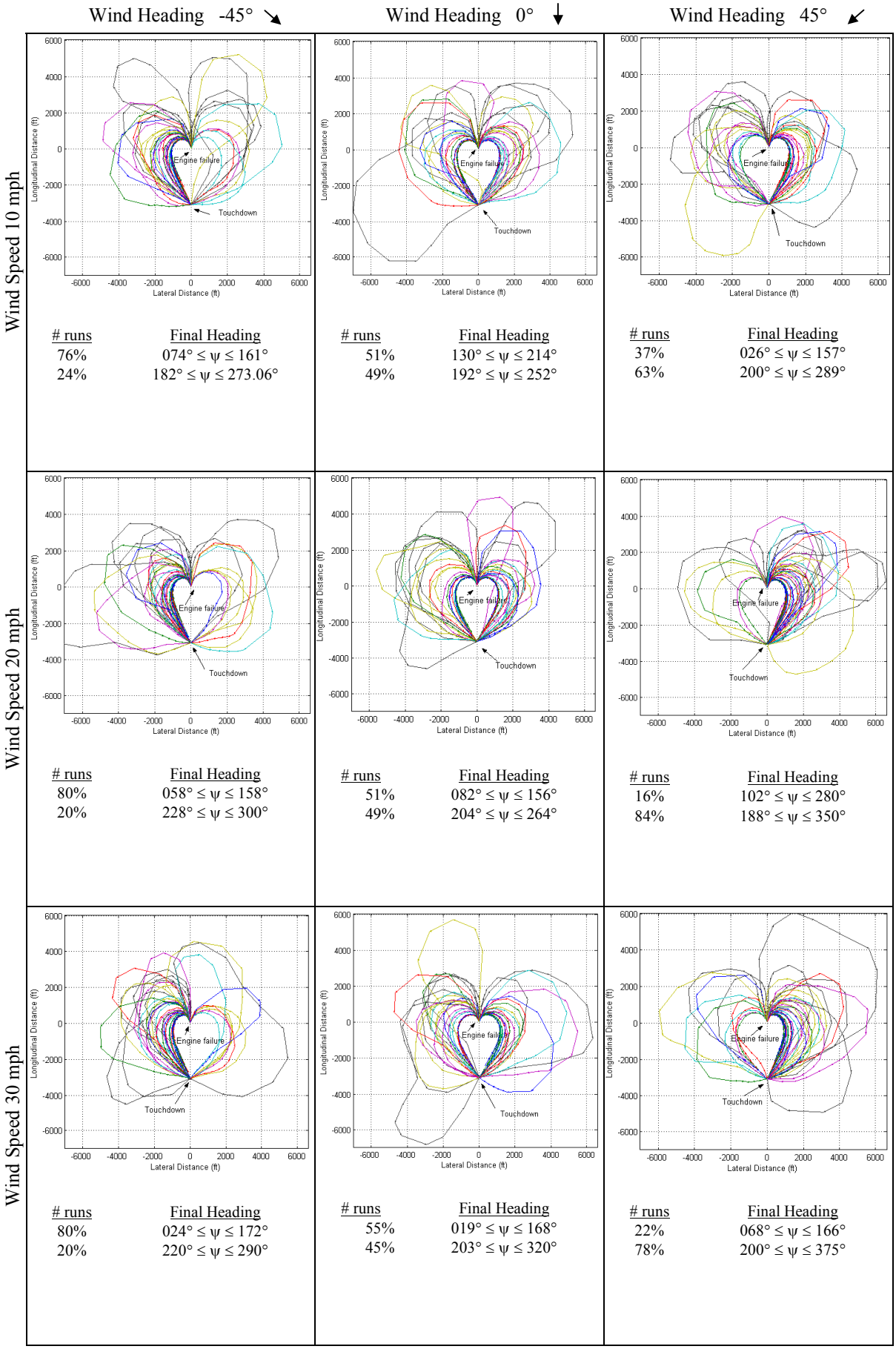

Figure 6.35 Optimal Forced Landing Trajectory – (0 ft, -3100 ft) Variable Speed and Variable Bank Angle for Engine Failure at 650 ft AGL with Horizontal Wind and Vertical Thermals

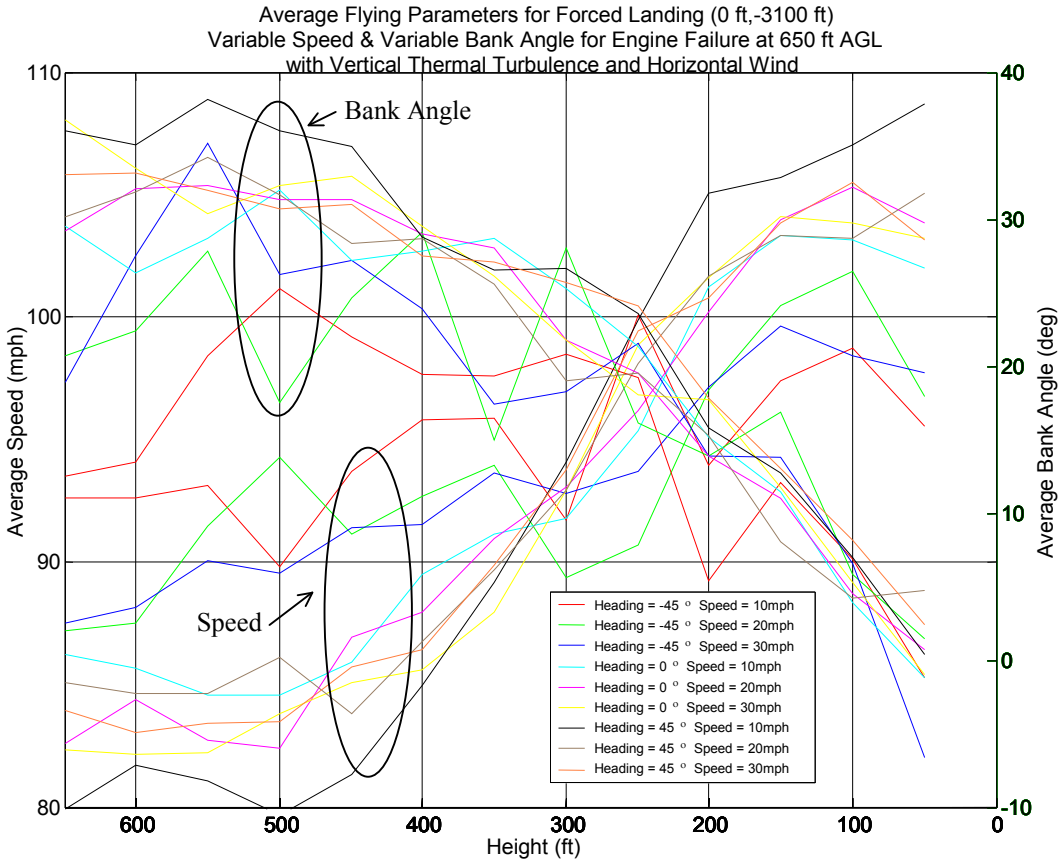

Figure 6.36 Average Flying Parameters for Forced Landing – (0 ft, -3100 ft) Variable Speed and Variable Bank Angle for Engine Failure at 650 ft AGL with Horizontal Wind and Vertical Thermals

The results for the pre-selected location (3000 ft, 3000 ft) with vertical thermals are shown in Figures 6.37 – 6.38. These results show similar general trend compare to the results obtained without vertical atmospheric disturbances as shown in Figures 6.25 – 6.26. However, the strong vertical thermals accentuate the flight path and flying parameters characteristics significantly. It traces a much longer and wider flight path, increases the number of flight paths with final heading ranging from 180° to 360°, and have a wider range of flying parameters compare to without vertical disturbances as described in Chapter 6.6.1.

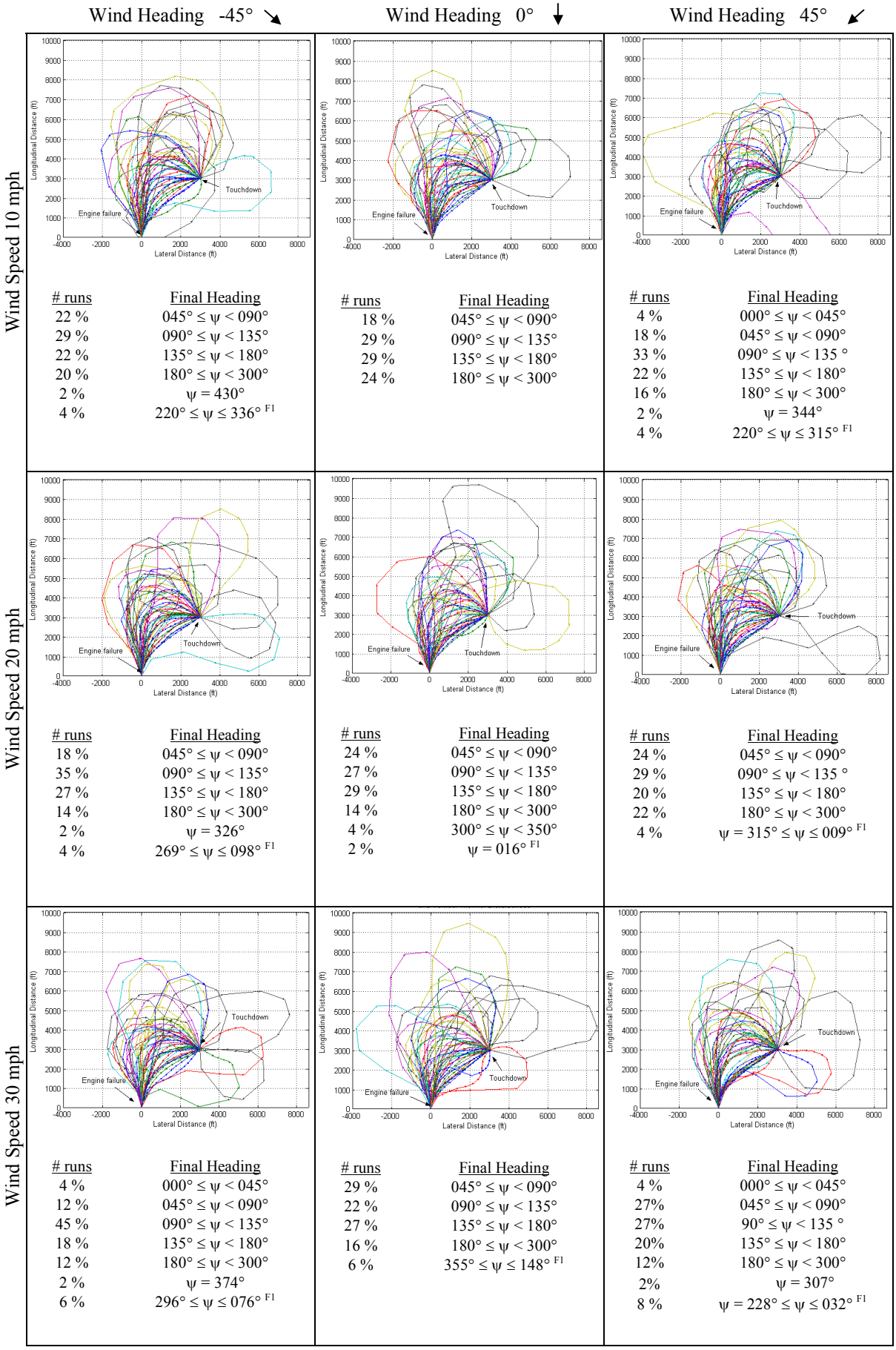

Wind Speed 10 mph	# runs	Final Heading
Wind Heading -45°	22 %	045° ≤ ψ < 090°
	29 %	090° ≤ ψ < 135°
	22 %	135° ≤ ψ < 180°
	20 %	180° ≤ ψ < 300°
	2 %	ψ = 430°
	4 %	220° ≤ ψ ≤ 336° [F1]
Wind Heading 0°	18 %	045° ≤ ψ < 090°
	29 %	090° ≤ ψ < 135°
	29 %	135° ≤ ψ < 180°
	24 %	180° ≤ ψ < 300°
Wind Heading 45°	4 %	000° ≤ ψ < 045°
	18 %	045° ≤ ψ < 090°
	33 %	090° ≤ ψ < 135 °
	22 %	135° ≤ ψ < 180°
	16 %	180° ≤ ψ < 300°
	2 %	ψ = 344°
	4 %	220° ≤ ψ ≤ 315° [F1]

Wind Speed 20 mph	# runs	Final Heading
Wind Heading -45°	18 %	045° ≤ ψ < 090°
	35 %	090° ≤ ψ < 135°
	27 %	135° ≤ ψ < 180°
	14 %	180° ≤ ψ < 300°
	2 %	ψ = 326°
	4 %	269° ≤ ψ ≤ 098° [F1]
Wind Heading 0°	24 %	045° ≤ ψ < 090°
	27 %	090° ≤ ψ < 135°
	29 %	135° ≤ ψ < 180°
	14 %	180° ≤ ψ < 300°
	4 %	300° ≤ ψ < 350°
	2 %	ψ = 016° [F1]
Wind Heading 45°	24 %	045° ≤ ψ < 090°
	29 %	090° ≤ ψ < 135 °
	20 %	135° ≤ ψ < 180°
	22 %	180° ≤ ψ < 300°
	4 %	ψ = 315° ≤ ψ ≤ 009° [F1]

Wind Speed 30 mph	# runs	Final Heading
Wind Heading -45°	4 %	000° ≤ ψ < 045°
	12 %	045° ≤ ψ < 090°
	45 %	090° ≤ ψ < 135°
	18 %	135° ≤ ψ < 180°
	12 %	180° ≤ ψ < 300°
	2 %	ψ = 374°
	6 %	296° ≤ ψ ≤ 076° [F1]
Wind Heading 0°	29 %	045° ≤ ψ < 090°
	22 %	090° ≤ ψ < 135°
	27 %	135° ≤ ψ < 180°
	16 %	180° ≤ ψ < 300°
	6 %	355° ≤ ψ ≤ 148° [F1]
Wind Heading 45°	4 %	000° ≤ ψ < 045°
	27%	045° ≤ ψ < 090°
	27%	90° ≤ ψ < 135 °
	20%	135° ≤ ψ < 180°
	12%	180° ≤ ψ < 300°
	2%	ψ = 307°
	8 %	ψ = 228° ≤ ψ ≤ 032° [F1]

Figure 6.37 Optimal Forced Landing Trajectory – (3000 ft, 3000 ft) Variable Speed and Variable Bank Angle for Engine Failure at 650 ft AGL with Horizontal Wind and Vertical Thermals

[F1] Double Base Leg Manoeuvre

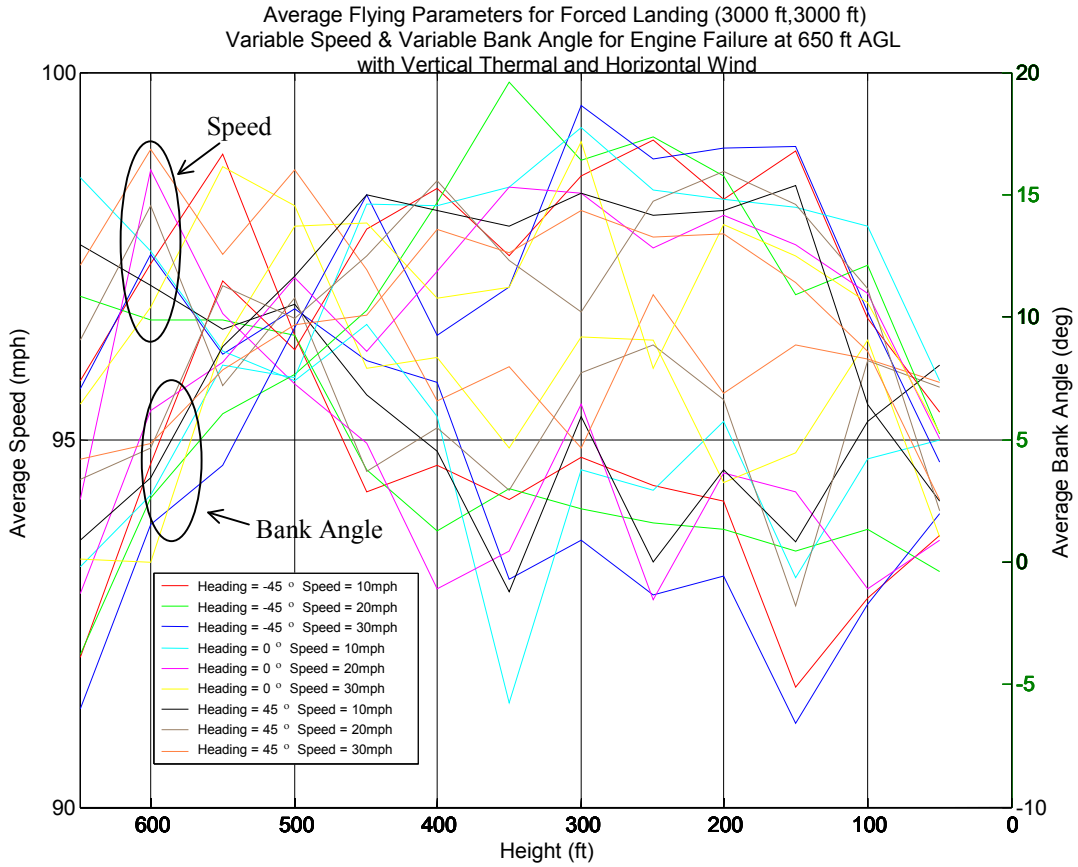

Figure 6.38 Average Flying Parameters for Forced Landing – (3000 ft, 3000 ft) Variable Speed and Variable Bank Angle for Engine Failure at 650 ft AGL with Horizontal Wind and Vertical Thermals

The results for the pre-selected location (500 ft, 200 ft) with vertical thermals are shown in Figures 6.39 – 6.40. These results show similar general trend compare to the results obtained without vertical atmospheric disturbances as shown in Figures 6.27 – 6.28. However, the strong vertical thermals accentuate the flight path characteristics significantly. It traces a much longer and wider flight path, increases the final heading range, and have a wider range of flying parameters compare to without vertical disturbances as described in Chapter 6.6.1.

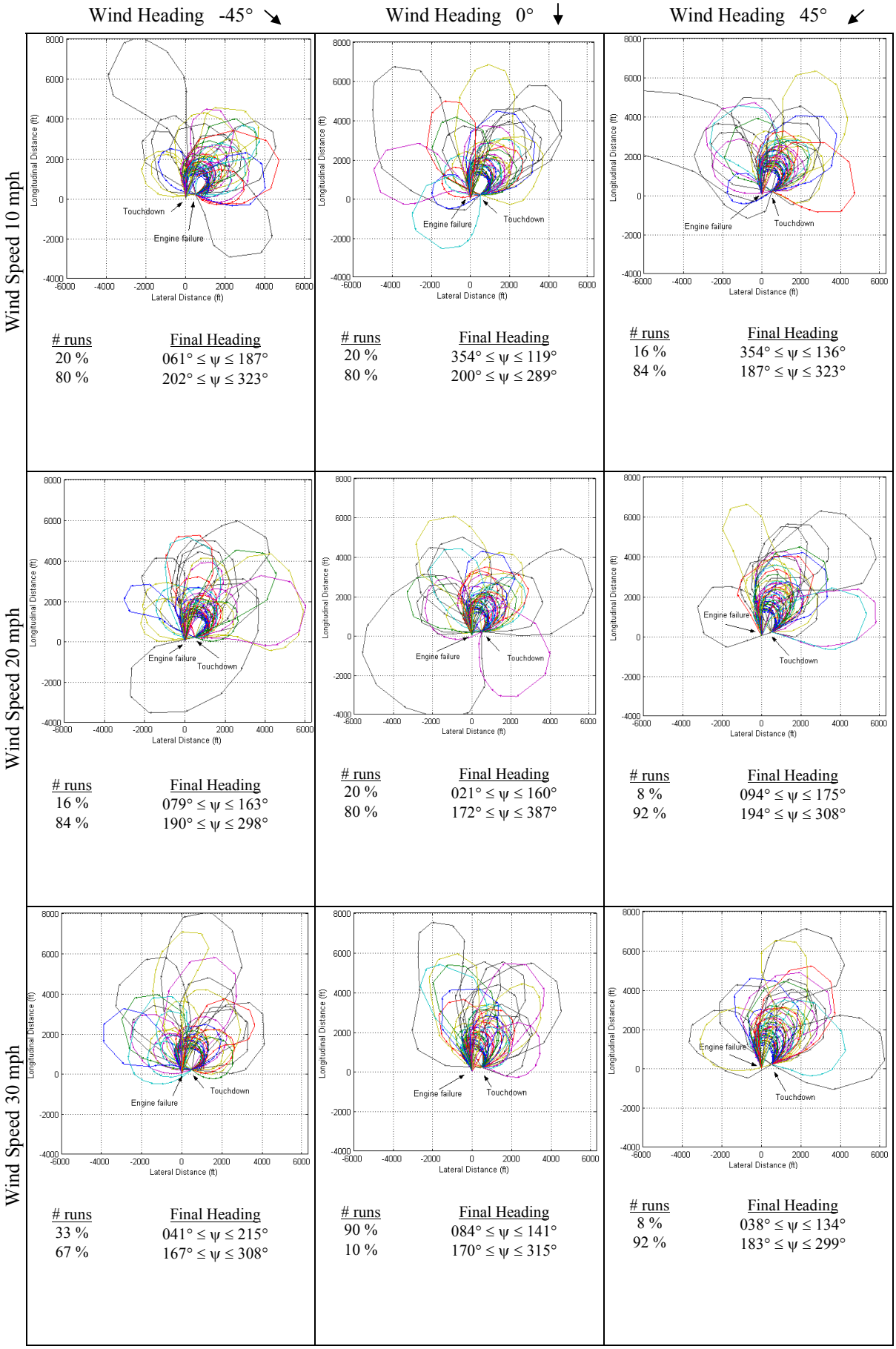

Figure 6.39 Optimal Forced Landing Trajectory – (500 ft, 200 ft) Variable Speed and Variable Bank Angle for Engine Failure at 650 ft AGL with Horizontal Wind and Vertical Thermals

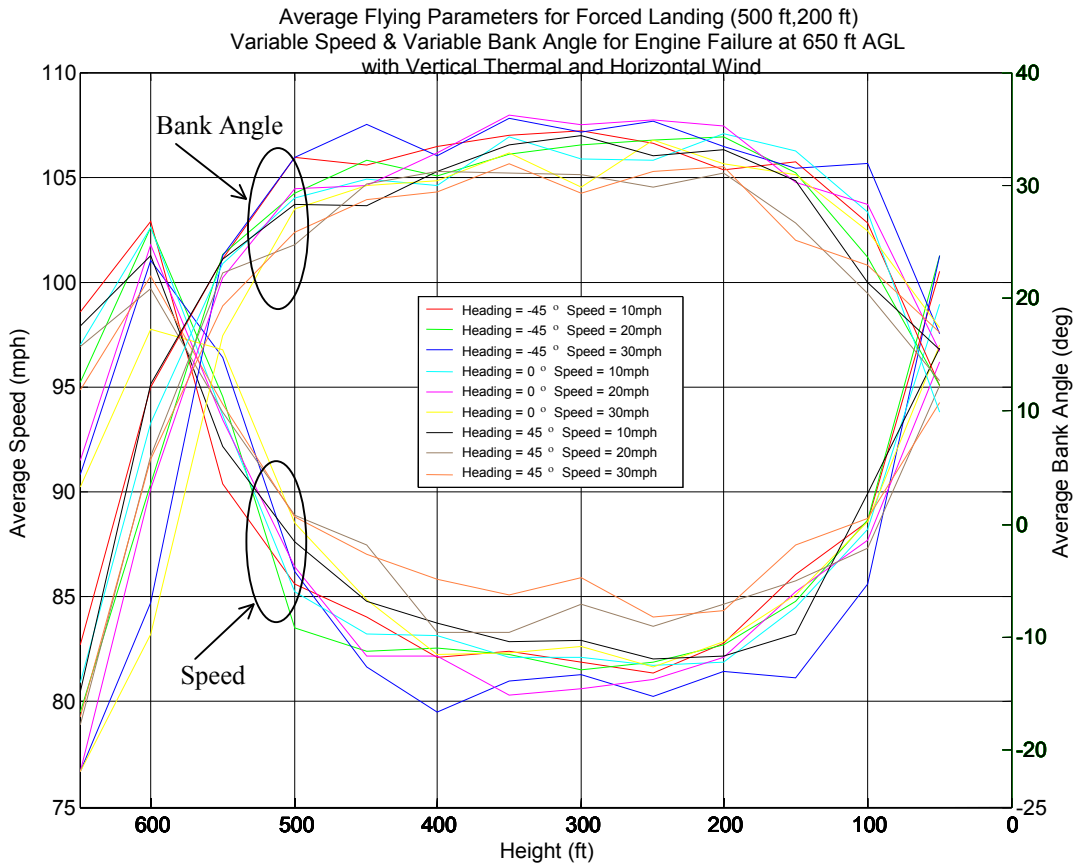

Figure 6.40 Average Flying Parameters for Forced Landing – (500 ft, 200 ft) Variable Speed and Variable Bank Angle for Engine Failure at 650 ft AGL with Horizontal Wind and Vertical Thermals

Overall, the effects thermal disturbances with maximum updrafts and downdrafts of 9.84 ft/sec have on a forced landing resemble the results obtained without vertical disturbances but the flight path characterises are accentuated moderately for all the three pre-selected locations.

6.7 Genetic Algorithm in a Forced Landing Manoeuvre with Pre-selected Location and Specified Final Heading

The GA program prior to this chapter has successfully located touchdown locations very close the pre-selected locations. This section implements an additional objective of touching down closest to a specified final heading. Using the similar GA search method as described in Chapter 6.4 and the forced landing Matlab program developed, the GA's fitness function has the additional criteria of assessing the final heading in addition to the pre-selected touchdown location. Several multiplier factors were tested and a factor of 1/100 and 1/10 for the distance error and final heading error respectively were found suitable for the fitness function. There is more weighting on landing closer to the pre-selected location since in a real-life forced landing manoeuvre, landing at or very close to the pre-selected location has precedence over the final heading. The fitness function can be expressed:

$$Fitness\ Function = \sum \frac{distance\ error}{100} + \sum \frac{final\ heading\ error}{10}$$

Analyses were carried out for several specific final headings for each of the pre-selected touchdown locations of touching down at (0 ft, -3100 ft), (3000 ft, 3000 ft) and (500 ft, 200 ft), where the 1st component represents the lateral distance and the 2nd component represents the longitudinal distance from the engine failure point. The specific final headings tested were selected based on the forced landing trajectory results as shown in Figures 6.14 – 6.16 as presented in Chapter 6.4.3.

6.7.1 Results with Specified Final Heading

The results for the forced landing manoeuvre with pre-selected touchdown location and specific final heading carried out are shown in Table 6.10. Three final headings at 180°, 225° and 270° were specified for the pre-selected touchdown location of (0 ft, -3100 ft). They were chosen based on the results as shown in Figure 6.14 where the final headings range between 206° and 240°. Five final headings at 0°, 90°, 150°, 180° and 315° were specified for the pre-selected touchdown location of (3000 ft, 3000 ft). They were chosen based on the results as shown in Figure 6.15 where the final headings range between 0° and 340° with varying probability within different range of final headings. Three final headings at 45°, 180° and 255° were specified for the pre-selected touchdown location of (500 ft, 200 ft).

They were chosen based on the results as shown in Figure 6.16 where the final headings range between 222° and 288°, and between 32° and 73° with the former having a much higher probability since it flies toward the pre-selected touchdown location.

Table 6.10 Results for GA with Pre-selected Location and Specific Final Heading

Pre-selected Location	Specified Final Heading (deg)	Average Final Heading Computed (deg)	Heading error (deg)	Distance Error (ft)
(0 ft, -3100 ft)	225	224.7660	0.2340	1.7575
(0 ft, -3100 ft)	180	195.1083	15.1083	9.9459
(0 ft, -3100 ft)	270	249.3819	20.6181	10.9365
(3000 ft, 3000 ft)	150	149.8836	0.1164	0.5547
(3000 ft, 3000 ft)	90	90.9225	0.9225	2.4420
(3000 ft, 3000 ft)	180	171.0022	8.9978	4.9323
(3000 ft, 3000 ft)	0	26.5977	26.5977	12.1306
(3000 ft, 3000 ft)	315	-13.8415	31.1585	12.6317
(500 ft, 200 ft)	255	255.0017	0.0017	0.1919
(500 ft, 200 ft)	180	187.8298	7.8298	11.6859
(500 ft, 200 ft)	45	166.8710	121.8710	20.1884

The results obtained for the pre-selected touchdown location of (0 ft, -3100 ft) show that the smallest final heading error was obtained for the specific final heading of 225° and that both the heading error and distance error increases as the specified final heading deviated from it. This is as expected since if no final heading were specified, the aircraft has the highest probability of touching down between 206° and 240° as shown in Figure 6.14. The forced landing flight paths and their flying parameters for the pre-selected touchdown location (0 ft, -3100 ft) for the three specific final headings are shown in Figures 6.41 – 6.43. Overall, the flight trajectories for all three specified final headings have similar flight path and flying parameters for approximately first 30 secs of the flight. Thereafter, the flight paths change accordingly to suit each specific final heading. A heading error of 15° was found for the specified final heading of 180° while a largest error of 20.62° in final heading was found for the case of the specified final heading of 270°. Large final heading errors for the above two cases are because the aeroplane lacks the height to further re-align itself more towards the specified final heading.

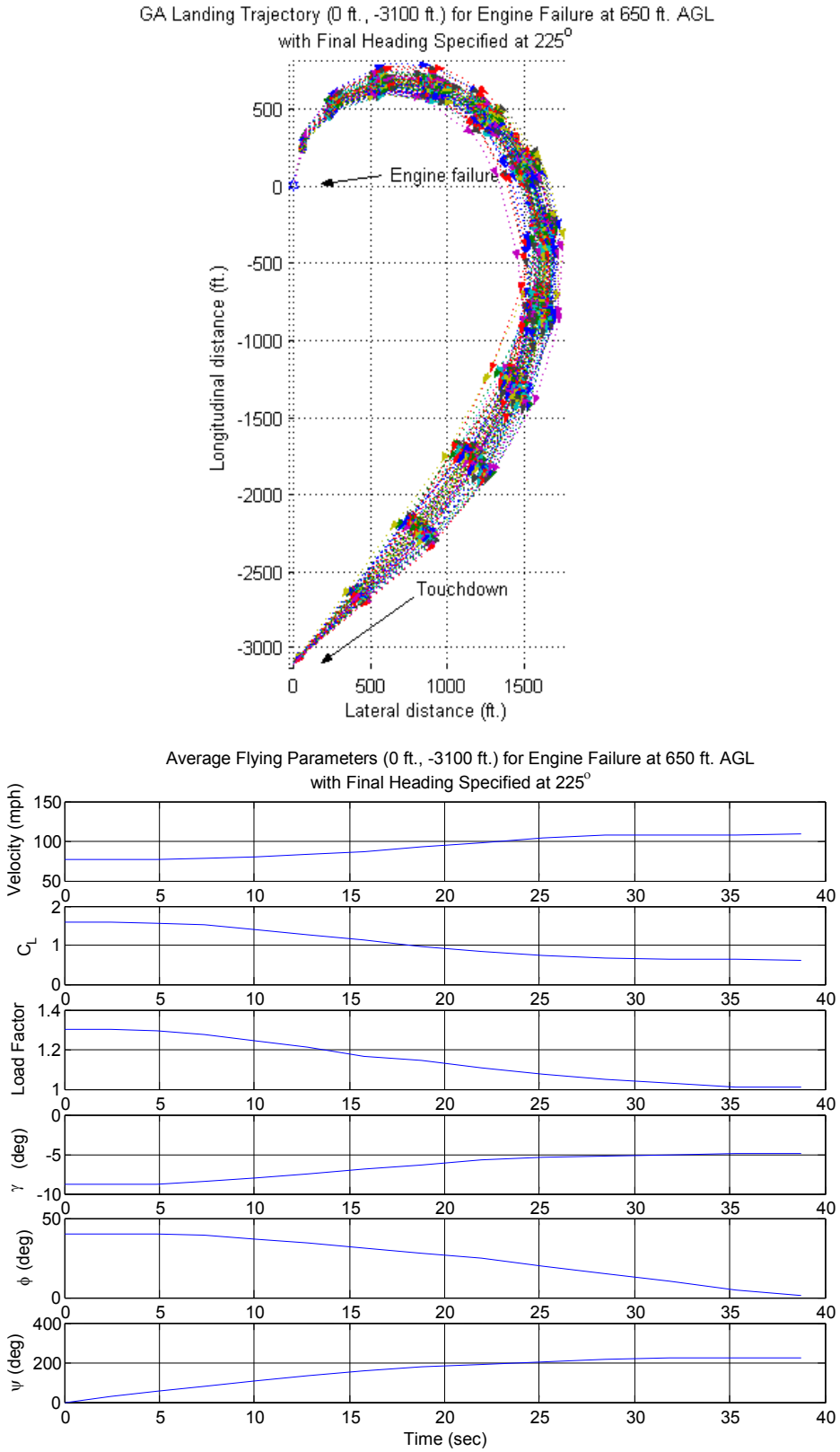

Figure 6.41 Forced Landing (-3100 ft, 0 ft) with Specified Final Heading at 225° for Engine Failure at 650 ft AGL

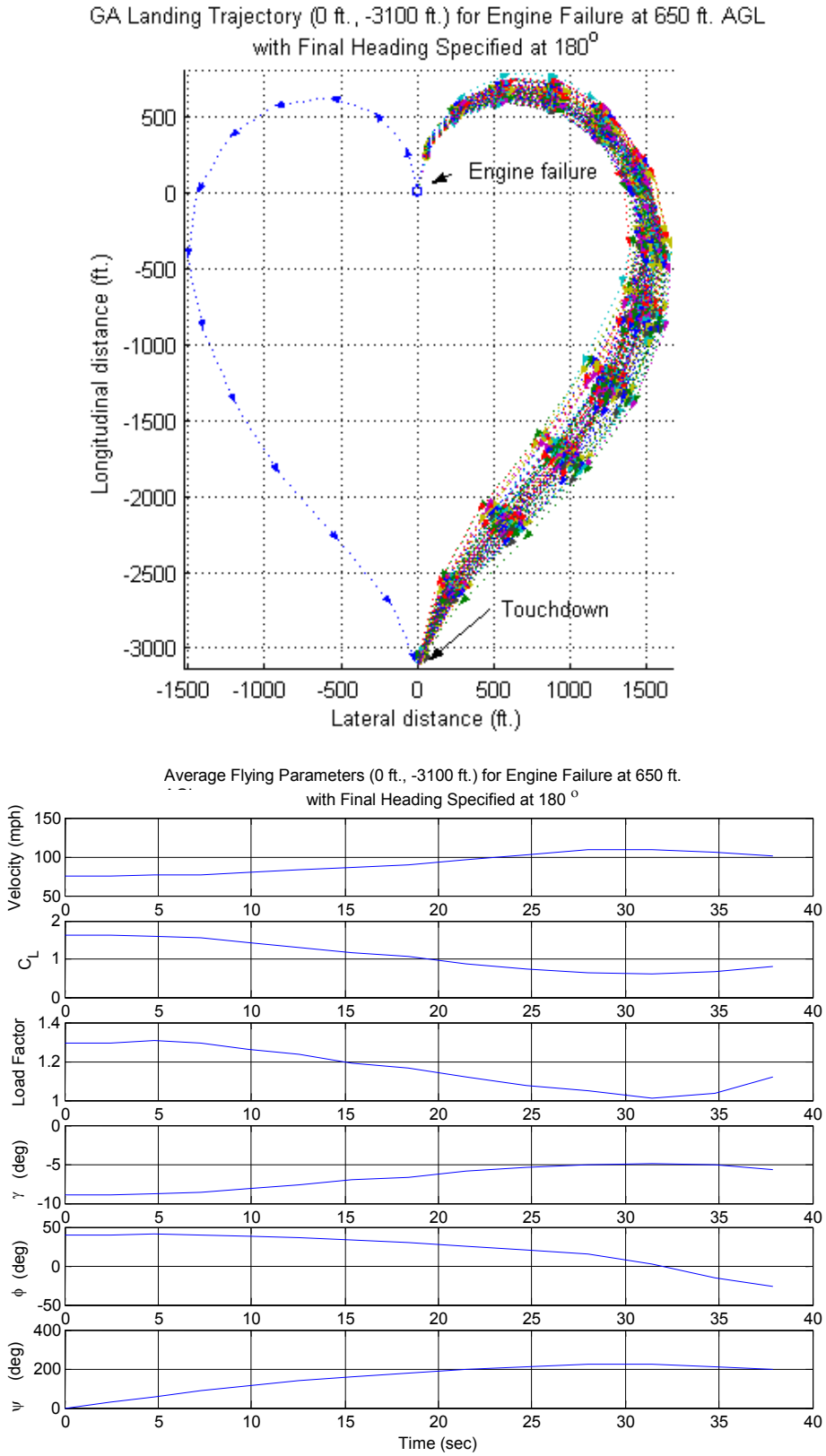

Figure 6.42 Forced Landing (-3100 ft, 0 ft) with Specified Final Heading at 180° for Engine Failure at 650 ft AGL

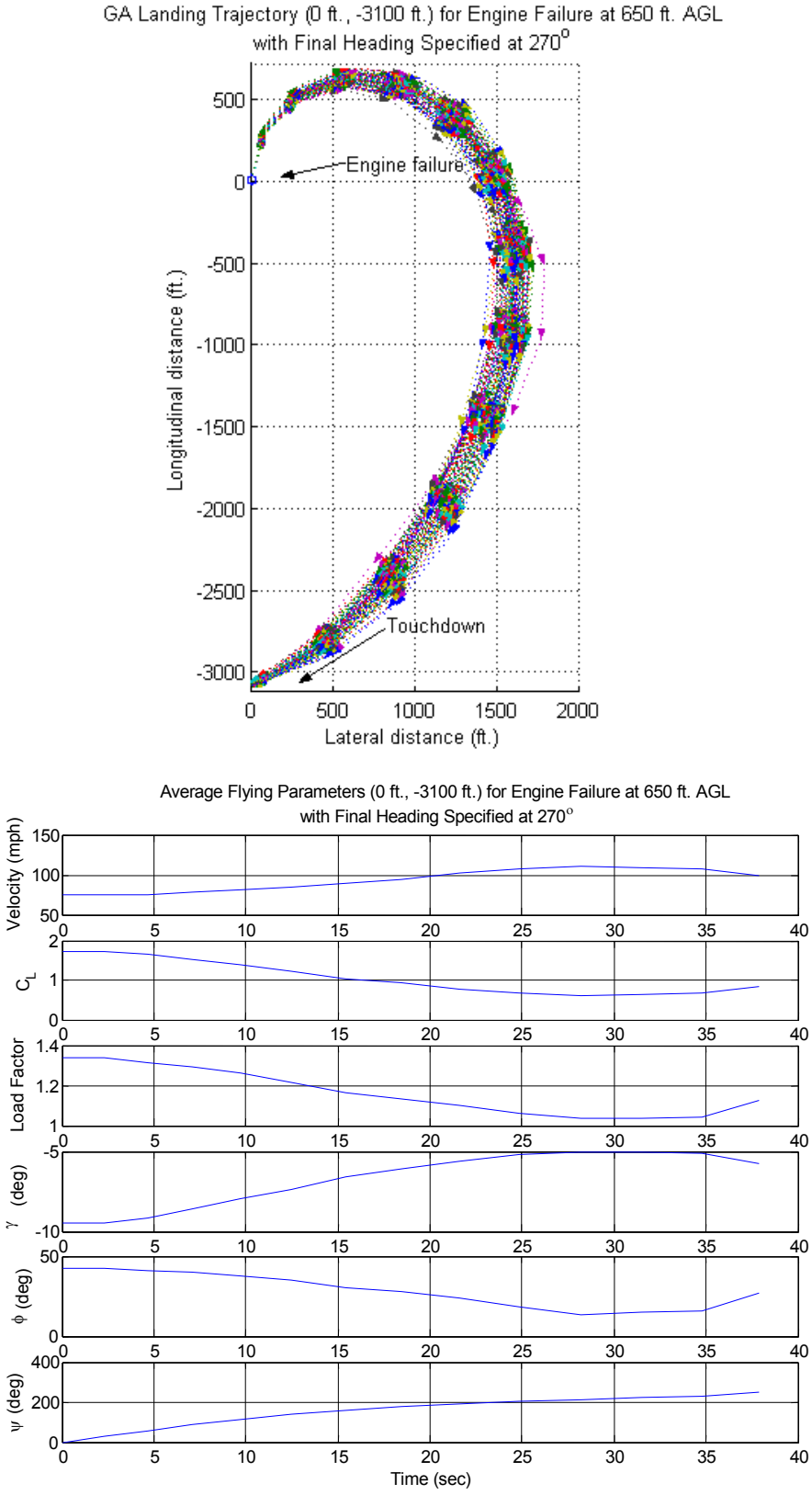

Figure 6.43 Forced Landing (-3100 ft, 0 ft) with Specified Final Heading at 270° for Engine Failure at 650 ft AGL

The forced landing flight paths and their flying parameters for the pre-selected touchdown location (3000 ft, 3000 ft) for the three specific final headings are shown in Figures 6.44 – 6.48. The results obtained for the pre-selected touchdown location of (3000 ft, 3000 ft) show that the smallest final heading error and distance error were obtained for the specified final heading of 150°, followed by 90°, 180°, 0° and 315° as shown in Table 6.10. The increase in error is consistent with the touchdown probability obtained for the different range of final headings if no final heading was specified as shown in Figure 6.15. An error of 26.6° and 31° in final heading was found for specified final heading of 0° and 315° respectively. Such large error in final heading is due to the location and is consistent with the results as shown in Figure 6.15 where the probability in touching down with certain final headings are very low.

For specified final headings of 90°, 150° and 180°, the forced landings have similar flight paths and flying parameters for approximately the first 35 seconds. Thereafter, the airplane's bank angle changes accordingly to manoeuvre itself towards the specified final heading. For specified final headings of -45° and 0°, the airplane flies the double base leg manoeuvre and takes a few seconds longer to touchdown compare to the 90° approach to landing manoeuvre. The flight paths and flying parameters are similar for approximately the first 23 seconds. Thereafter, the airplane manoeuvres itself to head towards the specified final heading.

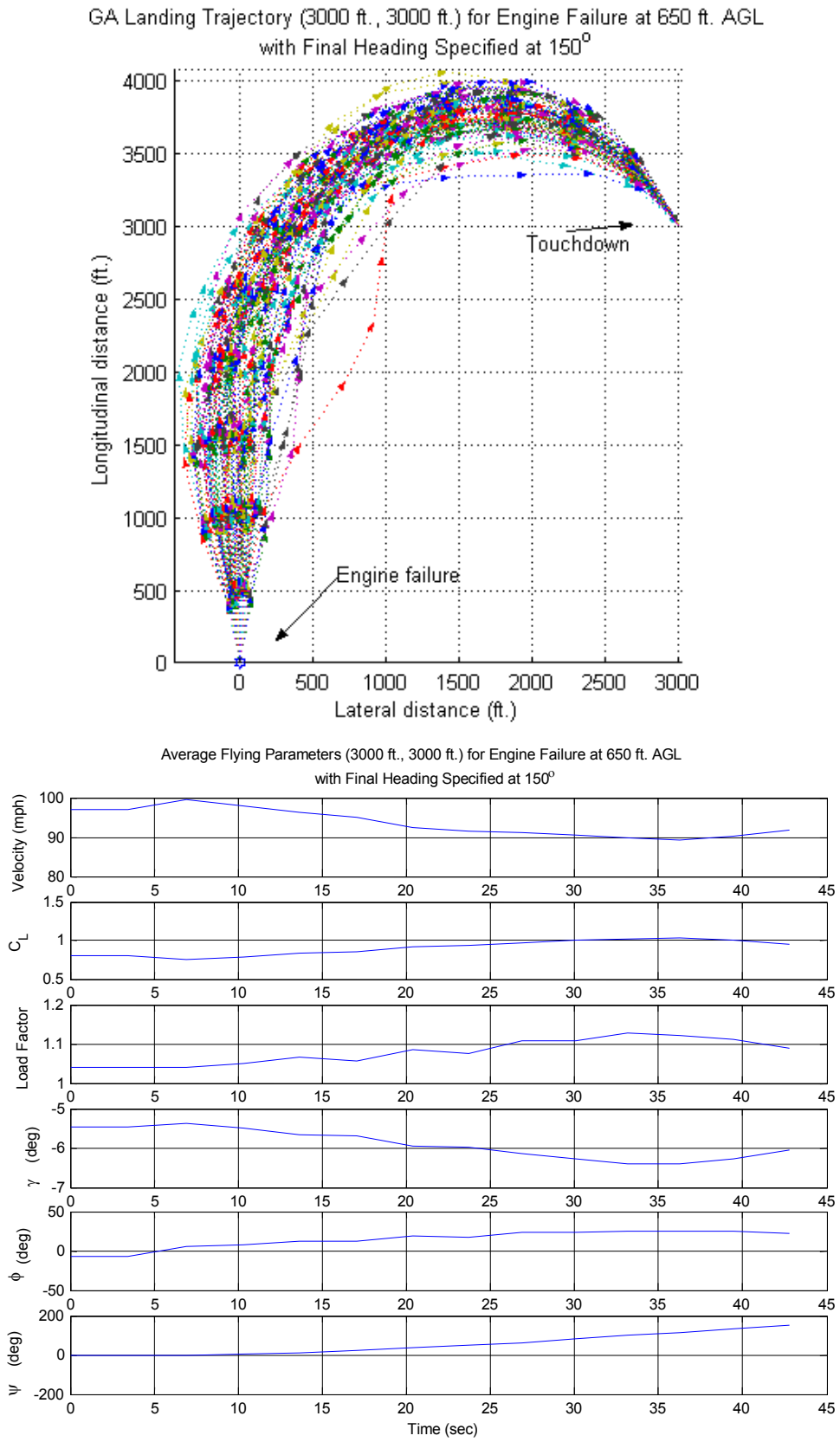

Figure 6.44 Forced Landing (3000 ft, 3000 ft) with Specified Final Heading at 150° for Engine Failure at 650 ft AGL

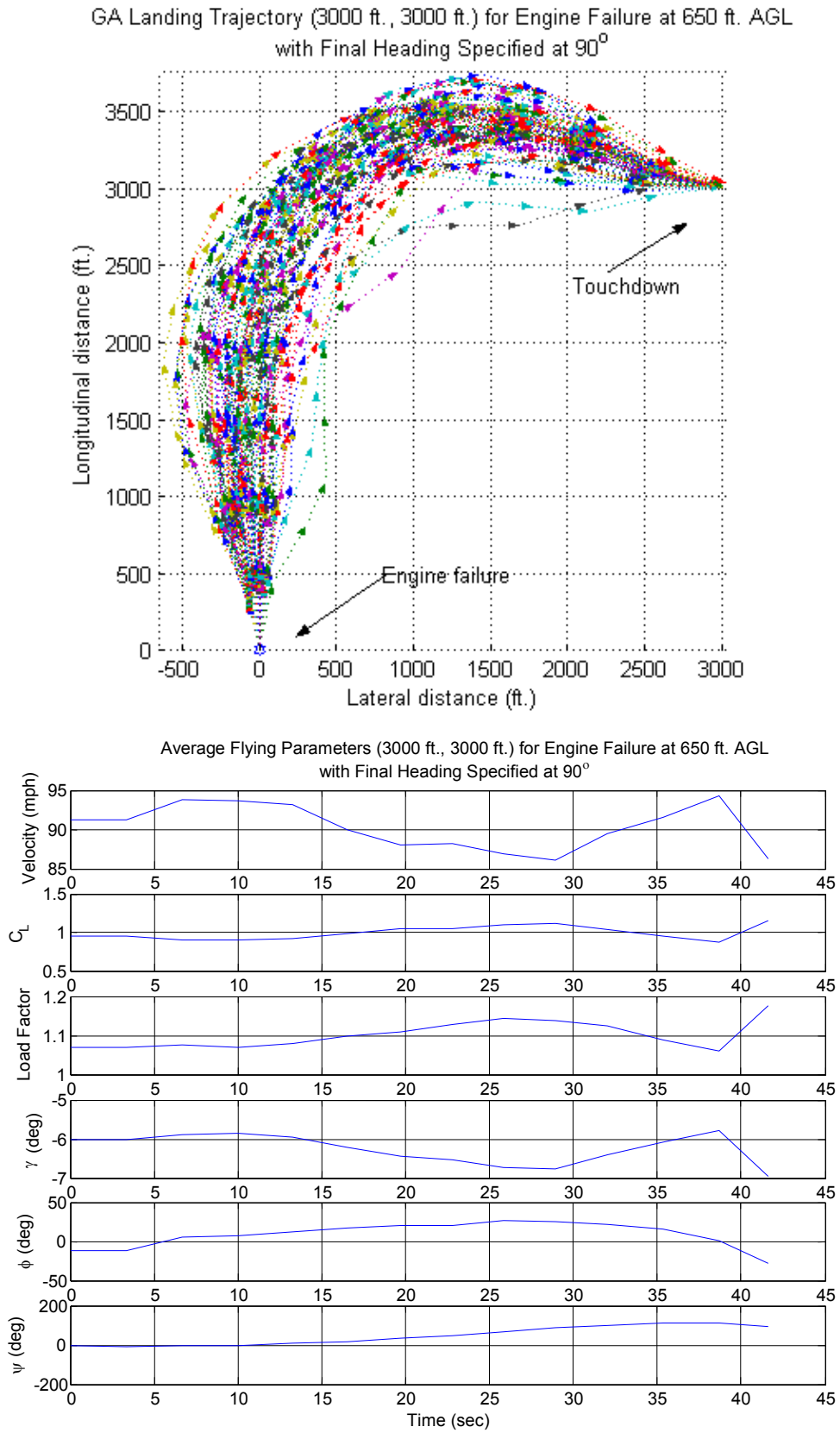

Figure 6.45 Forced Landing (3000 ft, 3000 ft) with Specified Final Heading at 90° for Engine Failure at 650 ft AGL

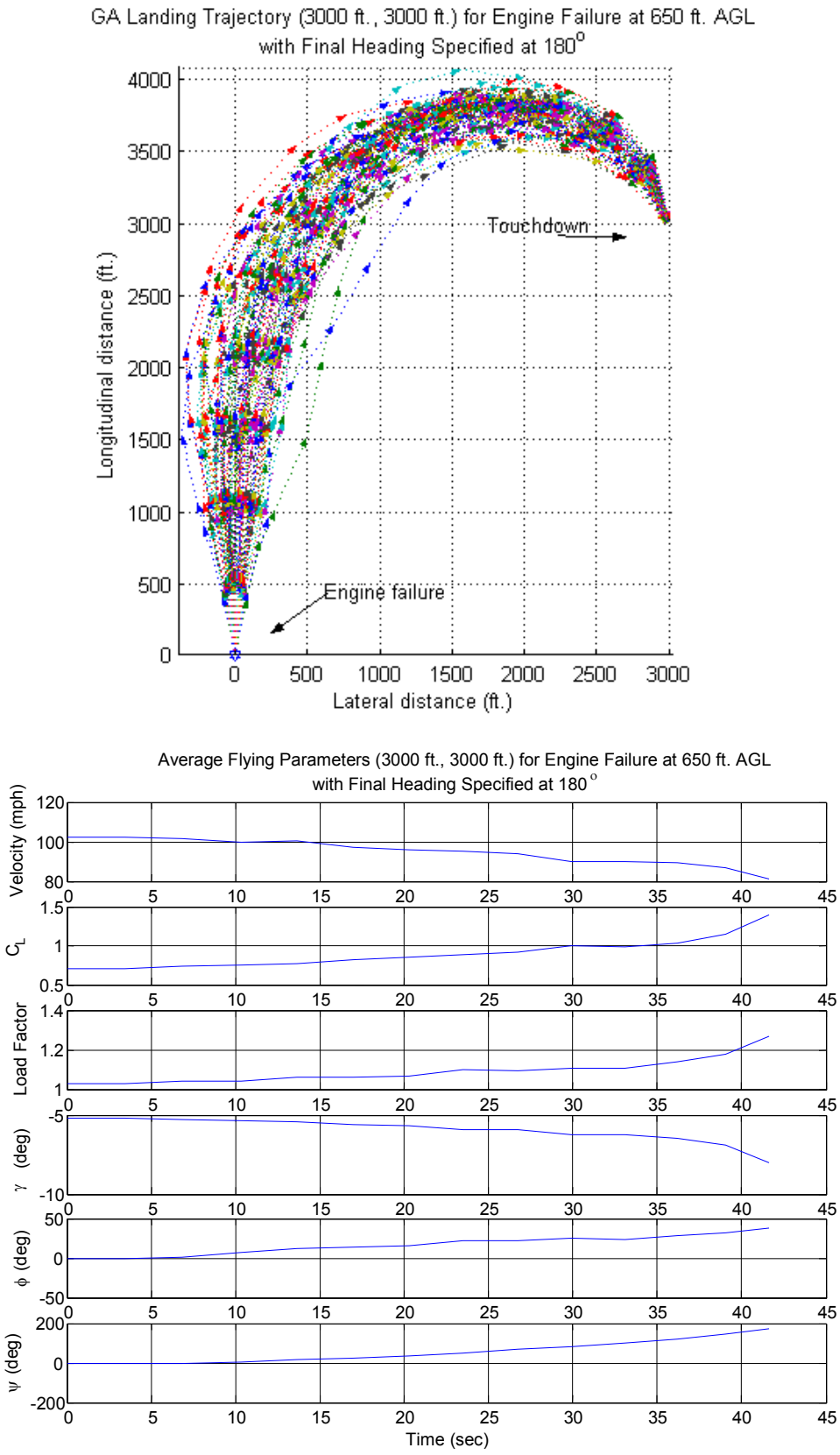

Figure 6.46 Forced Landing (3000 ft, 3000 ft) with Specified Final Heading at 180° for Engine Failure at 650 ft AGL

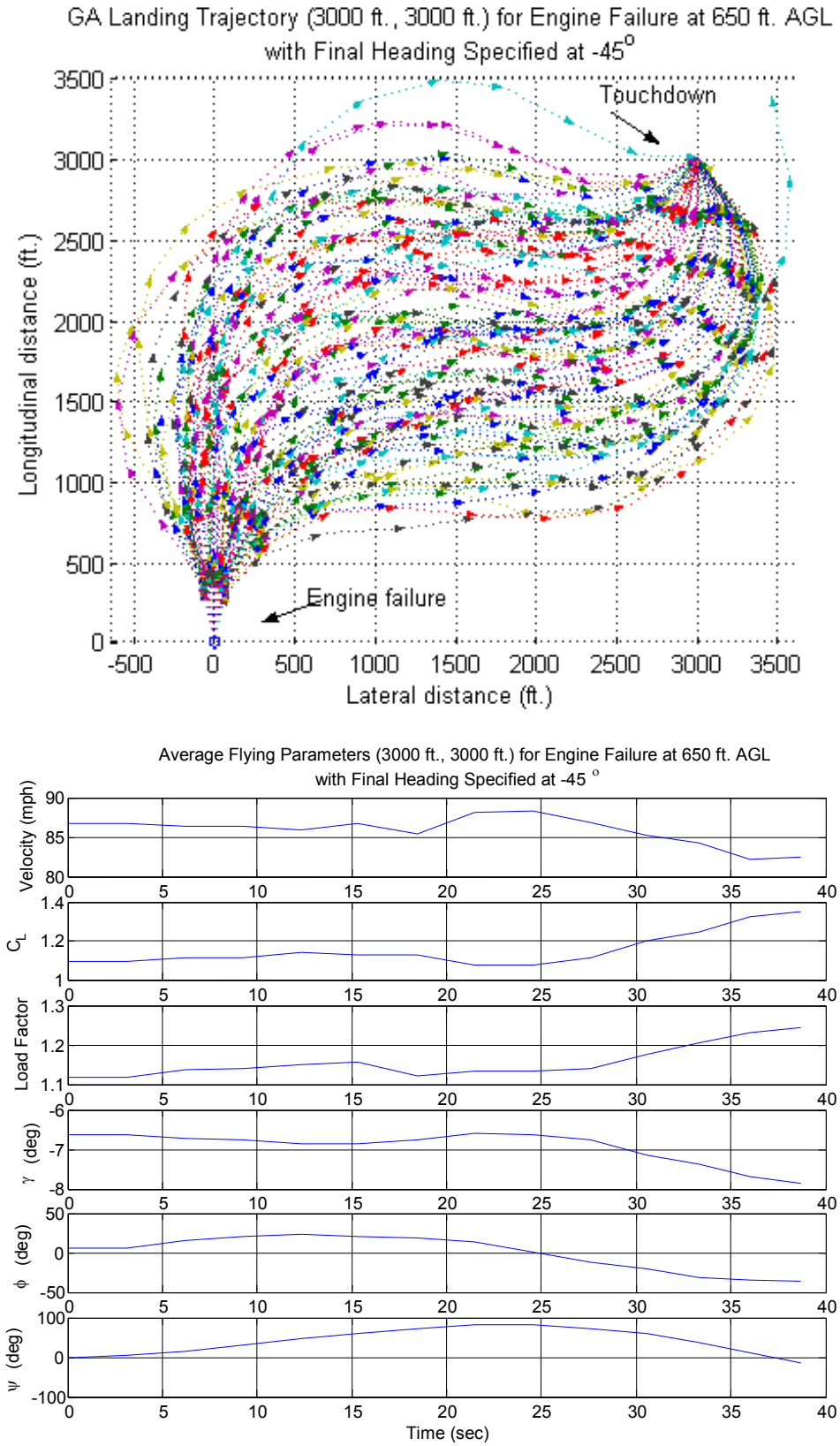

Figure 6.47 Forced Landing (3000 ft, 3000 ft) with Specified Final Heading at 315° for Engine Failure at 650 ft AGL

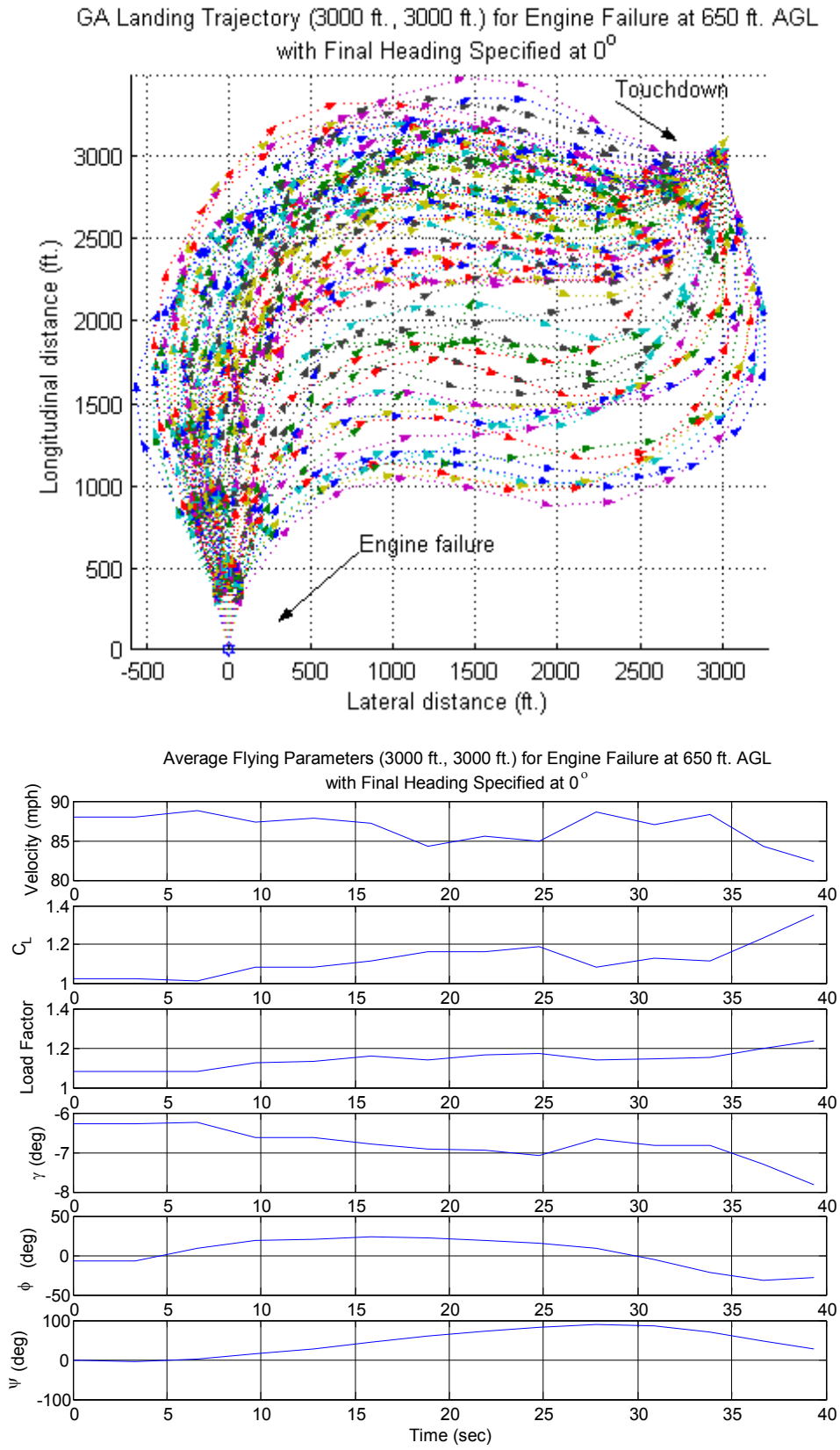

Figure 6.48 Forced Landing (3000 ft, 3000 ft) with Specified Final Heading at 0° for Engine Failure at 650 ft AGL

The forced landing flight paths and their flying parameters for the pre-selected touchdown location (500 ft, 200 ft) for the three specific final headings are shown in Figures 6.49 – 6.51. The results obtained for the pre-selected touchdown location of (500 ft, 200 ft) show that the smallest final heading error and distance error was obtained for the specified final heading of 255°, followed by 180° and 45° as shown in Table 6.10. The increase in error is consistent with the probability in the results obtained as if no final heading was specified as shown in Figure 6.16. The largest final heading error of 122° was found for the specified final heading of 45°. Such large error in result indicates that it is impossible for the airplane land at the pre-selected touchdown location with the specified final heading of 45°. This is due to the lack of altitude or energy for the airplane to manoeuvre to this particular specific final heading at this location. In summary, for this particular location the forced landing manoeuvre has the highest tendency to touchdown with a final heading of approximately 255° as indicated by the small error in heading.

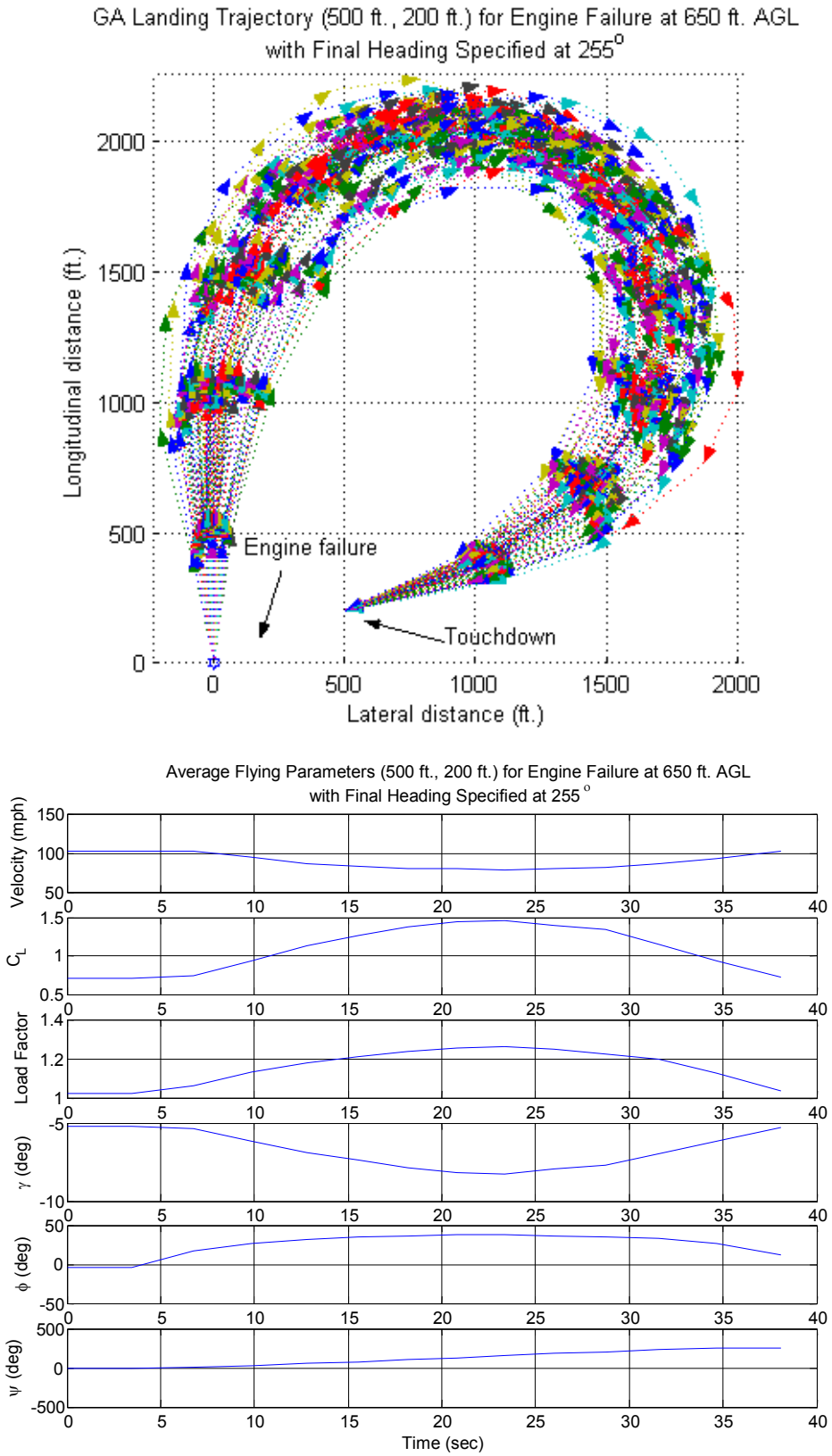

Figure 6.49 Forced Landing (500 ft, 200 ft) with Specified Final Heading at 255° for Engine Failure at 650 ft AGL

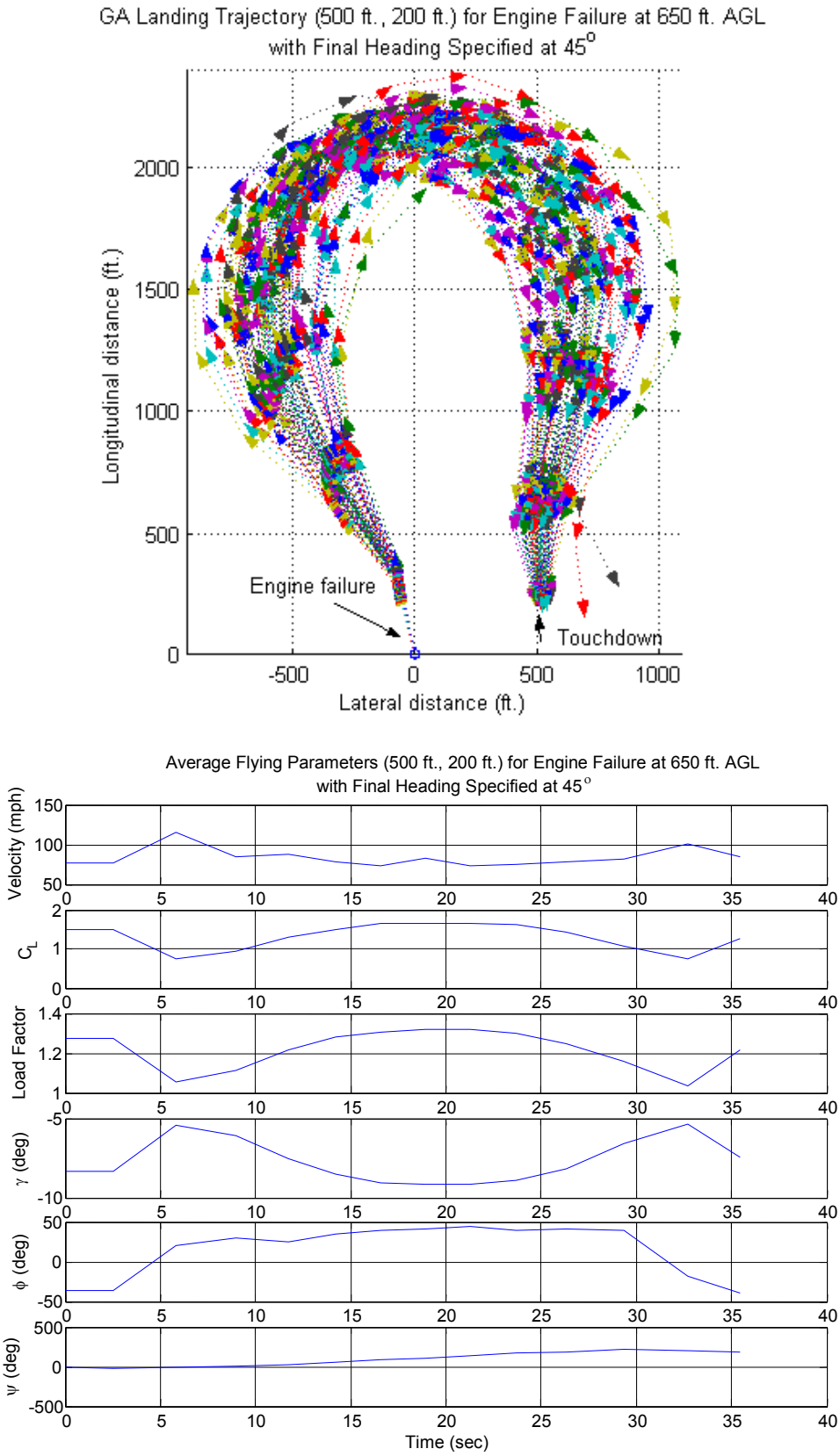

Figure 6.50 Forced Landing (500 ft, 200 ft) with Specified Final Heading at 45° for Engine Failure at 650 ft AGL

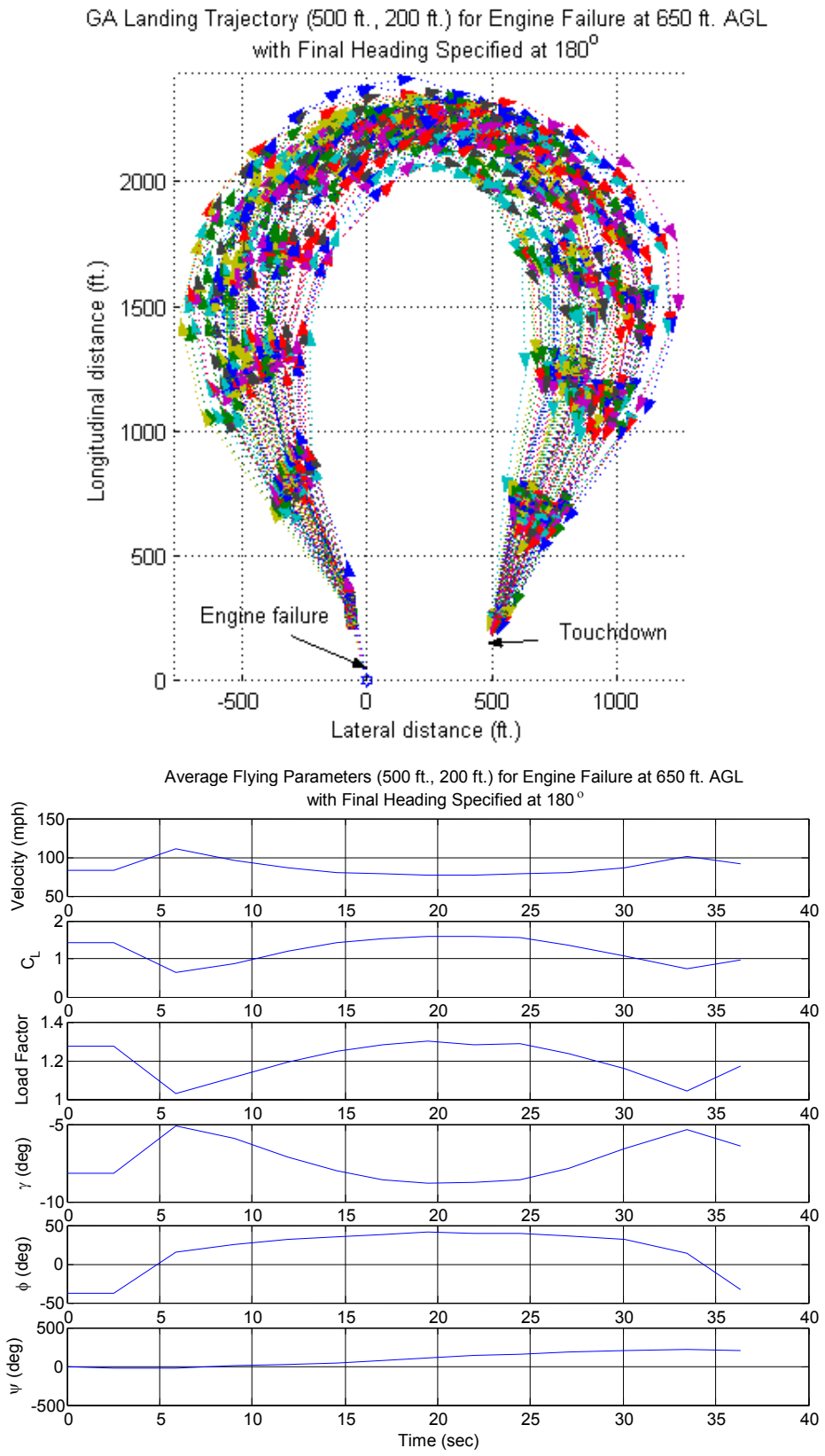

Figure 6.51 Forced Landing (500 ft, 200 ft) with Specified Final Heading at 180° for Engine Failure at 650 ft AGL

In summary, for certain locations and specific final headings, the results show that there is a trade off between heading error and the distance error as illustrated in the case for the pre-selected touchdown location (3000 ft, 3000 ft) for the specified final heading of 0° and 315° where a distance error of 12.1306 ft and 12.6317 ft is relatively small but a heading error of 26.5977° and 31.1585° is large. Another example can be seen in the case of the pre-selected touchdown location of (500 ft, 200 ft) for the specified final heading of 45° where a heading error of 121.8710° is much more apparent than the distance error of 20.1884 ft. Therefore, in conclusion, for certain pre-selected touchdown location and certain final heading, the airplane may either touchdown very close to the pre-selected touchdown location but with greater final heading error or touchdown with minimal final heading error but further from the pre-selected touchdown location.

6.7.2 Results with Specified Final Heading and Horizontal Wind

This section examines the effects constant horizontal winds have on a forced landing manoeuvre to a pre-selected touchdown location with specific final heading. It uses the aircraft model described in Chapters 3.2 and 3.3 and similar GA search method as described in Chapter 6.4. For similar comparisons with the results obtained in previous sections, the analyses were carried out for constant horizontal wind at three different combinations of wind speed: 10 mph, 20 mph and 30 mph, and at three wind headings: 45° left of head on wind, 0° (head on wind) and 45° right of head on wind were carried out for a specific final heading for each of the three pre-selected touchdown locations. The results are shown in Table 6.11.

Table 6.11 Results for GA with Pre-selected Location and Specified Final Heading with Horizontal Crosswinds

Pre-selected Location	Specified Final Heading (deg)	Wind Azimuth (deg)	Average Final Heading Computed (deg)	Heading error (deg)	Distance Error (ft)
(0 ft, -3100 ft)	225	-45	225.0946	0.0946	2.0504
(0 ft, -3100 ft)	225	-45	225.1949	0.1949	1.4008
(0 ft, -3100 ft)	225	-45	225.2673	0.2673	3.7748
(0 ft, -3100 ft)	225	0	225.0009	0.0009	1.3668
(0 ft, -3100 ft)	225	0	225.0845	0.0845	1.3919
(0 ft, -3100 ft)	225	0	225.1234	0.1234	1.4686
(0 ft, -3100 ft)	225	+45	224.9214	0.0786	1.6254
(0 ft, -3100 ft)	225	+45	224.9802	0.0198	1.1050
(0 ft, -3100 ft)	225	+45	225.0424	0.0424	0.9445
(3000 ft, 3000 ft)	150	-45	149.8220	0.1780	0.6617
(3000 ft, 3000 ft)	150	-45	149.9187	0.0813	0.6002
(3000 ft, 3000 ft)	150	-45	149.7600	0.2400	1.1036
(3000 ft, 3000 ft)	150	0	149.8246	0.1754	0.8841
(3000 ft, 3000 ft)	150	0	149.3516	0.6484	1.4830
(3000 ft, 3000 ft)	150	0	148.7076	1.2924	2.4297
(3000 ft, 3000 ft)	150	+45	149.8402	0.1598	1.0404
(3000 ft, 3000 ft)	150	+45	149.4807	0.5193	1.2826
(3000 ft, 3000 ft)	150	+45	148.5421	1.4579	2.2681
(500 ft, 200 ft)	255	-45	255.0037	0.0037	0.2845
(500 ft, 200 ft)	255	-45	255.0068	0.0068	0.3703
(500 ft, 200 ft)	255	-45	255.0374	0.0374	1.4152
(500 ft, 200 ft)	255	0	255.0025	0.0025	0.2041
(500 ft, 200 ft)	255	0	255.0043	0.0043	0.2212
(500 ft, 200 ft)	255	0	255.0054	0.0054	0.2350
(500 ft, 200 ft)	255	+45	255.0019	0.0019	0.2246
(500 ft, 200 ft)	255	+45	255.0011	0.0011	0.1828
(500 ft, 200 ft)	255	+45	255.0001	0.0001	0.1520

The results for the pre-selected touchdown location (0 ft, -3100 ft) with specified final heading of 225° are shown in Figure 6.52 while its flying parameters are shown in Figure 6.53. The forced landing trajectory for this case have very similar results as shown in Figure 6.23 in Chapter 6.61 – Results with Horizontal Wind. The effect of a horizontal 30 mph wind at -45° is a slightly bigger and a longer trajectory path since this crosswind has an effect of a tail wind for part of the flight. Meanwhile, the effect of a horizontal 30 mph wind at +45° is a tighter turn in the flight trajectory. In general, the flying parameters for the constant horizontal wind of different speed and direction have very similar characteristics for different crosswinds and have very small heading error and distance error. The variation in bank angle is approximately 4° during mid flight and approximately 10° towards the end of the flight trajectory or from approximately 27 seconds into the flight. The bank angle in the final league before touchdown is the greatest for a horizontal wind of 30 mph at –45° and the least for a horizontal wind of 30 mph at +45°.

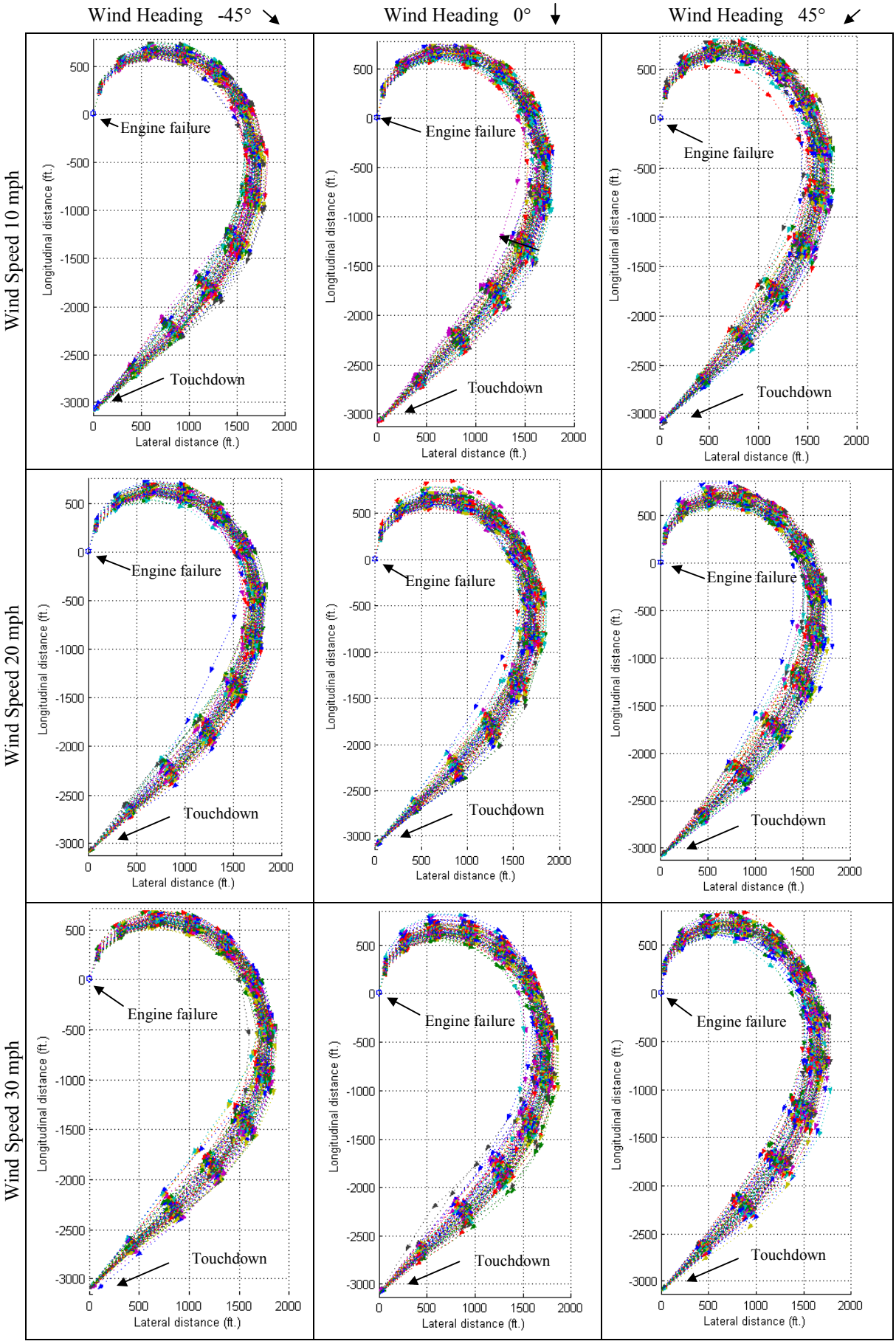

Figure 6.52 Forced Landing Trajectory – (0 ft, -3100 ft) with Horizontal Wind and Specified Final Heading at 225° for Engine Failure at 650 ft AGL

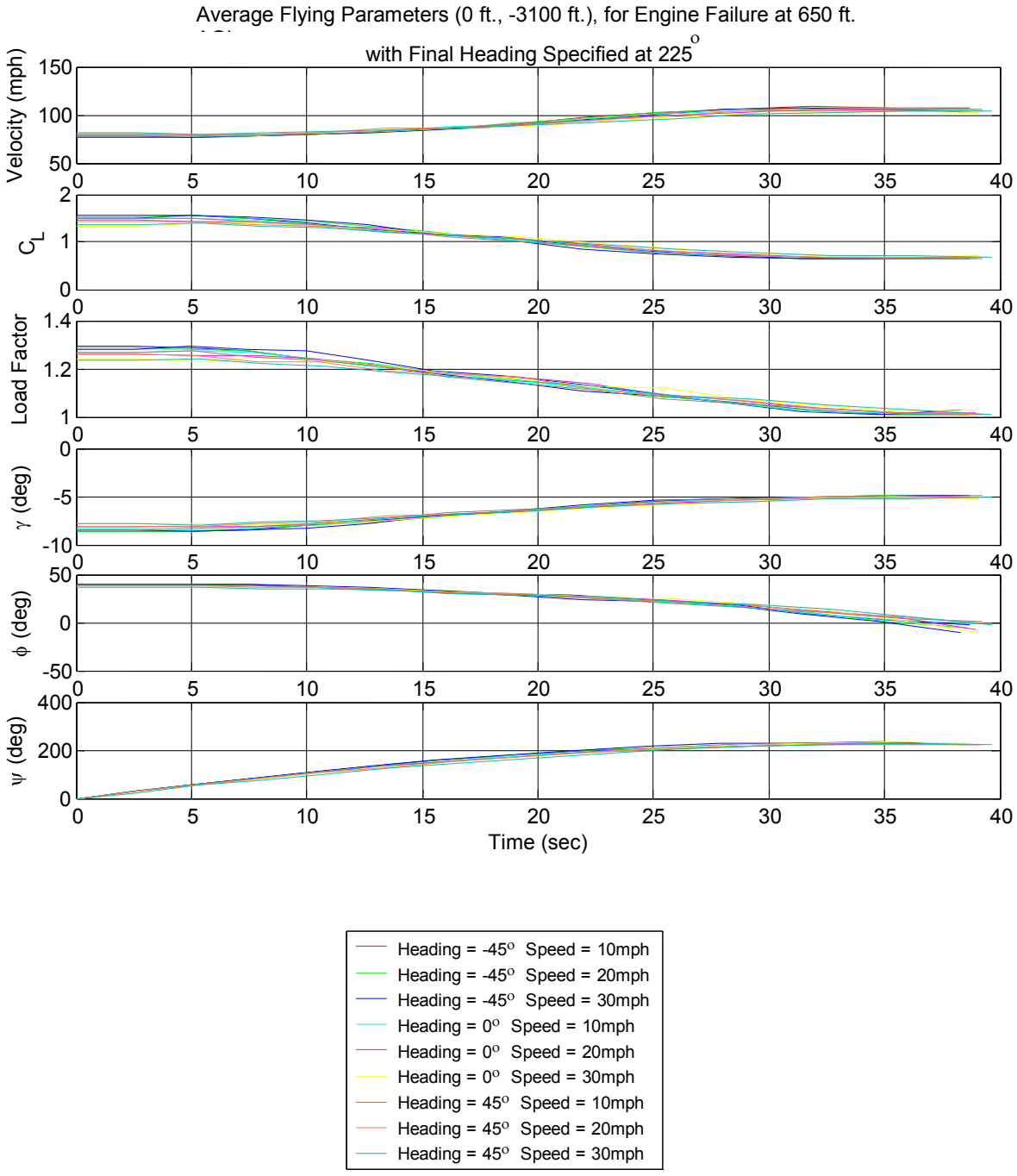

Figure 6.53 Average Flying Parameters for Forced Landing Trajectory – (0 ft, -3100 ft) with Specified Final Heading at 255° for Engine Failure at 650 ft AGL

The results for the pre-selected touchdown location (3000 ft, 3000 ft) with specified final heading of 150° are shown in Figure 6.54 while its flying parameters are shown in Figure 6.55. The forced landing trajectory for this case have very similar results as shown in Figure 6.25 in Chapter 6.61 – Results with Horizontal Wind. The effects of stronger horizontal wind at -45° are that the ensemble of flight trajectories are closer together and a larger bank angle near the end of the flight while the effect of a stronger horizontal wind at +45° are that the ensemble of flight trajectories are a slightly more scattered flight trajectories for the initial part of the flight and lesser bank angle near the end of the flight. Overall, the flying parameters are very similar for the different crosswinds and small variations in bank angle of approximately 7° and glide angle, which in effect changes the airplane's speed, were used to compensate for the different crosswinds.

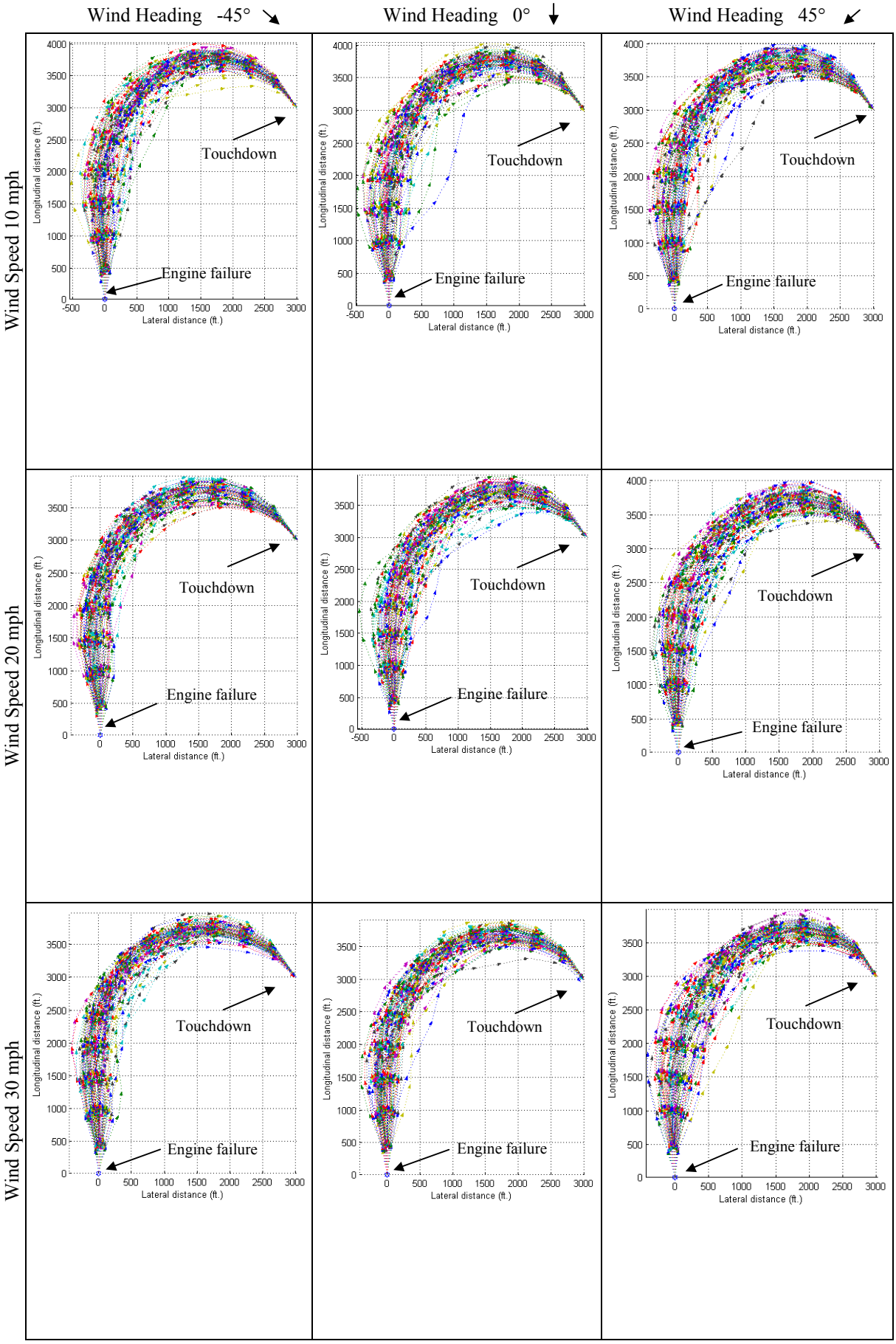

Figure 6.54 Forced Landing Trajectory – (3000 ft, 3000 ft) with Horizontal Wind and Specified Final Heading at 150° for Engine Failure at 650 ft AGL

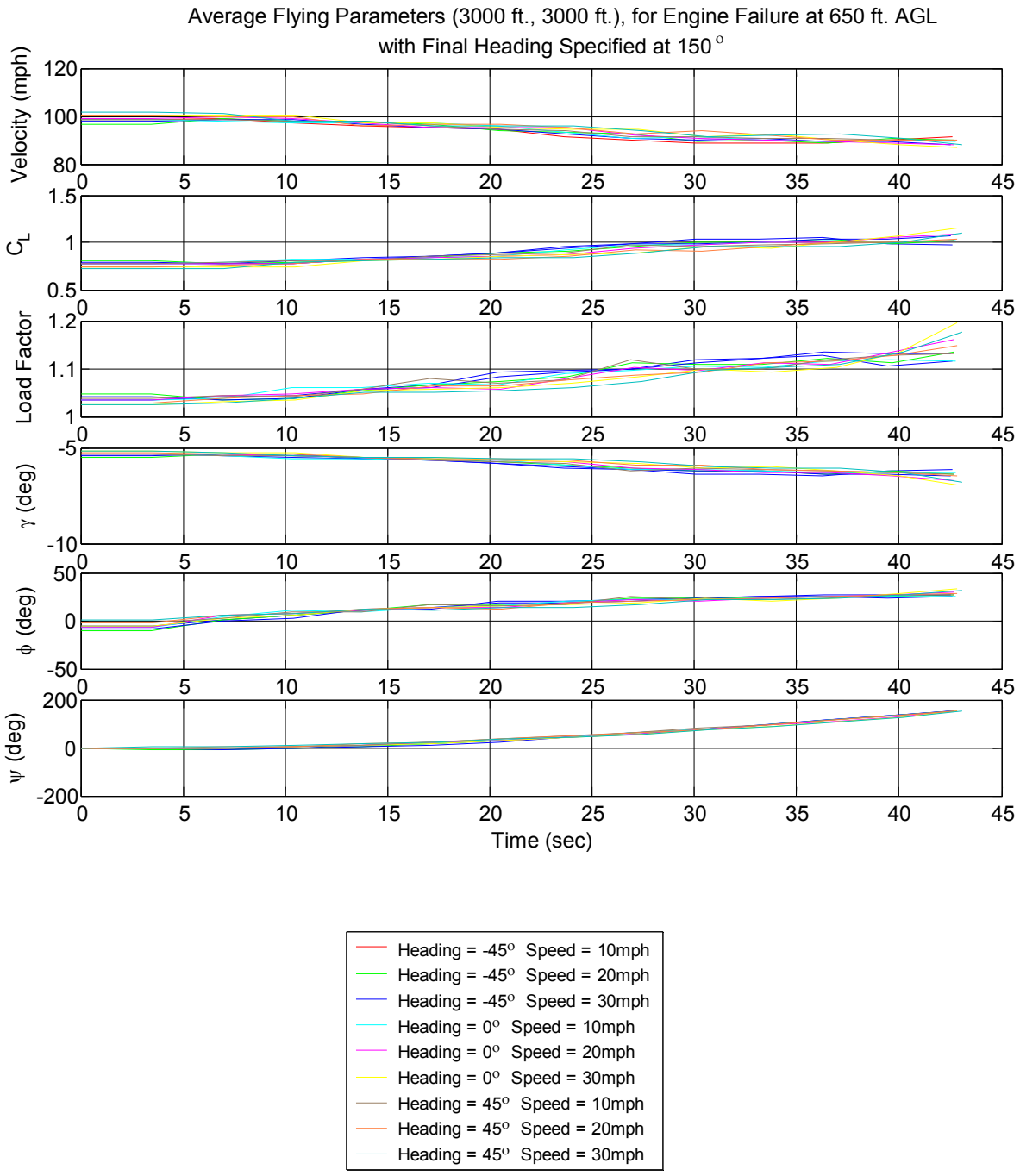

Figure 6.55 Average Flying Parameters for Forced Landing Trajectory – (3000 ft, 3000 ft) with Horizontal Wind and Specified Final Heading at 150° for Engine Failure at 650 ft AGL

The results for the pre-selected touchdown location (3000 ft, 3000 ft) with specified final heading of 150° are shown in Figure 6.56 while its flying parameters are shown in Figure 6.57. The forced landing trajectory for this case have very similar results as shown in Figure 6.27 in Chapter 6.61 – Results with Horizontal Wind. The effects of stronger horizontal wind at -45° is a larger bank angle near the end of the flight while the effects of a stronger horizontal wind at +45° is a lesser bank angle near the end of the flight. Overall, the flying parameters are very similar, with very small error for the specified heading and error distance. The flying parameters for the different crosswinds have variations in a bank angle of approximately 10° and glide angle, which in effect changes the airplane's speed, were used to compensate for the different crosswinds.

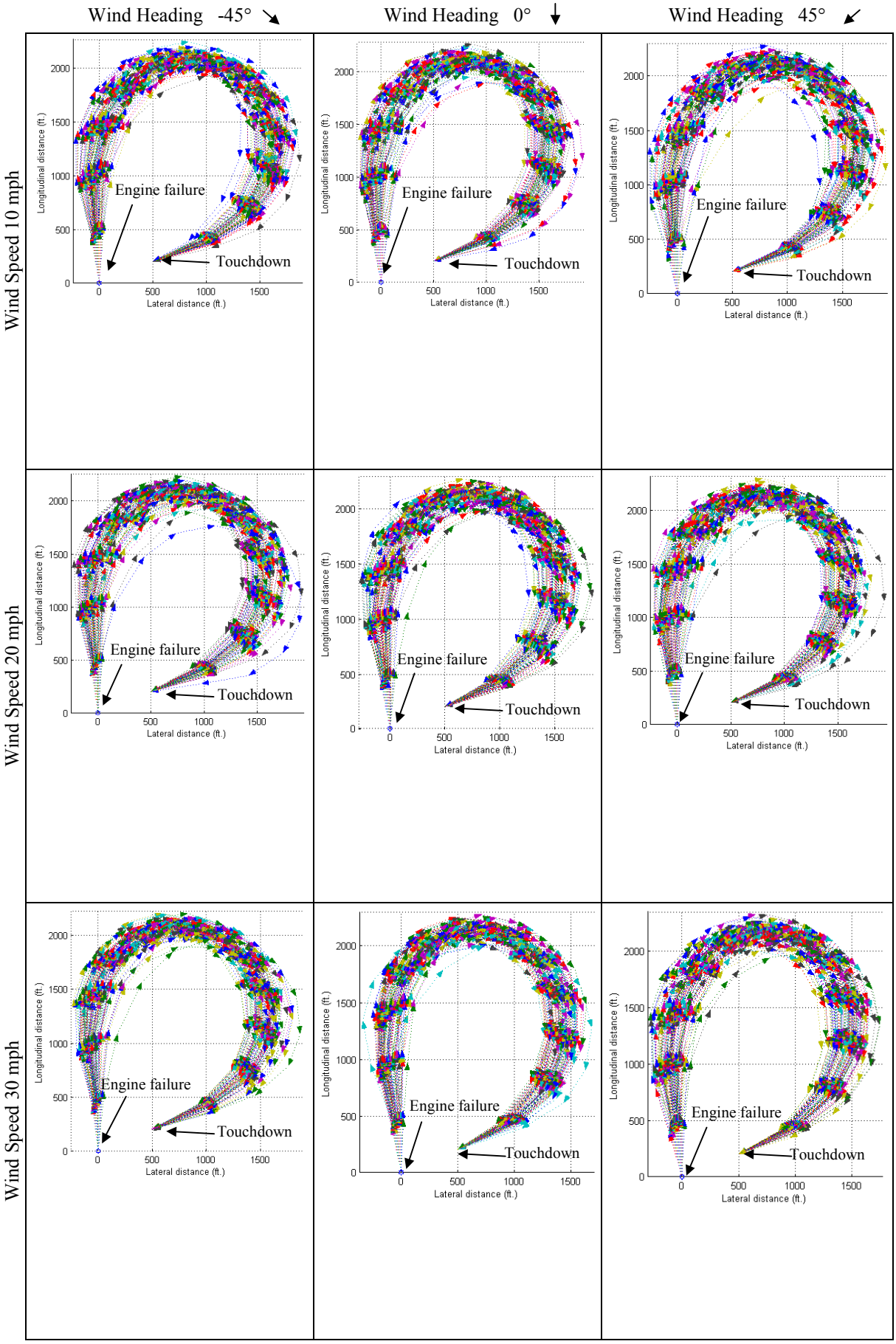

Figure 6.56 Forced Landing Trajectory – (500 ft, 200 ft) with Horizontal Wind and Specified Final Heading at 255° for Engine Failure at 650 ft AGL

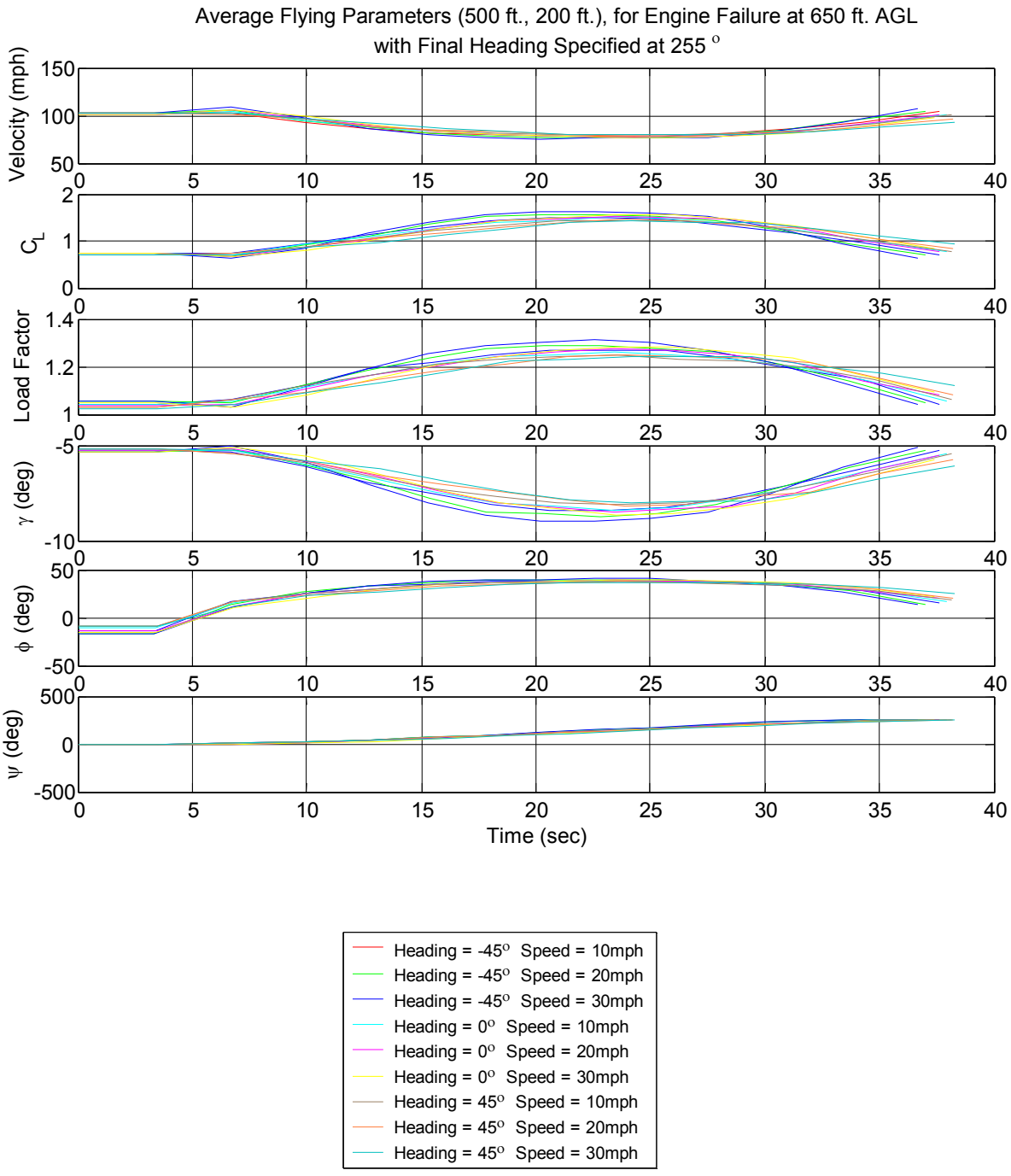

Figure 6.57 Average Flying Parameters for Forced Landing Trajectory – (500 ft, 200 ft) with Horizontal Wind and Specified Final Heading at 255° for Engine Failure at 650 ft AGL

6.8 Genetic Algorithm in an Obstacle Avoidance Forced Landing Manoeuvre

Forced landing of an aircraft after engine failure may occur in a built up area where there are buildings or transmission towers in the vicinity. Here, the pilot will have to fly an alternate flight path following a forced landing compare to without obstructions in the intended flight path. Therefore, an extension to the previous GA program developed on the forced landing manoeuvre analysis included the search for flight trajectories where there was an obstacle in the intended flight path without obstruction. The obstruction was represented by a cylinder shaped obstacle placed in the flight path computed in the previous sections. An obstacle was placed in the way of the flight paths found in the previous sections to observe how different the flight paths may be and if the GA program developed can successfully find an alternate flight path avoiding the obstacle. A single obstacle with a height of 650 ft AGL and different radius sizes was placed at various locations to each of the three pre-selected touchdown locations for the GA forced landing simulation. Analyses for different obstacles sizes with radius 250 ft, 300 ft and 500ft for different locations were carried out for each of the pre-selected touchdown locations of touching down at (0 ft, -3100 ft), (3000 ft, 3000 ft) and (500 ft, 200 ft), where the 1st component represents the lateral distance and the 2nd component represents the longitudinal distance from the engine failure point.

6.8.1 Results for Forced Landing Manoeuvre with Obstacle

Analyses for forced landing with obstructions and unspecified final heading were carried out for various obstacle sizes at different locations for three different locations as shown in Table 6.12. In order to compare how different the flight paths maybe for forced landing trajectory without obstacle, the obstacle was intentionally placed in the earlier sector, mid sector and later sector of the flight path without obstacle as found in previous sections.

Table 6.12 GA Forced Landing Analyses with Obstacle

Pre-selected Location	Obstacle Location	Obstacle Radius	Average Final Heading (deg)	Distance Error (ft) (Path A)
(0 ft, -3100 ft)	(1000 ft, 500 ft)	500 ft	215.2056	449.6586
(0 ft, -3100 ft)	(1500 ft, -1000 ft)	500 ft	232.1243	605.5853
(0 ft, -3100 ft)	(1000 ft, -2250 ft)	500 ft	227.0394	904.8637
(3000 ft, 3000 ft)	(1000 ft, 3250 ft)	250 ft	134.4788	0.0553
(3000 ft, 3000 ft)	(2000 ft, 3500 ft)	250 ft	147.0487	0.6068
(3000 ft, 3000 ft)	(0 ft, 750 ft)	300 ft	101.7792	0.0711
(500 ft, 200 ft)	(1500 ft, 1000 ft)	250 ft	269.1462	2.1770
(500 ft, 200 ft)	(1000 ft, 2000 ft)	250 ft	234.1587	8.8617
(500 ft, 200 ft)	(-1250 ft, 1000 ft)	250 ft	257.8785	0.0538

For the (0 ft, -3100 ft) pre-selected location, a cylindrical shaped object with radius 500 ft was intentionally placed at (1000 ft, 500 ft), (1500 ft, -1000 ft) and (1000 ft, -2250 ft) relative to the engine failure position. As shown in Figures 6.58 – 6.60, the GA forced landing program developed successfully found flight trajectories that will avoid the obstacle in all three cases with touchdown distances varying from 450 ft. to 905 ft. away from the pre-selected touchdown location and final headings ranging from 215° to 232°. The distance errors are unavoidable given the low engine failure position of 650 ft AGL, the pre-selected touchdown location and the relative locations of the obstacles. This is due to the lack of altitude or energy to manoeuvre the airplane for a successful touchdown at the pre-selected touchdown location. In the event that, there are more than one general groupings of flight path, only the average flying parameters of one general grouping of flight paths that fly around the obstacle touching down with the least distance error are presented as shown in Figure 6.60. The results show larger distance error when obstacle was placed closer to the pre-selected location as shown in Table 6.12. This is because of the lack in altitude or energy at the end of the forced landing manoeuvre to fly the airplane for a closer touchdown at the pre-selected location.

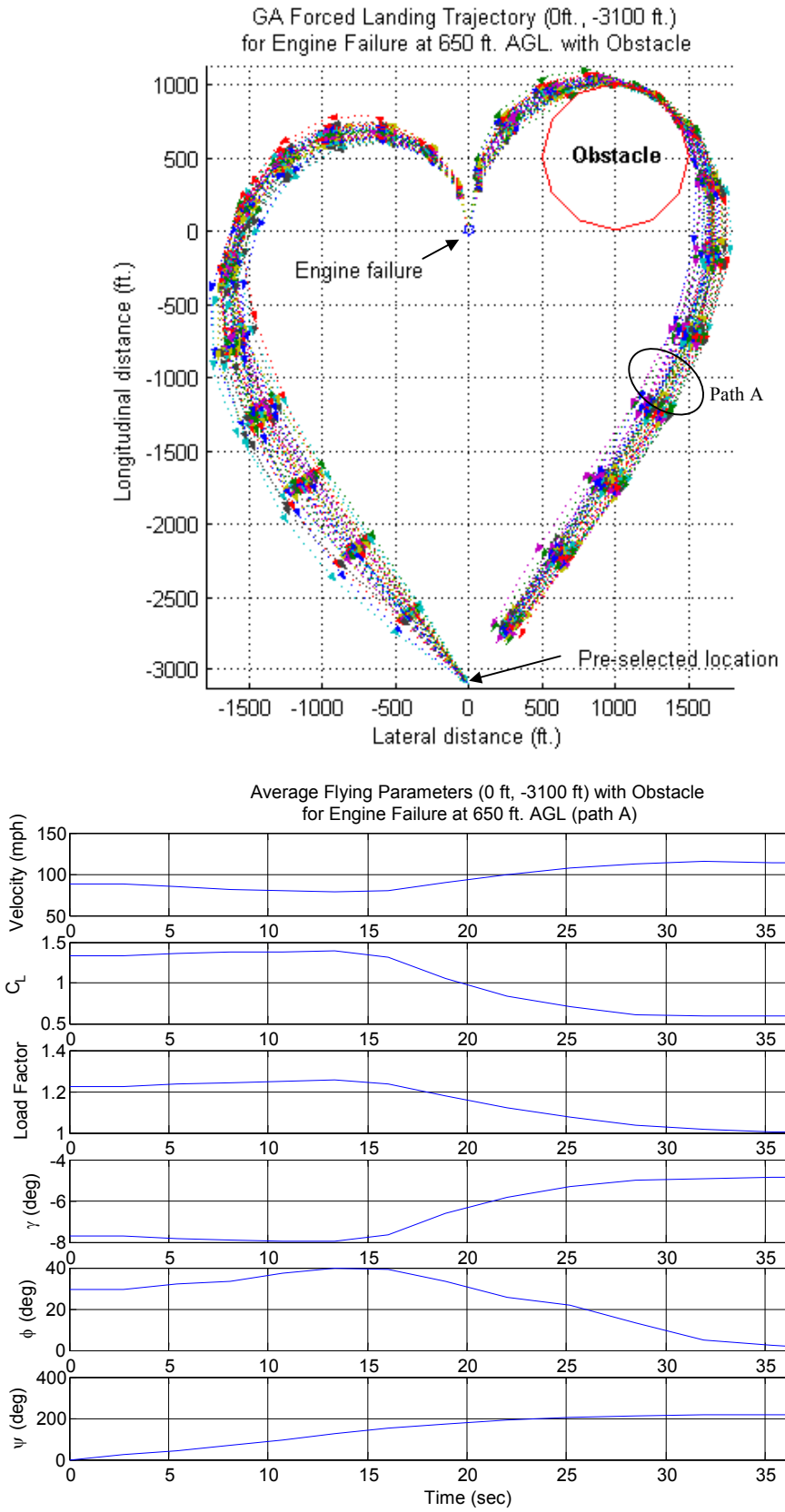

Figure 6.58 Forced Landing (0 ft, -3100 ft) with Obstacle at (1000 ft, 500 ft)

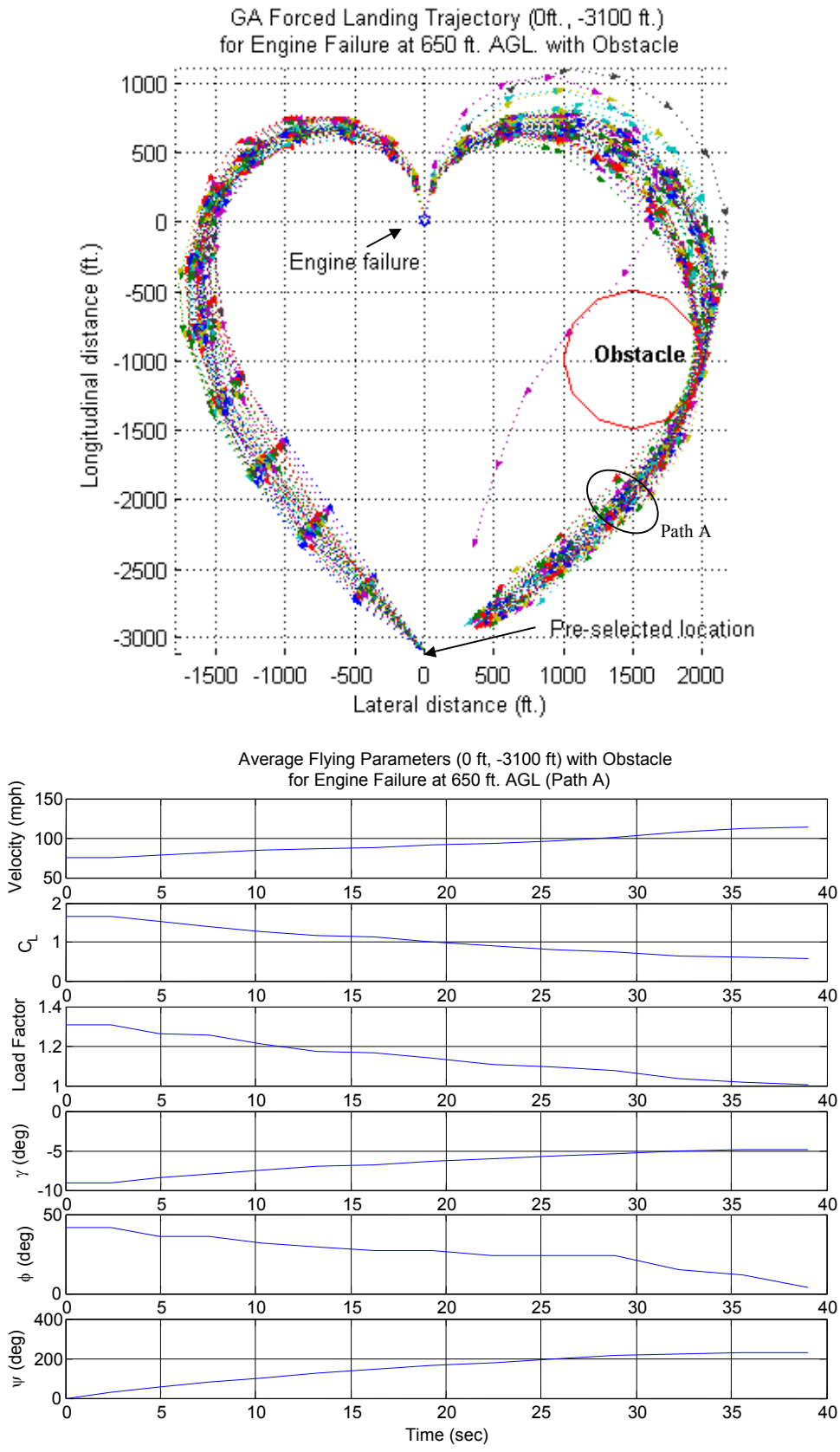

Figure 6.59 Forced Landing (0 ft, -3100 ft) with Obstacle at (1500 ft, -1000 ft)

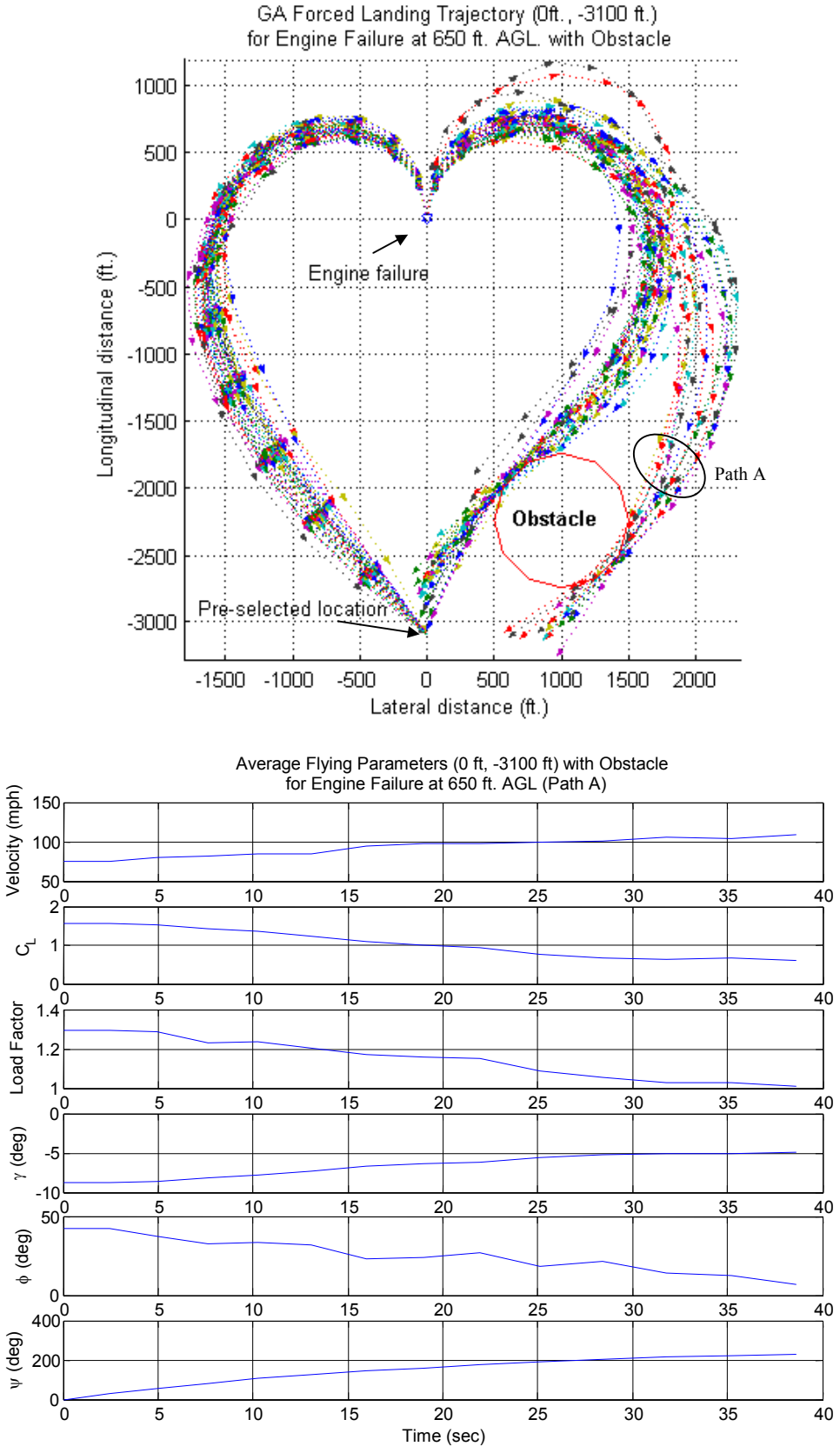

Figure 6.60 Forced Landing (0 ft, -3100 ft) with Obstacle at (1000 ft, -2250 ft)

For the (3000 ft, 3000 ft) pre-selected location, a cylindrical shaped object with radius 250 ft., 250 ft. and 500 ft. was intentionally placed at (1000 ft, 3250 ft), (2000 ft, 3500 ft) and (0 ft, 750 ft) respectively relative to the engine failure position. As shown in Figures 6.61 – 6.63, the GA forced landing program developed successfully found flight trajectories that will avoid the obstacle in all three cases and touchdown at the pre-selected locations. The location for this particular pre-selected location is not being affected by the positioning of the obstacle as indicated by the small distance error as shown in Table 6.12. In the event that, there are more than one general groupings of flight path, only the average flying parameters of one general grouping of flight paths that fly around the obstacle touching down with the least distance error are shown. In Figure 6.61, some flight trajectories were seen flying through the obstacle. This is simply due to numerical error and the problem can be avoided if a larger radius or finer computation step sizes were used.

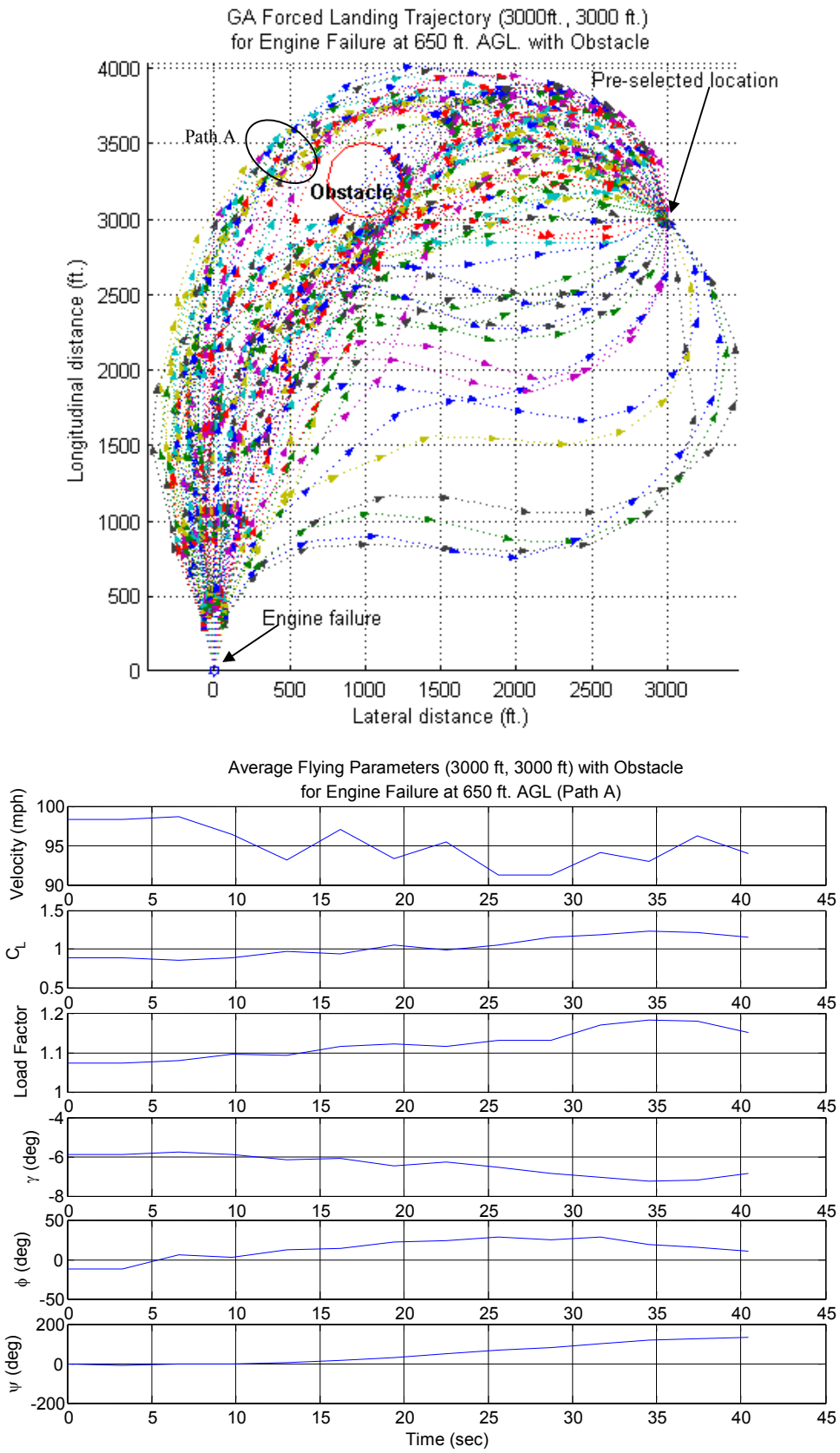

Figure 6.61 Forced Landing (3000 ft, 3000 ft) with Obstacle at (1000 ft, 3250 ft)

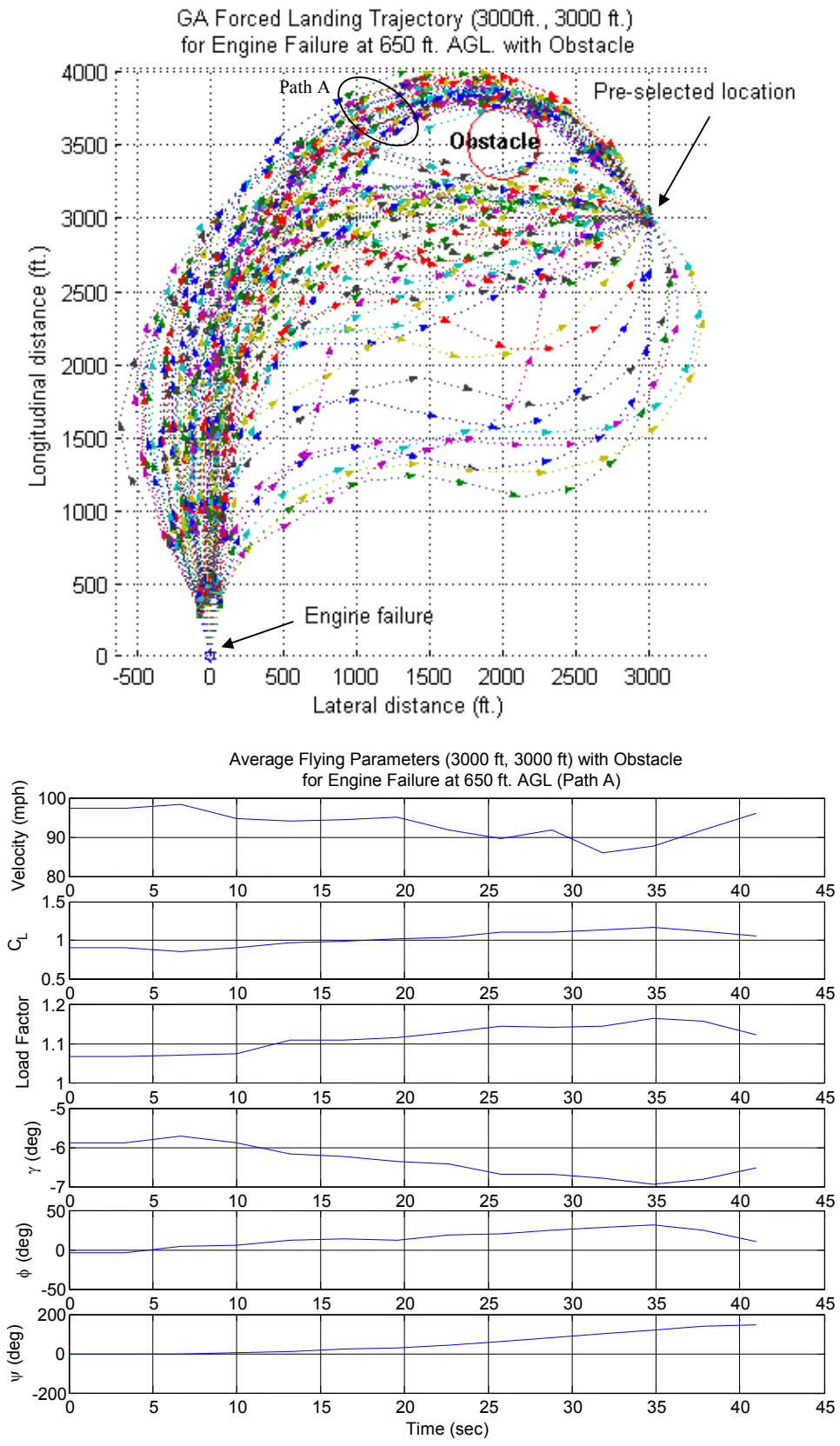

Figure 6.62 Forced Landing (3000 ft, 3000 ft) with Obstacle at (2000 ft, 3500 ft)

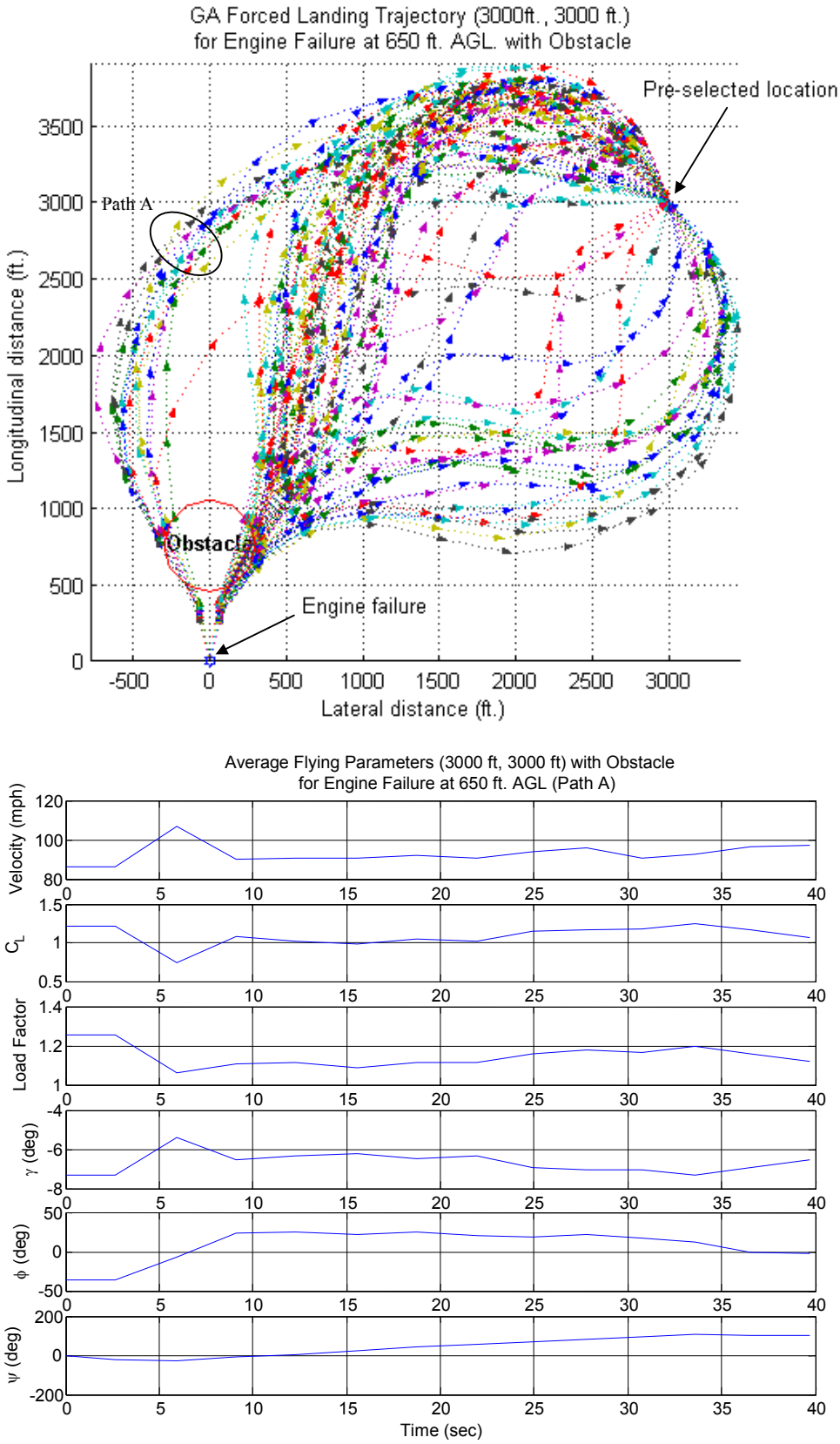

Figure 6.63 Forced Landing (3000 ft, 3000 ft) with Obstacle at (0 ft, 750 ft)

For the (500 ft, 200 ft) pre-selected location, a cylindrical shaped object with radius 250 ft. was intentionally placed at (1500 ft, 1000 ft), (1000 ft, 2000 ft) and (-1250 ft, 1000 ft) relative to the engine failure position. As shown in Figures 6.64 – 6.66, the GA forced landing program developed successfully found flight trajectories that will avoid the obstacle in all three cases and touchdown at the pre-selected locations. The location for this particular pre-selected location does not seem to be affected by the positioning of the obstacle as indicated by the small distance error as shown in Table 6.12. In the event that, there are more than one general groupings of flight path, only the average flying parameters of one general grouping of flight paths that fly around the obstacle touching down with the least distance error are shown. The location of the obstacle will have an effect on the general grouping of the forced landing trajectory as shown in Figure 6.65 where there are two distinct general groupings of flight paths that will successfully avoid the obstacle.

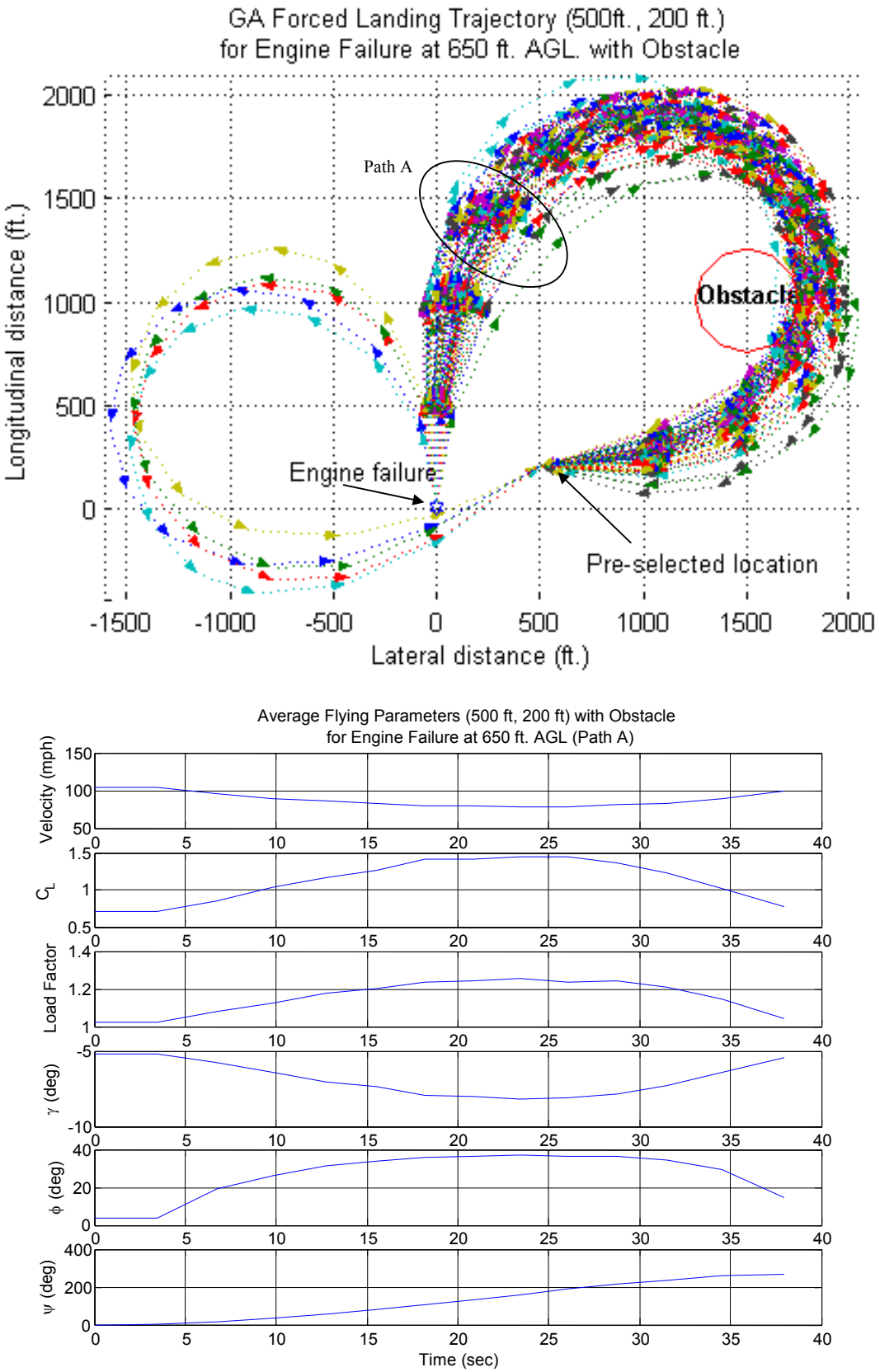

Figure 6.64 Forced Landing (500 ft, 200 ft) with Obstacle at (1500 ft, 1000 ft)

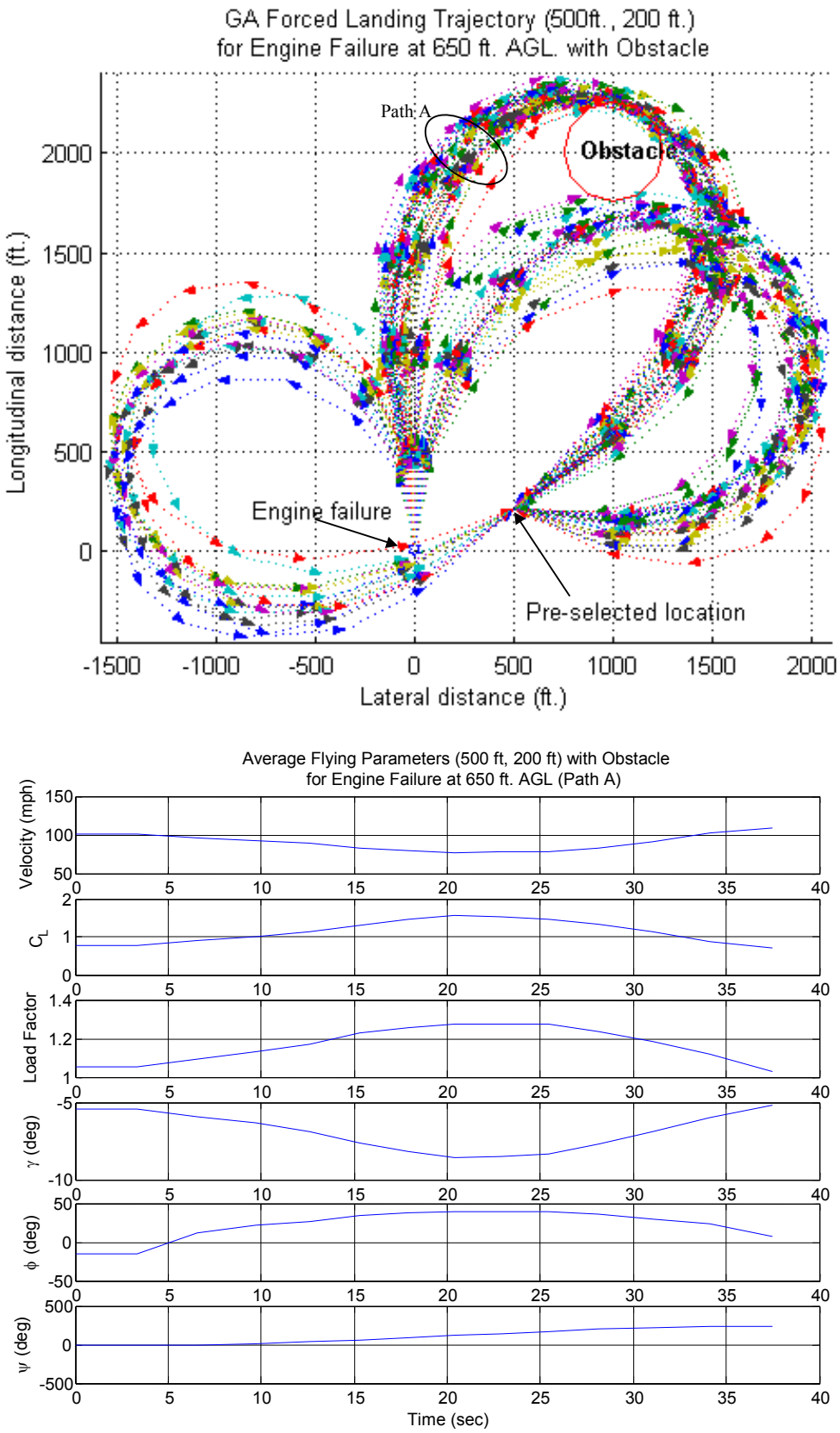

Figure 6.65 Forced Landing (500 ft, 200 ft) with Obstacle at (1000 ft, 2000 ft)

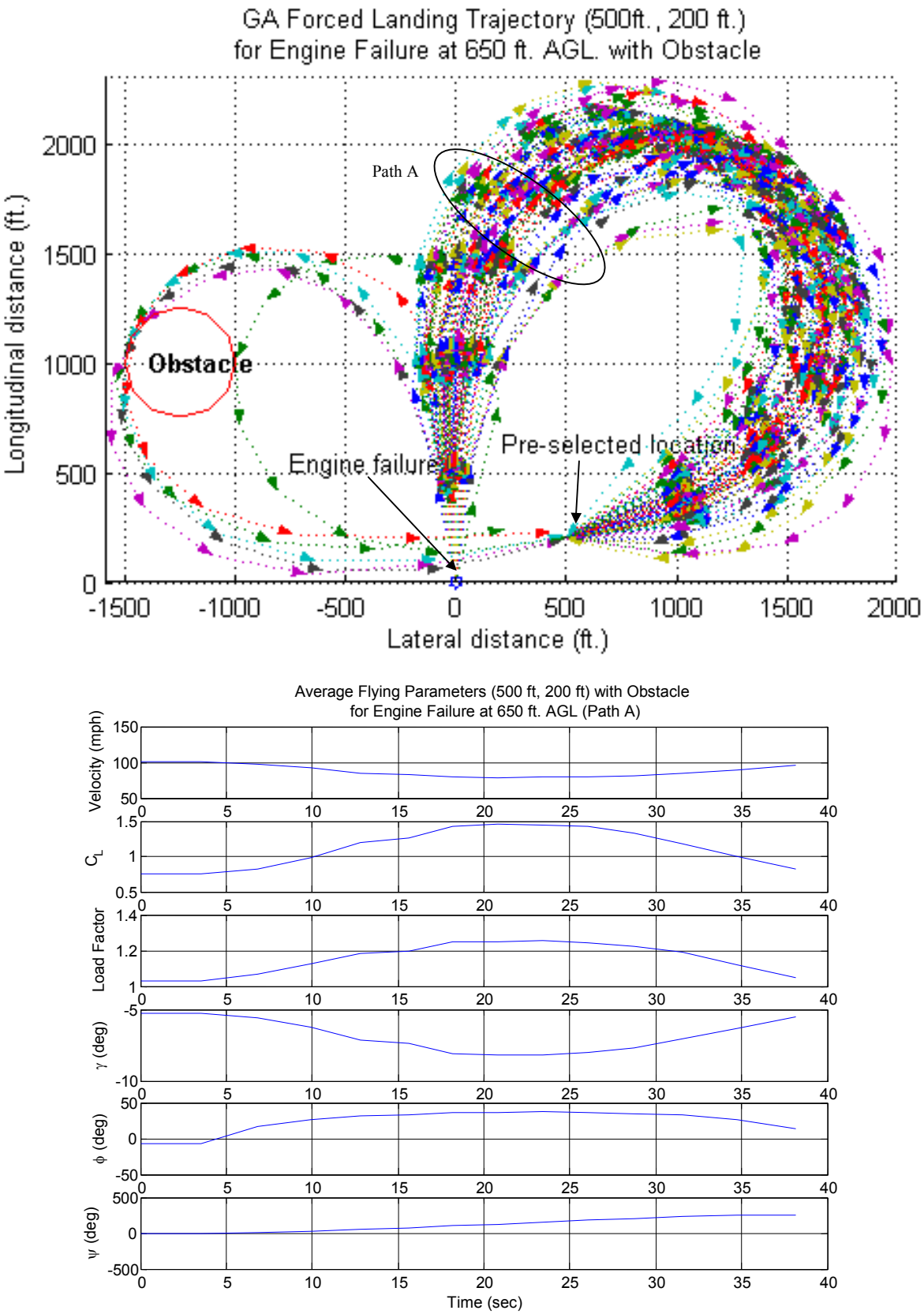

Figure 6.66 Forced Landing (500 ft, 200 ft) with Obstacle at (-1250 ft, 1000 ft)

6.8.2 Results for Forced Landing Manoeuvre with Obstacle and Specified Final Heading

Analyses for forced landing with specific final heading and with obstructions were carried out for various obstacle sizes at different locations for three different locations as shown in Table 6.13. The obstacles were intentionally placed in the earlier sector, mid sector and later sector of the flight path as found in previous sections without obstacle. They were chosen to illustrate the GA forced landing program's ability to locate flight paths around the obstacle that will land as close as possible to the pre-selected touchdown location with specific final headings.

Table 6.13 GA Forced Landing Analyses with Obstacle and Specified Final Heading

Pre-selected Location	Obstacle Location	Obstacle Radius	Specified Final Heading (°)	Average Final Heading (°)	Heading Error (°)	Distance Error (ft)
(0 ft, -3100 ft)	(1000 ft, 500 ft)	500 ft	225	223.8445	1.1555	535.7652
(0 ft, -3100 ft)	(1000 ft, 500 ft)	500 ft	180	191.8184	11.8184	542.2849
(0 ft, -3100 ft)	(1000 ft, -2250 ft)	500 ft	225	223.8123 (path A)	1.1877	602.4221
				226.8771 (path B)	1.8771	911.0503
(3000 ft, 3000 ft)	(0 ft, 1500 ft)	250 ft	150	150.0530	0.0530	1.3255
(3000 ft, 3000 ft)	(2000 ft, 3500 ft)	500 ft	90	109.3001 (path A)	19.3001	349.8519
				89.7423 (path B)	0.2577	79.3937
(500 ft, 200 ft)	(1000 ft, 2000 ft)	250 ft	255	251.8474 (path A)	3.1526	32.7532
				255.6363 (path B)	0.6363	4.8401
(500 ft, 200 ft)	(1000 ft, 2000 ft)	250 ft	180	182.2980 (path A)	2.2980	93.6797
				202.0793 (path B)	22.0793	102.0667
				231.2302 (path C)	51.2302	48.7608

The forced landing trajectory results and average flying parameters for the pre-selected touchdown location at (0 ft., -3100 ft.) with the specified final heading of 225° and with a cylindrical shaped radius of 500 ft placed at (1000 ft., 500 ft.) are shown in Figure 6.67. The GA forced landing program successfully found flight paths that will land with specific final heading with a minimal final heading error of 1.15° and a distance error of 536 ft as shown in Table 6.13. The error in distance is mainly due to having to avoid the obstacle and the results are consistent with the results as shown in Figure 6.58 for the case without specific final heading. The flight paths are similar to the all the previous forced landing trajectory for this pre-selected location. The results for the forced landing trajectory and average flying parameters at the same pre-selected touchdown location and obstacle location with the specified final heading of 180° and with a cylindrical shaped radius of 500 ft are shown in Figure 6.68. For this case, the distance error is 542 ft and the final heading error is 11.8°. A third case was tested for a cylindrical shaped obstacle with the same radius of 500 ft located at (1000 ft, -2250 ft) and a specified final heading of 225°. For this particular obstacle

location, there are two general flight paths that will avoid the obstacle as shown in Figure 6.69. However, the distance error is 602 ft and 911 ft for paths A and B respectively, which is larger than the first case. Again, the results are consistent with the previous results where larger error distance tends to prevail when the obstacle is located closer to the pre-selected location.

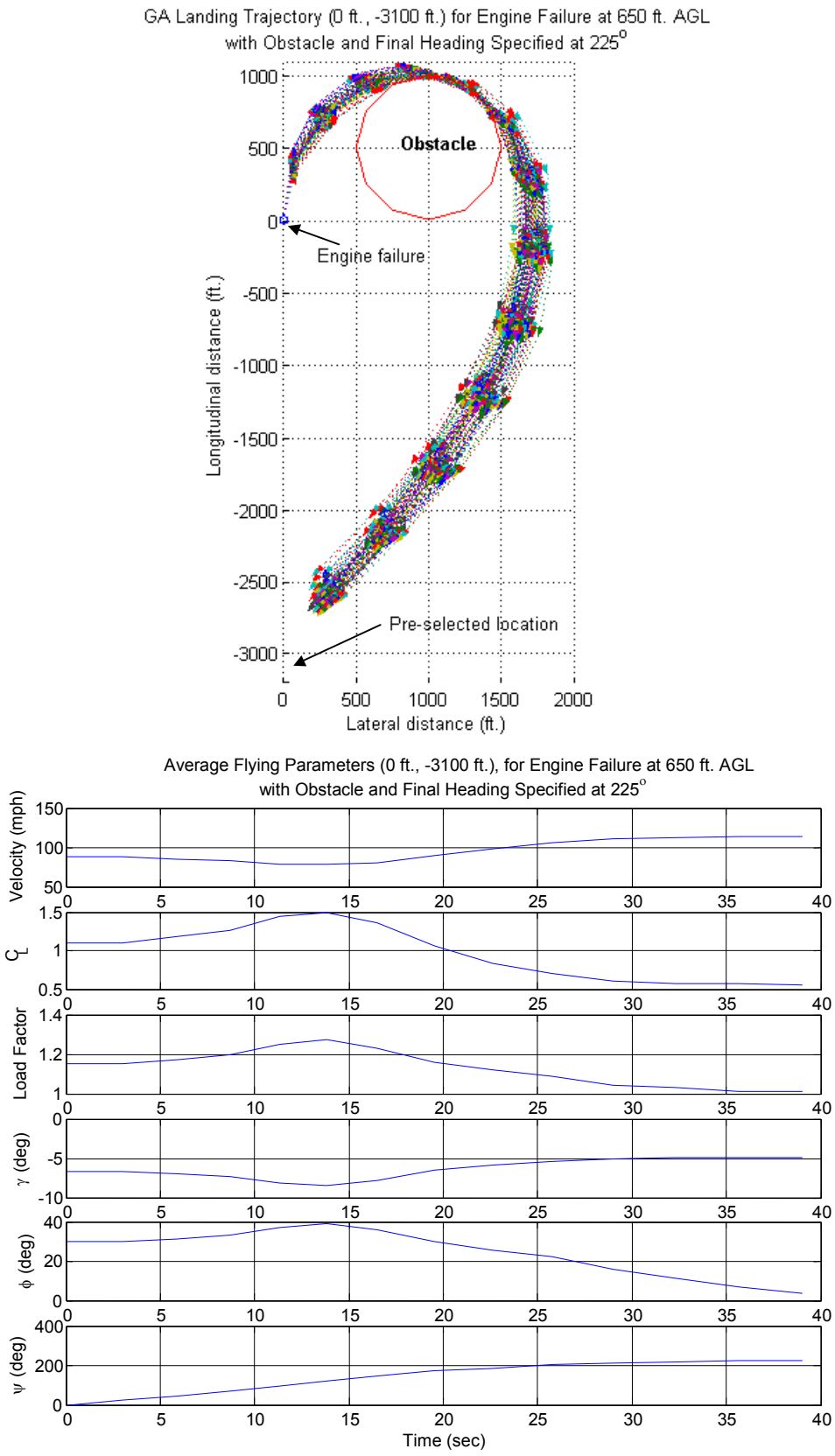

Figure 6.67 Forced Landing (0 ft, -3100 ft) with Specified Final Heading at 225° and Obstacle (1000 ft, 500 ft) for Engine Failure at 650 ft AGL

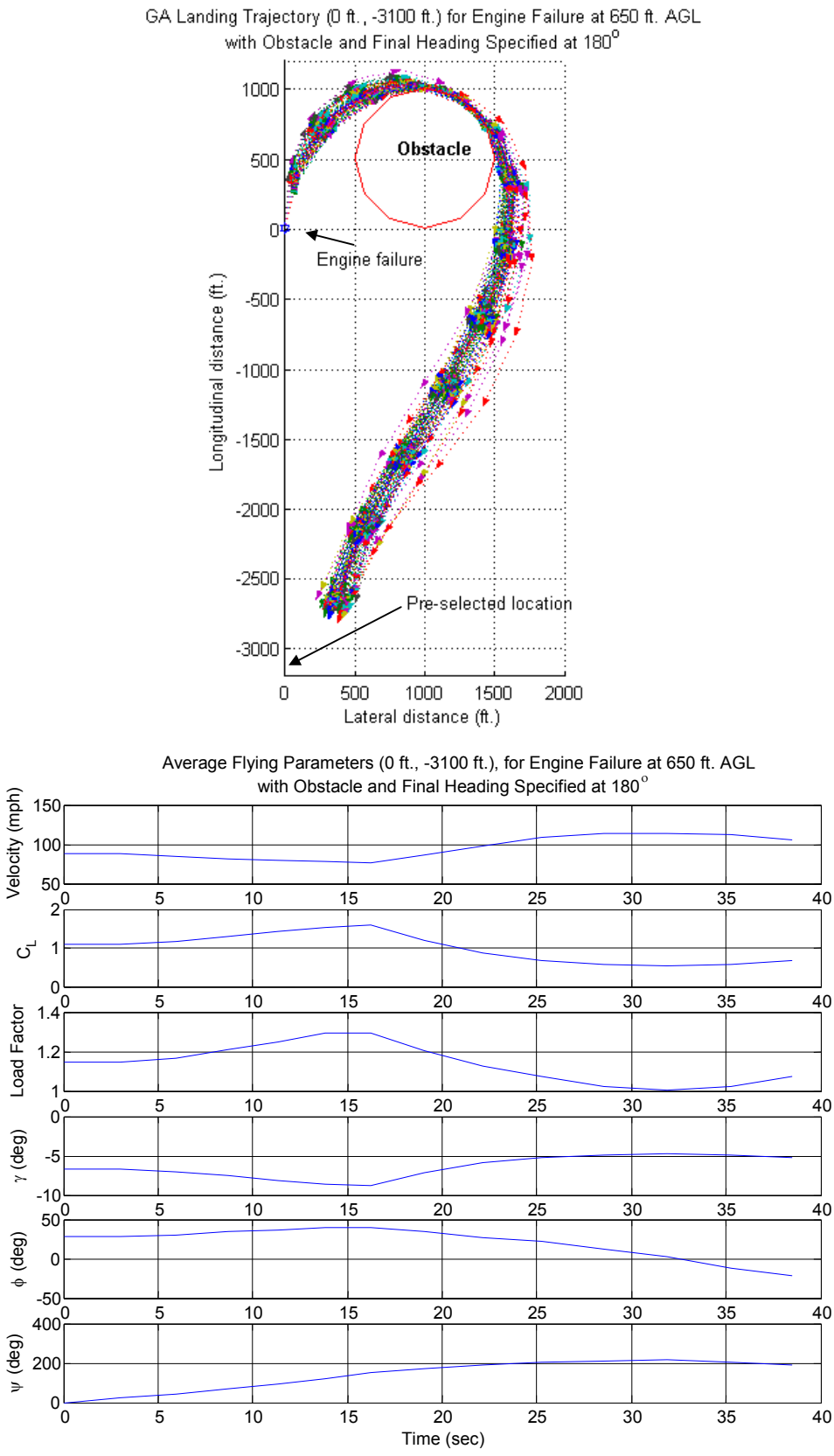

Figure 6.68 Forced Landing (0 ft, -3100 ft) with Specified Final Heading at 180° and Obstacle (1000 ft, 500 ft) for Engine Failure at 650 ft AGL

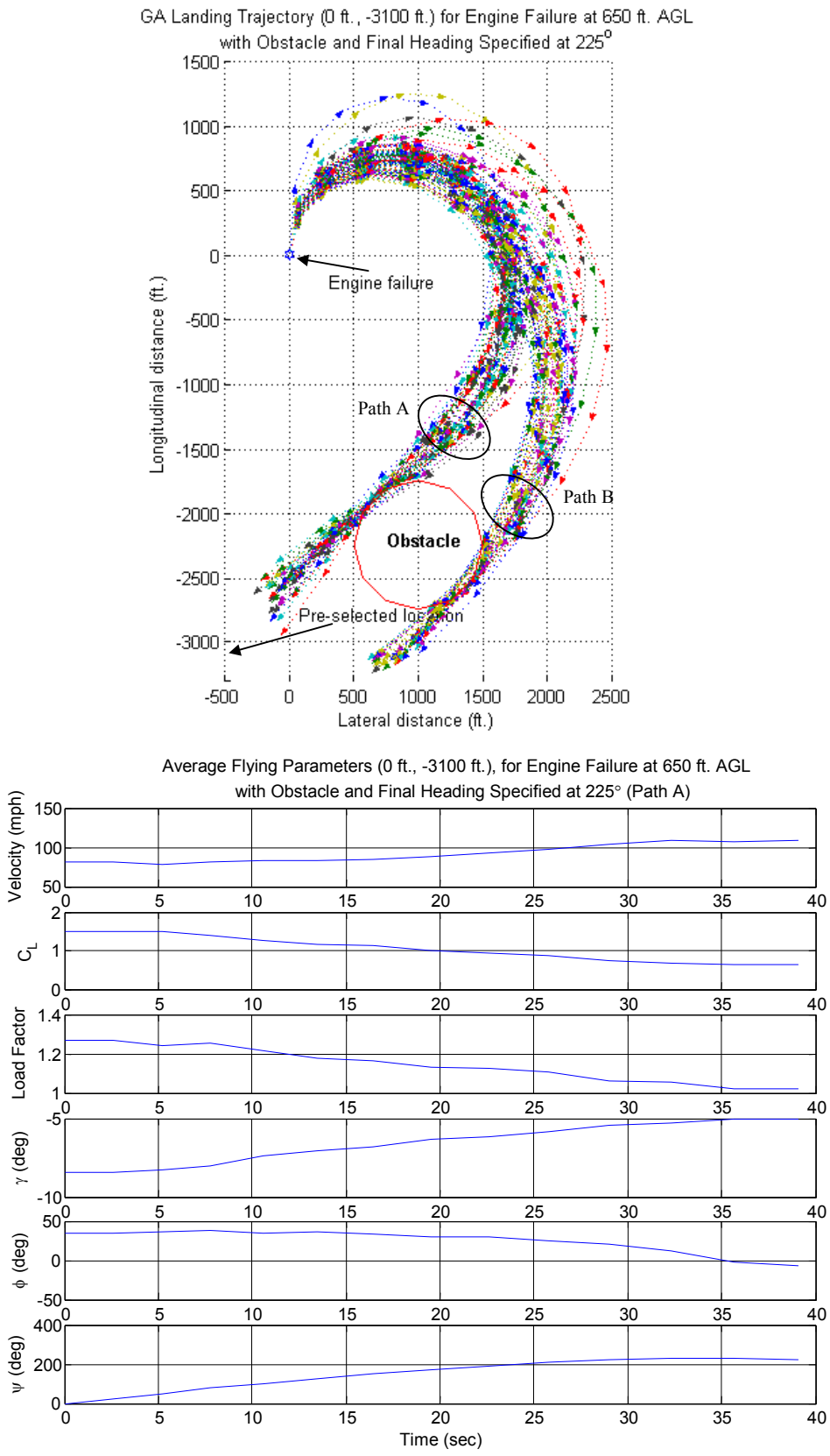

Figure 6.69 Forced Landing (0 ft, -3100 ft) with Specified Final Heading at 225° and Obstacle (1000 ft, -2250 ft) for Engine Failure at 650 ft AGL

The forced landing trajectory results and average flying parameters for the pre-selected location at (3000 ft., 3000 ft.) with the specified final heading of 150° and with a cylindrical shaped radius of 250 ft at (0 ft., 1500 ft.) are shown in Figure 6.70. For this particular obstacle location, the GA forced landing program found flight trajectories that will land at the pre-selected location and specific final heading with great accuracy as shown in Table 6.13. The results for the same pre-selected location with the specified final heading at 90° with a cylindrical shaped radius of 500 ft at (2000 ft., 3500 ft.) are shown in Figure 6.71. Two general flight paths were found; path A and path B with final heading error of 19° and distance error of 350 ft, and final heading error of 0.25° and distance error of 79 ft respectively as shown in Table 6.13. For this particular case, flying path B will allow the airplane to touchdown closer to the pre-selected location and the specified final heading.

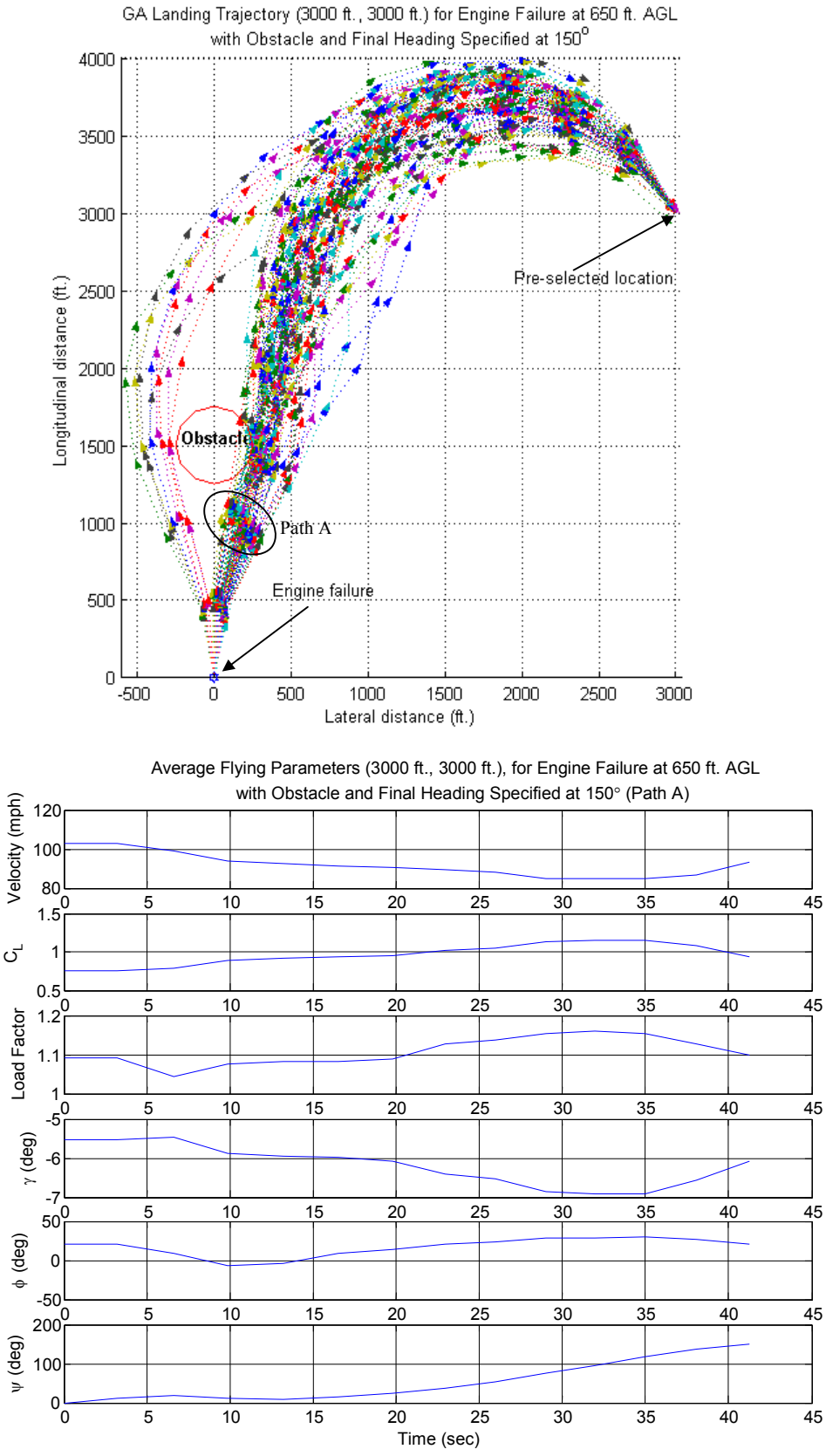

Figure 6.70 Forced Landing (3000 ft, 3000 ft) with Specified Final Heading at 150° and Obstacle (0 ft, 1500 ft) for Engine Failure at 650 ft AGL

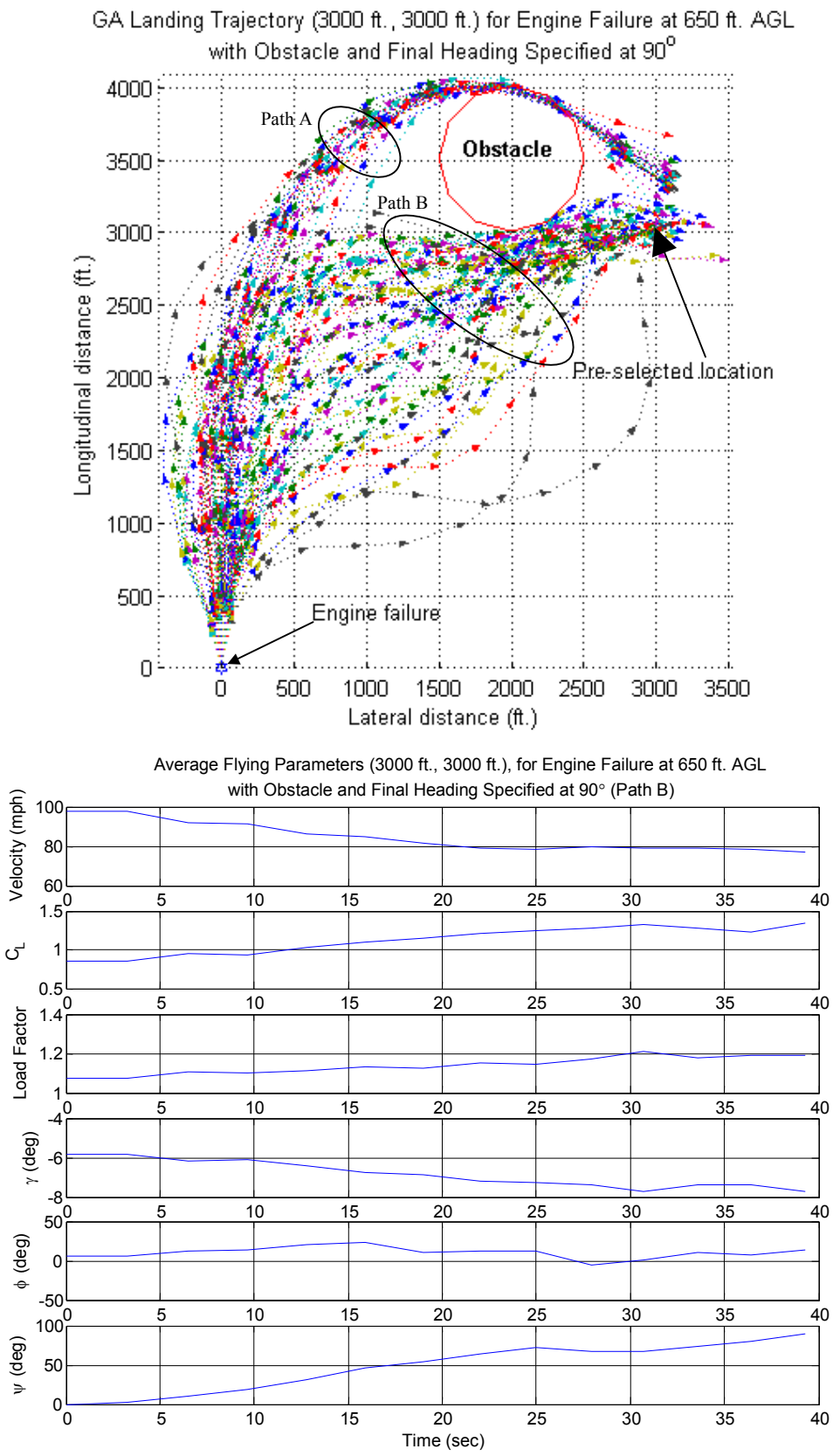

Figure 6.71 Forced Landing (3000 ft, 3000 ft) with Specified Final Heading at 90° and Obstacle (2000 ft, 3500 ft) for Engine Failure at 650 ft AGL

The forced landing trajectory results and average flying parameters for the pre-selected location at (500 ft., 200 ft.) with a cylindrical shaped radius of 250 ft at (1000 ft., 2000 ft.) are shown in Figure 6.72. The results show two general groupings of flight paths; path A and path B with final heading error of 3° and distance error of 33 ft., and final heading error of 0.6° and distance error of 5 ft. respectively as shown in Table 6.13. For this particular obstacle location, path B will allow the airplane to touchdown closer to the touchdown objectives specified.

The results for another specified final heading 180° for the same pre-selected touchdown and obstacle are shown in Figure 6.73. The results show three general groupings of flight paths; path A, path B and path C with final heading error of 2.3° and distance error of 94 ft., final heading error of 22° and distance error of 102 ft., and with final heading error of 51° and distance error of 49 ft. respectively as shown in Table 6.13. For this particular obstacle location, the pilot may elect to either landing closer to the pre-selected location (path C) or landing with direction that is closer to the specified final heading (path A).

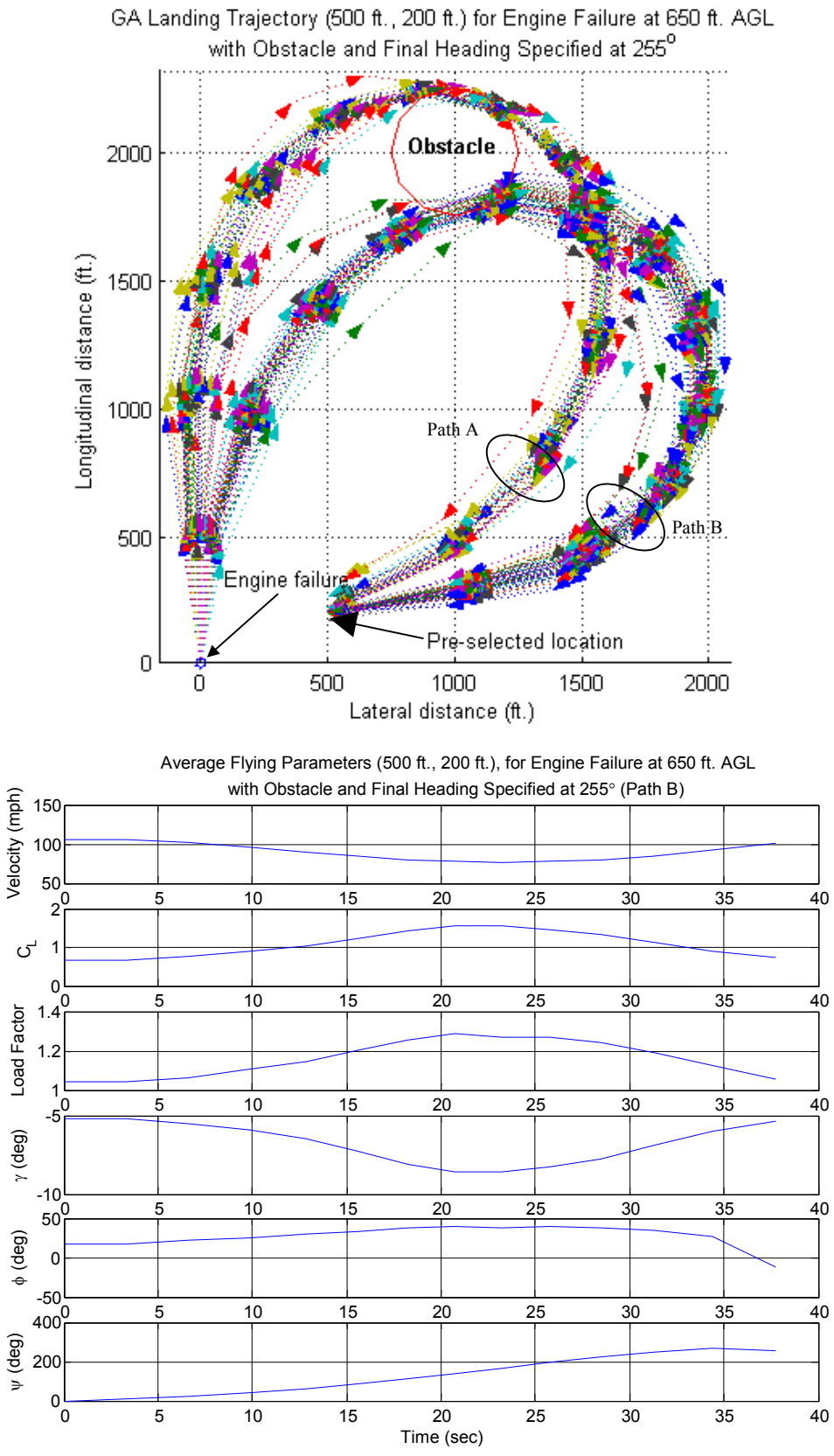

Figure 6.72 Forced Landing (500 ft, 200 ft) with Specified Final Heading at 255° and Obstacle (1000 ft, 2000 ft) for Engine Failure at 650 ft AGL

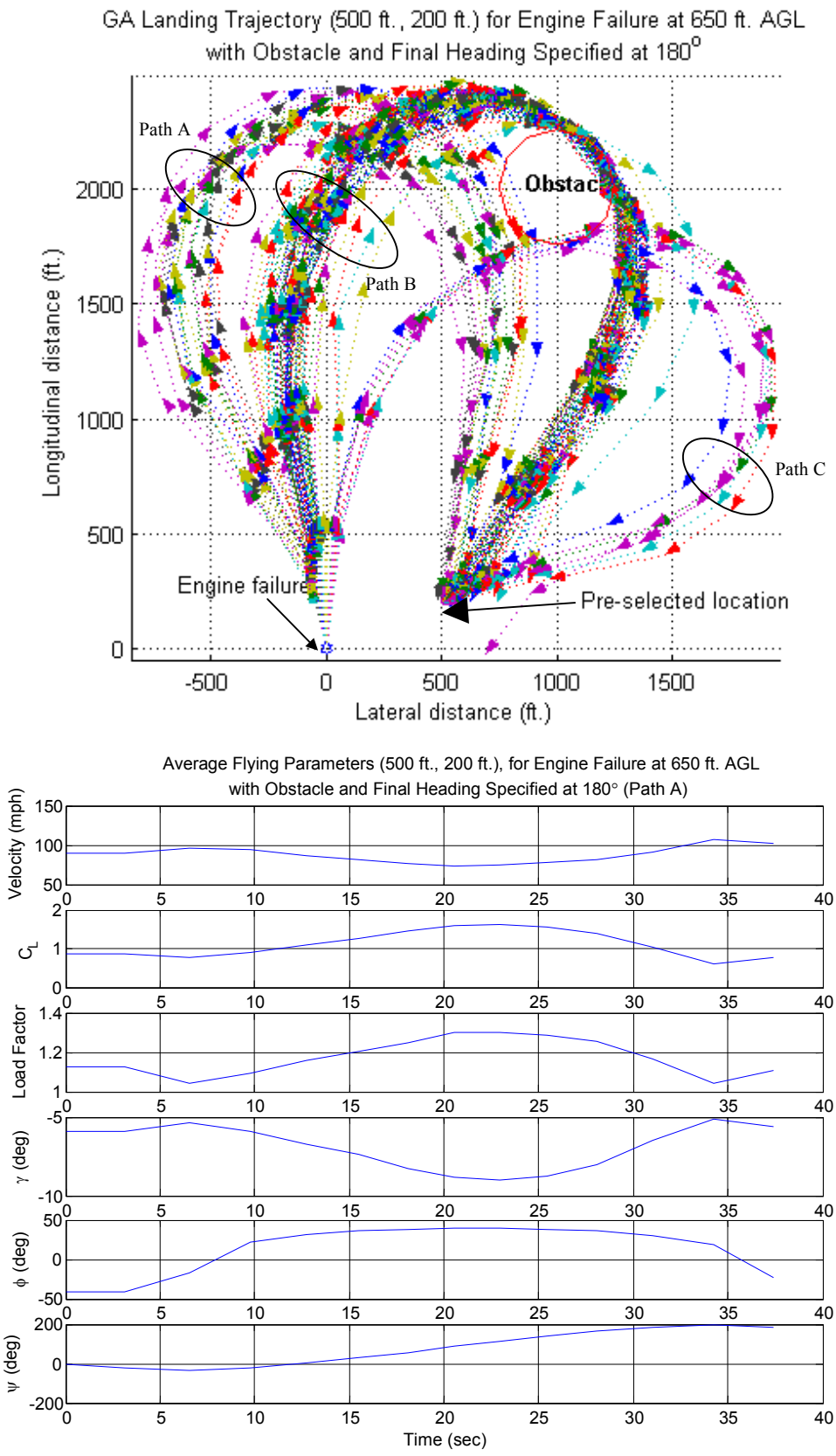

Figure 6.73 Forced Landing (500 ft, 200 ft) with Specified Final Heading at 180° and Obstacle (1000 ft, 2000 ft) for Engine Failure at 650 ft AGL

6.9 Concluding Remarks

The GA results for different GA variations on a forced landing of an aeroplane after an engine failure: discrete speed & discrete bank angle; variable speed and variable bank angle; with vertical atmospheric turbulence and with vertical thermal disturbances; and horizontal crosswinds found results with similar general characteristics for each of the three test locations considered. The results for GA with variable speed and variable bank angle improved significantly over GA with discrete speed and discrete bank angle since continuous real values are used to represent the chromosomes. Therefore, the use of real-value GA representation over direct-value representation produces more accurate results simply because there are more combinations to finding a more precise solution but this is at the expense of computational time.

The results obtained trace an envelope for the most probable landing paths for each of the pre-selected landing location considered, touching down very close to the intended touchdown point on the ground. The vertical disturbances have the effect of widening the flight path envelope for each of the three locations considered. This is as expected since vertical turbulence velocity components effectively changes the vertical descent rate, forcing a change in the forced landing manoeuvre to land at the pre-selected landing locations. As mentioned in Chapter 5, the vertical disturbances have the most effect on the straight glide manoeuvres and are less sensitive to the turn manoeuvres. This effect is very well depicted in the forced landing analyses with vertical disturbances where longer and wider the flight paths are obtained for forced landings with vertical atmospheric and more so for the case with vertical thermal disturbances.

One of the GA's limitations is not being able to locate all the possible trajectories and neither can it provide a single best solution since it is a stochastic process based on randomness. The lack of gradient information in GA is responsible for its inability to mathematically prove whether the results found are optimum but the results obtained show that GA successfully locate results with very minute distance error from the pre-selected touchdown locations as shown in Table 6.3. The trade off in its ability to search a large solution space is the performance sacrifice as a true optimisation procedure. In fact, different GA runs may produce different optimal results, possibly more than one unique landing path, perhaps causing uncertainty as to which is the best landing path as can be seen for the pre-selected landing locations tested in this analysis.

GA may also generate results that are intuitive, those may provide more information that would not have been thought of otherwise or results that are counter intuitive as illustrated by the three test locations. For the test location at (0 ft, -3100 ft), it is intuitive that there are 2 general paths as shown in Figure 6.17 since the pre-selected touchdown location lies along the airplane's line of symmetry at engine failure. For the location (3000 ft, 3000 ft), a double base leg landing can also be clearly seen in Figure 6.18 but this flying manoeuvre is not a recommended because it is more complicated to fly than the typical base leg to final leg landing manoeuvre that resembles the 90° approach to landing and it will also increase the pilot's workload. However, there is a possibility that training may make this manoeuvre feasible and pilots may be more proficient in flying it, if needed. Such a scenario may arise should there be an obstruction in the flight path for the typical approach for this particular landing location. Based on the results obtained, GA also found more flying paths that for the typical base leg to final leg manoeuvre than for the double base leg landing manoeuvre. Lastly, for the location (500 ft, 200 ft), it is possible to land at the pre-selected touchdown location by turning in the opposite direction from the intended location as shown in Figure 6.19. This is possible because the pre-selected touchdown location is located at close proximity to the airplane's initial line of symmetry at engine failure. It is not recommended to fly this manoeuvre to land at this particular landing location because statistically, GA found more paths in flying the manoeuvre that continuously turning towards the pre-selected touchdown location.

The results on the effects horizontal crosswinds have on a forced landing show that certain pre-selected touchdown locations are more susceptible to the horizontal crosswind directions. This is because certain crosswinds headings may represent a headwind or a tailwind which may affect the landing manoeuvre. The horizontal crosswinds have the effect of either improving or degrading the probability in landing at the pre-selected location and may change the character of the optimal forced landing trajectory. Overall, the GA procedure used in this forced landing manoeuvre study clearly identified an ensemble of the most promising landing paths within the search domain.

An improvement to the GA forced landing manoeuvre included the criteria of landing with specific final heading. In general, the GA forced landing program developed is able to find trajectories that will land the airplane very close to the pre-selected location with minimal distance error. However, the final heading error varies with the pre-selected location and the specified final heading. This is as expected since for certain pre-selected location and

specific final heading, for example landing at (500 ft, 200 ft) with a specified final heading of 45°, there may not be sufficient altitude or energy to further manoeuvre the airplane to that particular final heading as shown in Figure 6.50. In other words, some specific final headings are simply not attainable or impossible but the GA program will provide the solution with minimal distance or final heading error. The effect of constant horizontal wind on the forced landing manoeuvre with specific final heading for the conditions tested is a slight variation on the flight path.

An extension to the GA forced landing manoeuvre is GA in obstacle avoidance forced landing manoeuvre. Obstacles were placed based on the flight path results found from the various forced landing situations without obstacles. This is to test the GA forced landing program's capability in searching for paths that will successfully avoid obstacles that were placed in the flight paths. The results show that the GA forced landing program is capable of finding such flight paths. However, the degree to which the program is capable of finding flight paths that will touchdown at the pre-selected location depend on where the obstacle's location and the intended touchdown location.

The addition of a specific final heading was implemented as an improvement to the GA obstacle avoidance forced landing manoeuvre. The results show that in general the program is able to find flight paths that will land close to the pre-selected location subject to the obstacle's size and location. However, due to the additional boundary condition of landing with a specified final heading, the results found are not as close to the case without specified final headings. In some cases, more than one ensemble grouping of flight paths were revealed from the results where certain paths are better as illustrated in the case of landing at the pre-selected location of (3000 ft., 3000 ft.) with an obstacle whose radius is 500 ft located at (2000 ft., 3500 ft.) and a specified final heading of 90° as shown in Figure 6.71. The results also revealed the trade offs between landing closer to the pre-selected location with a larger final heading error or landing further from the pre-selected location with a smaller final heading error as shown in the case of landing at the pre-selected location of (500 ft., 200 ft.) with an obstacle whose radius is 250 ft located at (1000 ft., 2000 ft.) and a specified final heading of 180° as shown in Figure 6.73.

The results from various GA search have confirmed GA's effectiveness to explore the solution domain as well as its capability to successfully identify the most promising trajectory paths to a forced landing manoeuvre. The GA search method can also be easily catered for

both discrete and for continuous variables, which allows the genetic optimisation procedure high flexibility in searching for optimal forced landing trajectories. GA is a relatively new optimisation method compared to the traditional gradient search method, which has difficulties for discontinuous or non-smooth functions. In solving optimisation problems, GAs have the advantage that no derivatives have to be found but they have only to utilise the governing equations in the problem considered.

The trade off in not using gradient information is that it does not guarantee a minimum point but it will locate results that are very close to the optimal solution. Other optimisation methods such as gradient method may be able to locate better optimal solutions but may suffer computational time. GA is not an alternative nor is it a replacement method to other traditional optimisation methods but it is a valid complementary optimisation technique. In simulation, obtaining acceptable results rapidly is more valuable than spending an enormous time searching for the optimal point. In this study, the objective is to be able to obtain a solution quickly in a short time, namely a fast algorithm that can be used on board a small aircraft and can calculate the optimum trajectory quickly in the case of a forced landing.

CHAPTER 7

SEQUENTIAL QUADRATIC PROGRAMMING IN A FORCED LANDING MANOEUVRE

7.1 Introduction

In the event of a forced landing, flying an optimal trajectory may allow the aircraft to land safely and the criterion applied depends on the type of emergency landing. For example, in the case of a flame out forced landing, a minimum-time trajectory criterion will be imposed. However, if an energy-preserving manoeuvre is flown, valuable time could be gained and this may allow the pilot more time to troubleshoot the aircraft even if there are no suitable landing locations. It is the later emergency landing that is being considered in this analysis. Therefore, flying the optimal trajectory could be a life-saving endeavour. The landing manoeuvre should be simple and general for pilots to carry out the manoeuvre and should not be overly sensitive to the flying manoeuvres.

As mentioned in the Chapter 6, although GA is capable of locating some of the best values for optimisation, it does not guarantee that it is a minimum value. Therefore, another optimisation technique is used to find a more accurate and precise solution. This chapter presents the analysis on a forced landing manoeuvre trajectory optimisation using Sequential Quadratic Programming (SQP), which is a branch of the enumerative search technique that incorporates both dynamic optimisation and constrained optimisation. This search technique was chosen because of its ability to locate minimum values. The use of GA as an optimisation technique coupled with another optimisation technique such as SQP has also been used for space plane trajectory optimisation (Yokoyama 2002). In his research work, GA was used to obtain values that were used as initial guesses for the SQP program, which was then used to refine the solution. The objective for this analysis is to find the lift coefficients and bank angles histories for optimal forced landing manoeuvres.

7.2 Sequential Quadratic Programming

SQP is a highly sequential iterative mathematical programming technique method where the objective function is approximated with a quadratic form and the non-linear constraints are

linearised at each iteration step. SQP solves nonlinear program directly rather than converting the problem to a sequence of unconstrained minimisation problems. It is widely used in solving non-linearly constrained optimisation problems and several implementations of SQP are available (Schittkowski 1985; Gill, W.Murray *et al.* 1986; Gill, Murray *et al.* 1994). The basic idea for SQP is analogous to Newton's method for unconstrained minimisation, where at each step a local model of the optimisation problem is constructed and solved, yielding a step toward the solution of the original problem. The SQP theoretical background can be found in (Stoer 1985; Spellucci 1993) while a more comprehensive overview of SQP can be found in (Fletcher 1980; Gill, W.Murray *et al.* 1981; Hock and K. Schittkowski 1983). The following is a brief description of the SQP technique compiled from several sources[††].

The general nonlinear constrained optimisation problems used in SQP take the following form:

$$\begin{aligned} &\text{Minimise} && f(x) \\ &\text{Subject to} && h(x) = 0 \\ & && g(x) \le 0 \end{aligned} \tag{7.1}$$

where: $f : R^n \to R$, $h : R^n \to R^m$, and $g : R^n \to R^p$.

The Quadratic Programming (QP), which is described later, solved at each SQP's iteration is an approximation of the original problem with linear constraints and quadratic objective:

$$\min_d f(x_k) + \nabla f(x_k)^T d + \frac{1}{2} d^T \nabla^2 L(x_k) d$$

subject to:

$$\begin{aligned} g_i(x_k) + \nabla g_i(x_k)^T d \le 0 \\ h_i(x_k) + \nabla h_i(x_k)^T d = 0 \end{aligned} \tag{7.2}$$

where the Lagrangian function, L, is defined as:

$$L(x) \triangleq f(x) + \lambda^T h(x) + \mu^T g(x) \tag{7.3}$$

where λ is a vector of approximate Lagrange multipliers and μ is a vector of the approximate Karush-Kuhn-Tucker (KKT) multipliers.

[††] http://www-personal.engin.umich.edu/~mepelman/teaching/IOE511/section11.pdf
http://www-fp.mcs.anl.gov/otc/Guide/OptWeb/continuous/constrained/nonlinearcon/section2_1_1.html
http://tomlab.biz/docs/nlpqlp.pdf

Instead of using the true Hessian of the Lagrangian, $\nabla^2 L(x)$ is replaced by H_k, which is the Broyden-Fletcher-Goldfarb-Shanno (BFGS) approximation of the Hessian:

$$H_{k+1} = Hk + \frac{q_k q_k^T}{q_k^T p_k} - \frac{H_k p_k p_k^T H_k}{p_k^T H_k p_k} \tag{7.4}$$

where:

$$\begin{aligned} pk &= x_{k+1} - x_k, \\ qk &= \nabla f(x_{k+1}) + \lambda^T \nabla h(x_{k+1}) - (\nabla f(x_k) + \lambda^T \nabla h(x_k)) \end{aligned} \tag{7.5}$$

A final superlinear convergence rate can be obtained using the BFGS quasi-Newton formula while avoiding the second derivatives calculation (Powell 1978; Stoer 1985).

The solution to the QP sub-problem produces a search direction vector, d_k, which is used to form a new iterate x_{k+1}, where:

$$x_{k+1} = x_k + \alpha d_k \tag{7.6}$$

A line search is carried out to choose an α, such that the following penalty function (also known as merit function) is minimised:

$$\psi(x) = f(x) + \rho \left[\sum_{i=1}^{p} |h_i(x)| + \sum_{i=1}^{m} \max\{0, g_i(x)\} \right] \tag{7.7}$$

where ρ is a penalty factor.

This line search sub-problem helps to improve the convergence of the algorithms and it balances the occasional conflicting objectives of reducing the objective function and of satisfying the constraints.

The following describes the QP process, which is used in SQP as described above. A QP is an optimisation problem with a quadratic objective and linear constraints:

$$\min_x \frac{1}{2} x^T Hx + gx$$

subject to:

$$\begin{aligned} Ax - b &= 0 \\ Cx - d &\le 0 \end{aligned} \tag{7.8}$$

where: H is constant and symmetric,

A and C are constant matrices,

g, b, and d are constant vectors.

The solution to an unconstrained QP problem with H positive definite is $x^* = -H^{-1}g$. The solution of an equality constrained QP problem with H positive definite can be found in the Lagrangian function:

$$L = \frac{1}{2}x^T Hx + g^T x + \lambda(A^T x - b) \tag{7.9}$$

The Lagrangian's gradient is:

$$\nabla L = Hx + g + A^T \lambda = 0 \tag{7.10}$$

This solution, along with the equality constraint $Ax\text{-}b = 0$ defines the following set of linear equations:

$$\begin{bmatrix} H & A^T \\ A & 0 \end{bmatrix}\begin{bmatrix} x \\ \lambda \end{bmatrix} = \begin{bmatrix} -g \\ b \end{bmatrix} \tag{7.11}$$

The solution is: $x^* = -H^{-1}(g + A^T \lambda)$

$$\lambda^* = -(AH^{-1}AT)^{-1}(b + AH^{-1}g)$$

If the QP includes inequality constraints, then a typical solution algorithm involves the active set strategy through which a sequence of equality constrained problems are solved.

$$\min_d \frac{1}{2}(x+d)^T H(x+d) + g(x+d) \tag{7.12}$$

subject to:

$$a_i(x+d) - b_i^* = 0, \quad i \in W_k \tag{7.13}$$

where d is a search direction.

The active set W_k includes all the equality constraints and the active inequality constraints at the current iteration. The active set is updated at every iteration according to a selection criterion.

The SQP algorithm can be summarised as follow:

1) Given the current iterate, x_k, and a current approximate Hessian, H_k, the QP sub-problem is solved to obtain the search direction d_k. Notice that the solution of the QP sub-problem provides estimates of the multipliers λ and μ.
2) Given d_k, the line search problem is solved to minimise the merit function $\psi(x)$ and then to find the next iterate x_{k+1}.
3) Update the Hessian approximation H_{k+1} using BFGS formula.

4) Check if the convergence criterion is satisfied, if not set $k = k + 1$ and repeat step 1.

This research uses the FMINCON tool from The Optimization Toolbox 2.0 for use with MATLAB V6.5. This software was selected for its versatility implementation and interactive nature, thus, allowing optimisation problems to be easily refined and adapted. It provides the user with valuable feedback and useful insight into a problem's "best" solution and has been successfully used in constrained non-linear optimization problems [‡‡]. Although it may not be the best choice for an off-the-shelve software package, it was selected simply as a basic tool to solve a large-scale optimisation problem. Further research may include better and more efficient software package for solving such problem. SQP has been successfully implemented in some of the aerospace problems as mentioned in Chapter 2.3.1.

7.3 Sequential Quadratic Programming Applied to a Forced Landing Manoeuvre

This section describes the forced landing manoeuvre optimisation using SQP and it utilises the aircraft model as described in Chapter 3.2. Although GA has successfully found some of the best forced landing trajectories, a different method was also used in the forced landing analysis to support the solutions found by the GA method. The objective in this optimisation is to land at a pre-selected location after an engine failure in mid air. Since this method was employed simply as a comparison to the solutions found by the GA method, only the simplest case of a forced landing after an engine failure was being considered, which was to touchdown at a pre-selected location and the final heading of the aircraft was not being imposed. The optimisation procedure consists of a two parts: (1) optimise to reach a point above the pre-selected location with minimum altitude lost and (2) follows by a "circle to touchdown" approach to land directly below with minimum descent rate. Since SQP requires the variables to be smooth up to second-order, the forced landing for different atmospheric disturbances was not being carried out because the atmospheric disturbances would create sudden velocity jumps in the flight model. A two-part optimisation criterion was being applied in order to have better consistency in the forced landing trajectories for various engine failure altitudes. The optimisation procedure for this problem consists of flying to a position directly above the pre-selection with minimum altitude lost and then circle to touchdown to a location directly below with minimum descent rate.

[‡‡] http://www.cqm.nl/eng/publications/pdf/asmo2001sequem.pdf

The objective functions can be formulated as follow:

Objective function for Part 1:

Maximum altitude at pre-selected location

Objective function for Part 2:

Circle to touchdown with minimum descend rate

Constraints for Parts 1 & 2;

$$105.6\ ft/sec(V_{L/Dmax}) \leq Velocity \leq 305.49\ ft/sec\ (V_{max})$$

$$3° \leq Angle\ of\ attack \leq 12°$$

$$-45° \leq Bank\ angle \leq +45°$$

$$Roll\ rate \leq 45\ °/sec$$

$$Velocity\ jump\ between\ iteration\ steps \leq 20\ ft/sec$$

$$0\ ft \leq Error\ distance\ from\ pre\text{-}selected\ location \leq 10\ ft$$

The range of the parameters specified are based on the Beech Bonanza E33A. Some preliminary tests were carried out to determine an adequate number of discretisation points required and it was found that the results do not vary significantly when approximately one discretisation point is used for each 50 ft drop in altitude based on the results obtained using the GA program.

Despite the fact that nonlinear programming techniques have a large convergence domain, it was found that the initial guess for the decision variables has a significant impact to finding solutions to the optimisation problem considered in this analysis. Therefore, the SQP decision variables' initial guesses for Part 1 either used results from the GA analysis or heuristic rules that utilise the variables' initial and final states. The heuristic rule for any particular decision variable was obtained from a straight line connecting the initial ($_i$) and final state ($_f$);

$$x_i = x_1 + (x_f - x_1)\frac{(i-1)}{(N-1)}, \quad i = 1, \ldots N$$

where N is the number of discretisation points.

Since the objective for Part 2 is to land with minimum descend rate to a location directly below, the initial guesses used wee a velocity of 122 mph ($V_{L/Dmax}$) and a bank angle of 45°.

7.3.1 Results for Optimal Forced Landing Manoeuvre

Forced landing optimisations were conducted for pre-selected location at (3000 ft, 3000 ft), where the 1st component represents the lateral distance and the 2nd component represents the longitudinal distance from the engine failure position. The analyses were carried out from three altitude: 3000 ft AGL, 2000 ft AGL, 650 ft AGL and for three different initial engine failure velocities: 76 mph (5% above stall speed), 122 mph ($V_{max\ L/D}$) and 208 mph (V_{max}). 13 discretisation points were used for Part 1 of the optimisation process and 39 discretisation points were used for Part 2 except for the case where the engine fails at 650 ft AGL. For this engine failure altitude, only Part 1 of the optimisation procedure was used and the optimisation procedure was modified to touchdown at the pre-selected location instead of arriving at the pre-selected location with minimum altitude lost. The low engine failure altitude does not require Part 2 of the optimisation procedure to be used.

The 2-D and 3-D optimal flight paths for an engine failure at 3000 ft AGL are shown in Figure 7.1 while the optimal flying parameters are shown in Figure 7.2. The flight time and altitude lost to reach a position above the pre-selected location for an initial engine failure speed of 76 mph, 122 mph, 208 mph are 23.69 secs, 20.74 secs, 16.79 secs and 384 ft, 381, 468 ft respectively. The results show that when the aircraft's maximum speed is flown at engine failure, the aircraft is required to fly a longer flight path in order to successfully reach the position above the pre-selected location with minimum altitude drop. The flight paths for an initial engine failure speed at 76 mph and at 122 mph show very similar flight paths and flying parameters. The flight paths for the circle to touchdown sector for all the different initial engine failure speed are very similar and require approximately 3.5 turns to touchdown. The solution resembles the holding of aircraft in stacks in the Airport Terminal Area.

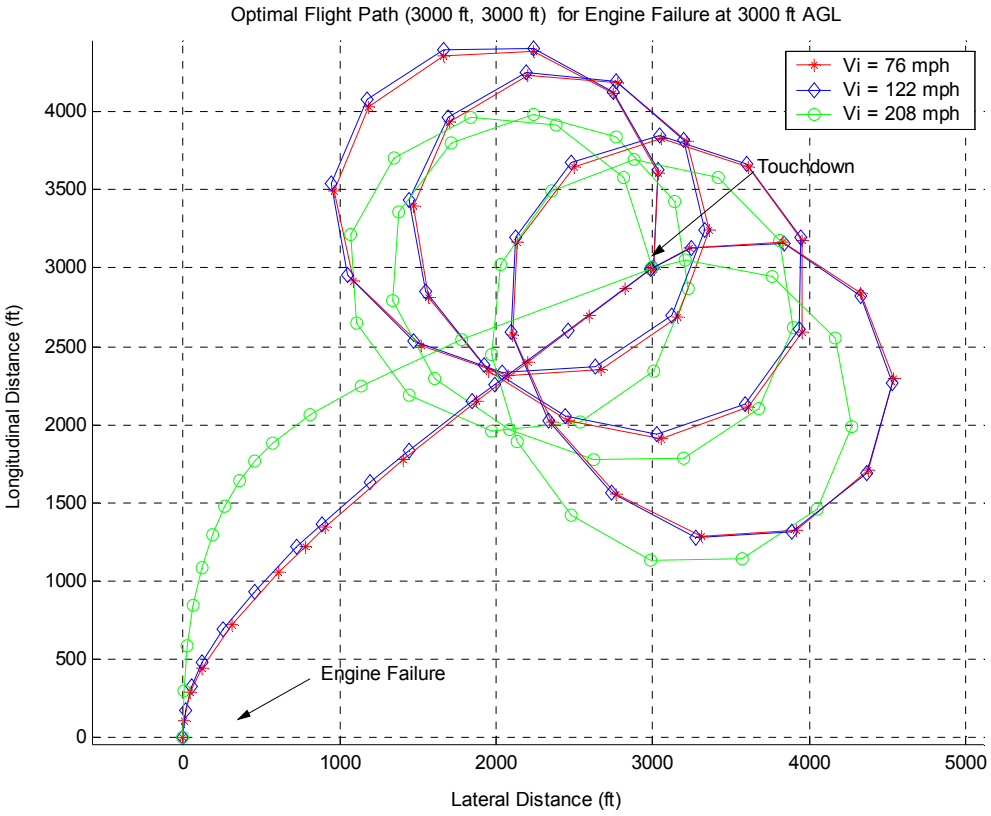

(a)

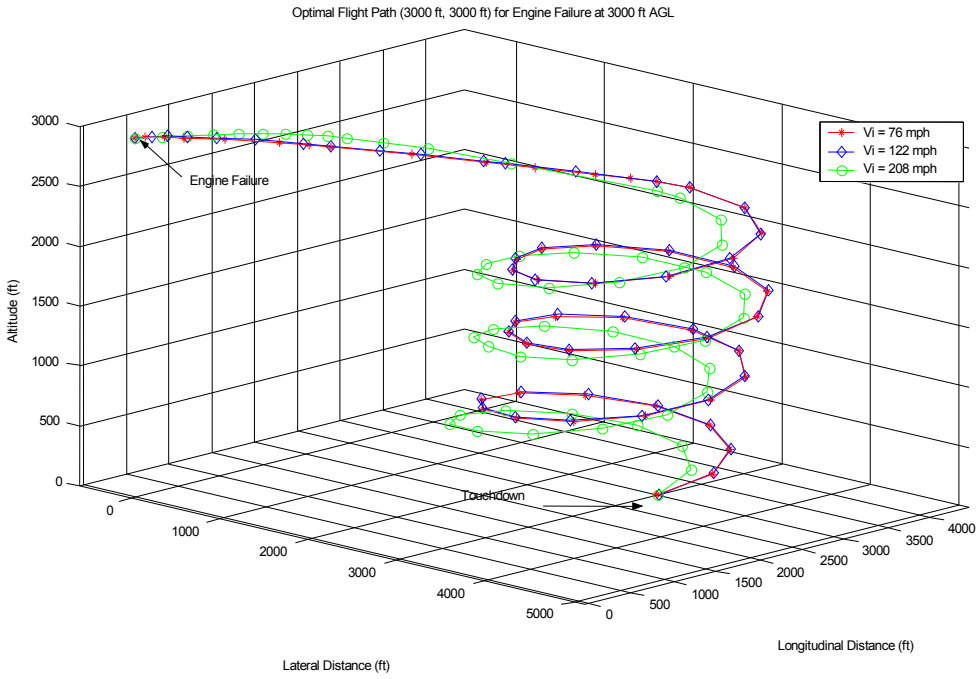

(b)

Figure 7.1 Optimal Flight Paths for Engine Failure at 3000 ft AGL for Different Initial Engine Failure Speed

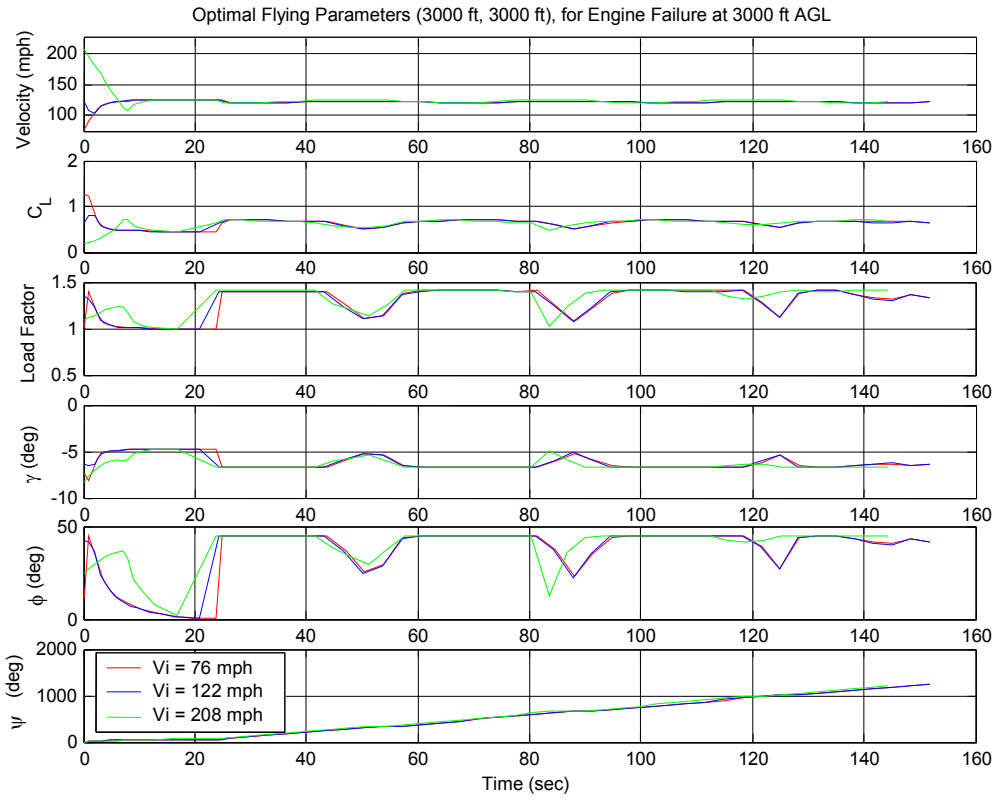

(b)

Figure 7.2 Optimal Flying Parameters for Engine Failure at 3000 ft AGL for Different Initial Engine Failure Speed

The 2-D and 3-D optimal flight paths for an engine failure at 2000 ft AGL are shown in Figure 7.3 while the optimal flying parameters are shown in Figure 7.4. The flight time and altitude lost to reach a position above the pre-selected location for an initial engine failure speed of 76 mph, 122 mph and 208 mph are consistent with the engine failure at 3000 ft AGL case since the first part of the optimisation process is independent of the engine failure altitude. The main difference between an engine failure at 2000 ft AGL and at 3000 ft AGL are (1) fewer turns are required to touchdown for the lower engine failure altitude and (2) the final heading at touchdown at the pre-selected location.

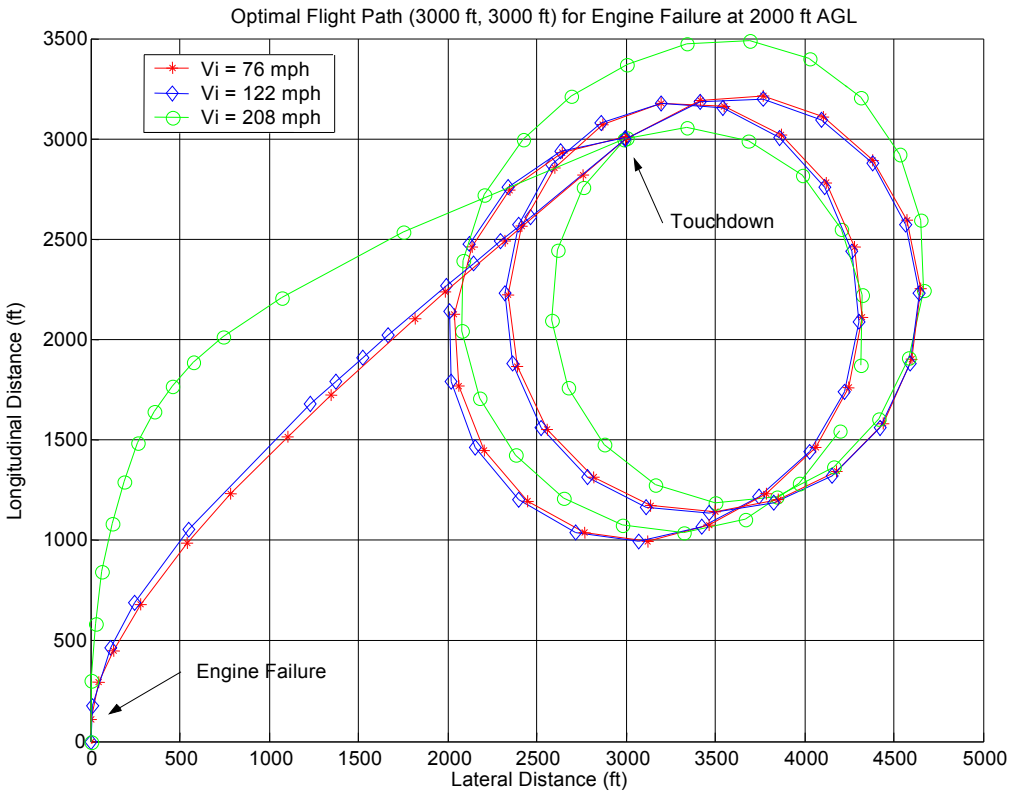

(a)

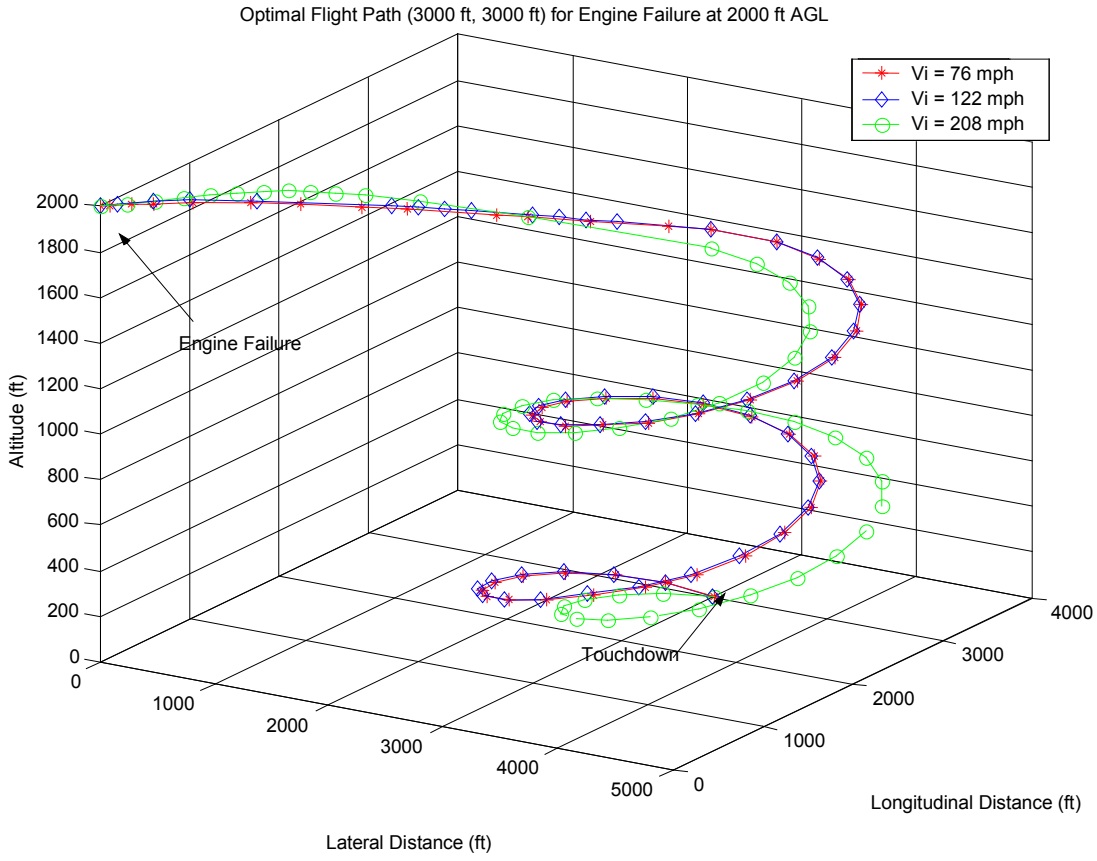

(b)

Figure 7.3 Optimal Flight Paths for Engine Failure at 2000 ft AGL for Different Initial Engine Failure Speed

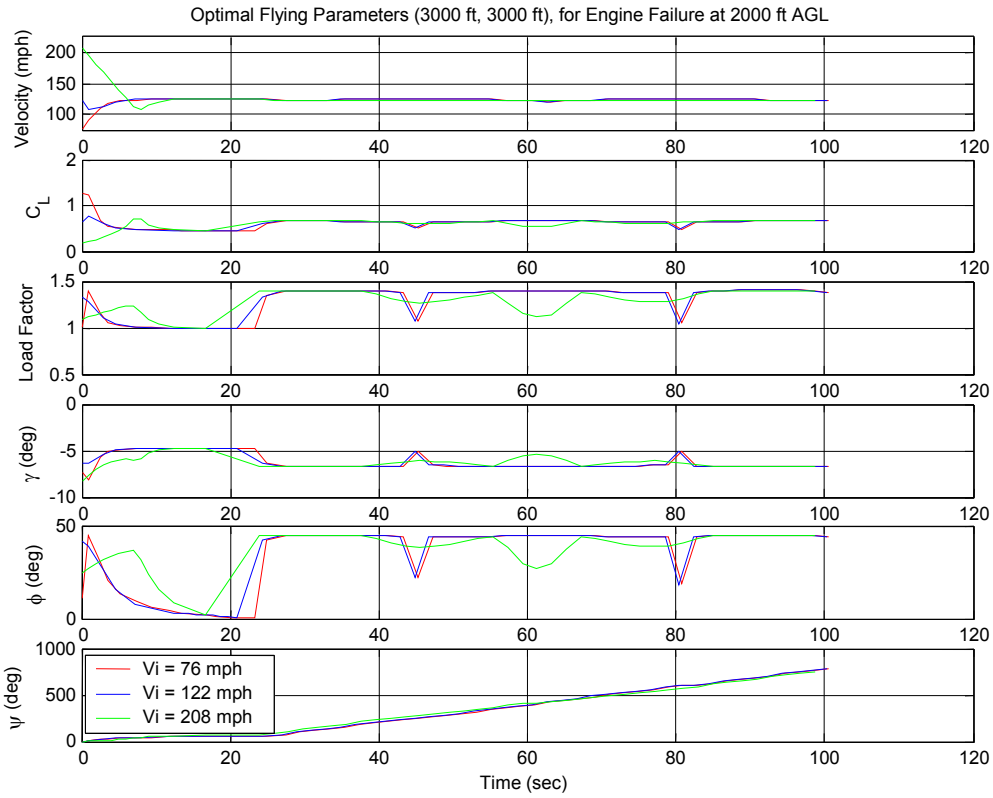

Figure 7.4 Optimal Flying Parameters for Engine Failure at 2000 ft AGL for Different Initial Engine Failure Speed

The effects for different initial engine failure speed at 650 ft AGL is different from the previous two cases considered since the aircraft is assumed to fail at lower altitude and it does not require Part 2 of the optimisation process. The 2-D and 3-D optimal flight paths for an engine failure at 650 ft AGL are shown in Figure 7.5 while the optimal flying parameters are shown in Figure 7.6. The results show a shorter flight path for an initial engine failure speed of 208 mph. The flight time for an initial engine failure speed of 76 mph, 122 mph and 208 mph are 25.1 secs, 21.7 secs and 17.9 secs respectively.

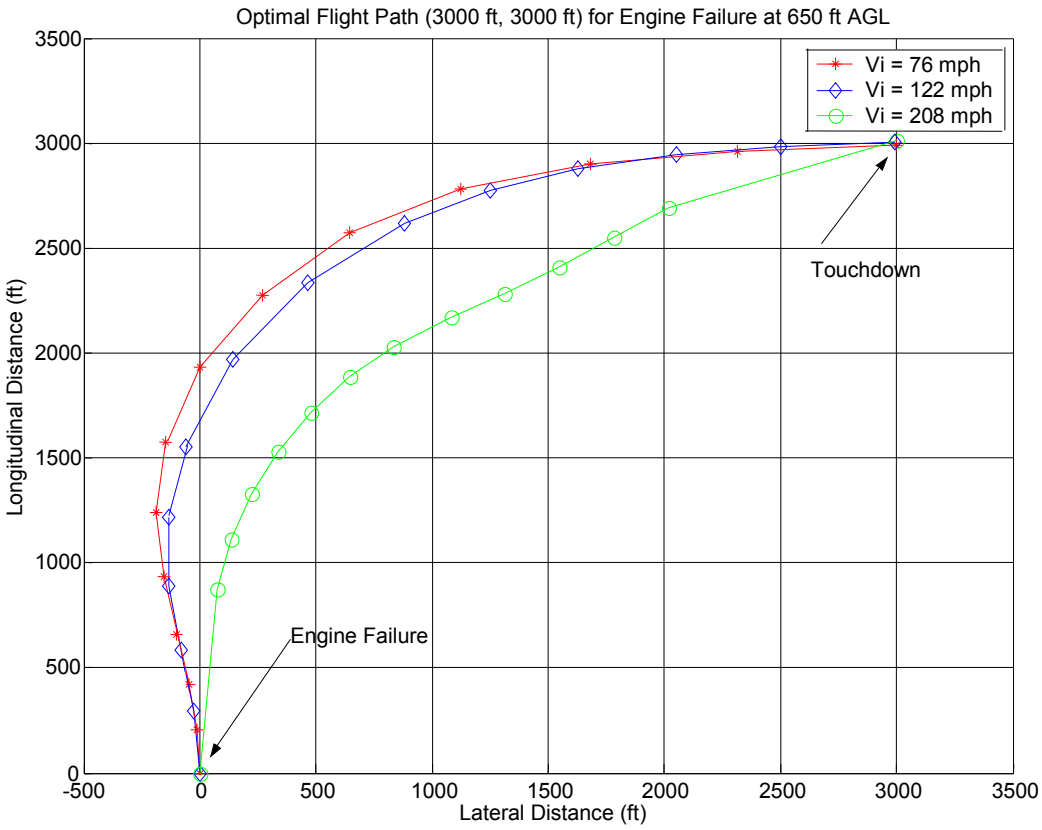

(a)

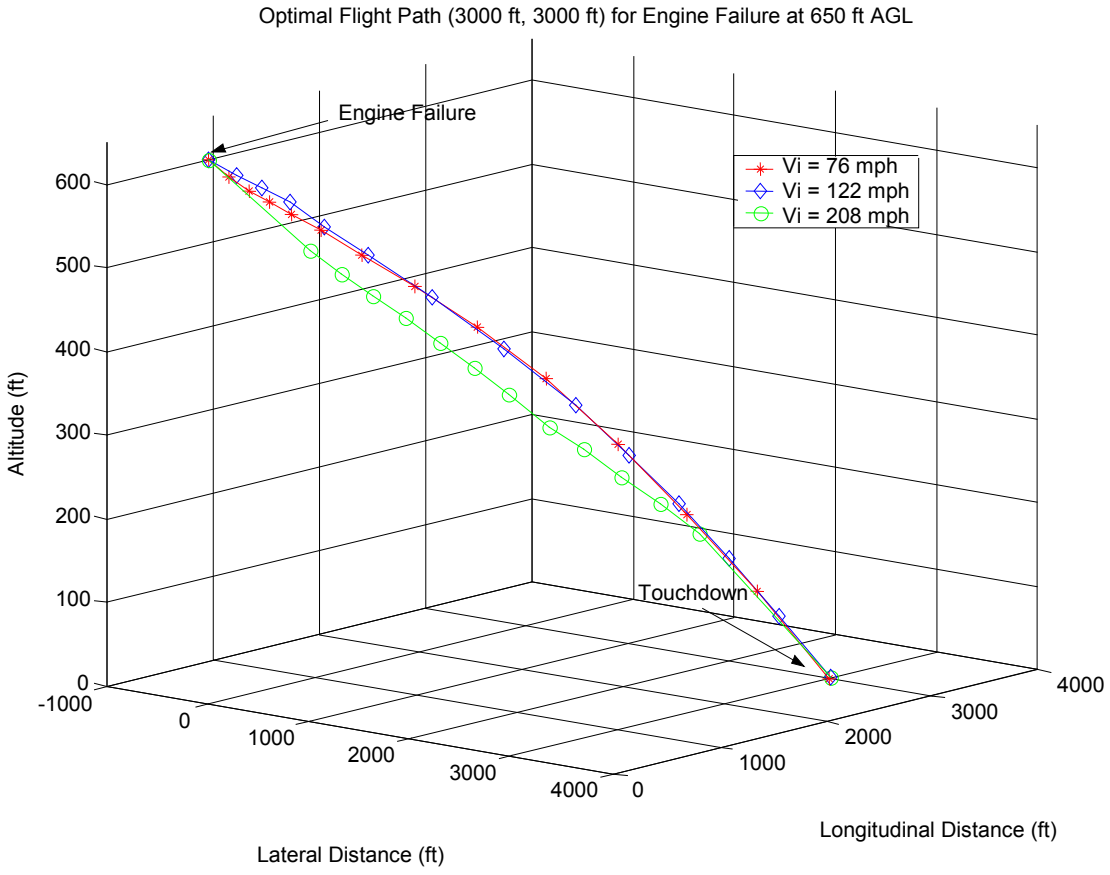

(b)

Figure 7.5 Optimal Flight Paths for Engine Failure at 650 ft AGL for Different Initial Engine Failure Speed

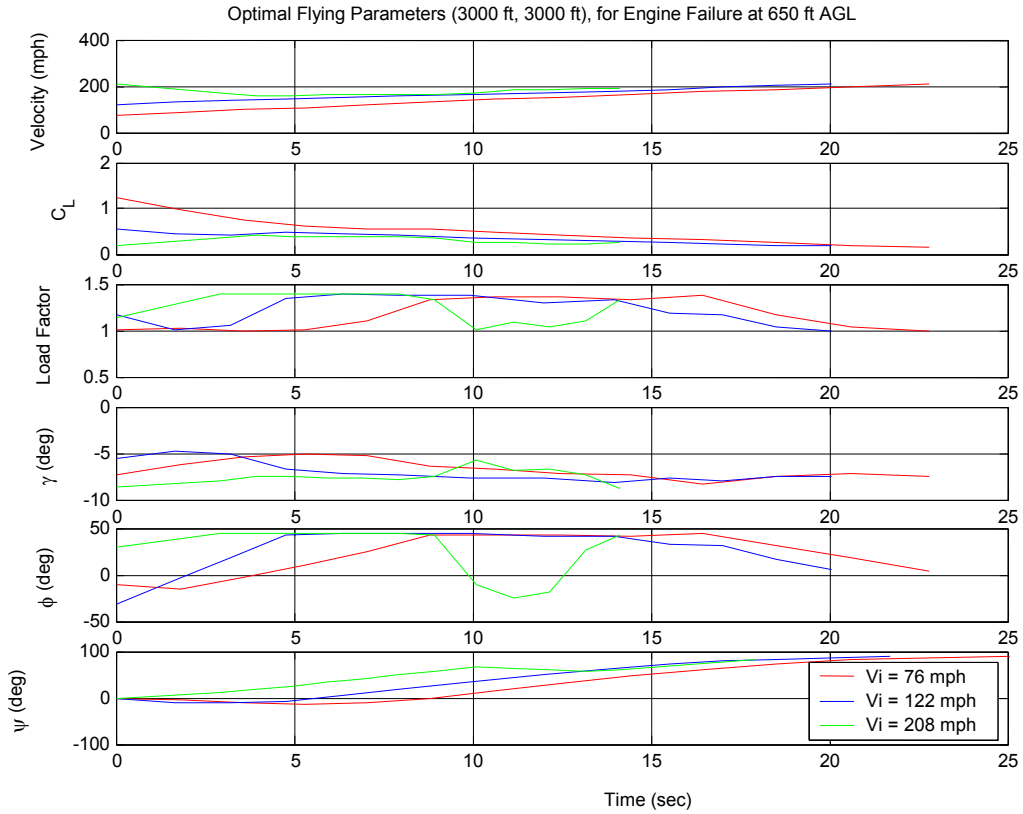

Figure 7.6 Optimal Flying Parameters for Engine Failure at 650 ft AGL for Different Initial Engine Failure Speed

7.4 Concluding Remarks

The solutions obtained using SQP are approximated solutions since the accuracy of the results are dependent on the number of discritisation points and on the initial guesses used. However, SQP is successful in locating optimal flight paths for the problem considered in this study. The accuracy can be improved either by increasing the number of discritisation points or by reallocating the current points adaptively.

In optimising for the aeroplane for a forced landing manoeuvre from 2000 ft AGL and 3000 ft AGL, a high engine failure speed requires the aeroplane to fly a longer flight path to reach the pre-selected location with minium altitude lost. The sector on circle to touchdown does not seem to be affected by the initial engine failure speed except for a shift in horizontal circling flight path for higher engine failure altitude. In the case of engine failure from 650 ft AGL, a high engine failure speed will require the aeroplane to fly a shorter route to touching down at the pre-selected landing location. For this case, the optimisation process was carried out without having to optimise to land at the pre-selected location with maximum altitude.

CHAPTER 8

PRACTICAL FORCED LANDING MANOEUVRE STRATEGY WITH UNKNOWN ATMOSPHERIC WIND CONDITIONS

8.1 Introduction

This chapter describes the how the analyses carried out in the two previous chapters can be applied to a practical piloting problem. The analyses in Chapter 6 involved the search for practical trajectories to a forced landing manoeuvre with and without specific final heading, and a forced landing manoeuvre with obstruction using the GA technique. Further observations of the results reveal how the results obtained can be applied to a forced landing strategy with unknown atmospheric wind conditions.

8.2 Optimal Forced Landing Manoeuvre for Pilots in Unknown Atmospheric Wind Condition

The GA analyses in Chapter 6 found solutions to a forced landing manoeuvre for two atmospheric models and for various crosswinds conditions. The vertical disturbances have the effect of changing the airplane's sink rate, hence, affecting the flight path to be flown for a forced landing trajectory. An updraft will require the airplane to fly a different flight path to bleed off the excess energy while a downdraft will require the airplane to fly a more direct and shorter flight path in an attempt to touchdown at the pre-selected location. The effects horizontal crosswinds have on the forced landing manoeuvre depend on the location of the pre-selected location since crosswinds may act as headwind, crosswind or tail wind for certain sectors of the forced landing trajectory. Inevitably, there will be certain pre-selected location and pre-selected final heading that can never be reached.

The proposed forced landing manoeuvre for an engine failure after take-off; (i) with unknown atmospheric wind conditions is to intuitively steer the airplane towards the pre-selected location and (ii) for engine failure from higher altitude is to arrive at the pre-selected location with minimum altitude lost and then circle to touchdown to the pre-selected location directly below. A conservative approach would be for the airplane to fly the trajectory for the worst vertical disturbance, which is the one with the most downdrafts since any other vertical

disturbances will simply reduce the sink rate and the airplane can circle to touchdown to bleed off the excess energy.

The proposed technique is supported by the results obtained, which shows similarities in the flying parameters for the different vertical disturbances. The results suggest that a pilot could safely land an aeroplane after an engine failure using very similar flying manoeuvres for different atmospheric disturbances, except for cases where the engine failure occurs at very low altitude such that it can only perform a straight glide to touchdown. A conservative flying manoeuvre will be to fly the flight path for the worst atmospheric disturbances since any other atmospheric disturbances will simply require the pilot to fly with minor changes during the later part of the flight manoeuvre.

There are three zones in engine failure altitude in which the pilot has to consider for a forced landing. The key to a successful forced landing is energy conservation. The strategy adopted for this study is to fly under the worst atmospheric condition and to land with minimum sink rate. The first zone is a low engine failure altitude where the airplane can never make it to the pre-selected landing location. The second engine failure altitude zone is where the airplane can land by flying at the velocity for maximum glide angle ($V_{L/Dmax}$) to the pre-selected landing location but there is insufficient altitude for it to orbit to touchdown, and the third engine failure altitude zone is where the airplane will fly to the pre-selected location at minimum sink rate and then fly the necessary number of orbits to touchdown to the pre-selected landing location and specific final heading.

The findings from this study suggest that if pilots were to fly the flight path for the worst atmospheric condition he can certainly safely land the aircraft in any other atmospheric conditions. Having to only learn one flying technique and applying it, in the unfortunately event of an engine failure will certainly decrease the pilot's workload and help minimise the stress level during such emergency situation allowing for a safer emergency landing.

8.3 Concluding Remarks

The forced landing analyses in this study suggested a practical forced landing manoeuvre strategy in the presence of unknown atmospheric disturbances for three zones in engine failure altitude.

CHAPTER 9

CONCLUSIONS

9.1 Conclusions

The reliability and advancements in flight simulators have led to the growth in using flight simulators to safely train pilots in today's aviation industry. Flight simulators allow pilots to fly some dangerous manoeuvres or to explore certain flying techniques without risking their lives.

The main objective of this work is to understand how artefacts such as delay may affect the transfer of training from flight simulators to flying a real aeroplane. In this study, the artefact, delay, is being represented by atmospheric disturbances and the particular case of a forced landing after an engine failure was chosen. It is assumed that the pilot's response to uncertainties in the atmospheric disturbances is analogues to the pilot's response due to delay in a flight simulator. These errors are relevant to the understanding of the development of transfer of training from flight simulators.

This study has demonstrated the importance of analyses of simulator requirements and the consideration of such requirements within the context of particular manoeuvres to be flown. It has identified certain issues to assist in flight simulators development and in better understanding on transfer of training from flight simulators.

Trajectory optimisation and the search for a forced landing manoeuvre after an engine failure has been successfully carried out using both the Genetic Algorithm (GA) and the Sequential Quadratic Programming (SQP) methods. The forced landing trajectory study also included the study on the effects atmospheric disturbances and crosswinds have on the forced landing manoeuvre.

The forced landing trajectory analyses conducted in this study has led to the suggestion of a practical forced landing manoeuvre strategy in the presence of unknown wind conditions. The results from this study can be used to form building blocks for many relevant research

that can evolve in this research area as suggested in the section on Chapter 9.4 - Further Work.

9.2 Discussions

This study has produced several key results. The first and foremost of these is related directly to the main aim of this thesis, restated here:

> To develop and to gain better understanding on skills transfer from flight simulators, especially on the effects artefacts have on a forced landing manoeuvre after an engine failure and to use genetic algorithm as a search method to generate an ensemble of probable flight paths to a forced landing manoeuvre with and without obstacle for simulator flight training purposes.

The research contained in this body of work has highlighted some of the issues associated with the transfer of training from flight simulators and on the effects internationally acceptable flight simulators tolerances have on the performance of flight simulators used for pilot training. This study found that the effect of the simulator tolerances is highly sensitive on the nature of the manoeuvre flown and that in some cases, negative transfer of training may be induced by the tolerances as described in Chapter 5.

This study used a point mass aircraft model in all the analyses carried out and found acceptable and realistic results. Practical flight scenarios were simulated using a time-averaged atmospheric turbulence model and a simplified thermal model. An exhaustive search technique to a flight trajectory optimisation was carried out to form benchmark results for comparisons with other search and optimisation techniques used in this study.

Two optimisation techniques were used in this study as described in Chapters 6 and 7. The advantage in using GA as an optimisation tool is that no derivatives have to be found but only to utilise the governing equations in the problem considered. The drawback for this method is the lack of gradient information and the results obtained cannot be proven for optimality. However, this method is capable of searching a large solution space in a relatively short time and the use of large population size will compensate for the lack of gradient information. The control parameter optimisation analyses for direct-value and real-value representations found parameters that are suitable for use in various engineering optimisation problems

(Tong and Bil 2004). Since solving the optimal forced landing problem using GA does not guarantee an optimal solution but are very close to the optimal solution the SQP technique was used to complement the results. The flight paths from the SQP optimisation method show very similar results, thus, indicating that it has successfully verified the results obtained using the GA method.

The analyses on the effects atmospheric and thermal disturbances have on forced landing show that the magnitude of the disturbance affects the forced landing flight paths significantly. The crosswinds from various speeds and directions change the aeroplane's flight trajectory and performance in some cases and degrade in others. It can be concluded that winds may change the character of the optimal trajectory and almost always affect the cost in either improving or degrading the performance.

The results from the forced landing trajectory analyses suggested a practical forced landing manoeuvre strategy in unknown atmospheric wind conditions. The suggested method is to fly the flight path for the worst atmospheric condition, which is the one with the worst downdraft. The suggested flying procedure is to arrive at the pre-selected location with minimal altitude lost and then circle to touchdown to the pre-selected landing location below. Any other more favourable atmospheric condition will simply require the aeroplane to fly more orbits to touchdown.

The results from the forced landing manoeuvre with obstacle suggested some flight paths that will land the airplane successfully at the pre-selected location and at the specified final heading. However, the touchdown distance error from the pre-selected location and the final heading error from the specified final heading depend on the pre-selected touchdown location and the location of the obstacle. It was found that larger distance error or final heading error tend to occur for obstacle placed closer to the pre-selected location. In some instances, the results present a trade off between touching down closer to the pre-selected location and touching down with a smaller final heading error.

9.3 Limitations of this Research

Like all research, several limitations do exist with the aircraft and atmospheric models used, the trajectory search and optimisation procedure developed and on the results obtained. These limitations will be examined in the following sections.

9.3.1 Limitations of Aircraft and Atmospheric Disturbance Models

The results obtained using a pure point mass model assumption lack the transients response to the flight trajectory since no moments are present. The analysis assumes constant speed (zero acceleration) and any changes in speed are assumed to be instantaneous.

Unfortunately, at present, there is no perfect atmospheric turbulence models or thermal distributions that are applicable to this particular research. Therefore, estimated atmospheric turbulence and thermal models were used for the trajectory optimisation analysis. The atmospheric disturbances effects were assumed to be of low frequency. The atmospheric disturbances frequency used was estimated using the phugoid period based on the aeroplane's stall speed.

Whilst the lack of accurate of models would slightly compensate for the results obtained for this research, the models used still represent reasonable expectations to the flight trajectories obtained. The models used can only possess a limited degree of fidelity and to completely verify the results, actual flight tests should be flown. However, some of the forced landing manoeuvres will never be flown since it is too dangerous or it is a manoeuvre for which flight-test data would be difficult if not impossible to obtain safely.

9.3.2 Limitations on the Trajectory Search Technique Used

The results generated by the GA analysis were carried out using a population size of four times the chromosome length. Better GA results could be obtained by using larger population size but at the expense of exponential growth in computational cost. Higher quality results can be obtained with additional objectives such as specific minimal touchdown speed and glide angle.

An increase in optimisation points in SQP may provide more accurate results. This optimisation method is dependent on the initial guesses used and there may be other solutions if different initial guesses were used. However, for the purpose of the problem considered for this study, which is to locate a practical flight trajectory to a forced landing after an engine failure, this does not pose an issue since educated guesses were used for the initial guesses.

9.3.3 Limitations on the Results Obtained

The feasibility of the results on the forced landing manoeuvre considered in this study is limited to the aircraft model, the type of vertical disturbance models and on the optimisation technique used. The results for the two very different types of vertical disturbances used: the timed averaged for the von Karman turbulence model and the thermal jump model, show that the forced landing trajectory depends considerably on the magnitude of the vertical velocity.

9.4 Further Work

As with every research, there can never seem to be an end to what else that can be researched upon. There are still some outstanding research that is of interest and relevance to this research topic. The following are some suggestions of further work that can be continued from here on:

1) The results obtained from any simulation are only as good as the model used in the simulation. An overly simplified model may not produce realistic results while and overly sophisticated model may not allow repeatability. In this study, the simple aircraft model used has yield feasible results. A more sophisticated rigid body aircraft model can be used to obtain more accurate results.

2) The effects of atmospheric disturbances are an important component in any flight simulations and for this study, the updrafts are always assumed to be less than the sink rate. Hence, the aircraft is always descending. A more realistic atmospheric disturbance model would be to have updrafts than can be greater than the aircraft's sink rate. An atmospheric model with variable frequencies will also allow the study on the effects different atmospheric disturbance frequencies have on a forced landing manoeuvre. The study on the effects wind has on a flight simulation may also include windshear, the effects of crosswinds with variable speeds and directions have on flight trajectory optimisation.

3) The search and optimisation objective for this study is to land closest to the pre-selected landing location and specified final heading. Additional objectives such as glide angle and velocity requirements may also be implemented in the search and optimisation procedure. The addition of more objectives will transform the current single/two objective optimisation problem into a multi-objective

optimisation and weighting factors may be used in the optimisation cost function. In the case of GA optimisation, multiple-pareto-optimality may be used to avoid comparison of different objective functions.

4) Another search method such as "A*" search algorithm which uses a heuristic estimate to be used to search for flight trajectories of an airplane after engine failure.

5) An issue in optimising non-linear functions or problems is that there may be more than one local minimum. Therefore, additional analysis maybe carried out to investigate how different initial guesses might affect the SQP optimisation results.

6) The problem considered in this study is on optimal landing manoeuvre to a pre-selected landing location, this problem can be extended to where is the best location to position an aeroplane given that there are a few known plausible landing locations at engine failure. An extension of such problem would be from a flight route planning point of view, "What is the best flight path to fly along any given route given that there are several possible safe-landing locations along the flight path?"

7) In the unfortunate event that a forced landing of an aeroplane may occur while flying over a suburban area or a well developed area with high-rise buildings. The aeroplane may also be required to land safely while avoiding obstacles. An extension of the current study may include optimisation of flight trajectories with several obstacles avoidance of various sizes and height.

8) The problem considered in this study is for an aeroplane with variable flying parameters to land at a fixed location on the ground. This problem may serve as a corner stone to an air combat pursuit-evasion problem by applying velocity and other flying parameters to the fixed touchdown location, hence, converting the fixed touchdown location into an evader allowing it to change role, whereby the evader may now become the pursuer. The focus of the research will then be, to gain better insight into the skills transfer of pilots' cognitive skills. The current work on the effects atmospheric disturbances have on the optimal flight trajectory

may also be used as the building block on the study of how uncertainties or artefacts such as delay may affect an air combat pursuit-evasion problem.

9.5 Potential Applications

The simple trajectory optimisation problem considered in this study has many potential avenues for development. The outcome from this study can be applied or form the basis to many practical aerospace problems. Two of which are suggested in the following sections.

9.5.1 Autopilot Systems

It is not uncommon for forced landings in both civil or military aviations to occur and the existence of better techniques or procedures to land an aeroplane after an engine failure will certainly increase the probability of a safer landing. Further understanding and development on the outcome of this study on a forced landing of an aeroplane after an engine failure can be implemented into the aeroplane's autopilot system, thereby, promoting higher chances of a safer landing. With the advanced of Global Positioning System (GPS) and faster computers, real-time simulation may be implemented into the auto-pilot system to constantly map out possible flight paths and to safely land an airplane upon engine failure. Such a system will certainly reduce the pilot's workload in case of emergency and increases the chances of a safe landing.

9.5.2 Pursuit-Evasion

The current study can also be used to form the basis to an air combat pursuit-evasion problem as recommended in Chapter 9.4 – Further Work.

A pursuit-evasion game is an intuitive notion indicating that one of the players, called the pursuer, is chasing and wants to capture the other, called the evader. Since, in application to combat aircrafts scenario, the gain of one player is the loss of the other, the game is called a zero-sum game and the theory applied is zero-sum pursuit-evasion game theory. This notion is well suited to, for example, an interception scenario, where the pay-off is the probability of destruction of a ballistic missile. The pursuer wants to maximise this pay-off and the evader wants to minimise it. Armed with the guidance law based on games theory, an interceptor would be provided with a set of equations covering all possibilities and generating a

gradually shortening list of end coordinates. By knowing exactly where its target must be at a certain point in time, the pursuer would have a vastly improved chance of homing in on its target. It could even ignore certain evasive actions by knowing that they would not affect the outcome. Current aircraft and cruise missile interceptors, like the Patriot, have only a limited ability to think ahead, generally being reduced to reacting after every manoeuvre and then playing catch-up. They rely purely on speed to get close to their targets and then detonate.

The model of a pursuit-evasion situation can be described by differential equations with the simplest version of two players when one of them wants to minimise some cost function while the other wants to maximise it. This is a two-person zero-sum Differential Game. Both players have perfect information on the state of the dynamic system jointly controlled by them and determine simultaneously their control strategies by mapping the available information into respective control actions. The players are not supposed to have any knowledge of the opponent's strategy or its current control action. The solution of a two-person zero-sum Differential Game is composed of three elements, the two optimal strategies (one for each player) and the outcome of the game when both players use these strategies, called the Value of the game. If the strategy of one player is known the Differential Game is degenerated and becomes an Optimal Control problem. Any Optimal Control problem with unknown bounded disturbances can be considered as a Differential Game against nature. The game solution provides not only the optimal control law, but also the worst disturbance and the guaranteed cost.

Thus, the Differential Game formulation introduces a more general viewpoint for the analysis of robust optimal control problems. Two well-known formulations of robust control methods, namely the min-max control (introduced in the late sixties) and the more recent H-infinity control (formulated in 1981) are in this category. A Pursuit-Evasion zero-sum differential game serves for many aerospace applications such as missile guidance, interception, collision avoidance and rendezvous. The Differential Game formulation can also be used in other aerospace control problems, such as take-off or landing in wind shear, re-entry to an uncertain atmosphere, and terrain following/avoidance.

9.6 Concluding Remarks

This research on transfer of training from flight simulators using the specific example of a forced landing of an aeroplane has expressed the importance of analyses of simulator

equipments. Regulatory authorities around the world are beginning to approve — or are considering the approval of — single engine gas turbine (SEGT) aircraft for regular public transport (RPT) operations. This will require the flight simulator industry to consider exploring the use of flight simulators for SEGT aircraft in RPT operations.

The analyses on trajectory optimisation as part of this study has contributed in the area of forced landing by suggesting a practical forced landing manoeuvre strategy. Further extensions on the current work will pave the way to many practical aerospace problems.

REFERENCES

Adams, J. A. (1979). On the Evaluations of Training Devices. *Human Factors,* 21 (6) pp. 711-720.

Ali, N. & Behdinan, K. (2002). Conceptual Aircraft Design - A Genetic Search and Optimization Approach. 23rd International Congress of Aeronautical Sciences (ICAS), Toronto, Canada, pp. 114.1-114.11.

Anderson, M. B. (1995). Potential of Genetic Algorithms for Subsonic Wing Design AIAA Paper 95-3925.

Anderson, M. B. (1996). Using Pareto Genetic Algorithms for Preliminary Subsonic Wing Design AIAA Paper 96-4023.

Anderson, M. B., Burkhalter, J. E. & Jenkins, R. M. (2000). Missile Aerodynamic Shape Optimization Using Genetic Algorithm. Journal of Spacecraft and Rockets, 37 (5) pp. 663-669.

Andrews, D. H., Edwards, B. J., Mattoon, J. S. & Thurman, R. A. (1996). Potential Modeling and Simulation Contributions to Specialized Undergraduate Pilot Training. Educational Technology, (July-August) pp. 6-15.

Anon (1980) "Flying Qualities of Piloted Airplanes". US Department of Defence, 5 November 1980, MIL-F-8785C.

Arho, R. (1972). Optimal Dolphin Soaring as a Variational Problem. ACTA Polytechnica Scandinavica ME, 68 pp. 1-17.

Asselin, M. (1997). An Introduction to Aircraft Performance, AIAA.

Baarspul, M. (1990). A Review of Flight Simulation Techniques. Progress in Aerospace Science, 27 (1) pp. 1-120.

Bailey, R. E., Knotts, L. H., Horowitz, S. J. & Malone, H. L. (1987). Effect of Time Delay on Manual Flight Control and Flying Qualities During In-Flight and Ground-Based Simulation. Montery, CA. AIAA Paper 87-2370.

Bakker, J. T. C. (1982). Effect of Control System Delays on Flying Qualities. Criteria for Handling Qualities of Military Aircraft, Fort Worth, Texas, pp. 19-1-19-3 AGARD.

Barnes, A. G. (1994). Modelling requirements in flight simulation. Aeronautical Journal, (December) pp. 395-404.

Beal, T. R. (1993). Digital Simulation of Atmospheric Turbulence for Dryden and von Karman Models. Journal of Guidance, Control, and Dynamics, 16 (1) pp. 132-138.

Benichou, P. & Santurette, P. (1998). Synergie as a Powerful Integrated Tool for Gliding Meteorology. Technical Soaring, XXII (no. 4 October) pp. 107-111.

Berkmann, P. & Pesch, H. J. (1995). Abort Landing of an Airplane under Different Windshear Conditions: An Optimal Control Problem with a Third-Order State Constraint and a Multifarious Switching Structure. Journal of Optimization Theory & Applications, 85 (1) pp. 21-57.

Berry, D. T., Powers, B. G., Szalai, K. J. & Wilson, R. J. (1982). In-Flight Evaluation of Control Systems Pure Delay Time Delays. Journal of Aircraft, 19 (4) pp. 318-323.

Betts, J. T. & Huffman, W. P. (1992). Application of Sparse Nonlinear Programming to Trajectory Optimization. Journal of Guidance, Control, and Dynamics, 15 (1) pp. 198-206.

Betts, J. T. & Huffman, W. P. (1993). Path-Constraint Trajectory Optimization Using Sparse Sequential Quadratic Programming. Journal of Guidance, Control, and Dynamics, 16 (1) pp. 59-68.

Betts, J. T. (1998). Survey of Numerical Methods for Trajectory Optimization. Journal of Guidance, Control, and Dynamics, 21 (2) pp. 193-207.

Blasi, L., Iuspa, L. & Core, G. D. (2000). Conceptual Aircraft Design Based on a Multiconstraint Genetic Optimizer. Journal of Aircraft, 37 (2) pp. 350-354.

Bramlette, M. & Cusic, R. (1989). A Comparative Evaluation of Search Methods Applied to the Parametric Design of Aircraft. Proceedings of the Third International Conference on Genetic Algorithms, San Mateo, CA, pp. 213-218.

Bramson, A. F. (1982). Glide, flapless and other abnormal landings, Martin Dunitz Ltd, London.

Brigger, P. (1995). Optimization of Structuring Elements by Genetic Algorithms. http://ltswww.epfl.ch/pub_files/brigger/thesis_html/node56.html.

Brinkman, K. & Visser, H. G. (2007). *Optimal Turn-Back Maneuver after Engine Failure in a Single-Engine Aircraft during Climb-Out*. 45th AIAA Aerospace Sciences Meeting and Exhibit. Reno, Nevada. AIAA Paper 2007-252.

Brown, A. D. (1971) "Category 2 - A simulation Study of Low Visibility Approaches and Landings at Night". Royal Aircraft Establishment, March 1971, Technical Report 71044, pp. 1-69.

Bulirsch, R., Montrone, F. & Pesch, H. J. (1991). Abort Landing in the Presence of Windshear as a Minimax Optimal Control Problem, Part 1: Necessary Conditions. Journal of Optimization Theory & Applications, 70 (1) pp. 1-23.

Bulirsch, R., Montrone, F. & Pesch, H. J. (1991). Abort Landing in the Presence of Windshear as a Minimax Optimal Control Problem, Part 2: Multiple Shooting and Homotopy. Journal of Optimization Theory & Applications, 70 (2) pp. 223-254.

Cochrane, J. H. (1999). MacCready theory with uncertain lift and limited altitude. Technical Soaring, XXIII (no. 3 , July) pp. 88-96.

Conklin, J. E. (1957). Effect of Control Lag on Performance in a Tracking Task. Journal of Experimental Psychology, 53 (4) pp. 261-268.

Cooper, G. E. & Harper, R. P. (1969). The Use of Pilot Rating in the Evaluation of Aircraft Handling Qualities. AGARD.

Crossley, W. A. & Laananen, D. H. (1996). Conceptual Design of Helicopters via Genetic Algorithm. Journal of Aircraft, 33 (6) pp. 1062-1070.

Crossley, W. A., Cook, A. M. & Fanjoy, D. W. (1999). Using the Two-Branch Tournament Genetic Algorithm for Multiobjective Design. Journal of Aircraft, 37 (2) pp. 261-267.

Dumas, J. D., II & Klee, H. I. (1996). Design, Simulation, and Experiments on the Delay Compensation for a Vehicle Simulator. Transactions, 13 (3) pp. 155-167.

Eckalbar, J. C. (1992). The Optimum Turn. Newsletter of the American Bonanza Society. 92 pp. 3037,3038,3044.

Edwards, A. (1983). A Stochastic Cross-country or Festina Lente. Australian Gliding pp. 16-18.

Erkelens, L. J. J. (1988) "Flight Simulations on MLS-Guided Interception Procedures and Curved Approach Path Parameters". National Aerospace Laboratory NLR, The Netherlands, NLR MP 88035 U, pp. 1-14.

Erzberger, H. & Lee, H. Q. (1971). Optimum Horizontal Guidance Techniques for Aircraft. Journal of Aircraft, 8 (2) pp. 95-101.

Eshelman, L. J. & Schaffer, J. D. (1991). Preventing Premature Convergence in Genetic Algorithms by Preventing Incest. Proceedings of the Fourth International Conference on Genetic Algorithms, University of California at San Diego, San Diego, California, USA, pp. 115-122.

Eshelman, L. J. & Schaffer, J. D. (1993). Crossover's Niche. Proceedings of the Fifth International Conference on Genetic Algorithms, University of Illinois at Urbana-Champaign, Urbana, Illinois, USA, pp. 9-14.

Etkin, B. (1981). Turbulence Wind and Its Effect on Flight. Journal of Aircraft, 18 (15) pp. 327-345.

Fan, Y., Lutze, F. H. & Cliff, E. M. (1995). Time-Optimal Lateral Maneuvers of an Aircraft. Journal of Guidance, Control, and Dynamics, 18 (5) pp. 1106-1112.

Farrow, D. R. (1982). Reducing The Risks Of Military Aircrew Training Through Simulation Technology. NSPI Journal, (March) pp. 13-15.

Filho, J. L. R. & Treleavan, P. C. (1994). Genetic-Algorithm Programming Environments. Membership Magazine of the IEEE Computer Society, (June) pp. 29-43.

Firebaugh, J. M. (1967). Evaluations of a Spectral Gust Model Using VGH and V-G Flight Data. Journal of Aircraft, 4 (6) pp. 518-525.

Fletcher, R. (1980). Unconstrained Optimization, John Wiley and Sons.

Frank, L. H., Casali, J. G. & Wierwille, W. W. (1988). Effects of Visual Display and Motion System Delays on Operator Performance and Uneasiness in a Driving Simulator. Human Factors, 30 (2) pp. 201-217.

Frost, W. & Reddy, K. R. (1978) "Investigation of Aircraft Landing in Variable Wind Fields". NASA, December 1978, NASA Contract Report 3073, pp. 1-84.

Fukada, Y. (2000). Speed to Fly With Management of the Risk of Landing Out. Technical Soaring, XXV (no. 3 July) pp. 88-94.

Gage, P. & Kroo, I. (1993). A Role of Genetic Algorithms in a Preliminary Design Environment AIAA Paper 93-3933.

Galanis, G., Jennings, A. & Beckett, P. (1997). Towards a General Model of Perception for Simulation. SimTecT 97, Canberra, Australia.

Galanis, G., Jennings, A. & Beckett, P. (1998). A Mathematical Model of glide slope Perception in the Visual Approach to Landing. The International Journal of Aviation Psychology, 8 (2) pp. 83-101.

Gath, P. F. & Well, K. H. (2001). Trajectory Optimization using a Combination of Direct Multiple Shooting and Collocation. AIAA Guidance, Navigation, Control Conference and Exhibit. Montreal, Canada. AIAA Paper 01-37026.

Gedeon, J. (1972). Dynamic Analysis of Dolphin-Style Thermal Cross-Country Flight. OSTIV Publications.

Gedeon, J. (1996). Instationary Stochastic Modeling of Thermals. Technical Soaring, XX (1) pp. 11-15.

Gerlach, O. H., Bray, R. S., Covelli, D., Czinczenheim, J., Hass, R., Lean, D. & Schmidtlein, D. (1975). Approach and Landing Simulation. AGARD.

Gill, P. E., Murray, W. & Saunders, M. A. (1994). Large-scale SQP Methods and Their Applications in trajectory Optimisation. Computational Optimal Contr. R. Bulirsch and D. Kraft. Basel, Germany, pp. 29-42.

Gill, P. E., W.Murray & Wright, M. H. (1981). Practical Optimization, London, Academic Press,.

Gill, P. E., W.Murray & Wright, M. H. (1986) "User's guide for NPSOL (Version 4.0)". Department of Operation Research, Standford University, Stanford, CA, Report SOL 86-2.

Gillespie, A. J. & Handley, S. J. (1996). Development of a Real-time Simulation of a VSTOL Aircraft. Aeronautical Journal, (November) pp. 397-405.

Goldberg, D. E. (1985) "Optimal Initial Population Size for Binary-Coded Genetic Algorithms". The Clearing House for Genetic Algorithms, The University of Alabama, Tuscaloosa, Al., Alabama, November 1985, TCGA Report No. 85001, pp. 1-14.

Goldberg, D. E. (1989). Genetic Algorithms in Search, Optimization, and Machine Learning, Addison-Wesley Publishing Company Inc.

Gopher, D., Weil, M. & Bareket, T. (1992). The Transfer of Skill from a Computer Game Transfer to Actual Flight. Proceedings of the Human Factors Society 36th Annual Meeting 1992, pp. 1285-1290.

Grefenstette, J. J. (1986). Optimization of Control Parameters for Genetic Algorithms. IEEE Transactions on Systems, Man, and Cybernetics, SMC-16 (1) pp. 122-128.

Gum, D. R. & Albery, W. B. (1977). Time-Delay Problems Encountered in Integrating the Advanced Simulator for Undergraduate Pilot Training. Journal of Aircraft, 14 (4) pp. 327-332.

Gum, D. R. & Martin, E. A. (1987). The Flight Simulator Time Delay Problem. AIAA Simulation Technology Conference. Montery, CA. AIAA Paper 87-2369.

Hahn, K.-U., Heintsch, T., Kaufmann, B., Schanzer, G. & Swolinsky, M. (1990). Effect of Wind and Wind Variation on Aircraft Flight - Paths. AGARDograph No. 301 Aircraft Trajectories Computation - Prediction - Control, pp. 6-1-6-22.

Hahn, K.-U., Heintsch, T., Kaufmann, B., Schanzer, G. & Swolinsky, M. (1990). Wind Models for Flight Simulation. AGARDograph No. 301 Aircraft Trajectories Computation - Prediction - Control, pp. 9-1-9-32.

Hajela, P. (1990). Genetic Search - An Approach to the Nonconvex Optimization Problem. AIAA Journal, 28 (7) pp. 1205-1210.

Hargaves, C. R. & Paris, S. W. (1987). Direct Trajectory Optimization Using Nonlinear Programming and Collocation. Journal of Guidance, Control, and Dynamics, 10 (4) pp. 338-342.

Haupt, R. L. & Haupt, S. E. (1998). Practical Genetic Algorithms, John Wiley & Sons, Inc.

Hedrick, J. K. & Arthur E. Bryson, J. (1971). Minimum Time Turns for a Supersonic Airplane at Constant Altitude. Journal of Aircraft, 8 (3) pp. 182-187.

Hedrick, J. K. & Arthur E. Bryson, J. (1972). Three-Dimensional, Minimum-Time Turns for a Supersonic Aircraft. Journal of Aircraft, 9 (2) pp. 115-121.

Heise, R. (1999). Future Aspects of Meteorology Support for Competition Flights. Technical Soaring, XXII (no. 1 January) pp. 13-16.

Hess, R. A. (1984). Effects of Time Delay on Systems Subject to Manual Control. Journal of Guidance, Control, and Dynamics, 7 (7) pp. 416-421.

Heymann, V. I. & Ben-Asher, J. Z. (1997). Aircraft Trajectory Optimization in the Horizontal Plane. Journal of Guidance, Control, and Dynamics, 20 (6) pp. 1271-1274.

Hill, R. R., McIntyre, G. A. & Narayanan, S. (2002). Genetic Algorithms for Model Optimization. SimTect 2002, Melbourne, Australia, pp. 133-138.

Hock, W. & K. Schittkowski (1983). Comparative Performance Evaluation of 27 Nonlinear Programming Codes. Computing, 30 pp. 335.

Hoffren, J. & Raivio, T. (2000). Optimal Maneuvering After Engine Failure. AIAA Proceedings of the Atmospheric Flight Mechanics Conference. Denver, Colorado. AIAA Paper 2000-3992.

Holland, J. H. (1975). Adaptation in Natural and Artificial Systems: An introduction Analysis with Applications to Biology, Control, and Artificial Intelligence, Ann Arbor, The University of Michigan Press.

Horowitz, S. J. (1987) "Measurement and Effects of Transport Delays in a State-of-the-Art F-16C flight Simulator". Operations Training division, Williams Air Force Base, Arizona, September 1987, AFHRL-TP-87-11, pp. 1-11.

Houbolt, J. C. (1973). Atmospheric Turbulence. AIAA Journal, 11 (4) pp. 421-437.

Houghton, E. L. & Brock, A. E. (1960). Aerodynamics for Engineering Students, London, edward Arnold (Publishers) Ltd.

Howe, R. M. (1990). Some Methods for Reducing Time Delays in Flight Simulations. AIAA Flight Simulation Technologies Conference AIAA Paper 90-3154.

ICAO (1995) "Manual of Criteria for the Qualification of Flight Simulators". International Civil Aviation Organization, Doc 9625-AN/938, pp. 27- 45.

Irving, F. (1999). The Paths of Soaring Flight, Imprerial College Press.

Jacobson, I. D. & Joshi, D. S. (1978). Handling Qualities of Aircraft in the Presence of Simulated Turbulence. Journal of Aircraft, 15 (4) pp. 254-256.

Jardin, M. R. & Arthur E. Bryson, J. (2001). Neighboring Optimal Aircraft Guidance in Winds. Journal of Guidance, Control, and Dynamics, 24 (4) pp. 710-715.

Jett, B. W. (1982). *The Feasibility of Turnback from a Low Altitude Engine Failure During the Takeoff Climb-out Phase*. AIAA 20th Aerospace Sciences Meeting. Orlando, FL. AIAA paper 82-0406.

Johns, L. (1988). A Study of the Effects of Delay Times in a Dome-To-Dome Simulation Link. AIAA Flight Simulation Technologies Conference, Atlanta, Georgia, pp. 122-127.

Johnson, R. H. (1978). Measurements of Sailplane Sink Rates Between Thermals. OSTIV Publications, XV.

Karatas, T. & Bullo, F. (2001). Randomized searches and nonlinear programming in trajectory planning. IEEE Conference on Decision and Control, Orlando, Florida.

Katz, A. (1991). Why Simulators are More Difficult to Fly Than Aircraft. SAE (Society of Automotive Engineers) Transactions, 100 (i Sect pt. 2) pp. 2331-2336.

Kindemann, C. & Asseng, J. (1998). Geographical Signatures for Thermal Convection Climatology. Technical Soaring, XXIi (no. 3 July) pp. 81-86.

Kishi, F. H. & Pfeffer, I. (1971). Approach Guidance to Circular Flight Paths. Journal of Aircraft, 8 (2) pp. 89-95.

Konovalov, D. A. (1970). On the Structure of Thermals. OSTIV Publications, XI.

Lampton, D. R., Kolasinski, E. M., Knerr, B. W., Bliss, J. P., Bailey, J. H. & Witmer, B. G. (1994). Side Effect and After Effects of Immersion in Virtual Environments. Proceedings of the Human Factors and Ergonomics Society 38th Annual Meeting 1994, pp. 1154-1157.

Lappe, U. O. (1966). Low-Altitude Turbulence Model for Estimating Gust Loads on Aircraft. Journal of Aircraft, 3 (1) pp. 41-47.

Lefebvre, M. (1998). A Bidimensional Optimal Landing Problem. Automatica, 34 (5) pp. 655-657.

Levison, W. H. & Papazian, B. (1987). The Effects of Time Delay and Simulator Mode on Closed-Loop Pilot/Vehicle Performance: Model Analysis and Manned Simulation Results. AIAA Simulation Technology Conference. Montery, CA. AIAA Paper 87-2371.

Liechti, O. & lorenzen, E. (1998). A New Approach to the Climatology of Convective Activity. Technical Soaring, XXII (no. 2 April) pp. 36-40.

Liechti, O. & Neininger, B. (1994). ALPTHERM - A PC-Based Model for Atmospheric Convection Over Complex Topography. Technical Soaring, XVIII (no. 3 July) pp. 73-78.

Lintern, G. (1991). An Informational Perspective on skill Transfer in Human-Machine Systems. Human Factors, 33 (3) pp. 251-266.

Lintern, G. (1992). Flight Simulation for the Study of Skill Transfer. Simulation/Games for Learning, 22 (4) pp. 336-349.

Lintern, G. (1999). Human Performance Research for Virtual Training Environments. SimTecT 99, pp. 239-244.

Lintern, G., Roscoe, S. N. & Sivier, J. E. (1990). Display Principles, Control Dynamics, and Environmental Factors in Pilot Training and Transfer. Human Factors, 32 (3) pp. 299-317.

Lintern, G., Roscoe, S. N., Koonce, J. M. & Segal, L. D. (1990). Transfer of Landing Skills in Beginning Flight Training. Human Factors, 32 (3) pp. 319-327.

Lu, P. & Khan, M. A. (1994). Nonsmooth Trajectory Optimization: An Approach Using Continuous Simulated Annealing. Journal of Guidance, Control, and Dynamics, 17 (4) pp. 685-691.

Lu, P. (1993). Inverse Dynamics Approach to Trajectory Optimization for an Aerospace Plane. Journal of Guidance, Control, and Dynamics, 16 (4).

Malone, H. L., Horowitz, S., Brunderman, J. A. & Eulenbach, H. (1987). The impact of network delay on two-ship air-to-air combat simulation. AIAA Flight Simulation Technologies Conference. New York, NY. AIAA Paper 87-2373.

Mason, R. P. & Eichner, R. B. (1996). U.S. Navy Refresher Physiology Training in Aircraft Simulators: A Case Study. Proceedings - Annual Symposium (Survivals and Flight), pp. 283-286.

Mathar, R. (1996). Stochastic Models of Thermal Convection: An Extended McCready Theory and a Simulation Tool. Technical Soaring, XX (4) pp. 113-117.

Matranga, G. J. & Armstrong, N. A. (1959). Approach and Landing Investigation at Lift-Drag Ratios of 2 to 4 Utilizing a Straight-Wing Fighter Airplane. NASA-TM-X-31 pp. 1-21.

Mattoon, J. S. (1996). Modeling and Simulation: A Rationale for Implementing New Training Technologies. Educational Technologies, (July-August) pp. 17-26.

McMinn, J. D. (1997). Extension of a Kolmogorov Atmospheric Turbulence Model for Time-Based Simulation Implementation. AIAA Guidance, Navigation and Control Conference. New Orleans, Louisiana, USA. AIAA 97-3532.

Menhaj, M. B. & Hagan, M. T. (1994). Analysis of Delays in Networked Flight Simulators. IEEE Transactions on Systems, Man, and Cybernetics, 24 (6) pp. 875-880.

Merriken, M. S., Johnson, W. V., Cress, J. D. & Riccio, G. E. (1988). Time Delay Compensation Using Supplementary Cues in Aircraft Simulator Systems. AIAA Flight Simulation Technologies Conference. New York. AIAA Paper 88-4626.

Metzger, D. E. & Hedrick, J. K. (1975). Optimal Flight Paths for Soaring Flight. Journal of Aircraft, 12 (11) pp. 867-871.

Michalewicz, Z. (1996). Genetic Algorithms + Data Structure = Evolution Programs, Springer-Verlag.

Middendorf, M. S. & Fiorita, A. I. (1991). The Effects of Simulator Transport Delay on Performance, Workload, and Control Activity During Low Level Flight. AIAA Flight Simulation Technologies Conference. New York. AIAA Paper 91-2965.

Miele, A. (1990). Optimal Trajectories of Aircraft and Spacraft. AGARDograph No. 301 Aircraft Trajectories Computation - Prediction - Control, pp. 2-1-2-56.

Miele, A., Wang, T., Tzeng, C. Y. & Melvin, W. W. (1987). Optimal Abort Landing Trajectories in the Presence of Windshear. Journal of Optimization Theory and Applications, 55 (2) pp. 165-202.

Milford, J. R. (1972). Some Thermal Sections Shown by an Instrumented Glider. 13th OSTIV Congress, Vrsac, Yugoslavia.

Newman, D. M. & Wong, K. C. (1993) "Six Degree of Freedom Flight Dynamic and Performance Simulation of a Remotely-Piloted Vehicle". The University of Sydney, Sydney, June 1993, Aero. Tech. Note 9301, pp. 22-27.

Obata, A. (1972). A Fundamental Study on Safe Landing. Vol. 37, No. 8 (ISAS Report no. 482) pp. 211-262.

Obayashi, S. & Yamaguchi, Y. (1997). Multiobjective Genetic Algorithm for Multidisciplinary Design of Transonic Wing Planform. Journal of Aircraft, 34 (5) pp. 690-693.

Obayashi, S. (1998). Pareto Genetic Algorithm for Aerodynamic Design Using the Navier-Stokes Equations. Genetic Algorithms and Evolution Strategy in Engineering and Computer Science Recent Advances and Industrial Applications. D. Quagliarella, J. Periaux, C. Poloni and G. Winter. New York, John Wiley & Sons Ltd., pp. 245-266.

Obitko, M. (1998). Introduction to Genetic Algorithms. http://cs.felk.cvut.cz/~xobitko/ga/.

Ohta, H. (1982). Analysis of Minimum Noise Landing Approach Trajectory. Journal of Guidance, Control, and Dynamics, 5 (3) pp. 263-269.

Oldaker, I. (1996). Pilot Decision Making - an Alternative to Judgement Training. Technical Soaring, XX (2) pp. 36-41.

Orlansky, J. & String, J. (1980). Reaping the Benefits of Flight Simulation. Defense Management Journal, (Fourth Quarter).

Pamadi, B. N. (1998). Performance, Stability, Dynamics, and Control of Airplanes, Virginia, AIAA.

Pierson, B. L. (1985). Optimal Aircraft Landing - Approach Trajectories: A comparison of Two Dynamics Models. Control Applications of Nonlinear Programming and Optimization. Proceedings of the Fifth IFAC Workshop, Capri, Italy. IFAC, pp. 139-145 Pergamon.

Pouliot, N. A., Gosselin, C. M. & Nahon, M. A. (1988). Motion Simulation Capabilities of Three-Degree-of-Freedom Flight Simulators. Journal of Aircraft, 35 (1) pp. 9-17.

Powell, M. J. D. (1978). The convergence of variable metric methods for nonlinearly constrained optimization calculations. Nonlinear Programming 3. O. L. Mangasarian, Meyer, R. R., Robinson, S. M., Academic Press.

Quast, A. (1965). Computer Calculations on Optimum Rate of Climb. OSTIV Publications, IX.

Rader, J. E. & Hull, D. G. (1975). Computation of Optimal Aircraft Trajectories Using Parameter Optimization Methods. Journal of Aircraft, 12 (11) pp. 864-866.

Raivio, T., Ehtamo, H. & Hämäläinen, R. P. (1996). Aircraft Trajectory Optimization Using Nonlinear Programming. System Modeling and Optimization. London, UK, Chapman & Hall.

Raivio, T., Virtanen, K., Ehtamo, H. & Hämäläinen, R. P. (1998). Microcomputer simulation of optimal flight paths. Proceedings of the EUROSIM'98 Simulation Congress, Espoo, Finland, pp. 288-289.

Ray, P. A. (1999). Quality Flight Simulation Proper and Improper Applications. Can Flight Simulation Do Everything? Flight Simulation Capabilities, Capability Gaps and Ways to Fill the Gaps, London, UK, pp. 14.1-14.11.

Reardon, K. A., Oliver, C. G. & Warren, R. (1987). Flight Simulation Training Using Standard and non-Standard Tasks. Proceedings of the Human Factors Society - 31st Annual Meeting 1987, pp. 1291-1295.

Ricard, G. L. & Harris, W. T. (1978). Time Delays in Flight Simulators Behaviour and Engineering Analyses. AIAA Simulation Technologies Conference AIAA Paper 78-1596.

Ricard, G. L. & Harris, W. T. (1980). Lead/Lag Dynamics to Compensate for Display Delays. Journal of Aircraft, 17 (3) pp. 212-217.

Ricard, G. L. (1994). Manual Control with Delays: A Bibliography. Computer Graphics, 28 (2 May) pp. 149-154.

Ricard, G. L. (1995). Acquisition of Control Skill with Delayed and Compensated Displays. Human Factors, 37 (3 September) pp. 652-658.

Riccio, G. E., Cress, J. D. & Johnson, W. V. (1987). The Effects of Simulator Delays on the Acquisition of Flight Control Skills: Control of Heading and Altitude. Proceedings of the Human Factors Society - 31st Annual Meeting 1987, pp. 1286-1290.

Ringertz, U. (2000). Flight Testing an Optimal Trajectory for the Saab J35 Draken. Journal of Aircraft, 37 (1) pp. 187-189.

Ringertz, U. (2000). Optimal Trajectory for a Minimum Fuel Turn. Journal of Aircraft, 37 (5) pp. 932-934.

Rogers, D. F. (1995). Possible "Impossible" Turn. Journal of Aircraft, 32 (2) pp. 392-397.

Sasaki, D., Obayashi, S. & Nakahashi, K. (2002). Navier-Stokes Optimization of Supersonic Wings with Four Objectives Using Evolutionary Algorithm. Journal of Aircraft, 39 (4) pp. 621-629.

Schanzer, G. (1989). Influence of Windshear, Downdraft and Turbulence on Flight Safety. Agard Conference Proceedings No. 470 - Flight in Adverse Environment Conditions, pp. 7-1-7-19 AGARD.

Schiff, B. J. (1985). The Proficient Pilot, New York, MacMillan.

Schittkowski, K. (1985). NLQPL: A FORTRAN-Subroutine Solving Constrained Nonlinear Programming Problems. Annals of Operations Research, 5 pp. 485-500.

Schoonover, P. L., Crossley, W. A. & Heister, S. D. (2000). Application of a Genetic Algorithm to the Optimization of Hybrid Rockets. Journal of Spacecraft and Rockets, 37 (5) pp. 622-629.

Schultz, R. L. & Zagalsky, N. R. (1972). Aircraft Performance Optimization. Journal of Aircraft, 9 (2) pp. 108-114.

Semonov, A. (1993). Numerical Optimization of Aircraft Trajectories in the Presence of Windshear. International Aerospace Planes and Hypersonics Technologies Conference, Germany, pp. 1-5 American Institute of Aeronautics and Astronautics, Inc.

Seywald, H., Cliff, E. M. & Well, K. H. (1994). Range Optimal Trajectories for an Aircraft Flying in the Vertical Plane. Journal of Guidance, Control, and Dynamics, 17 (2) pp. 389-398.

Sheu, D., Chen, Y. M. & Chang, Y.-J. (1998). Optimal Glide for Maximum Range. AIAA Atmospheric Flight Mechanics Conference and Exhibit. Boston, MA. AIAA Paper 98-4462.

Shevell, R. S. (1989). Fundamentals of Flight, New Jersey, Prentice-Hall, Inc.

Smith, R. E. & Bailey, R. E. (1982). Effect of Control System Delays on Fighter Flying Qualities. Criteria for Handling Qualities of Military Aircraft, Fort Worth, Texas, pp. 18-1-18-10 AGARD.

Smith, R. E. & Sarrafian, S. K. (1986). Effect of Time Delay on Flying Qualities: An Update. Journal of Guidance, Controls, and Dynamics, 9 (5) pp. 578-584.

Smith, R. M. (1991). A Method for Determining Transport Delays in the Flight Simulation Environment. AIAA Flight Simulation Technologies Conference. New Orleans, Lousiana. AIAA Paper 91-2964.

Smith, R. M. (1992). Reducing Transport Delay Through Improvements in Real-Time Program Flow. Flight Simulation Technologies Conference. South Carolina. AIAA Paper 92-4147.

Spellucci, P. (1993). Numerische Verfahren der nichtlinearen Optimierung, Birkhäuser.

Srinivas, M. (1994). Genetic Algorithms: A Survey. Membership Magazine of the IEEE Computer Society, (June) pp. 17-26.

Stark, E. A. (1989). Simulation. Aviation Psychology. R. S. Jensen. Ohio, Gower Publishing Company, pp. 109-153.

Stephens, C. & Seymour, M. (1999). Emergencies and Failures - How Well Can Simulation Train for Them. Can Flight Simulation Do Everything? Flight Simulation Capabilities, Capability Gaps and Ways to Fill the Gaps, London, UK, pp. 7.1-7.8.

Stewart, E. C. (1998). A Piloted Simulation Study of Wake Turbulence on Final Approach. AIAA Atmospheric Flight Mechanics Conference and Exhibit. Boston, MA. AIAA Paper 98-4339.

Stewart-Smith, J. (1999). Forced landings in light aircraft-the "constant aspect" approach. Flight Safety Bulletin. XXXV pp. 5-11.

Stoer, J. (1985). Foundations of recursive quadratic programming methods for solving nonlinear programs. Computational Mathematical Programming. K. Schittkowski, Springer. 15.

Syswerda, G. (1989). Uniform Crossover in Genetic Algorithms. Proceedings of the Third International Conference on Genetic Algorithms, George Mason University, Fairfax, VA, USA, pp. 2-9.

Teunissen, C. R. P. A. M. (1999). The Future of Simulation and Training. Can Flight Simulation Do Everything? Flight Simulation Capabilities, Capability Gaps and Ways to Fill the Gaps, London, UK, pp. 6.1-6.11 The Royal Aeronautical Society.

Thom, T. (1987). The Forced Landing Without Power. Private Pilot Flying Training Guide for the Student Pilot. Victoria, Australia, Aviation Theory Centre, pp. 17a-3 17c-3.

Thom, T. (1997). The Air Pilot's Manual, England, Airlife Publishing Ltd.

Tong, P. & Galanis, G. (2001). Simulator Requirements for Optimal Training of Pilots for Forced Landings. SimTecT 2001, Canberra, pp. 331-335.

Tong, P., Bil, C. & Galanis, G. (2003). The Effect of Vertical Atmospheric Turbulence Velocity on the Sensitivity Analysis to a Forced Landing Manoeuvre. Second MIT Conference on Computational Fluid and Solid Mechanics, Cambridge, Massachusetts.

Tong, P., Galanis, G. & Bil, C. (2003). Sensitivity Analysis to a Forced Landing Manoeuvre. Journal of Aircraft, 40 (1) pp. 208-210.

Tong, S. S. & Gregory, B. A. (1990). Turbine Preliminary Design Using Artificial Intelligence and Numerical Optimization Techniques ASME Paper 90-GT148.

Vinh, N. X. (1981). Optimal Trajectories in Atmospheric Flight, Elsevier Scientific Publishing Company.

Virtanen, K., Ehtamo, H., Raivio, T. & Hämäläinen, R. P. (1997). VIATO - Visual Interactive Aircraft Trajectory Optimization. IEEE International Conference on Systems, Man and Cybernetics, Orlando, Florida, USA, pp. 2280-2285.

Virtanen, K., Ehtamo, H., Raivio, T. & Hämäläinen, R. P. (1999). VIATO - Visual Interactive Aircraft Trajectory Optimization. IEEE Transactions on Systems, Man, and Cybernetics, Part C: Applications and Reviews, 29 (3) pp. 409-421.

Visser, H. G. & Wijnen, R. A. A. (2001). Optimization of Noise Abatement Arrival Trajectories. AIAA Guidance, Navigation, Control Conference and Exhibit. Montreal, Canada. AIAA Paper 2001-4222.

Visser, H. G. & Wijnen, R. A. A. (2001). Optimization of Noise Abatement Departure Trajectories. Journal of Aircraft, 38 (4) pp. 620-627.

Visser, H. G. (1994). Optimal Lateral-Escape Maneuvers for Microburst Encounters During Final Approach. Journal of Guidance, Control, and Dynamics, 17 (6) pp. 1234-1240.

Wang, J. (1997). Practical Forecasting of Thermal Soaring Weather. Technical Soaring, XXI (no. 1 January) pp. 27-32.

Whiteley, J. D. & Lusk, S. L. (1990). The Effects of Simulator Time Delays on a Sidestep Landing Maneuver: A Preliminary Investigation. Proceedings of the Human Factors Society 34th Annual Meeting 1990, pp. 1538-1541.

Williams, E. A. & Crossley, W. A. (1998). Empirically-Derived Population Size and Mutation Rate Guidelines for a Genetic Algorithm with Uniform Crossover. Soft Computing in Engineering Design and Manufacturing. P. K. Chawdhry, R.Roy and R. K. Pant. Berlin, Springer-Verlag, pp. 163-172.

Wu, S.-F. & Guo, S.-F. (1994). Optimum Flight Trajectory Guidance Based on Total Energy Control of Trajectory. Journal of Guidance, Control, and Dynamics, 17 (2) pp. 291-296.

Yakimenko, O. A. & Kaminer, I. L. (1999). Near- Optimal Trajectory Generation for Autonomous Aircraft Landing. Proceedings of the 1999 IEEE International Symposium on Computer Aided Control System Design, Kohala Coast-Island of Hawaii, USA, pp. 445-450.

Yakimenko, O. A. (2000). Direct Method for Rapid Prototyping of Near-Optimal Aircraft Trajectories. Journal of Guidance, Control, and Dynamics, 23 (5) pp. 865-875.

Yokoyama, N. (2002). Trajectory Optimization of Space Plane Using Genetic Algorithm Combined with Gradient Method. ICAS 2002 23rd International Congress of Aeronautical Sciences, Toronto, Canada, pp. 513.1-513.10.

APPENDIX A

CONTROL PARAMETERS SELECTION FOR REAL-VALUE ENCODING IN GA

A.1 Test Problems

The test problems used in this analysis represent simple two-dimensional, uni-modal problems with increasing number of state variables and complexity levels to multi-modal functions. These particular test problems were selected to allow direct comparisons between the control parameters for real value encoding and binary encoding as carried out by (Williams and Crossley 1998). The GA chromosomes are represented by a vector $\vec{x} = (x_1, \ldots x_n)$, where n is the chromosome length. The chromosome length (l) is equivalent to the number of variables used to represent the domain. Each gene, (x_k), in the chromosome is bounded by an upper limit (x_{max}) and a lower limit (x_{min}) specific to the gene.

Test problem 1 is a smooth, convex function with continuous derivatives which represents the "banana function" because of its distinctive geometry, can be described as minimising:

$$f(x) = 10x_1^4 - 20x_1^2 x_2 + 10x_2^2 + x_1^2 - 2x_1 + 5 \qquad \text{(A-1)}$$

The two variables, x_1 and x_2, that range from – 4 to +12 were encoded as two real values with chromosome length of 2.

Test problem 2 is a two-dimensional, multi-modal "egg-crate" problem, which is a difficult problem to solve using calculus-based methods. The function can be described as minimising:

$$f(x) = x_1^2 + x_2^2 + 25\left(\sin^2 x_1 + \sin^2 x_2\right) \qquad \text{(A-2)}$$

The two variables, x_1 and x_2, that range from $-\pi$ to $+\pi$ were encoded as two real values with chromosome length of 2.

Test problem 3 is a six-dimensional Rosenbrock's function which was chosen for the increased number of variables and to intensify the complexity to the problems tested. The function can be described as minimising:

$$f(x) = \sum_{i=1}^{5}\left[100\left(x_{i+1} - x_i^2\right)^2 + \left(1 - x_i\right)^2\right] \qquad \text{(A-3)}$$

The six variables, x_1, …, x_6, that range from –20 to +20 were encoded as six real values with chromosome length of 6.

Test problem 4 is a four-dimensional Griewank's function, which was chosen to represent a non-linear and multi-modal problem and to increase the complexity level of the problems tested. The function can be described as minimising:

$$f(x) = \sum_{i=1}^{4} \frac{x_i^{\,2}}{200} + \prod_{i=1}^{4} \cos\left(\frac{x_i}{\sqrt{i}}\right) + 1 \qquad \text{(A-4)}$$

The four variables, x_1, …, x_4, that range from –10 to +10 were encoded as four real values with chromosome length of 4.

The GA control parameter selection as shown in Table A.1 was carried out for an elitism of 10% of the population size. The actual population size based on the multiples of chromosome lengths tested may be adjusted, if necessary, to ensure that an even number of chromosomes were available for the crossover process since some chromosomes were kept for elitism. The GA in this analysis used three types of mutation (uniform mutation, boundary mutation, non-uniform mutation), three types of crossover (arithmetic crossover, simple crossover, heuristic crossover), coefficient for non-uniform mutation and tournament selection. A stopping criterion of 100 generations and a repetition of 100 genetic algorithm runs were carried out for each configuration.

Table A.1 Control Parameters Selection

GA Control Parameters	Range	Step Size
Coef. for non-uniform mutation (b)	2 – 8	2
Crossover rate	10% – 90%	20%
Population size	$2l$*– $10l$	$2l$
Mutation rate	1% – 9%	2 %

*l = chromosome length

For each run, the best fitness value was recorded as measure for the GA's performance. These values were averaged over 100 runs for every combination of population sizes, crossover rates, mutation rates, coefficient for non-uniform mutation (b), to provide a representative performance of a general GA run. The computation cost is defined as a product of the population size and the minimum number of generations it takes to obtain the minimum value for each trial limited to the stopping criterion of 100 generations used. The performance values for each configuration were normalized with respect to those values from

run with coefficients for non-uniform mutation of 2, crossover rate of 10%, mutation rate of 1% and population size of twice the chromosome lengths for each test problem.

A.2 Results

The results for all the different control parameters configurations to every test problem show similar trend in the best fitness value performance. Therefore, only some of the selected combinations of control parameter graphs are shown and the normalised best fitness graphs were "truncated" to highlight the minimal best fitness values. The normalised best fitness results for test problems 1, 2, 3 and 4 with normalised fitness values 72.25, 7.81, 25536, 0.51 are shown in Figures A.1a, A.2a, A.3a and A.4a respectively. All the test problems show that larger population sizes provide more accurate solution. However, for trials with the same crossover rate or mutation rate, there is relatively little improvement in fitness value for population size above 4*l*. This minimal improvement in fitness value is at the expense of greater computational cost, which in general is a linear increase of computational effort for an increase in population size as shown in Figures A.1b, A.2b, A.3b and A.4b for test problems 1, 2, 3 and 4 respectively. While there is minimal improvement in the best fitness for populations greater than 4*l*, the computational effort continues to increase as shown in the normalised computation cost graphs. Hence, increasing the population size beyond 4*l* does not appear to be worth the related computational cost. The results suggest that a population size of 4*l* is an appropriate compromise for a best fitness value and a reasonable computational effort which agrees well with (Williams and Crossley 1998).

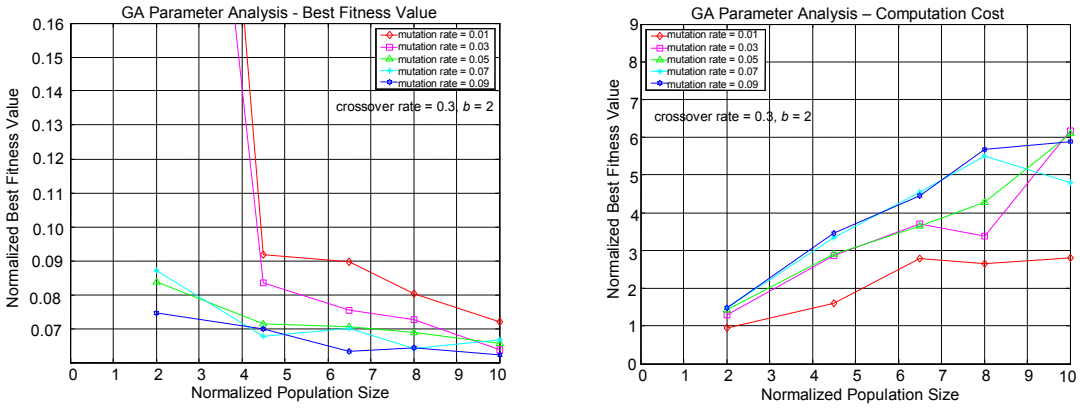

(a) (b)

Figure A.1 GA Control Parameter Analysis – Test Problem 1

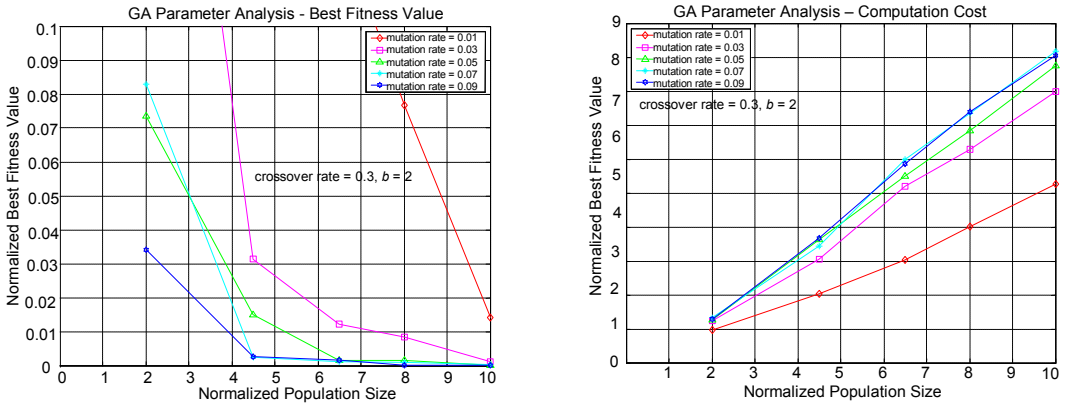

(a) (b)

Figure A.2 GA Control Parameter Analysis – Test Problem 2

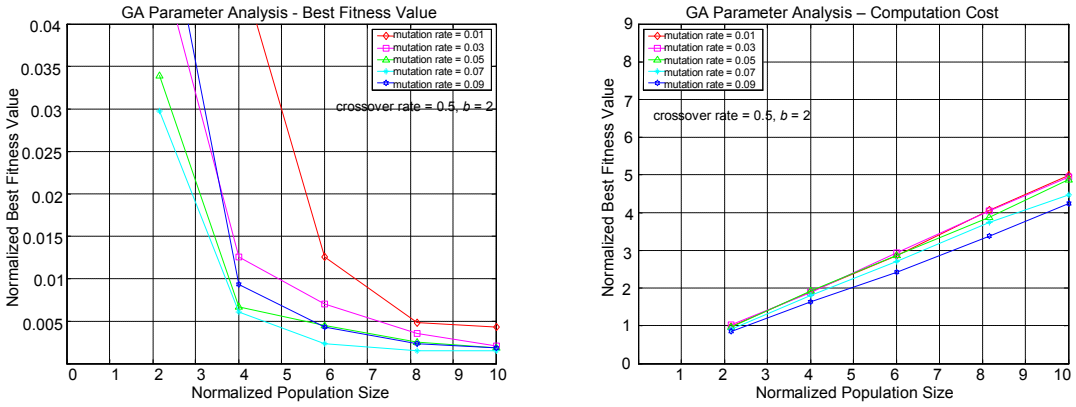

(a) (b)

Figure A.3 GA Control Parameter Analysis – Test Problem 3

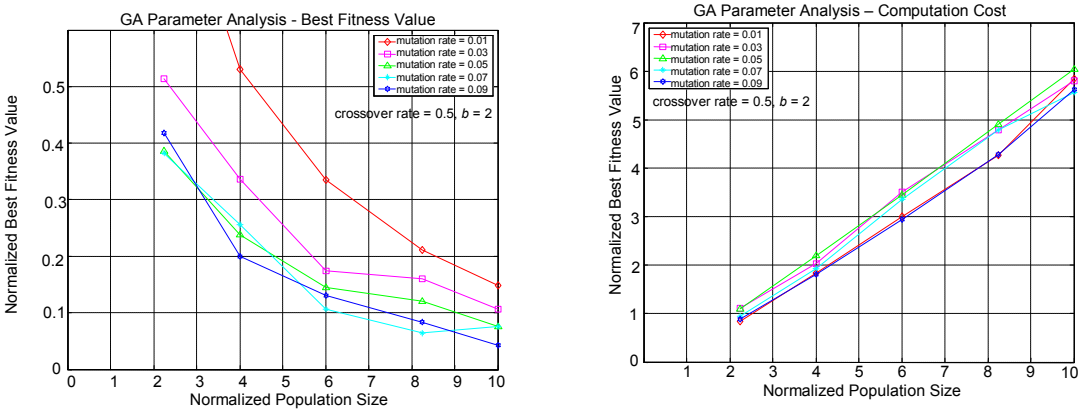

(a) (b)

Figure A.4 GA Control Parameter Analysis – Test Problem 4

GA convergence history is important to the understanding of its behaviour to ensure sufficient number of generations was run to obtain satisfactory results. Figure A.5 illustrates the typical convergence history for 100 generations for each of the 100 trials. No premature

convergence is observed and 100 generations has allowed a satisfactory development of the population.

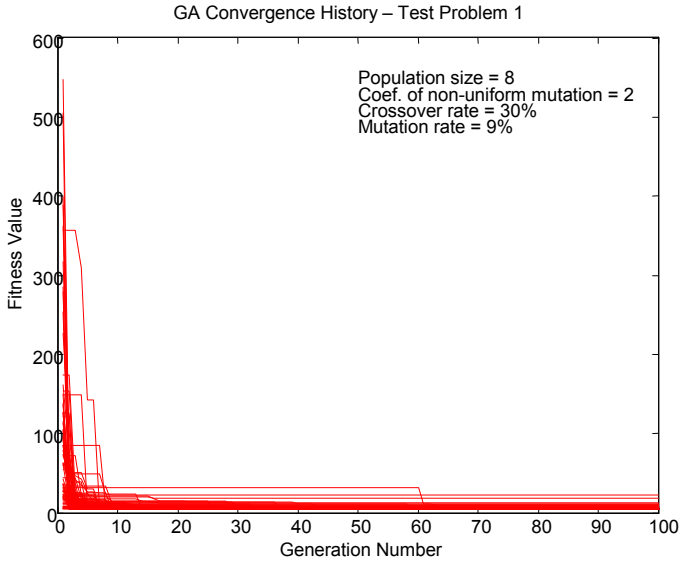

Figure A.5 GA Convergence History

The results for the best control parameter combinations are shown in Table A.2. A coefficient for non-uniform mutation of 2 consistently provides the best results for all the different combinations of population sizes, crossover rates and mutation rates tested for all four test problems. A crossover rate of 30% provides the best results for the test problems with two variables while a crossover rate of 50% provides the best results for the test problems with four or six variables. The results seem to indicate that a crossover rate of 50% is more suitable for problems with more variables. A mutation rate of 9% provides the best results for the test problems with up to four variables while a mutation rate of 7% provides the best results for the test problem with six variables. The decrease in mutation rate provides better results for test problems with more variables. This indicates that a higher mutation rate might create excessive mutation in the chromosomes. At small population size, the mutation rates appear to have a significant effect on the fitness performance but as the population sizes increases beyond $4l$, the effect becomes minimal. At larger population sizes, the improvement in fitness value in increased mutation rates are smaller than the improvement in fitness value in an increased in population size.

Table A.2 Control Parameters Selection Results

Test Problem	# Variables	Coefficient for non-uniform mutation	Crossover rate	Mutation rate	Population size
1	2	2	30%	9%	$4l$
2	2	2	30%	9%	$4l$
3	6	2	50%	7%	$4l$
4	4	2	50%	9%	$4l$